DETRIMENTAL AND BENEFICIAL EFFECTS OF INTERFERON-GAMMA ON OLIGODENDROCYTES AND THE MYELINATION/REMYELINATION PROCESS

Krystle D. Strand

A dissertation submitted to the faculty of the University of North Carolina at Chapel Hill in partial fulfillment of the requirements for the degree of Doctor of Philosophy in the Curriculum of Neurobiology.

Chapel Hill
2006

Approved by
Advisor: Brian Popko
Reader: Glenn Matsushima
Reader: Jenny Ting
Reader: Arrel Toews
Reader: Mohanish Deshmukh

ABSTRACT

KRYSTLE D. STRAND: Detrimental and Beneficial Effects of Interferon-gamma on Oligodendrocytes and the Myelination/Remyelination Process
(Under the direction of Brian Popko)

Interferon-gamma (IFN-γ) is a pro-inflammatory cytokine that is believed to play a key role in the pathogenesis of immune-mediated demyelinating disorders of the central nervous system by exerting direct deleterious effects on oligodendrocytes, the myelinating cells of the CNS. Increasing evidence predicts that the effect of IFN-γ on oligodendrocytes in culture and in vivo will depend on the developmental stage of the cells and the timing of IFN-γ expression relative to myelination/remyelination. We hypothesize that selected genes will be expressed by developmentally different oligodendrocytes when exposed to IFN-γ. In order to elucidate the molecular mechanisms driving these effects, we used microarrays to quantitatively compare the transcriptional response of 1) cultured developing and mature primary oligodendrocytes exposed to IFN-γ, and 2) the corpus collosum exposed to IFN-γ in vivo during, and two weeks following, a cuprizone-induced demyelinating insult, measured at the point of peak demyelination and at the crest of remyelination. There was a significant change in the expression of numerous genes in both the in vitro and in vivo systems as a result of IFN-γ exposure. Most dramatic were changes in the expression of genes involved in antigen presentation and protein processing, the immune response, the endoplasmic reticulum stress response, apoptosis, and the oxidative stress response. Moreover, immature oligodendrocytes appeared more responsive and vulnerable than mature oligodendrocytes to IFN-γ exposure in vitro, and the timing of IFN-γ induction influenced the transcriptional

response in vivo. Early IFN-γ exposure demonstrated evidence of a deleterious effect, while later IFN-γ suggested a protective effect, particularly during remyelination.

To my parents, Jan and Larry Strand,
and to my extraordinary friend Dr. Karla Thompson
for their never-ending love, encouragement and support.

ACKNOWLEDGEMENTS

This work was made possible by the many people who have participated in my education formation over the years. I would first like to acknowledge my advisor, Dr. Brian Popko, for his superb mentorship, patience, and constant support, as well as my committee members, Dr. Glenn Matsushima, Dr. Arrel Toews, Dr. Jenny Ting, and Dr. Mohanish Deshmukh. I thank members of Brian Popko's lab, Dr. Nathalie Doerflinger and April Kemper, for their scientific assistance and friendship. I thank Mike Vernon for his excellent skill in microarray processing, Dr. Wensheng Lin for his work on the cuprizone project, and Dr. Randy McKinnon for his work on the cell cultures. I also thank Dr. James Mattoon of the University of Colorado at Colorado Springs for his mentorship of my master's thesis. I especially thank Dr. Ellen Aho of Concordia College for her excellent teaching early in my scientific career and for her ongoing support and friendship. Finally, I thank friends Patricia Anderson Prasifka, Cathy Bozzo, Cindy Lempp, and Margaret Hensley for their continuous encouragement and faithful friendship. I would also like to express my gratitude, regrettably posthumously, to Dr. Pierre Morell for his scientific guidance, mentorship, and humor; and to Harold Smith for his uplifting spirit, kindness and friendship.

TABLE OF CONTENTS

LIST OF TABLES

LIST OF FIGURES

LIST OF ABBREVIATIONS AND SYMBOLS

BBB	blood-brain barrier
CNP	2', 3' cyclic nucleotide phosphodiesterase
CNS	central nervous system
dox	doxycycline
EAE	experimental autoimmune encephalomyelitis
EST	expressed sequence tag
FGF	fibroblast growth factor
Fig.	Figure
GFAP	glial fibrillary acidic protein
IFN-	interferon-gamma
IFN-γ-iOL	interferon-gamma-treated immature oligodendrocyte
IFN-γ-mOL	interferon-gamma-treated mature oligodendrocyte
iOL	immature oligodendrocyte
MAC	membrane attack complex
MBP	myelin basic protein
MHC	major histocompatibility complex
MOBP	myelin-associated oligodendrocytic basic protein
mOL	mature oligodendrocyte
MS	multiple sclerosis
OL	oligodendrocyte

OPC	oligodendrocyte progenitor cell
PDGF	platelet-derived growth factor
PLP	proteolipid protein
PND	postnatal day
PNS	peripheral nervous system
RMA	Robust MicroArray Algorithm
ROS	reactive oxygen species
T3	triiodothryonine
tx	treated

CHAPTER ONE

INRODUCTION

Myelin is a multilammelar sheath comprised of 70% lipid and 30% protein that serves to wrap neuronal axons in up to 1mm internode increments leaving 1μm of bare axon between internodes known as nodes of Ranvier (Smith, 1996). In the peripheral nervous system (PNS), axons are myelinated by Schwann cells, and each Schwann cell forms a single internode (Smith, 1996). In the central nervous system (CNS), oligodendrocytes (OLs) produce myelin. The conservation of space in the CNS is of much more importance, and a single OL can extend up to 50 membrane processes myelinating several different axons (Raine, 1997; Smith, 1996).

The term salutatory conduction is used to describe the series of depolarizing events that occur along the axon at the nodes of Ranvier. Sodium channels are clustered in high density at the nodes, resulting in low membrane resistance, which allows rapid charging and discharging and results in extremely fast propagation of electrical impulses down the axon. It is these electrical impulses that signal the release of neurotransmitters between axon terminals and dendrites, providing a line of communication between neurons (Smith, 1996).

Not all axons are myelinated, and those that aren't do not have the high density clustering of sodium channels, and therefore, propagate electrical impulses much more slowly (Smith, 1996). There are several neuropathies in which axons become demyelinated and the disruption to neuronal communication has marked phenotypic consequences.

In the CNS, the most common demyelinating disease is multiple sclerosis (MS), affecting over 2.5 million people world-wide with a bias for females (1.6:1) and persons of Northern European decent residing in temperate climates during the first 15 years of life (1 in 1000) (Compston and Coles, 2002; reviewed in Noseworthy, 1999). The onset of symptoms, which can be sensory, motor, visual, and/or autonomic, most often occurs in the second to forth decade of life. In 15% of MS cases, there is a steady progression of symptoms from the time of onset, but the majority of cases (85%) begin as relapsing-remitting with exacerbations generally lasting weeks followed by periods of nearly complete recovery lasting months to even years. Over time the number of partially remyelinated and fully demyelinated lesions increases such that patients no longer experience distinct recovery periods and enter a secondary progressive phase of the disease (Trapp et al., 1999). The etiology and contributing factors of MS remain elusive, in part due to the extreme variability of symptoms and rate of progression. It is now, however, widely accepted that MS is an autoimmune inflammatory disorder with both environmental and genetic elements influencing its course (Noseworthy, 1999; Raine, 1994).

The CNS is normally naïve to components of the immune system, protected by the blood-brain barrier (BBB) (Crone, 1986); however, in MS the BBB is compromised allowing infiltration of T cells and macrophages (Raine, 1994; Rodriquez and Scheithauer, 1994). These cells along with reactive astrocytes have been found at sites of demyelination, and biopsied lesions have indicated that OLs, not myelin itself, are the target of attack (Rodriguez and Scheithauer, 1994; Rodriguez et al., 1993). Moreover, examination of cerebral spinal fluid (CSF) from MS patients revealed antibodies to several myelin components, including myelin basic protein (MBP) and proteolipid protein (PLP) (reviewed in Miller et al., 1995).

The primary animal model for MS, experimental autoimmune encephalomyelitis (EAE), can be induced by immunizing animals with myelin or one of its components (Roland and McFarland, 1995). While not a perfect model for MS (reviewed in Steinman, 1999), EAE is T cell-mediated and displays many of the immunological, clinical, and pathological features and nuances of MS (Roland and McFarland, 1995).

One of the complicating factors, and likely significant contributors, to immune-mediated demyelination is the ectopic secretion of cytokines and growth factors by infiltrating immune cells. Significant clinical and experimental evidence has implicated the pro-inflammatory cytokine interferon-gamma (IFN-γ) in the pathogenesis of MS and EAE (reviewed in Steinman, 2001; Baerwald et al., 1999; reviewed in Popko et al., 1997). IFN-γ has been detected in and around demyelinated lesions and in the CSF of MS patients. Furthermore, administration of IFN-γ as a therapeutic agent instead caused rapid progression of the disease (Panitch, 1992; Panitch et al., 1987).

IFN-γ is a Type II pro-inflammatory cytokine and fundamental regulator of the immune and inflammatory responses that is expressed exclusively by T cells and natural killer cells and regulates their preponderance in response to injury or infection (reviewed in St. Pierre et al., 1996). It is a 34- to 50-kDa secreted protein that upon non-covalent homodimerization binds dimerized α and β subunits of its receptor, which is expressed by all cells types except erythrocytes (Tau and Rothman, 1999). Ligand-receptor binding initiates an intracellular signal transduction cascade whereby Janus protein tyrosine kinases (JAKs) associated with the receptor become phosphorylated. Signal transducer and activator of transcription-1 (STAT1) molecules bind phosphorylated JAKs and also become phosphorylated.

Phosphorylated STAT1 is then translocated to the nucleus where it binds γ-activation sites (GAS) and induces IFN-γ-sensitive genes containing GAS elements (Shuai et al., 1993).

Oligodendrocyte progenitor cells (OPCs) arise from the subventricular zone in the CNS (reviewed in Barres, 1999; McKinnon and Dubois-Dalcq, 1996) and migrate into areas of the CNS destined for myelination, where they then proliferate and differentiate into postmitotic mature OLs. Distinct stages of differentiation have been immunologically identified, beginning with PSA-NCAM$^+$ preprogenitors (Grinspan et al., 1990; Ben-Hur et al., 1998), followed by A2B5$^+$ early progenitors (Raff et al., 1978), O4$^+$ late progenitors/pro-oligodendrocytes (Dubois-Dalcq, 1987), galactocerebroside$^+$ oligodendrocytes (Raff et al., 1978), and O1$^+$ mature oligodendrocytes (Schachner et al., 1981; Sommer and Schachner, 1981) .

The survival, proliferation and differentiation of OPCs is regulated by numerous extracellular cues. Platelet-derived growth factor (PDGF) (Noble et al., 1988; Raff et al., 1988) and basic fibroblast growth factor (bFGF) (McKinnon, 1990) promote progenitor cell survival (Barres et al., 1992) and insulin-like growth factors (IGFs), neurotrophin-3 (NT-3), ciliary-neurotrophic factor (CNTF), leukemia inhibitory factor (LIF) and interleukin-6 (IL-6) promote the survival of mature cells (Barres et al.,1993). bFGF sustains high levels of PDGF-α receptors, the sole isoform expressed by OPCs and OLs (de Vries, 2000). In vitro, differentiation of progenitors can be stimulated by removing PDGF and bFGF from the culture medium (McKinnon et al., 1990, 1993), and this process is facilitated by IGF-1 and thyroid hormones (McMorris et al., 1986; Barres et al., 1992, 1994). PDGF-α knockout mice display hypomyelination and a decrease in the number of both progenitor cells and mature OLs (Fruttiger et al., 1999).

Several transcription factors have also been found to be transcriptionally regulated during various stages of progenitor differentiation and myelination (reviewed in Wegner, 2001). Members of the basic helix-loop-helix family, OLIG-1, OLIG-2, and OLIG-3 are expressed early in OL differentiation (Takebayashi et al., 2000; Zhou et al., 2001), while the expression of NKX6-2, a homeodomain protein, is restricted to mature OLs and parallels that of MBP and PLP proteins during postnatal brain development (Komuro et al., 1993; Awatramani et al., 1997). Still others, such as POU3F1, are expressed only transiently to activate myelin-associated genes (Collarini et al., 1992).

Exposing developing and mature OLs to IFN-γ in vitro has been shown to have varied, but principally detrimental consequences. Vartanian et al. (1995) reported apoptotic death in both immature and mature primary rodent OL cultures; whereas Agresti et al. (1996) determined IFN-γ only caused progenitor cells to halt mitosis and differentiation. Still others observed a retraction of membrane processes and flattened cell bodies in response to IFN-γ treatment of the MOCH-1 OL cell line (Li et al., 1995). Previous studies from our lab have indicated that immature cells of the O2-A cell line die by apoptosis after two days of IFN-γ exposure and mature cells die by necrosis after four to seven days (Baerwald and Popko, 1998).

In vivo, direct delivery of IFN-γ to the CNS of rodents (reviewed in Popko et al., 1997) stimulated major histocompatibility complex (MHC) expression (Wong et al., 1984; Sethna and Lampson, 1991; Steiniger and van der Meide, 1988). Evidence from these studies also suggests IFN-γ may induce cell adhesion molecule expression in endothelial cells of the blood-brain barrier, which may potentially play a role in the perturbation mediating

transepithelial migration of inflammatory cells into the CNS (Simmons and Willenborg 1990, Wong and Dorovini-Zis 1992, Steffen et al. 1994, McCarron et al. 1993).

Several transgenic lines of mice have been generated to examine the effects of ectopic IFN-γ expression in the CNS. Mice expressing IFN-γ under the transcriptional control of the oligodendrocyte-specific MBP promoter (MBP/IFN-γ) display a tremoring phenotype, severe hypomyelination, and astrogliosis (Corbin et al., 1996). Expression of IFN-γ in these mice is induced at the time of myelin production; however, the onset of MS occurs in adulthood after myelination has been established. Moreover, in MS and EAE, oligodendrocytes are bathed in IFN-γ; rather than synthesizing and secreting the cytokine. In an effort to create a more accurate model for adult onset demyelination, transgenic animals expressing IFN-γ in astrocytes under the tetracycline-inducible system were developed (Lin et al., 2004). This model provides temporal and spatial control of IFN-γ expression and permits evaluation of the effects of IFN-γ on mature OLs and myelination.

In MS and EAE, T cells and macrophages infiltrate the CNS and invoke the induction of cytokines and other immune response molecules. Demyelination by the toxicant cuprizone, however, is largely non-immune-mediated (Matsushima and Morell, 2001). Combining the cuprizone model of demyelination with the tetracycline-inducible model of IFN-γ has spawned an excellent system for studying the effects of a single cytokine, induced at different time points, on the demyelination and remyelination processes (Lin et al., 2006).

During remission, oligodendrocyte progenitor cells (OPCs) migrate to areas of demyelination where they differentiate into mature oligodendrocytes (OLs) and extend membrane processes that become the myelin sheath wrapping bare axons and restoring signal transduction (Mason et al., 2000; Matsushima and Morell, 2001). A single OL can extend up

to approximately 50 myelin processes, which requires the synthesis of enormous amounts of plasma membrane lipid and protein (Smith, 1996).

In non-pathological situations, oligodendrocytes do not constitutively express antigen presenting molecules; however, in the presence of IFN-γ, MHC class I is markedly induced (Wong et al. 1984, Suzumara et al. 1986, Calder et al. 1988, Satoh et al. 1991, Massa et al. 1993, Li et al. 1995). MHC class I is a trimolecular complex that is assembled in the endoplasmic reticulum (ER) and consists of the MHC class I heavy chain, beta-2 microglobulin (β_2M), and a peptide antigen. The complex is transported out of the ER to the cell surface via the secretory pathway involving the transporter TAP, but only when correctly assembled by protein folding chaperones. At the cell surface, MHC-bound antigen is presented to and recognized by circulating T cells.

Evidence suggests that robust MHC synthesis in OLs is detrimental. MHC class I was upregulated in the MBP/IFN-γ mice (Corbin et al., 1996), particularly enhanced in white matter tracts (Baerwald et al, 2000), and phenotype severity strongly correlated with the level of MHC class I induction (Corbin et al., 1996). Transgenic animals with MHC class I heavy chain expression targeted to OLs exhibit severe hypomyelination (Turnley et al., 1991; Yoshioka et al., 1991). The heavy chain is restricted to oligodendrocyte perikarya (Power et al., 1996) and is not transported past the ER, which is likely due to improper assembly of the trimolecule complex (Baerwald et al., 2000). In the *jimpy* mouse, oligodendrocytes express a mutant form of PLP, which accumulates in the ER and results in severe hypomyelination and apoptotic cell death of oligodendrocytes (Gow et al. 1994, 1996, 1998; Tosic et al., 1996; Skoff, 1995). Over expression of wild-type PLP also leads to aberrant myelin formation (Readhead et al., 1994; Kagawa et al., 1994).

Since actively myelinating oligodendrocytes must synthesize copious amounts of membrane lipid and protein via the secretory pathway, the deleterious effects of robust MHC class I expression may be a result of ER overloading and stress (Southwood et al., 2002; Leegwater et al., 2001; Popko and Baerwald, 1999). Concordantly, recent experiments in which IFN-γ was ectopically expressed in astrocytes during cuprizone-induced demyelination demonstrated evidence of an ER stress response in remyelinating OLs of the corpus collosum (Lin et al., 2005). The folding chaperones BIP and CHOP were increased in IFN-γ-expressing animals during remyelination and the phosphorylation of eIF2α, which halts most protein synthesis, was also increased (Lin et al., 2005).

IFN-γ expressed in mice heterozygous for the ER stress response kinase PERK (pancreatic ER kinase), did not survive as long as non-IFN-γ expressing $PERK^{+/-}$ animals (Lin et al., 2005). Furthermore, $PERK^{+/-}$ mice carrying the IFN-γ transgene were treated with cuprizone and IFN-γ was induced at the time of demyelination (Lin et al., 2006). These mice possessed fewer OLs and displayed an increase in the pro-apoptotic gene caspase-3 in the corpus collosum during the remyelination phase (Lin et al., 2006).

Although there is considerable clinical and experimental evidence indicating IFN-γ is detrimental in MS, to cultured OLs, and myelination in vivo, the complete role of IFN-γ remains controversial. Moreover, data suggests its effect may be time- and dose-dependent. IFN-γ levels in the CNS correlate with the severity of EAE (Renno et al., 1994) and the number of T cells secreting the cytokine increases just before the onset of symptoms (Issazadeh et al., 1995; Mustafa et al., 1991). Unexpectedly, however, antibodies to IFN-γ worsened the disease pathogenesis (Duong et al., 1992; Voorthius et al., 1990; Billiau et al., 1988) and intraventricular treatment of IFN-γ to rodents with active EAE reduced disease

severity (Voorthius et al., 1990). Furthermore, IFN-γ or IFN-γ receptor knock-out mice were more sensitive to EAE (Ferber et al., 1996; Willenborg et al., 1996).

Asymptomatic lines of mice expressing low levels of IFN-γ in OLs from the time of MBP synthesis were resistant to cuprizone-induced demyelination (Gao et al., 2000). Additionally, recent studies have shown that IFN-γ induction commensurate with cuprizone-induced demyelination results in fewer repopulating OLs and reduced remyelination; whereas, IFN-γ induction at the time the corpus collosum is fully demyelinated results in a greater number of migrating OLs and enhanced remyelination (Lin et al., 2006 and unpublished data).

It has been thought that the progenitor cells responsible for repopulating and remyelinating areas of demyelination undergo the same course of maturation as progenitors during development. There is now evidence to suggest that this may not be the case (reviewed in Balabanov and Popko, 2005; Arnett et al., 2004; Stidworthy et al., 2004; Franklin et al., 2002). Whether IFN-γ is harmful or beneficial to oligodendrocytes and myelination/ remyelination may depend on the dose and timing of its expression relative to the demyelinating event.

CHAPTER TWO

EFFECTS OF INTERFERON-GAMMA ON IMMATURE AND MATURE OLIGODENDROCYTES IN VITRO

INTRODUCTION

Proper neuronal signal conduction in the central nervous system (CNS) requires structural integrity of the myelin membrane ensheathing axonal processes, and in the CNS, axons are myelinated by oligodendrocytes (OLs). The loss of myelin results in several neuropathies, including multiple sclerosis (MS) in humans and experimental autoimmune encephalomyelitis (EAE) in rodents. Based on clinical and experimental evidence, the pro-inflammatory cytokine interferon-gamma (IFN-γ) has been implicated in the pathogenesis of such immune-mediated demyelinating disorders (reviewed in Popko et al., 1997; reviewed in Popko and Baerwald, 1999; reviewed in Steinman, 2001). Whereas the CNS is normally naïve to IFN-γ, in these disorders IFN-γ-secreting T cells migrate across a disrupted blood-brain-barrier (Miller et al., 1995; reviewed in Roland and McFarland, 1995), and indeed, IFN-γ has been detected in the cerebral spinal fluid and in and around demyelinated lesions of individuals with MS. Furthermore, IFN-γ administered as a therapeutic agent to MS patients instead rapidly worsened the disease course (Panitch et al., 1987; Panitch, 1992).

Oligodendrocyte progenitor cells (OPCs) arise from the subventricular zone in the CNS (reviewed in Barres, 1999; McKinnon and Dubois-Dalcq, 1996). OPCs migrate into areas of the CNS destined for myelination, where they then proliferate and differentiate into postmitotic mature OLs. Distinct stages of differentiation have been immunologically

identified, beginning with PSA-NCAM$^+$ preprogenitors (Grinspan et al., 1990; Ben-Hur et al., 1998), followed by A2B5$^+$ early progenitors (Raff et al., 1978), O4$^+$ late progenitors/pro-oligodendrocytes (Dubois-Dalcq, 1987), galactocerebroside$^+$ oligodendrocytes (Raff et al., 1978), and O1$^+$ mature oligodendrocytes (Schachner et al., 1981; Sommer and Schachner, 1981) .

Many extracellular cues play a role in proper progenitor proliferation and survival. Platelet-derived growth factor (PDGF) (Noble et al., 1988; Raff et al., 1988) and basic fibroblast growth factor (bFGF) (McKinnon, 1990) promote progenitor cell survival (Barres et al., 1992), with bFGF maintaining high levels of PDGF-α receptors, the sole isoform expressed by OPCs and OLs (de Vries, 2000). In vitro, removal of PDGF and bFGF from culture medium stimulates OPC differentiation (McKinnon et al., 1990, 1993). Furthermore, insulin-like growth factor-1 (IGF-1) and thyroid hormones facilitate this process (McMorris et al., 1986; Barres et al., 1992, 1994). PDGF-α knockout mice display hypomyelination and a decrease in the number of both progenitor cells and mature OLs (Fruttiger et al., 1999). Barres et al. (1993) have also shown that IGFs along with neurotrophin-3 (NT-3), ciliary-neurotrophic factor (CNTF), leukemia inhibitory factor (LIF) and interleukin-6 (IL-6) promote OL survival in vivo.

Despite the substantial knowledge gained regarding environmental and extracellular factors influencing the survival, proliferation, and development of oligodendrocytes, the intracellular responses of these cells to such cues, and the pathways into which these responses are organized remain elusive. Several transcription factors undergo changes in expression during various stages of progenitor differentiation and myelination (reviewed in Wegner, 2001). Members of the basic helix-loop-helix family, OLIG-1, OLIG-2 and

OLIG-3 are expressed early in OL differentiation (Zhou et al., 2001). The expression of NKX6-2, a homeodomain protein, is restricted to mature OLs and parallels that of MBP and PLP proteins during postnatal brain development (Komuro et al., 1993; Awatramani et al., 1997). Still others, such as POU3F1, are expressed only transiently to activate myelin-associated genes (Collarini et al., 1992).

In recent years, there has been a torrent of new sequence information for several model organisms, including yeast, fly, mouse, rat, and human (reviewed in Lander and Weinberg, 2000). Much of the sequenced genomes represents characterized genes; however, a large portion contains information for genes of unknown function or expressed sequence tags (ESTs). The advent of such a wealth of new sequence information has fostered the development of microarray technology, which has become a powerful tool for simultaneously comparing the expression of thousands of genes across genetic and environmental parameters. In this study, we have employed microarray technology to scrutinize gene expression changes of OPCs in response to IFN-γ exposure during an early and later stage of differentiation.

MATERIALS AND METHODS

Primary Oligodendrocyte Isolation and Cytokine Incubation

Oligodendrocyte progenitor cell cultures were maintained according to previously established protocols (McKinnon et al., 1990). Briefly, primary mixed glial cultures were established from postnatal day two (PND2) Sprague-Dawley rats (Taconic Farms, NY) and immunoselected for $A2B5^+$ early (O2A) progenitor cells. Purified cells were plated on poly-L-ornithine-coated (100μg/ml, Sigma) Falcon dishes (Becton Dickenson) at 37°C in a

humidified atmosphere of 90% air/10% CO_2 and cultured in DMEM with 4.5g/L D-glucose, 50U/ml penicillin and 50μg/ml streptomycin (Gibco/BRL, Bethesda, MD), 50μg/ml transferrin, 30nM sodium selenite, 30nM triiodothryonine (T3), 50ng/ml bovine insulin and 100μg/ml bovine serum albumin (basal defined medium, BDM). Cells were expanded as A2B5-immunoreactive progenitors in BDM containing 10ng/ml PDGF and 5ng/ml FGF-2 (R&D, Inc., Minneapolis, MN). Growth factors were replenished every 48 hours and the culture medium was replenished every four days. After three days, progenitor differentiation was initiated by switching the cells to medium without PDGF and FGF-2. Recombinant rat IFN-γ (100U/ml, Gibco BRL, Gaithersburg, MD) was added to cells either at the time of switching to PDGF- and FGF-2-free media (immature OLs) or after cells had been allowed to differentiate for three days (mature OLs). Total RNA was isolated from cell cultures using TRIzol Reagent (Gibco BRL), then further purified through an RNeasy column (QIAGEN).

Immunocytochemistry

Monoclonal antibodies A2B5, O4 and O1 were obtained from hybridoma cell lines as supernatant fluids (Eisenbarth et al., 1979; Sommer and Schachner, 1981, respectively). Anti-bromodeoxyuridine (BrdU) was purchased from Sigma and rabbit MBP antisera was a gift from David Colman (Mt. Sinai, NY). To identify the stage of progenitor differentiation at the time of RNA isolation, cells were fixed in 2% paraformaldehyde for 10 min, exposed to primary antibodies for 30 min, washed in phosphate-buffered saline (PBS; 10mM sodium phosphate, 0.15mM NaCl, pH 7.2), detected by incubating in secondary anti-mouse IgM-RITC and IgG-FITC antibodies (Pierce, Rockford, IL) for 30 min at room temperature. Coverslips were mounted on glass slides in 10mM Tris, pH 8.6, 90% glycerol, 2% 1-4-

diazabicyclo(2.2.2) octane (Sigma) and visualized with a Zeiss Axiovert 100TV inverted fluorescent microscope equipped with a 40X Achrostigmat objective (McKinnon et al., 1990).

RNA Amplification, Labeling, and Microarray Hybridization

From each cell culture, 100ng of total RNA was used to synthesize cDNA according to the GeneChip® Eukaryotic Small Sample Target Labeling Protocol (Affymetrix). Two rounds of amplification were conducted using T7-$(dT)_{24}$ primer (Life Technologies). Biotinylated cRNA was then generated using the BioArray High Yield RNA Transcription Kit (Life Technologies), then subsequently fragmented in 5X fragmentation buffer (200mM Tris-acetate pH 8.1, 500mM KOAc and 150mM MgOAc) at 94°C for 35 min. 15μg of fragmented cRNA was added to hybridization cocktail (50pM control oligonucleotide [B2, *BioB*, *BioC*, *BioD* and *Cre*], 0.01mg/ml herring sperm DNA, 0.5mg/ml acetylated BSA, 100mM MES, 1M $[Na^+]$, 20mM EDTA and 0.01% Tween 20). 10μg of cRNA in cocktail was hybridized to each array for 16 hours at 45°C in the GeneChip® Hybridization Oven 640 (Affymetrix). Microarrays were then washed, stained with R-phycoerythrin streptavidin in the GeneChip® Fluidics Station 400 (Affymetrix), and scanned in the Hewlett Packard GeneArray Scanner using Microarray Suite 5.0 (Affymetrix). cRNA quality was assessed by examining the intensity ratio of 5':3' probe pair binding of control genes.

Microarray Analysis

The rat genome RG_U34 GeneChip® set (Affymetrix) containing probe sets representing over 26,000 genes and expressed sequence tags (ESTs) was used for all hybridization

reactions. Three independent hybridizations were performed with the RG_U34A array for cells that had been allowed to differentiate for 1 day (immature OLs [iOLs]), 5 days (mature OLs [mOLs]), and 3 days + 2 days with IFN-γ (IFN-γ-treated mature OLs [IFN-γ-mOLs]). Two independent hybridizations were completed with the RG_U34A array for cells that had been allowed to differentiate for 1 day in the presence of IFN-γ (IFN-γ-treated immature OLs [IFN-γ-iOLs]). On the RG_U34B and RG_U34C arrays, two hybridizations were carried out for the IFN-γ-treated immature OLs, and one hybridization was conducted for each of the remaining samples. Hybridization intensities were summarized using Robust MultiArray Analysis (RMA) (Irizarry et al., 2003) to generate an expression estimate for each probe set (gene). Expression estimates were normalized using GeneSpring® software (Agilent Technologies) as follows: 1) negative expression estimates were floored to 0.01, 2) the top 90% of expression estimates was used to calculate the 50th percentile for each array, and 3) expression estimates were normalized to the 50th percentile value of the corresponding array. Normalized expression estimates were averaged across replicate samples and significance of difference between treatment groups was determined by Student's t-test (p-value<0.1). We report here differential mRNA expression as the fold change between IFN-γ-treated and non-treated cell populations. Gene function information and probe set annotations were obtained from GeneSpring GX (Agilent Technologies), Netaffx™ (Affymetrix; www.affymetrix.com), the National Center for Biotechnology Information (NCBI; www.nbci.nlm.nih.gov) and literature review. ESTs were identified, when possible, by BLAST search of the nucleotide database (www.ncbi.nlm.nih.gov/BLAST). Pathway information was obtained from the Gene Map Annotator and Pathway Profiler (GenMAPP; Gladstone Institutes, University of

California at San Francisco; www.genmapp.org), PathArt© (Jubilent Biosys), NetAffx™, and primary literature.

Quantitative Real-Time Reverse Transcription-Polymerase Chain Reaction

RNA was treated with DNAse I and column purified (QIAGEN). cDNA was then synthesized with random hexomers and Superscript II (Invitrogen). Amplification was carried out by combining 4ng or 20ng of cDNA with the following reagents (in final concentrations): 0.2mM dATP, 0.2mM dGTP, 0.2mM dCTP, 0.4mM dUTP, 200mM forward primer, and 200mM reverse primer (Invitrogen), 3mM $MgCl_2$, 0.02U/µl UNG, 0.01U/µl AmpliTaq DNA polymerase, and 1X SYBR Green Dye in buffer (Applied Biosystems). Real-time PCR amplification reactions were performed in triplicate wells for each gene per starting amount of cDNA on the Applied Biosystems 7700 Real Time PCR System (1 cycle at 50°C for 2 min, 1 cycle at 95°C for 10 min, 40 cycles at 95°C for 15 sec, 1 cycle 60°C for 1 min). GAPDH was used as an internal and normalization control, and the amplified transcripts were quantified by relative threshold cycle (C_T) comparison. Primers were designed with Primer Express software (Applied Biosystems) to amplify the following sequences:

Accession#	Gene	Fwd Primer	Rev Primer
AA850495	EST	CGCCCATGGCGTTCAT	CAGAGGCCAAACGATCAAAAC
AA899109	EST	ACTCTATCACCCACCTCTAGTTCCAA	ATACTCACTGAGAACACCTGGACAGAGA
AA997015	EST	TGAATGAATGATAACAAGTAACATTGAGA	CAACCCCTTCCCCTGCTT
AA997255	EST	CCAGGGTGGCCTTAAATTCA	GTGGCTGGCACAGGACATT
AA998964	EST	CCGCCAATGGAAAATCCTAG	AAAATCACAATACCAATTAAACCCACT
AI073001	EST	CATGGTCCAAAAATACAGCTTCAG	GCCTACCTGTCGTATCACCAGAA
AI112362	EST	CTACTTGGGAGTGCATAATGAGGAT	TGGAAAACTTTGTAAGACAGGGAATATA
AI175346	EST	CAGCTAGGGTGACGGCAAA	TATGGAAGGCTTAAGTACGTTCAAAA
AI232326	EST	CCCTCGGTCAGCTCAACAAT	CACCCCCAGCGCATACC
AF106860	GAPDH	GGCCTACATGGCCT	CTCTCTTGCTCTCAGTATCCTTGCT
M34253	IRF1	CCCAAGACTTGGAAGGCAAAC	TGGTCCTTCACTTCCTCGATGT
AI235890	MHC CI	CACACCCCCAGCTCACAAA	GGTTTCCAACAGTGTAACGCAGTA

X17053	SIGJE	GAATCGCACCTTCATACAGTTCCT	AACCAACCCAAGCCCTTCTTT
AA999171	STAT1	GCTGCATTAAGGAACACGACTGT	CGTATGGCATGGTTCAAAGTCA
AA799569	STAT2	AACGCCCATAGTACAGGTTCTCA	GCCAACTGCTGCTGCTCTAAG

RESULTS AND DISCUSSION

Primary oligodendrocyte progenitor cells (OPCs) were expanded from PND2 Sprague-Dawley rats (Fig. 2.1) and relative mRNA expression was measured after cells had differentiated for 1 day (iOLs), 1day with IFN-γ (IFN-γ-iOLs), 5 days (mOLs), or 3 days followed by 2 days with IFN-γ (IFN-γ-mOLs). We report here differential mRNA expression as fold change between IFN-γ-treated and non-treated cell populations. Out of 26,263 genes surveyed 2647 (10%) were significantly up- or downregulated in IFN-γ-iOLs and 1293 (4.9%) were significantly up- or downregulated in IFN-γ-mOLs.

The hybridization cocktail contained poly-A (*Trp, Thr, Phe, Lys,* and *Dap*) and hybridization (B2, *BioB, BioC, BioD,* and *Cre*) control genes. The ratios of 5':3' probe pair binding for the poly-A controls ranged from 1:1 to 1:1.2, indicating that the RNA was of excellent quality. Expression estimates of the hybridization controls were also normal, demonstrating that the hybridization reactions worked properly. Furthermore, relative expression for several genes showing differential expression on the arrays was measured by quantitative real-time polymerase chain reaction (qRT-PCR), and these data corroborated the array findings (data not shown).

Differential Expression of Genes Involved in Myelin Formation
(Figure 2.2 and Table 2.1)

2',3'-cyclic nucleotide 3'-phosphodiesterase (CNP), myelin basic protein (MBP), and proteolipid protein (PLP) are structural components of the myelin sheath. MBP and PLP aid

in stabilizing the compact lamellar domains and in forming the intraperiod- and major dense lines, while CNP is present in the cytoplasmic channels traversing the sheath (De Angelis and Braun, 1996). CNP interacts with tubulin to promote microtubule assembly and facilitates F-actin and microtubule organization, suggesting that it may play a role in directing myelin process extension (Lee et al., 2005). As shown in Fig. 2.2, CNP, MBP, and PLP were upregulated in response to IFN-γ treatment of iOLs, but remained unchanged in mature cells treated with the cytokine. We also saw an increase in microtubule-associated tubulins TUBA6, TUBB2B and TUBB3 in IFN-γ-iOLs, and an increase in TUBB3 in IFN-γ-mOLs.

Myelin-associated oligodendrocytic basic protein (MOBP) was downregulated in mOLs treated with IFN-γ. While MOBP is not essential for myelin formation (Yool et al., 2002), it is thought to be involved in myelin sheath compaction (Holz and Schwab, 1997) and evidence suggests it may be necessary for controlling axonal diameter and establishing proper arrangement of the radial component of the intraperiod line (Yoshikawa, 2001).

Claudin11 (CLDN11, OSP) is a major element of CNS myelin forming the tight junctions within myelin sheaths that create a paracellular barrier and avenue of signal transduction, which may regulate processes such as cell growth and differentiation (Gow et al., 1999; Morita et al., 1999; Tiwari-Woodruff et al., 2001). CLDN11 is expressed in the O2-A line of OLs from the early progenitor to mature OL stage (Bronstein et al., 2000), and overexpression induces proliferation and migration in these cells (Tiwari-Woodruff et al., 2001). In our experiments, CLDN11 was upregulated in IFN-γ-iOLs and downregulated in IFN-γ-mOLs.

Protein tyrosine phosphatase, receptor type Z, polypeptide 1 (PTPRZ1) has been shown to be important for remyelination after immune-mediated demyelination, as mice deficient in PTPRZ1 recovered more slowly and less completely from MOG-induced EAE than PTPRZ1 expressing controls (Harroch et al., 2002). We found PTPRZ1 to be downregulated in IFN-γ-iOLs and unchanged in IFN-γ-mOLs.

Taken together, it appears that immature OLs may react to IFN-γ exposure by transcriptional upregulation of genes encoding structural and tight junction components of myelin, and downregulation of a remyelination-promoting gene. Mature OLs treated with IFN-γ were less responsive, downregulating genes that may affect myelin sheath compaction and tight junction signaling. Given the deleterious effects observed previously by IFN-γ exposure to OLs and myelination, it was surprising to find an increase in myelin gene expression in the IFN-γ-iOLs. The role of IFN-γ is controversial, however, and in low doses has had a protective effect against CNS demyelination (Gao et al., 2000), thus, the increase in certain myelin genes observed here could possibly be a result of such protection.

Differential Expression of Genes Involved in Cholesterol Biosynthesis
(Figure 2.3 and Table 2.2)

Cholesterol is a major component of myelin comprising approximately 30% of the total lipid in myelin, thus, we were interested in whether IFN-γ affected cholesterol biosynthesis. As shown in Fig. 2.3, several genes in the pathway were differentially regulated in response to IFN-γ exposure. In particular, HMGCR, NSDHL and APOE were upregulated in IFN-γ-iOLs. HMGCR is the rate-limiting enzyme in cholesterol biosynthesis, and APOE is thought to help transport cholesterol from degraded myelin into storage cells where it can later be

recovered by new remyelinating OLs (Mauch et al., 2001; Mahley, 1998; Sullivan et al., 1997; Venezie et al., 1995; Poirier et al., 1993; Page et al., 1993). SQLE, which converts squalene to squalene 2,3 epoxide in the second half of the pathway was downregulated in IFN-γ-iOLs, perhaps reflecting feedback regulation in response to the increase in the rate-limiting enzyme upstream. In IFN-γ-mOLs, there was a decrease in HMGCS2 and SC5D, the latter possibly indicating a shift toward 24-dehydrocholesterol rather than 7-dehydrocholesterol. It would appear from these data that iOLs exposed to IFN-γ may exhibit an increase in cholesterol synthesis and the recycling of existing cholesterol; whereas, in mature cells, cholesterol synthesis seems to be reduced. These data parallel the increase in structural and tight junction gene expression in IFN-γ-iOLs and the decrease in sheath compaction and tight junction gene expression in IFN-γ-mOLs, again suggesting a possible protective role for IFN-γ in early OL development.

Differential Expression of Genes Involved in Lipid Metabolism
(Figure 2.4 and Table 2.3)

Maturing oligodendrocytes send out branches of membrane that become myelin sheath, and this process requires the generation of a large amount of lipid in addition to cholesterol. In that connection, we found numerous genes involved in lipid metabolism to be differentially regulated in response to IFN-γ in both immature and mature OLs. In particular, lysophospholipase 1 (LYPLA1), which hydrolyzes lipophosphotidylcholine, was expressed at very low levels in both iOLs and mOLs was most robustly upregulated in both IFN-γ-treated populations. In addition, the lipid transport gene APOL2, and fatty acid degradation gene CTE1 were also upregulated in both IFN-γ-iOLs and IFN-γ-mOLs. In contrast, the

triglyceride hydrolases LPL and PNLIP were downregulated in IFN-γ-mOLs, and down- and upregulated in IFN-γ-iOLs, respectively.

Differential Expression of Genes Involved in Complement Activation
(Figure 2.5 and Table 2.4)

In the classical complement activation pathway, complement component 1 (C1) peptides join antigen-bound antibody on the cell membrane to form C1 complexes. These complexes then initiate a cascade of activation steps through various complement components that eventually results in the formation of membrane attack complexes (MACs). MAC formation has several consequences including the upregulation of c-JUN, c-FOS, PDGF, bFGF, cytokines, proto-oncogenes, diacylglycerol, and ceramide; and an increase in PKC activity, MBP hydrolysis, mitosis, cell proliferation, cytosolic calcium ions, and reactive oxygen species (ROS). Differential expression of genes involved in the complement activation pathway in response to IFN-γ treatment of immature and mature OLs is significantly higher than every other group of genes with the exception of those involved in antigen processing and presentation. As shown in Fig. 2.5, genes involved in complement activation were upregulated in both IFN-γ-iOLs and IFN-γ-mOLs, and the MAC formation inhibitor CD59 was downregulated in IFN-γ-mOLs. Given the number of downstream effects of MAC formation, perhaps complement activation is an early key factor and is, at least partially, driving the sundry of other cellular effects we observed in response to IFN-γ exposure.

Differential Expression of Genes Involved in Antigen Processing and Presentation, and ER Stress
(Figure 2.6 and Table 2.5)

As evidenced by aforementioned data and our present study, IFN-γ clearly elicits a significant immune response via antigen processing and presentation. As shown in Fig. 2.6, genes for several subtypes of MHC class I and II, the class I assembly protein β_2-microglobulin (β_2M), the class II transactivator (CIITA), and several MHC assembly proteins were substantially upregulated in both immature and mature cells exposed to IFN-γ.

Consistent with an increase in antigen presenting genes, we also found several genes involved in the processing of antigen via peptide degradation by the 20S proteasome, ubiquination, and proteolysis to also be upregulated in response to IFN-γ exposure in both immature and mature OLs. Specifically, PSMA and PSMB subunits of the 20S proteasome along with cytokine-responsive PA28 "immunoproteasome" genes PSME1/2 were strongly upregulated in both IFN-γ-treated cell populations. Also upregulated, but less so, was PSMF1, an inhibitor of the PA28 immunoproteasome, which may indicate feedback regulation. Peptides broken down by the proteasome are transported into the ER lumen through the transporter TAP, and both TAP1 and TAP2 were upregulated in IFN-γ-iOLs and IFN-γ-mOLs. Inside the ER, peptide antigens bind MHC class I associated with β_2M and the trimolecule complex is exported out of the ER via TAP. The complex then travels to the cell surface where the antigen can be recognized by T cells.

Peptide antigens can also be degraded by targeted ubiquination and proteolysis by the 26S proteasome. This process is not only used for antigen presentation; it is also used to break down mal-folded, surplus, or aggregated proteins. Synthesis, processing, and release of secretory and membrane proteins takes place in the ER. Among other events, an

accumulation of unfolded or mal-folded proteins in the ER can initiate a stress response (Rutkowski and Kaufman, 2004; Ma and Hendershot, 2001).

Developing OLs are generating copious amounts of membrane and extending numerous membrane processes destined to become multilamellar myelin sheath. This process alone heavily employs the ER; the added demand for large amounts of MHC, antigen and accessory protein synthesis and folding that occurs in response to IFN-γ has great potential for initiating an ER stress response. Recent work has demonstrated that IFN-γ exposure during myelination in vivo induces ER stress (Lin et al., 2005; Lin et al., 2006), and we find evidence of the same here as well (Figs. 2.7 and 2.8).

Cells respond to unfolded proteins by 1) upregulating ER chaperones that promote folding and help prevent protein aggregation, 2) removing mal-folded proteins from the ER via retrograde transport and subsequent degradation by the 26S proteasome, and 3) decreasing translation of additional proteins. If these responses are not enough to relieve the ER, or if the cause of stress is sustained, cells eventually succumb to death (Rutkowski and Kaufman, 2004; Rao et al., 2004; Ma and Hendershot, 2001).

In this work, we found genes involved in protein folding (HSPA9A, TOR3A, FKBP4, and HSPCA) to be upregulated in IFN-γ-iOLs. Numerous genes involved in ubiquination and proteolytic degradation of proteins were also highly upregulated in IFN-γ-treated iOLs, and to a lesser extent also in IFN-γ-treated mOLs. In particular, the cathepsin family of genes was upregulated in IFN-γ-iOLs, including CTSB and CTSS, which are involved in processing MHC class II antigen complexes. Additionally, gene expression of the poly (ADP-ribose) polymerases 9 and 10 (PARP9/10), along with the E3 ligase and Notch signaling gene DELTEX3 were strongly upregulated in both IFN-γ-treated cell populations.

Phosphorylation of eIF2α has been shown to inhibit translation in response to ER stress (Harding et al., 1999; Okada et al., 2002); whereas, PPP1R15B (CReP) inhibits the stress response by dephosphorylating eIF2α (Jousse et al., 2003). In these experiments, eIF2α message was increased in both IFN-γ-treated groups with higher expression in the immature population, and PPP1R15B was also upregulated in the immature cells. Since eIF2α phosphorylation has been shown to increase in response to IFN-γ (Lin et al., 2005), the upregulation of PPP1R15B could be a competing or feedback response. Other translation initiation factors, including eIF2C1, eIF4B1, eIF4E, and eIF4EBP2 were downregulated in IFN-γ-iOLs; and eIF2B1 expression was downregulated in IFN-γ-mOLs. Together, these data further support an IFN-γ-driven response to ER stress, particularly in immature OLs.

Differential Expression of Genes Involved in the Immune Response
(Figure 2.7 and Table 2.6)

In addition to complement activation and antigen presentation, IFN-γ treatment resulted in a significant increase in other immune response genes. Not surprisingly, expression levels of several genes for IFN-γ-inducible proteins, GTPases, transmembrane proteins, and binding proteins increased significantly in both IFN-γ-iOLs and IFN-γ-mOLs. Also increased significantly were GBP2, MX1 and MX2, which respond to viral infections; and CXCL10 and CXCL11, which have been shown to recruit CD4+ and CD8+ T cells in the CSF in other diseases and whose receptors are expressed on the surface of these cells (Lepej et al., 2005; Iijima et al., 2003). The FcIgG receptors, particularly FCGRIII, were also upregulated in both IFN-γ-treated populations. These pro-inflammatory receptors promote macrophage activation and cytokine release. In response to IFN-γ signaling, Janus tyrosine kinases

(JAKs) bind the IFN-γ-receptor and become phosphorylated. STAT1 molecules bind the phosphorylated JAKs, dissociate and translocate to the nucleus where they induce transcription of GAS element-containing genes. STAT-1 and STAT-2 showed robust upregulation in both IFN-γ-treated cell populations.

Differential Expression of Genes Involved in Oxidative Stress Response
(Figure 2.8 and Table 2.7)

We observed an increase in several genes that respond to reactive oxygen species (ROS) in IFN-γ-treated iOLs. Four transcription factor activators, NFE2L2, NFκB1, ATF-1 and TGM2 were all upregulated in IFN-γ-iOLs, and TGM2 was also unregulated in IFN-γ-mOLs. These transcription factors induce several antioxidant genes, including HMOX1, UGT1A6 and SOD2, which, along with the oxidase inhibitor CYBA, were also upregulated in the immature but not mature cultures treated with IFN-γ. GRP75 is a member of the heat shock protein family of chaperones and there is evidence to suggest that it may inhibit the accumulation of ROS (Liu et al., 2005). We observed an increase in GRP75 in IFN-γ-iOLs, but not IFN-γ-mOLs. In addition, FTL1, an iron transporter that is induced by oxidative stress and has a protective role against oxidative insults (Kim and Kim, 2002), was highly expressed in non-treated OLs at both stages of development, and more than doubled in cytokine-treated immature cells. TXN1, PRDX1 and PRDX4 are ROS scavengers. TXN1 and PRDX1 were upregulated, and PRDX4 was downregulated in IFN-γ-iOLs. None of these genes were differentially expressed in IFN-γ-mOLs. Overall, immature OLs appear to mount a stronger oxidative stress response than mature OLs.

Differential Expression of Genes Involved in Apoptosis
(Figure 2.9 and Table 2.8)

The events leading to and preventing programmed cell death, or apoptosis, are intricate. We have previously reported that developing OL cultures die by apoptosis after two days of IFN-γ exposure and that mature OLs withstand its effects for approximately four to seven days, at which point they die by necrosis (Baerwald and Popko, 1998). Accordingly, we found several genes involved in programmed cell death, both pro-apoptotic and survival, to be differentially expressed in response to IFN-γ exposure.

Pro-Apoptotic Gene Expression

Of the 34 genes involved in promoting apoptosis that were differentially regulated, two (IRAK and DAP) were slightly downregulated in IFN-γ-iOLs and two (NME3 and CIDEB) were slightly downregulated in IFN-γ-mOLs; all others were upregulated in response to IFN-γ. Most significantly upregulated in both populations was the IFN-γ-induced transcription factor IRF1, which as been shown to induce apoptosis via TRAIL (Park et al. 2004). Many of the upregulated apoptosis genes are involved in the extrinsic signaling pathways of FAS, TNF-α and IL-1, which result in caspase activation and DNA fragmentation. Intrinsic apoptosis-promoting molecules include ITM2, BTG1, DAPK3, CIDEB, PKCD and NDG2. In IFN-γ-iOLs, ITM2, BTG1, DAPK3, CIDEB and PKCD were strongly upregulated. ITM2 and NDG2 message was also increased in IFN-γ-mOLs, while CIDEB was decreased.

Survival Gene Expression

With the exception of IGF1, all survival genes with differential expression were upregulated in cytokine-treated immature OLs and seemed to stem largely from the induction of TRAF2BP, which activates NFκβ and PIM1, and PIM1 induces SOCS-1 (Fig 2.11(g-h)). The induction of SOCS-1 is interesting in that it is capable of binding phosphorylated JAKs interrupting JAK-STAT signaling and the subsequent transcription of IFN-γ-sensitive genes. In the mature cell population, IFN-γ again elicited a downregulation of IGF1, as well as an upregulation of PIM1, TRAF2BP, CCL2 and SOCS-1.

In agreement with previous observations, immature oligodendrocytes appeared more vulnerable to apoptosis by the overall greater upregulation of pro-apoptotic genes in response to IFN-γ. There was also a greater overall increase in survival genes in the immature cells, which perhaps reflects a concomitant protective defense response.

Differential Expression of Genes in Various Other Functional Groups
(Table 2.9)

It is clear from our data that IFN-γ treatment of developing and mature OLs elicits a diverse and complex response at the transcriptional level. Table 2.11 lists expression changes in genes involved in several cellular functions including cell adhesion; cell cycle; cell growth and metabolism; cell motility and cytoskeleton organization; protein synthesis, metabolism, and modification; development, differentiation, and proliferation; signal transduction; transcription, and translation regulation; and transport. While it is clear that IFN-γ affects the expression level of genes involved in many different functions, the effects are quite varied within most functional groups, and underscore the complexity of cytokine

signaling. Genes of particular interest based on degree of differential regulation and function are discussed below.

In IFN-γ-iOLs, certain cell adhesion genes that play a role in mediating T cell attachment to the endothelium were upregulated, including the integrins ITGA4 and ITGAL, which are necessary for T cell induction of EAE (Graesser et al., 2000). ITGAL was also upregulated in IFN-γ-mOLs. Neuropilin 1 (NRP1), which binds VEGF and mediates endothelium permeability, was upregulated in IFN-γ-iOLs.

A host of cell cycle regulating genes was differentially expressed in both immature and mature OLs treated with IFN-γ. Most notably was the robust upregulation of PBEF1, a gene that has not only been implicated in cell cycle regulation (Kitani et al., 2003), but also as a suppressor of apoptosis in response to inflammatory stimuli via inhibition of caspase-3 and caspase-8 (Jia et al., 2004).

Another large group of genes with differential regulation was those involved in cytoskeleton organization. There were moderate, varied responses from several genes, but most significantly upregulated were coronin actin-binding genes, microtubule-associated and neurofilament genes, myosin, pleckstrin, and especially matrix Gla protein (MGP). MGP is generally associated with bone formation, but it is also upregulated by T3 and TGFβ (Sato et al., 2005; Bostrom et al., 2004). The developing OL cultures used in these experiments were treated with T3 to facilitate differentiation, and in this study TGFβ expression did not change in IFN-γ-iOLs and decreased in IFN-γ-mOLs. It would seem, therefore, that MGP is also upregulated by IFN-γ and perhaps plays a role in the cytoskeletal changes necessary for process extension by maturing OLs.

The development-associated gene TNFAIP2 displayed robust upregulation in both IFN-γ-treated groups. Additionally, estrogen-responsive finger protein (EFP, TRIM25) was strongly upregulated in IFN-γ-mOLs, and its expression was nearly twice as high in IFN-γ-iOLs. EFP responds to estrogen and has been implicated in cell proliferation associated with breast cancer (Suzuki et al., 2005). Another gene product, VDUP1, inhibits proliferation by arresting cell cycle progression, and its expression was downregulated in both IFN-γ-iOLs and IFN-γ-mOLs.

Numerous signal transduction genes were differentially regulated in both IFN-γ-treated cell populations. The most significant change was the upregulation of a sequence similar to interferon-inducible GTPase designated RGD1309362. Lymphocyte cytosolic protein 2 (LCP2, SLP-76), which plays a role in mediating T cell function (Kumar et al., 2005), increased substantially in cytokine-treated immature, but not mature OLs.

Equally abundant were differentially expressed transcription regulation genes. In particular, STAT-1 and STAT-2 message (discussed in the immune response section) was greatly increased in IFN-γ-mOLs, and even more so in IFN-γ-iOLs. Likewise, there was an upregulation of the interferon stimulated gene factor ISGF3G in both IFN-γ-treated groups. Upon stimulation by Type I or Type II interferon, STAT-1, STAT-2 and ISGF3G form a complex and translocate to the nucleus. STAT molecules are dephosphorylated once inside the nucleus, then shuttled back out into the cytoplasm via nucleoporins 153 and 214 (NUP153, NUP214) as well as exportin 1 (XPO1) (Zimmerman et al., 2005; Marg et al., 2004). Neither of the nucleoporins was represented on the arrays, but XPO1 showed a slight decrease at both time points.

Numerous ESTs were also differentially regulated in both immature and mature OLs treated with IFN-γ. For reference, these sequences along with their fold change values are listed in Table 2.10.

CONCLUSION

Rat primary immature and mature oligodendrocyte cultures were treated with the pro-inflammatory cytokine IFN-γ, and the transcriptional response was quantitated using microarray analysis. It is clear from our data that IFN-γ elicits a dramatic immune response. The most significant differential regulation in both cytokine-treated immature and mature oligodendrocytes was seen in antigen processing and presenting genes, followed by genes that activate complement via the classical pathway. We also observed significant differential expression of genes involved in consequential events of MHC induction and complement activation, including response to ER stress, ROS accumulation, and apoptosis. Moreover, there was an overall greater response from immature than mature OLs exposed to IFN-γ, possibly rendering immature OLs more vulnerable to the detrimental effects of this cytokine.

Figure 2.1 Expression of lineage-specific markers in oligodendrocyte cultures. Panels a-b: oligodendrocyte progenitor cells; panels c-d: mature oligodendrocytes. OPCs isolated from neonatal rat forebrain were maintained in defined medium containing OPC mitogens PDGF-α and FGF2, while mature oligodendrocytes were derived from OPCs by culturing cells for 72 hrs in defined medium containing T3 and insulin (see Materials and Methods). Panel e: the numbers (percent) of cells expressing either progenitor or mature oligodendrocyte markers under either condition. OPC cultures (orange bars) contained >80% A2B5, 97% NG2-progenitors with 7% O1-oligodendrocytes and <2% GFAP-astrocytes (n=624 cells counted). OL cultures contained >90% O1-oligodendrocytes with <10% O4, GFAP-astrocytes (n=368 cells counted). Coverslips for immune cytochemistry were harvested from the same culture plates used to generate RNA for microarray analysis.

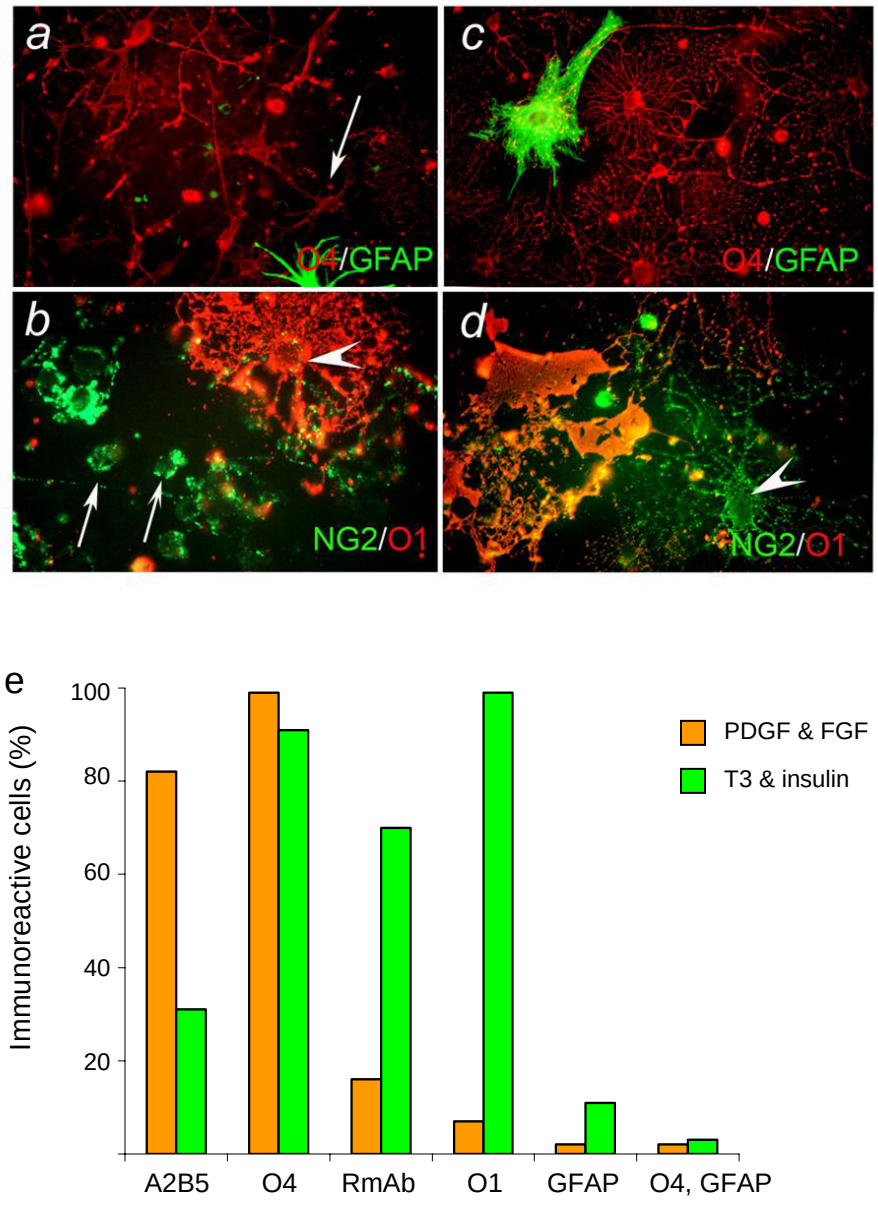

Figure 2.2 Expression Estimates of Genes Involved in Myelin Formation. a-b) Gene symbols and Accession numbers are plotted on the x-axis; the average of replicate normalized expression values for each treatment group (as described in Materials and Methods) is plotted on the y-axis. In some cases, a gene is represented on the microarray set more than once by different accession numbers. Fold change values for genes in a-b) are listed in Table 2.1.

a.

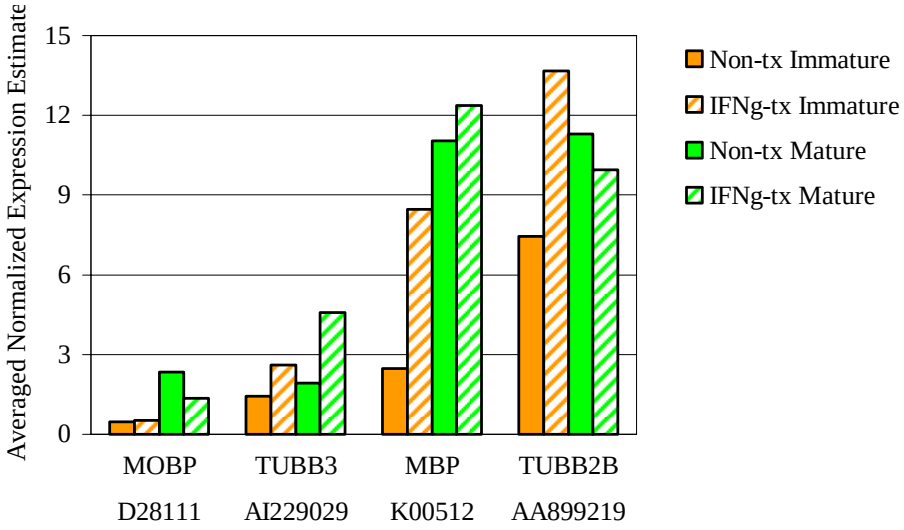

b.

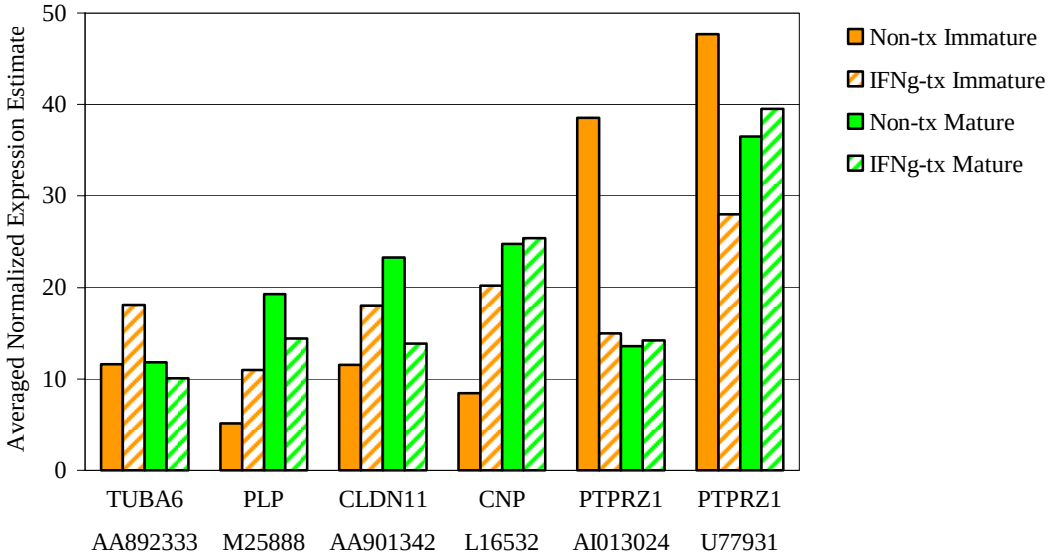

Table 2.1 Differential Expression of Genes Involved in Myelin Formation. Replicate RNA samples from each treatment group were hybridized to separate arrays. The average of replicate normalized expression estimates for each sample group was used to calculate the fold change difference in expression for each gene in Figure 2.2. Positive fold change values indicate an increase, and negative values indicate a decrease in gene expression in the IFNγ-treated groups. The dagger indicates the Student's t-test p-value was greater than 0.1; the asterisk indicates there was one sample for each treatment.

			Fold Change (IFN-γ-tx OLs / Non-tx OLs)	
Accession No.	Gene Symbol	Gene Name	Immature	Mature
AA901342	CLDN11	claudin 11	1.56	-1.68*
L16532	CNP	2',3'-cyclic nucleotide 3'-phosphodiesterase	2.38	1.03†
K00512	MBP	myelin basic protein	3.43	1.12†
D28111	MOBP	myelin-associated oligodendrocytic basic protein	1.02	-1.50
M25888	PLP	proteolipid protein	2.14	-1.34†
AI013024	PTPRZ1	protein tyrosine phosphatase, receptor type Z, polypeptide 1	-2.57	1.05*
U77931	PTPRZ1	protein tyrosine phosphatase, receptor type Z, polypeptide 1	-1.70	1.08†
AA892333	TUBA6	tubulin, alpha 6	1.55	-1.17†
AA899219	TUBB2B	tubulin, beta 2b	1.84	-1.14*
AI229029	TUBB3	tubulin, beta 3	1.83	2.37*

Figure 2.3 Expression Estimates of Genes Involved in Cholesterol Biosynthesis. a) Cholesterol biosynthetic pathway: Genes highlighted in yellow are upregulated and genes highlighted in green are downregulated in one or both IFN-γ-treated cultures. b) Gene symbols and Accession numbers are plotted on the x-axis; the average of replicate normalized expression values for each treatment group (as described in Materials and Methods) is plotted on the y-axis. In some cases, a gene was represented on the microarray set more than once by different accession numbers. Multiple accession numbers for a single gene have been graphed separately to provide replicate information for fold change values with a Student's t-test p-value greater than 0.1 or only one sample for each treatment group. Fold change values for genes in b) are listed in Table 2.2.

a.

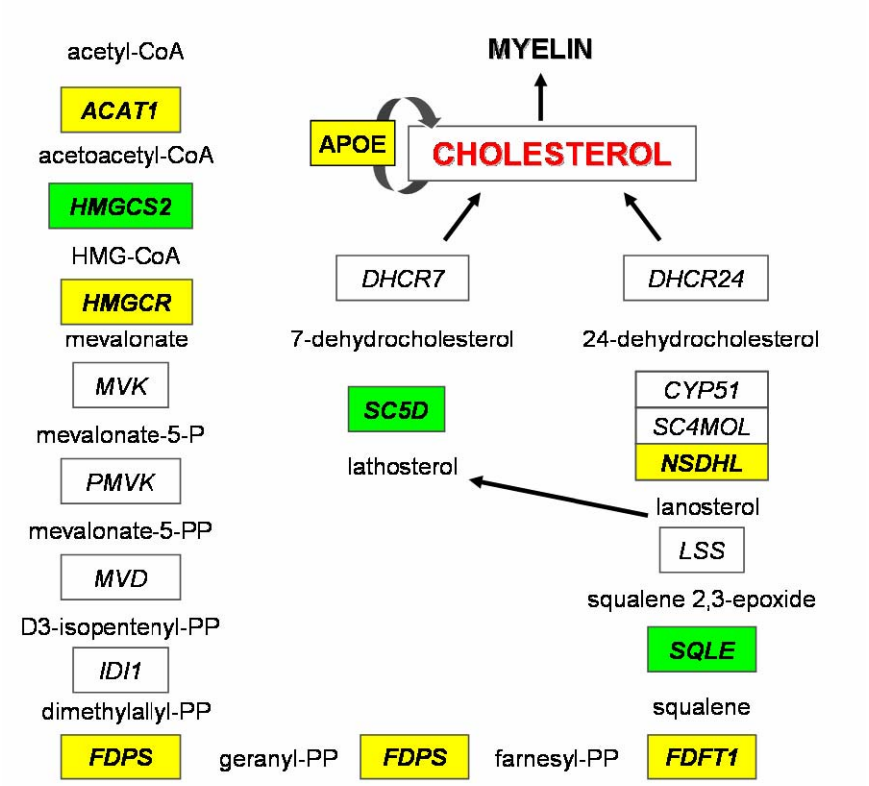

Figure 2.3 Expression Estimates of Genes Involved in Cholesterol Biosynthesis.

b.

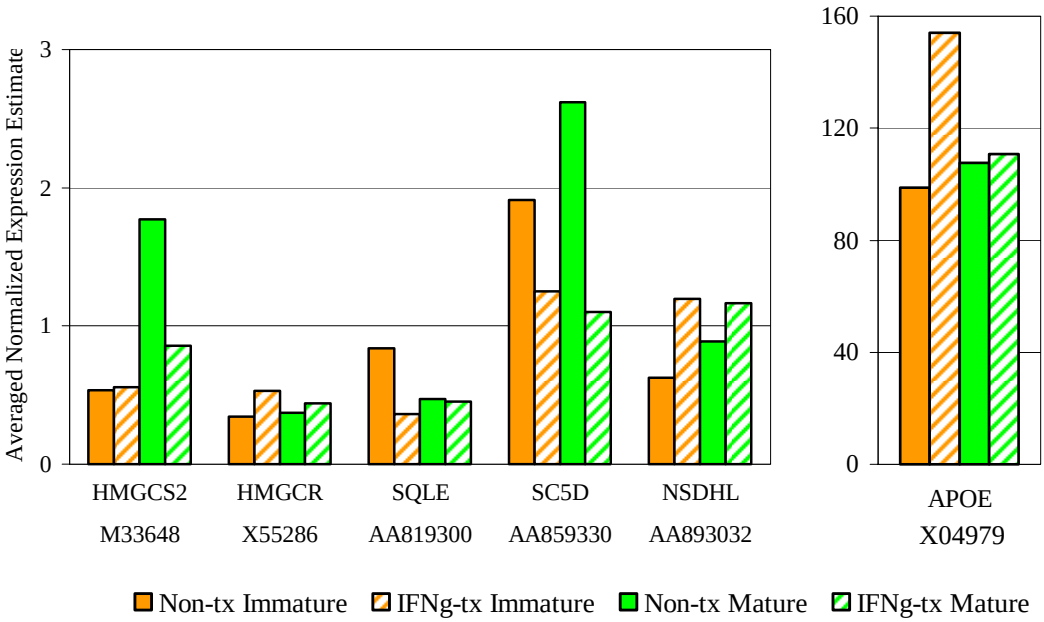

Table 2.2 Differential Expression of Genes Involved in Cholesterol Biosynthesis. Replicate RNA samples from each treatment group were hybridized to separate arrays. The average of replicate normalized expression estimates for each sample group was used to calculate the fold change difference in expression for each gene in Figure 2.3. Positive fold change values indicate an increase, and negative values indicate a decrease in gene expression in the IFNγ-treated groups. The dagger indicates the Student's t-test p-value was greater than 0.1; the asterisk indicates there was one sample for each treatment.

			Fold Change (IFN-γ-tx OLs / Non-tx OLs)	
Accession No.	Gene Symbol	Gene Name	Immature	Mature
D13921	ACAT1	acetyl-CoA acetyltransferase 1	1.92†	-1.09†
X04979	APOE	apolipoprotein E	2.13	1.09
M95591	FDFT1	farnesyl diphosphate farnesyl transferase 1	1.69†	-1.14†
M89945	FDPS	farnesyl diphosphate synthase	1.84†	-1.06†
X55286	HMGCR	3-hydroxy-3-methylglutaryl-CoA reductase	1.54	1.18†
M33648	HMGCS2	3-hydroxy-3-methylglutaryl-CoA synthase 2	1.05†	-2.07
U31352	LSS	lanosterol synthase	1.32	-1.02†
U53706	MVD	mevalonate (diphospho) decarboxylase	1.48†	-1.03†
M29472	MVK	mevalonate kinase	1.40†	-1.21
AA893032	NSDHL	NAD(P) dependent steroid dehydrogenase-like	1.91	1.31†
AA859330	SC5D	sterol-C5-desaturase	-1.53†	-2.37*
AA819300	SQLE	squalene epoxidase	-2.30	-1.03*

Figure 2.4 Expression Estimates of Genes Involved in Lipid Metabolism. a-f) Gene symbols and Accession numbers are plotted on the x-axis; the average of replicate normalized expression values for each treatment group (as described in Materials and Methods) is plotted on the y-axis. In some cases, a gene is represented on the microarray set more than once by different accession numbers. Fold change values for genes in a-f) are listed in Table 2.3.

a.

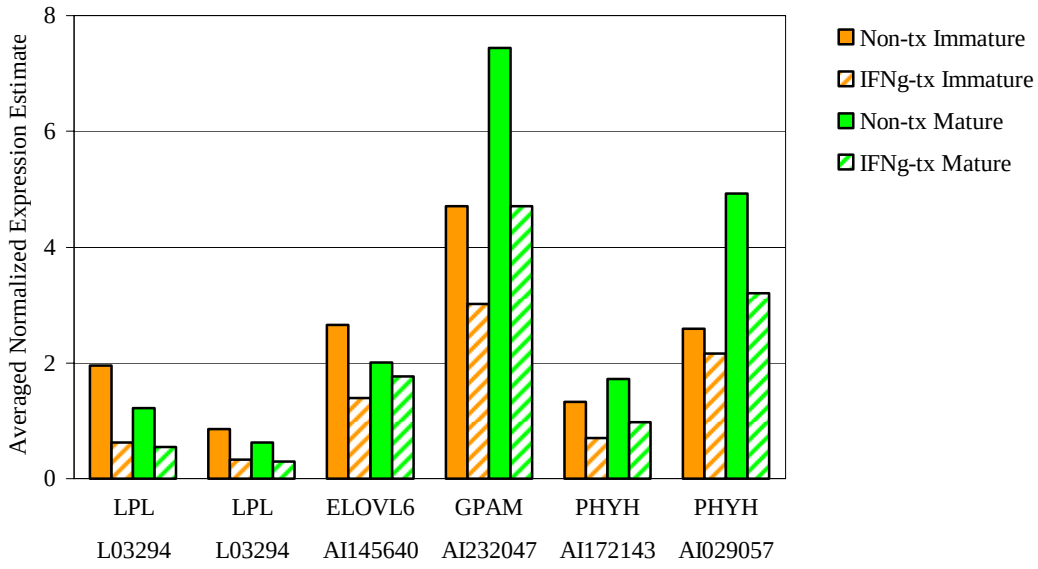

b.

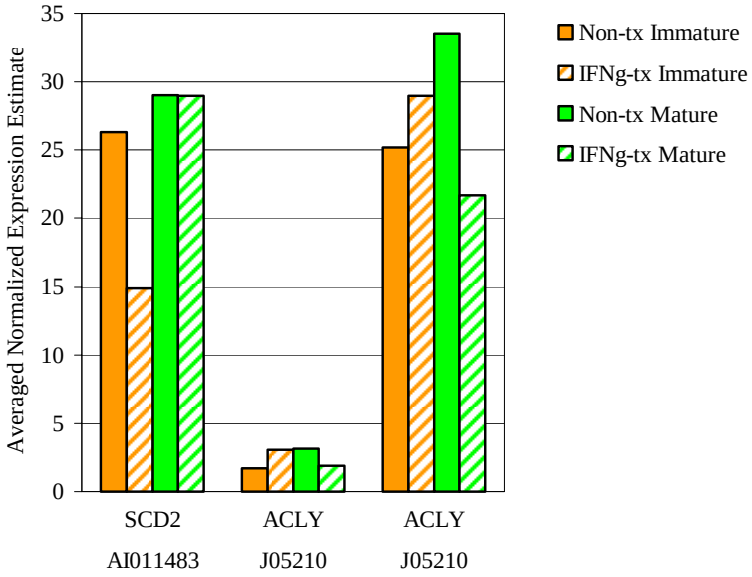

Figure 2.4 Expression Estimates of Genes Involved in Lipid Metabolism.

c.

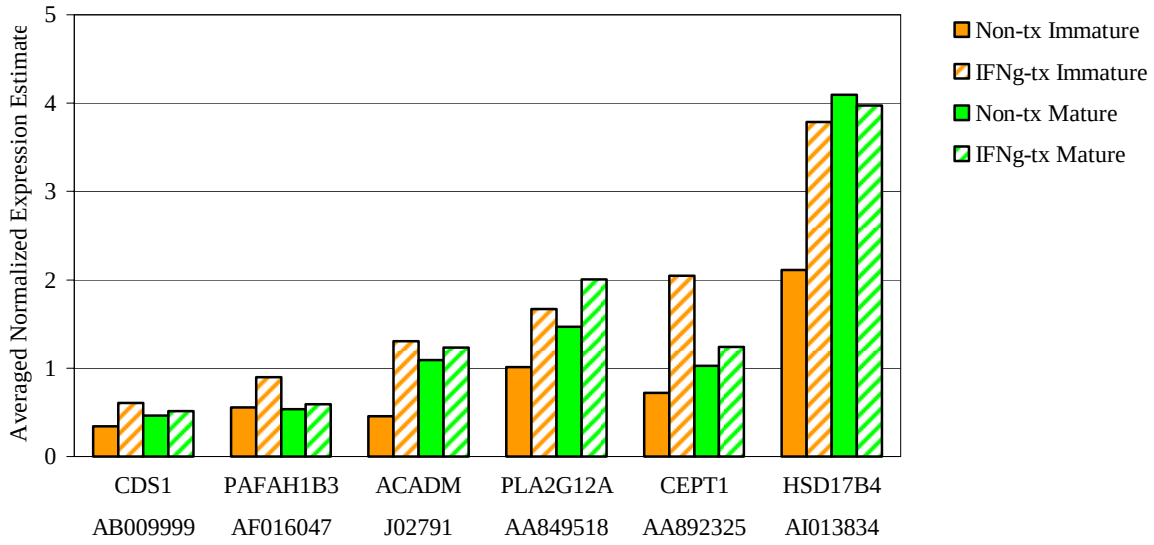

d.

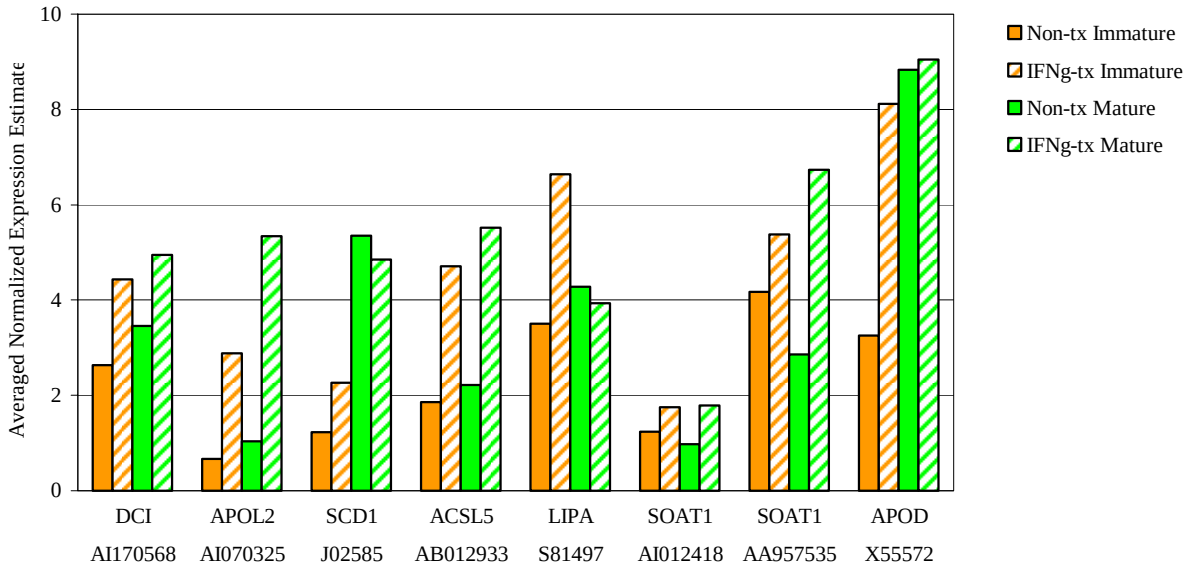

Figure 2.4 Expression Estimates of Genes Involved in Lipid Metabolism.

e.

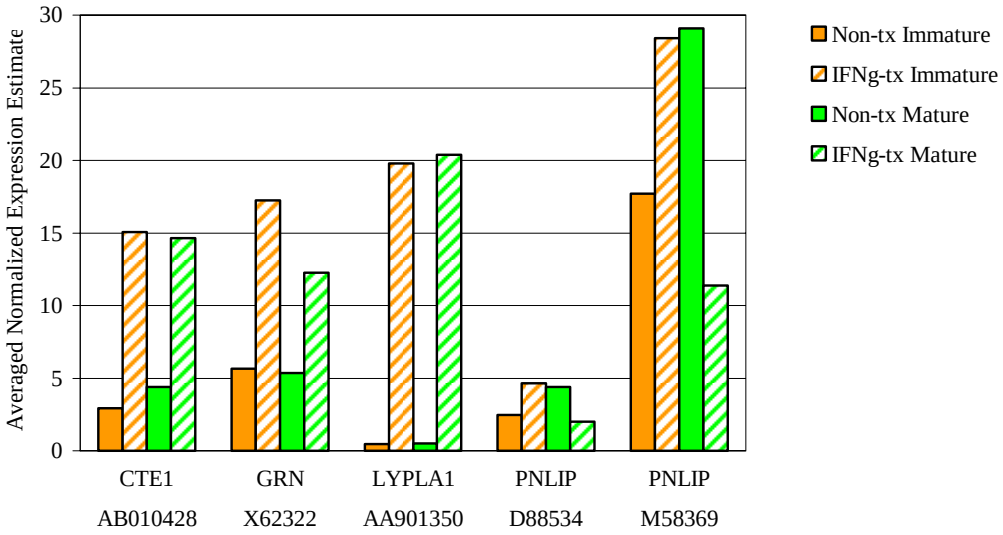

f.

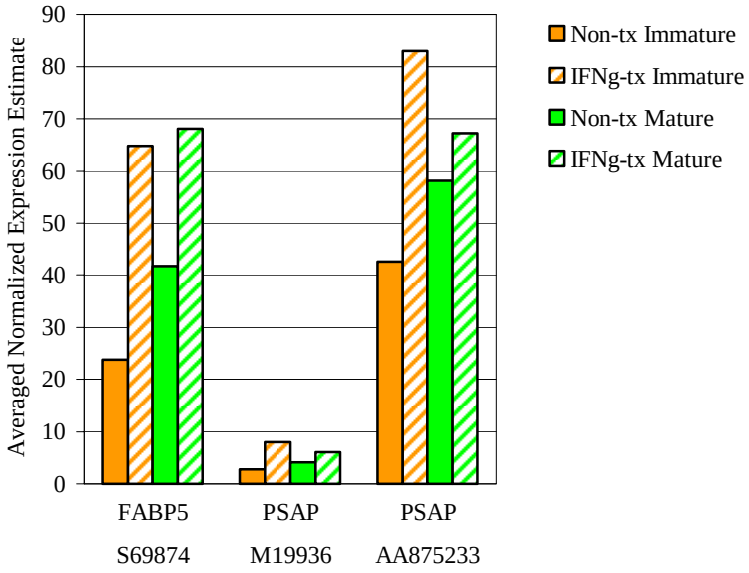

Table 2.3 Differential Expression of Genes Involved in Lipid Metabolism. Replicate RNA samples from each treatment group were hybridized to separate arrays. The average of replicate normalized expression estimates for each sample group was used to calculate the fold change difference in expression for each gene in Figure 2.4. Positive fold change values indicate an increase, and negative values indicate a decrease in gene expression in the IFNγ-treated groups. The dagger indicates the Student's t-test p-value was greater than 0.1; the asterisk indicates there was one sample for each treatment.

			Fold Change (IFN-γ-tx OLs / Non-tx OLs)	
Accession No.	Gene Symbol	Gene Name	Immature	Mature
J02791	ACADM	acetyl-CoA dehydrogenase, medium	2.85	1.13†
J05210	ACLY	ATP citrate lyase	1.15†	-1.55
J05210	ACLY	ATP citrate lyase	1.77†	-1.67
AB012933	ACSL5	acyl-CoA synthetase long-chain family member 5	2.54	2.48
X55572	APOD	apolipoprotein D	2.50	1.02†
AI070325	APOL2	apolipoprotein L2	4.30	5.13*
AB009999	CDS1	CDP-diacylglycerol synthase 1	1.79	1.12†
AA892325	CEPT1	choline/ethanolaminephosphotransferase 1	2.84	1.21†
AB010428	CTE1	acyl-CoA hydrolase, cytosolic	5.18	3.33
AI170568	DCI	dodecenoyl-coenzyme A delta isomerase	1.69	1.43†
AI145640	ELOVL6	elongation of long chain fatty acids, member 6	-1.90	-1.14*
S69874	FABP5	fatty acid binding protein 5	2.72	1.63
AI232047	GPAM	glycerol-3-phosphate acyltransferase, mitochondrial	-1.56	-1.58*
X62322	GRN	granulin	3.05	2.29
AI013834	HSD17B4	17-beta hydroxysteroid dehydrogenase 4	1.80	-1.03†
S81497	LIPA	lipase A, lysosomal acid	1.89	-1.09†
L03294	LPL	lipoprotein lipase	-3.10†	-2.25
L03294	LPL	lipoprotein lipase	-2.61†	-2.08
AA901350	LYPLA1	lysophospholipase	42.6	40.8*
AF016047	PAFAH1B3	platelet-activating factor acetylhydrolase, isoform 1b, alpha1 subunit	1.62	1.12†

Accession No.	Gene Symbol	Gene Name	Fold Change (IFN-γ-tx OLs / Non-tx OLs) Immature	Mature
AI172143	PHYH	phytanoyl-CoA hydroxylase	-1.89	-1.76*
AI029057	PHYH	phytanoyl-CoA hydroxylase	-1.20	-1.53*
AA849518	PLA2G12A	phospholipase A2, group XIIA	1.64	1.36*
D88534	PNLIP	pancreatic triglyceride lipase	1.88	-2.21
M58369	PNLIP	pancreatic triglyceride lipase	1.61	-2.55
M19936	PSAP	prosaposin	2.91	1.47†
AA875233	PSAP	prosaposin	1.95	1.16†
J02585	SCD1	stearoyl-Coenzyme A desaturase 1	1.83	-1.10†
AI011483	SCD2	stearoyl-Coenzyme A desaturase 2	-1.77	1.00*
AI012418	SOAT1	sterol O-acyltransferase 1	1.41	1.83*
AA957535	SOAT1	sterol O-acyltransferase 1	1.29	2.35*

Figure 2.5 Expression Estimates of Genes Involved in Complement Activation. a) Genes highlighted in yellow are upregulated and genes highlighted in green are downregulated in one or both IFN-γ-treated cultures. b-c) Gene symbols and Accession numbers are plotted on the x-axis; the average of replicate normalized expression values for each treatment group (as described in Materials and Methods) is plotted on the y-axis. In some cases, a gene was represented on the microarray set more than once by different accession numbers. Multiple accession numbers for a single gene have been graphed separately to provide replicate information for fold change values with a Student's t-test p-value greater than 0.1 or only one sample for each treatment group. Fold change values for genes in b-c) are listed in Table 2.4.

a.

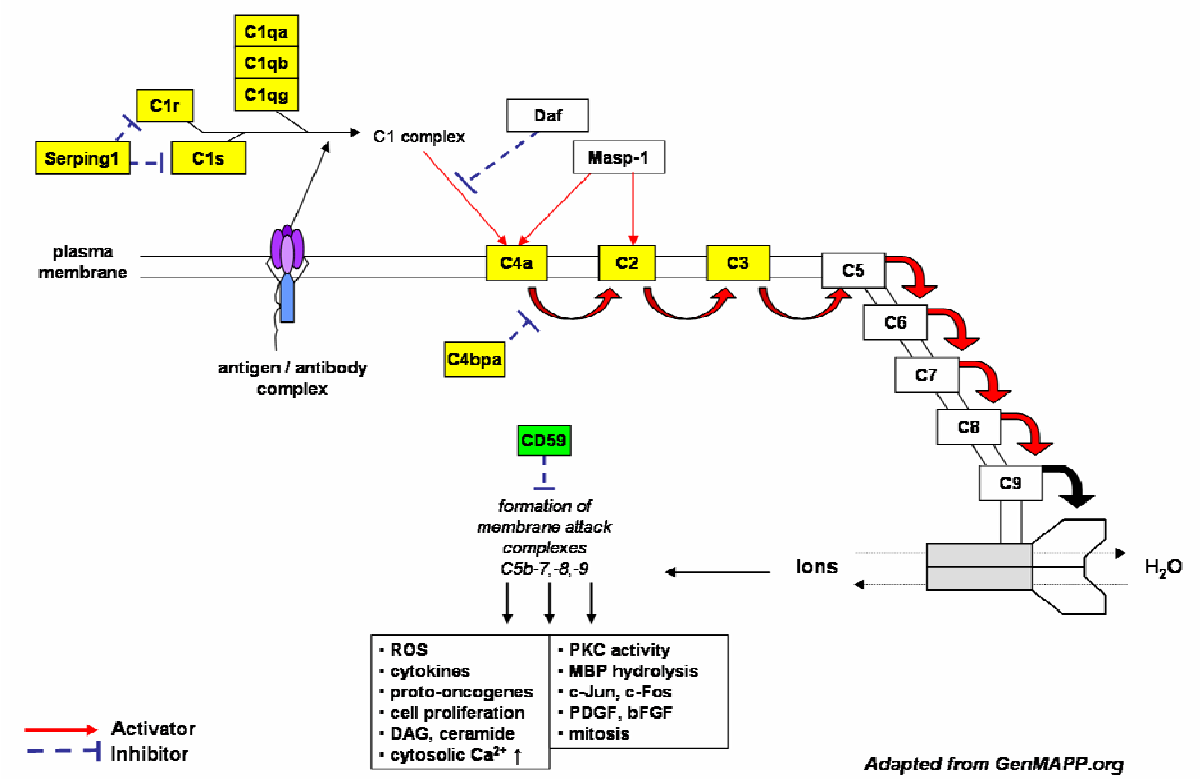

Figure 2.5 Expression Estimates of Genes Involved in Complement Activation.

b.

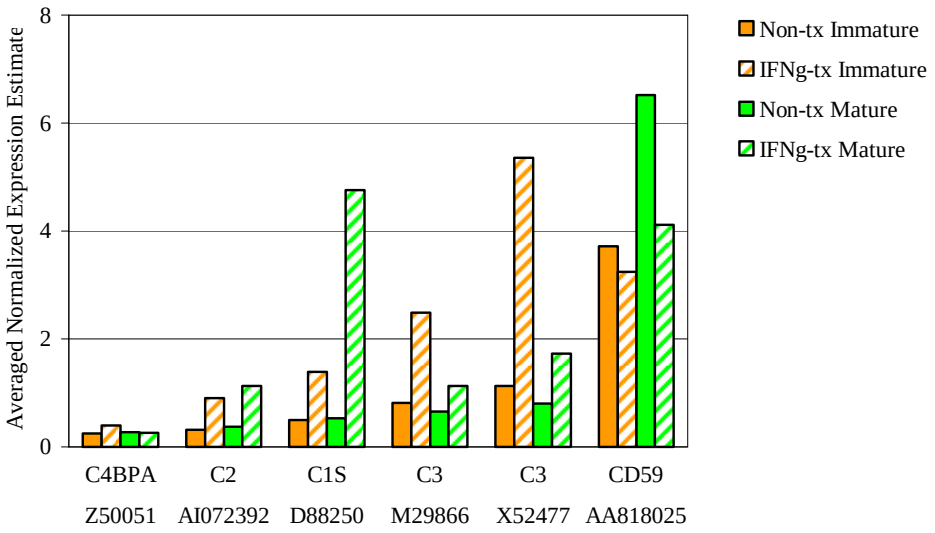

c.

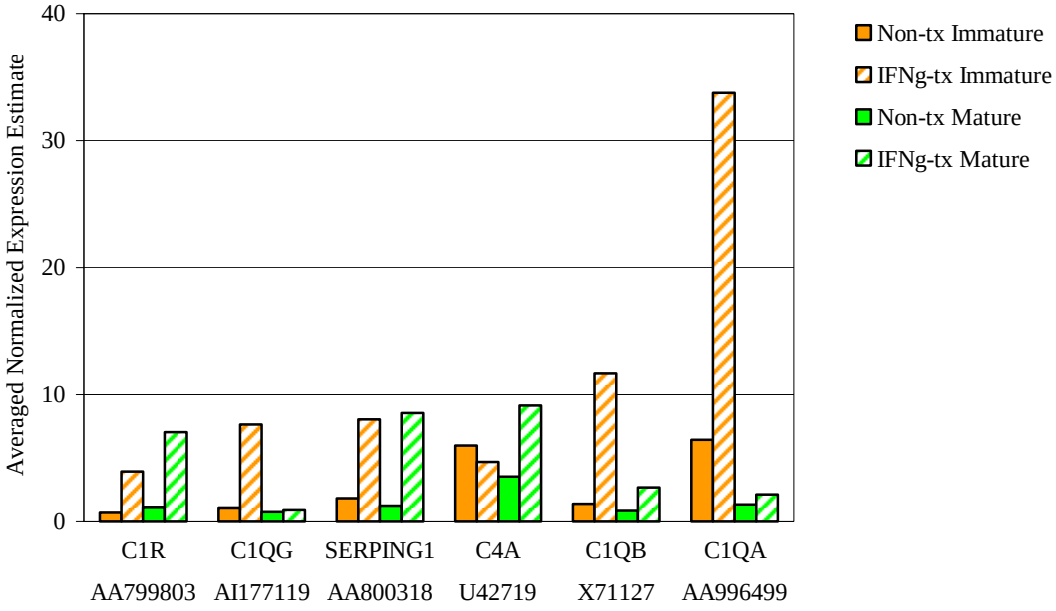

Table 2.4 Differential Expression of Genes Involved in Complement Activation. Replicate RNA samples from each treatment group were hybridized to separate arrays. The average of replicate normalized expression estimates for each sample group was used to calculate the fold change difference in expression for each gene in Figure 2.5. Positive fold change values indicate an increase, and negative values indicate a decrease in gene expression in the IFNγ-treated groups. The dagger indicates the Student's t-test p-value was greater than 0.1; the asterisk indicates there was one sample for each treatment.

			Fold Change (IFN-γ-tx OLs / Non-tx OLs)	
Accession No.	Gene Symbol	Gene Name	Immature	Mature
AA996499	C1QA	complement component 1, q subcomponent, alpha polypeptide	5.27	1.64*
X71127	C1QB	complement component 1, q subcomponent, beta polypeptide	8.65	3.20†
AI177119	C1QG	complement component 1, q subcomponent, gamma polypeptide	7.31	1.26*
AA799803	C1R	complement component 1, r subcomponent	5.39	6.47
D88250	C1S	complement component 1, s subcomponent	2.79	9.03†
AI072392	C2	complement component 2	2.85	3.03*
M29866	C3	complement component 3	3.04	1.73†
X52477	C3	complement component 3	4.74†	2.15†
U42719	C4A	C4 complement protein, palmitoyl-protein thioesterase 2	-1.28†	2.60
Z50051	C4BPA	complement component 4 binding protein, alpha	1.60	-1.02†
AA818025	CD59	CD59 antigen	-1.15†	-1.59
AA800318	SERPING1	serine (or cysteine) proteinase inhibitor, clade G (C1 inhibitor), member 1	4.44	7.09

Figure 2.6 Expression Estimates of Genes Involved in Antigen Processing and Presentation. a-o) Antigen processing and presentation genes and representative Accession numbers are plotted on the x-axis; the average of replicate normalized expression values for each treatment group (as described in Materials and Methods) is plotted on the y-axis. In some cases, a gene is represented on the microarray set more than once by different accession numbers. Multiple accession numbers for a single gene have been graphed separately to provide replicate information for fold change values with a Student's t-test p-value greater than 0.1 or only one sample for each treatment group. Fold change values for genes in a-o) are listed in Table 2.5.

a.

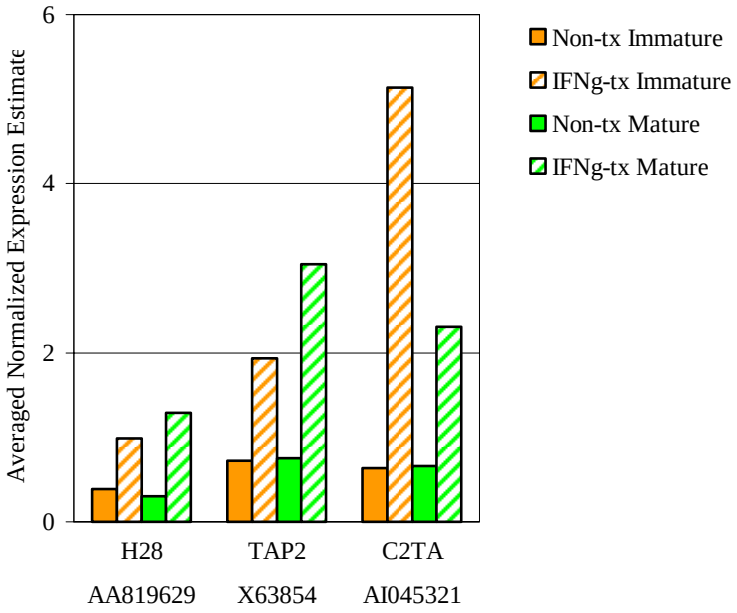

Figure 2.6 Expression Estimates of Genes Involved in Antigen Processing and Presentation.

b.

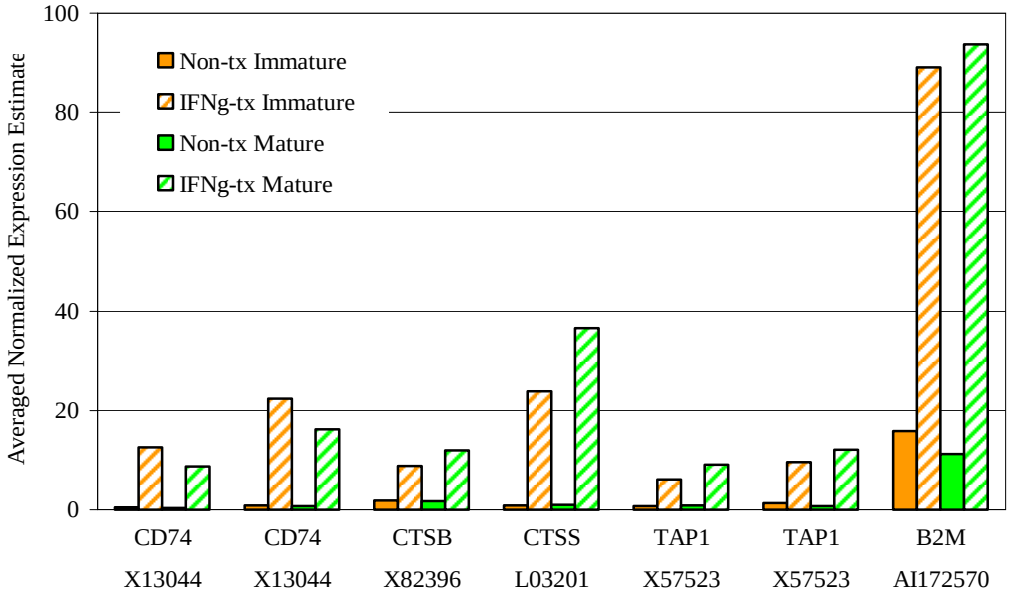

c.

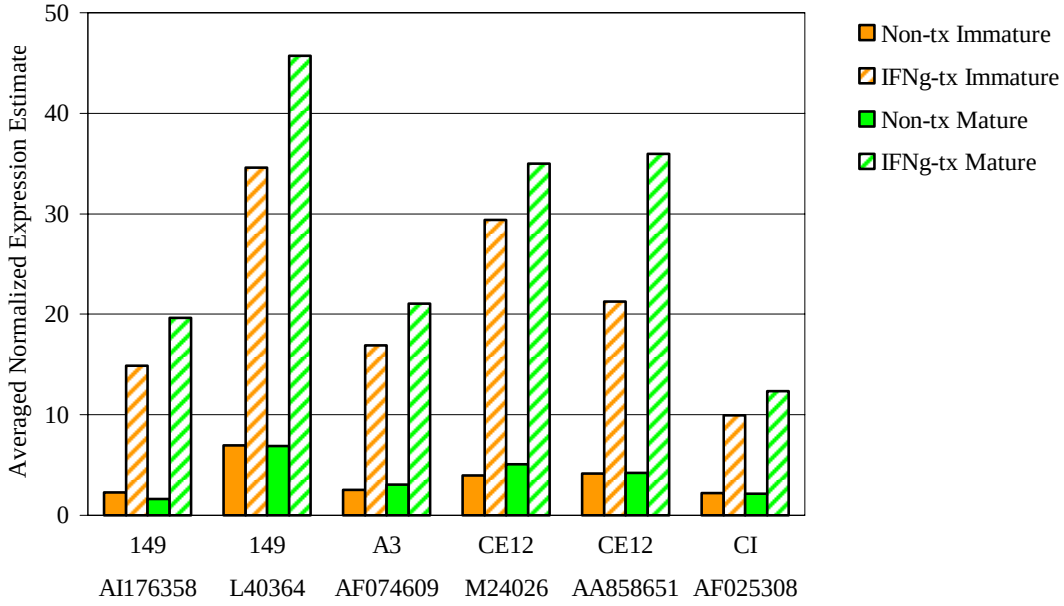

Figure 2.6 Expression Estimates of Genes Involved in Antigen Processing and Presentation.

d.

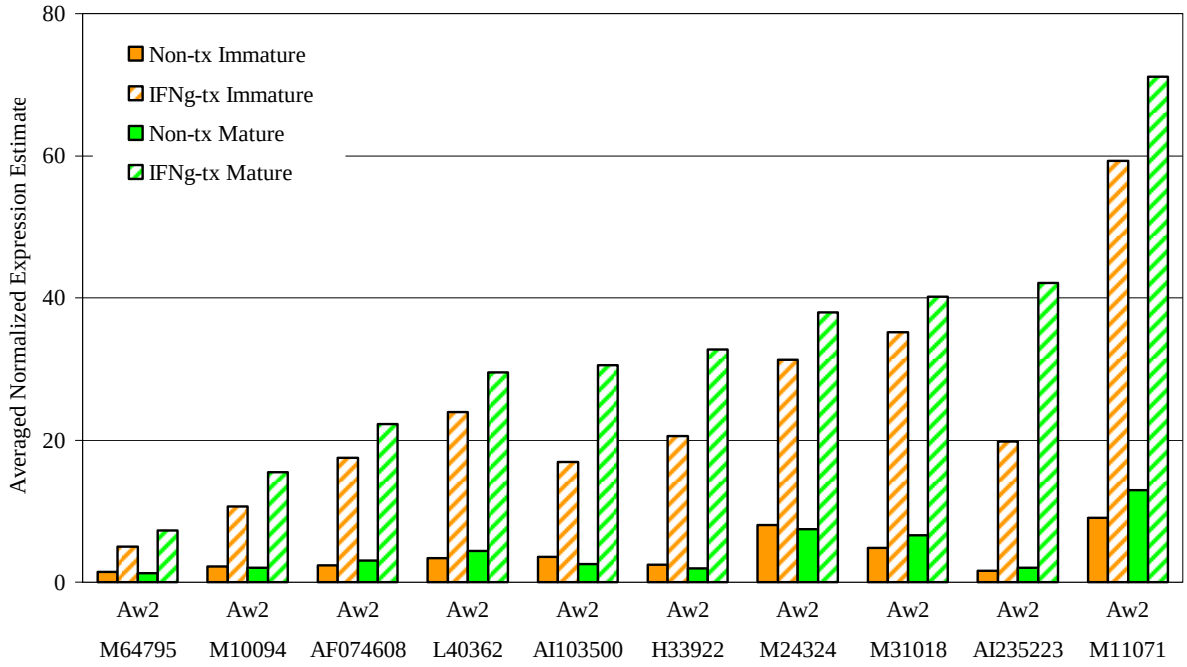

e.

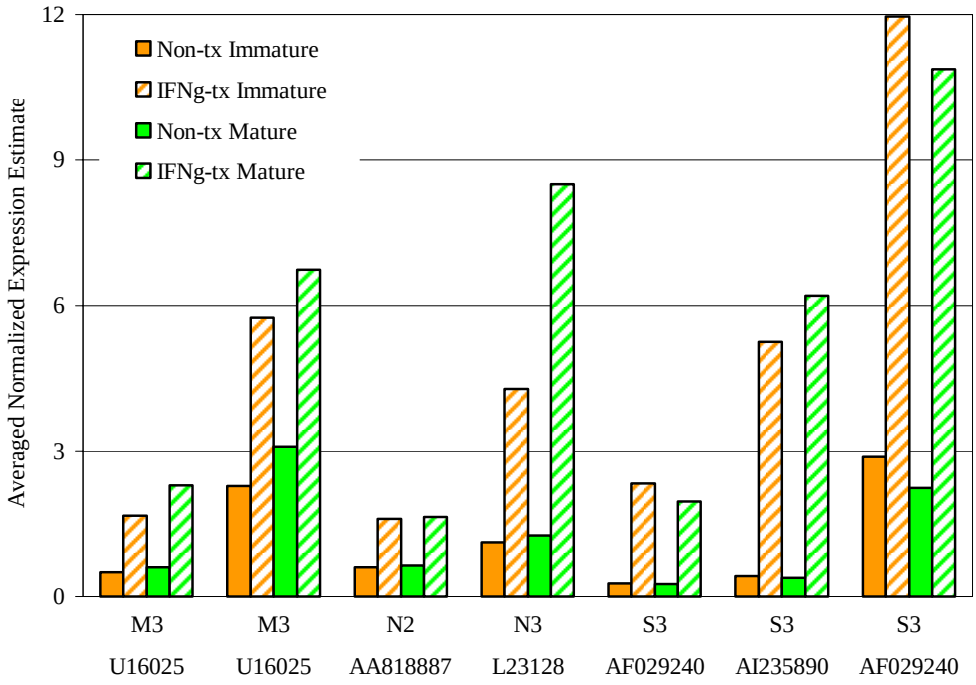

Figure 2.6 Expression Estimates of Genes Involved in Antigen Processing and Presentation.

f.

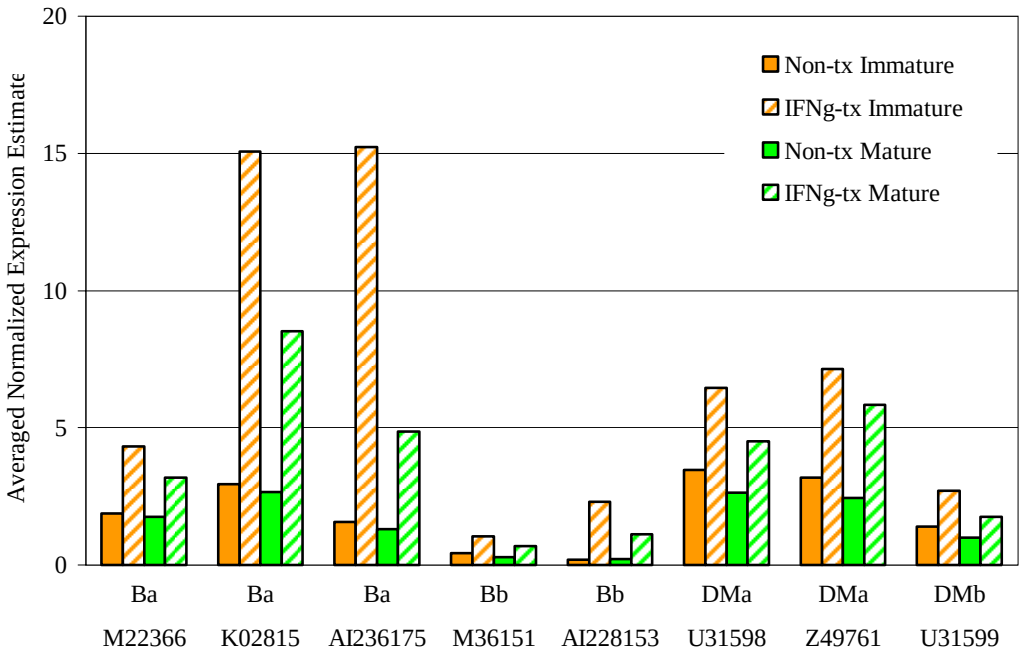

g.

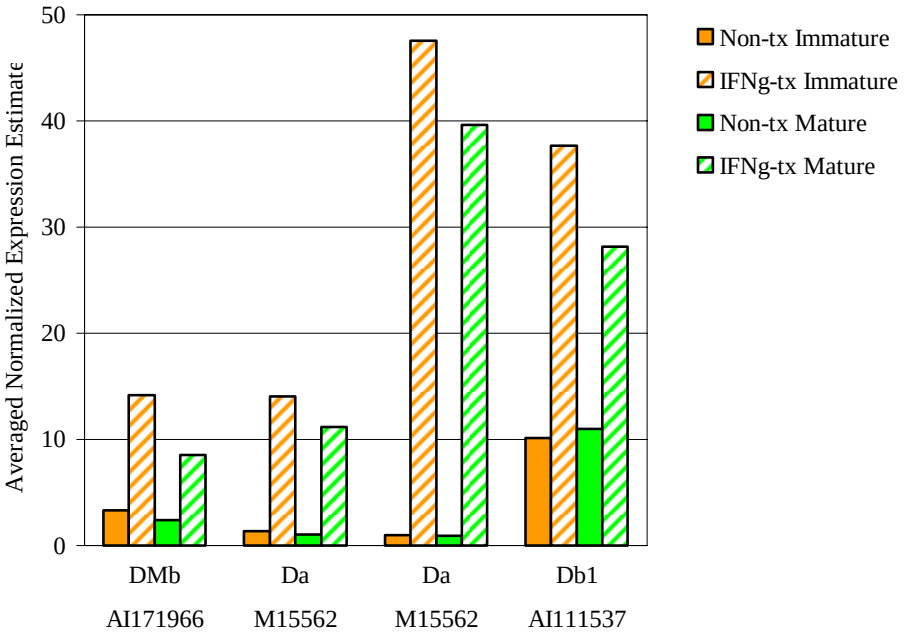

Figure 2.6 Expression Estimates of Genes Involved in Antigen Processing and Presentation.

h.

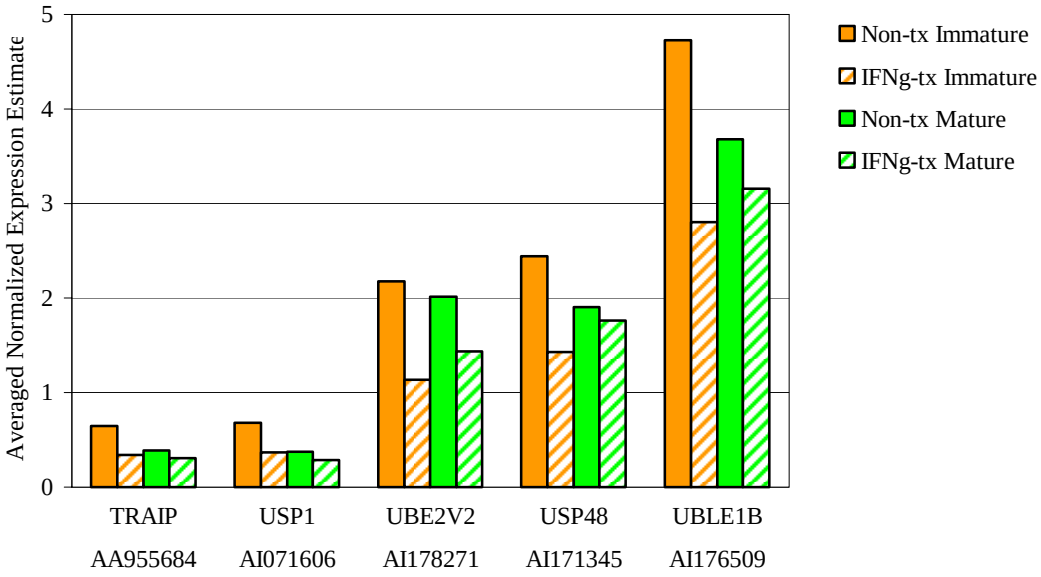

i.

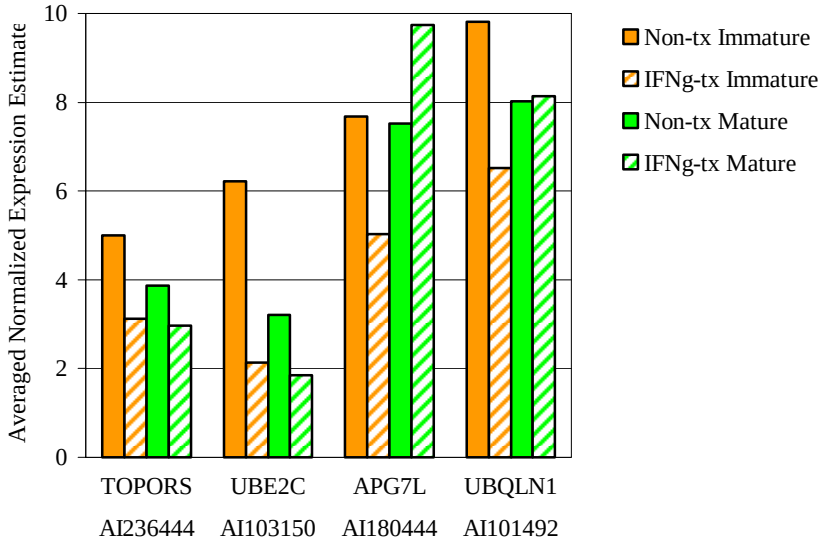

Figure 2.6 Expression Estimates of Genes Involved in Antigen Processing and Presentation.

j.

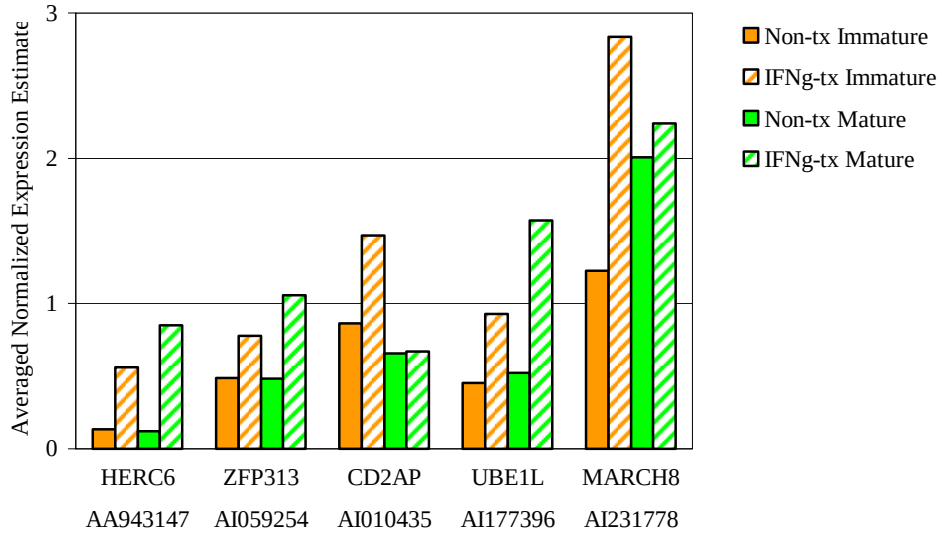

k.

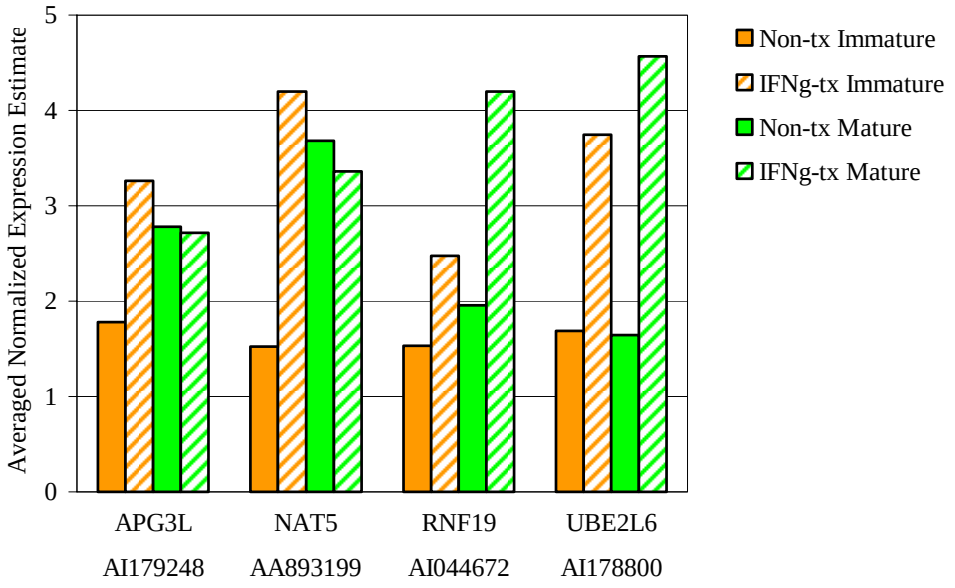

Figure 2.6 Expression Estimates of Genes Involved in Antigen Processing and Presentation.

l.

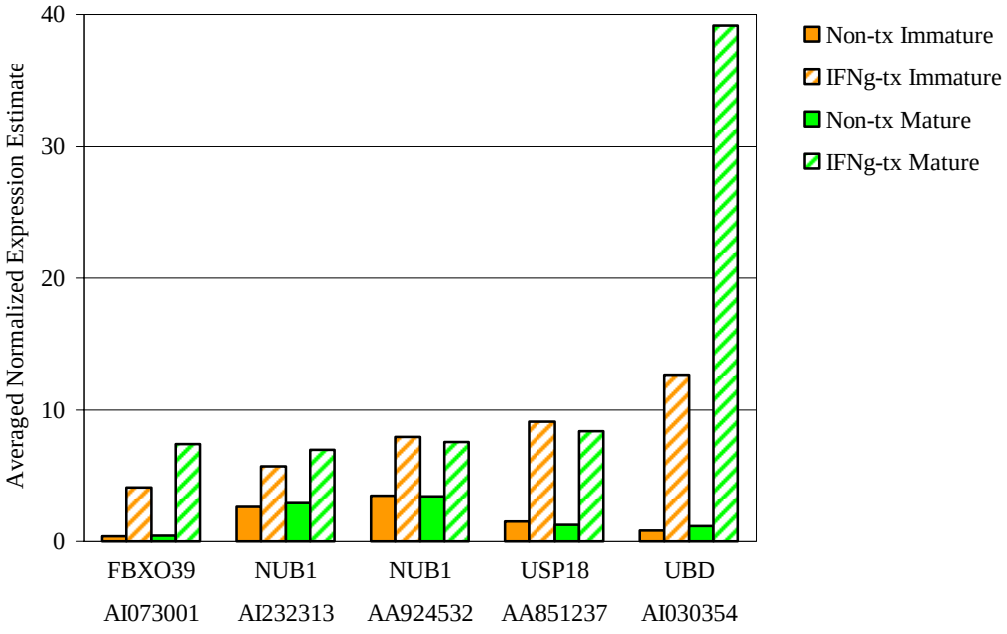

m.

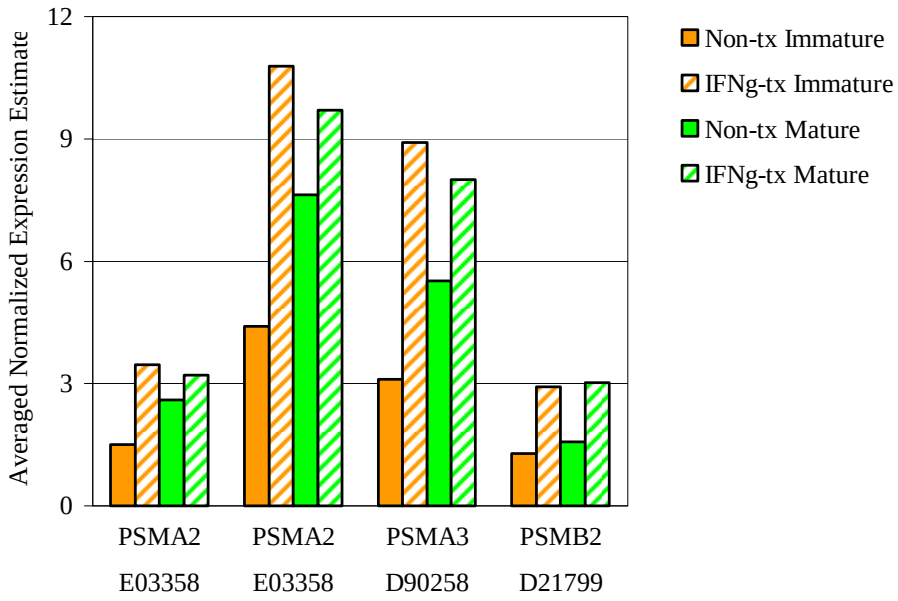

Figure 2.6 Expression Estimates of Genes Involved in Antigen Processing and Presentation.

n.

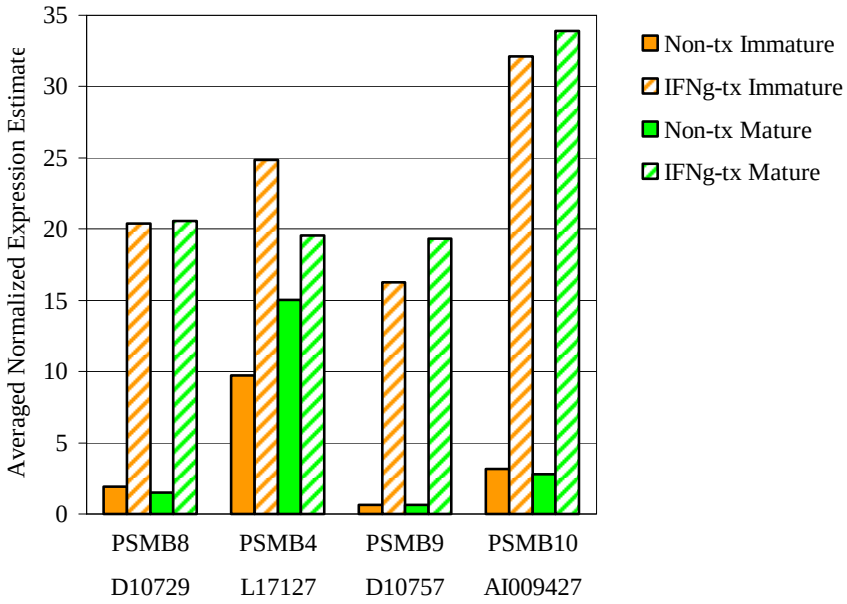

o.

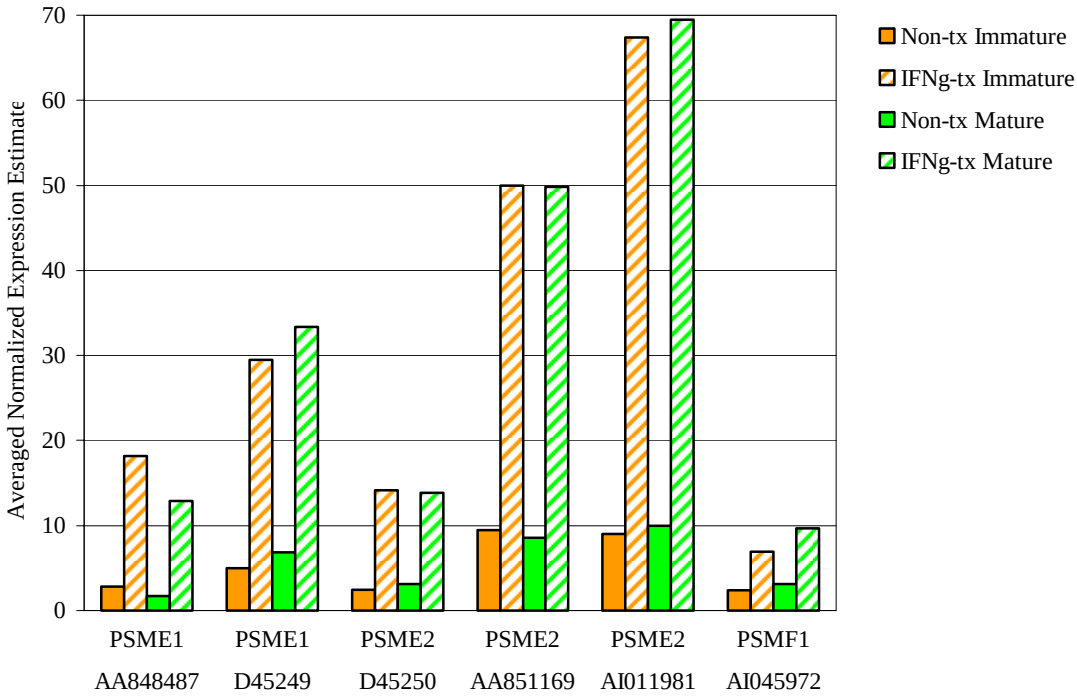

Table 2.5 Differential Expression of Genes Involved in Antigen Processing and Presentation. Replicate RNA samples from each treatment group were hybridized to separate arrays. The average of replicate normalized expression estimates for each sample group was used to calculate the fold change difference in expression for each gene in Figure 2.6. Positive fold change values indicate an increase, and negative values indicate a decrease in gene expression in the IFNγ-treated groups. The dagger indicates the Student's t-test p-value was greater than 0.1; the asterisk indicates there was one sample for each treatment.

			Fold Change (IFN-γ-tx OLs / Non-tx OLs)	
Accession No.	Gene Symbol	Gene Name	Immature	Mature
MHC class I presentation				
AI172570	B2M	beta-2 microglobulin	8.18	10.7*
AA848811	B2M	beta-2 microglobulin	7.05	15.3*
AA848811	B2M	beta-2 microglobulin	5.64	8.40*
AA819629	H28	histocompatibility 28	2.54	4.29*
AI176358	RT1-149	RT1 class I, type 149	6.62	12.1*
L40364	RT1-149	RT1 class I, type 149	4.98	6.66
AF074609	RT1-A3	RT1 class Ib, locus A3	6.62	6.96
M64795	RT1-Aw2	RT1 class Ib, locus Aw2	3.51	5.53
M10094	RT1-Aw2	RT1 class Ib, locus Aw2	4.84	7.53
AF074608	RT1-Aw2	RT1 class Ib, locus Aw2	7.31	7.40
L40362	RT1-Aw2	RT1 class Ib, locus Aw2	7.11	6.71
AI103500	RT1-Aw2	RT1 class Ib, locus Aw2	4.78	12.0*
H33922	RT1-Aw2	RT1 class Ib, locus Aw2	8.31	17.1*
M24324	RT1-Aw2	RT1 class Ib, locus Aw2	3.91	5.09
M31018	RT1-Aw2	RT1 class Ib, locus Aw2	7.36	6.11
AI235223	RT1-Aw2	RT1 class Ib, locus Aw2	12.2	21.1*
M11071	RT1-Aw2	RT1 class Ib, locus Aw2	6.56	5.51
M24026	RT1-CE12	RT1 class Ib, locus CE12	7.38	6.89
AA858651	RT1-CE12	RT1 class Ib, locus CE12	5.14	8.53*

Accession No.	Gene Symbol	Gene Name	Fold Change (IFN-γ-tx OLs / Non-tx OLs) Immature	Mature
AF025308	RT1-CI	RT1 class Ib, locus Cl	4.47	5.76
U16025	RT1-M3	RT1 class Ib, locus M3	3.36†	3.84
U16025	RT1-M3	RT1 class Ib, locus M3	2.52	2.18
AA818887	RT1-N2	RT1 class Ib, H2-TL-like, grc region (N2)	2.63	2.57*
L23128	RT1-N3	RT1 class Ib, H2-TL-like, grc region (N3)	3.83	6.78
AF029240	RT1-S3	RT1 class Ib, locus S3	8.72†	7.76
AI235890	RT1-S3	RT1 class Ib, locus S3	12.6†	16.0
AF029240	RT1-S3	RT1 class Ib, locus S3	4.15	4.85
X57523	TAP1	transporter 1, ATP-binding cassette, sub-family B	4.79	6.73
X57523	TAP1	transporter 1, ATP-binding cassette, sub-family B	26.5†	36.3
X63854	TAP2	transporter 2, ATP-binding cassette, sub-family B	2.67	4.03
MHC class II presentation				
AI045321	C2TA	MHC class II transactivator	8.11	3.49*
X13044	CD74	CD74 antigen (invariant polpypeptide of major histocompatibility class II antigen-associated)	25.9	20.1†
X13044	CD74	CD74 antigen (invariant polpypeptide of major histocompatibility class II antigen-associated)	24.5†	23.1†
X82396	CTSB	cathepsin B	2.76	1.25†
L03201	CTSS	cathepsin S	3.51	2.37†
M22366	RT1-Ba	RT1 class II, locus Ba	2.29†	1.82
K02815	RT1-Ba	RT1 class II, locus Ba	5.14†	3.20
AI236175	RT1-Ba	RT1 class II, locus Ba	9.76	3.73*
M36151	RT1-Bb	RT1 class II, locus Bb	2.37	2.35†
AI228153	RT1-Bb	RT1 class II, locus Bb	11.5	5.38*
M15562	RT1-Da	RT1 class II, locus Da	10.3	10.5
M15562	RT1-Da	RT1 class II, locus Da	49.4	42.8

Accession No.	Gene Symbol	Gene Name	Fold Change (IFN-γ-tx OLs / Non-tx OLs) Immature	Mature
AI111537	RT1-Db1	RT1 class II, locus Db1	3.73	2.56*
U31598	RT1-DMa	RT1 class II, locus DMa	1.86	1.71
Z49761	RT1-DMa	RT1 class II, locus DMa	2.24	2.38
U31599	RT1-DMb	RT1 class II, locus DMb	1.94†	1.76
AI171966	RT1-DMb	RT1 class II, locus DMb	4.31	3.57†
20S proteasome				
E03358	PSMA2	proteasome (prosome, macropain) subunit, alpha type 2	2.31	1.23†
E03358	PSMA2	proteasome (prosome, macropain) subunit, alpha type 2	2.44	1.27†
D90258	PSMA3	proteasome (prosome, macropain) subunit, alpha type 3	2.87	1.45†
D21799	PSMB2	proteasome (prosome, macropain) subunit, beta type 2	2.27	1.93
L17127	PSMB4	proteasome (prosome, macropain) subunit, beta type 4	2.55	1.30
D10729	PSMB8	proteasome (prosome, macropain) subunit, beta type 8	10.5	13.7
D10757	PSMB9	proteasome (prosome, macropain) subunit, beta type 9	25.5	30.5
AI009427	PSMB10	proteasome (prosome, macropain) subunit, beta type 10	10.2	12.2*
AA848487	PSME1	proteasome (prosome, macropain) 28 subunit, alpha	6.39	7.55*
D45249	PSME1	proteasome (prosome, macropain) 28 subunit, alpha	5.90	4.88
D45250	PSME2	proteasome (prosome, macropain) 28 subunit, beta	5.71	4.40
AA851169	PSME2	proteasome (prosome, macropain) 28 subunit, beta	5.27	5.81*
AI011981	PSME2	proteasome (prosome, macropain) 28 subunit, beta	7.45	6.97*
AI045972	PSMF1	proteasome (prosome, macropain) inhibitor subunit 1	2.87	3.11*
Ubiquitin Pathway				
AI179248	APG3L	autophagy 3-like	1.84	-1.02*
AI180444	APG7L	autophagy 7-like	-1.53	1.30*

Accession No.	Gene Symbol	Gene Name	Fold Change (IFN-γ-tx OLs / Non-tx OLs) Immature	Mature
AI010435	CD2AP	CD2-associated protein	1.70	1.02*
AI073001	FBXO39	F-box protein 39	10.3	16.2*
AA943147	HERC6	hect domain and RLD 6 ubiquitin ligase	4.22	7.01*
AI231778	MARCH8	membrane-associated ring finger (C3HC4) 8	2.32	1.12†
AA893199	NAT5	N-acetyltransferase 5	2.75	-1.09†
AI232313	NUB1	NEDD8 ultimate buster-1	2.14	2.36*
AA924532	NUB1	NEDD8 ultimate buster-1	2.33	2.24*
AI044672	RNF19	ring finger protein (C3HC4 type) 19	1.61	2.14*
AI236444	TOPORS	topoisomerase I binding, arginine/serine-rich	-1.60	-1.30*
AA955684	TRAIP	TRAF-interacting protein	-1.88	-1.27*
AI030354	UBD	ubiquitin D	14.9	33.9*
AI177396	UBE1L	ubiquitin-activating enzyme E1-like	2.05	3.01*
AI103150	UBE2C	ubiquitin-conjugating enzyme E2C	-2.92	-1.74*
AI178800	UBE2L6	ubiquitin-conjugating enzyme E2L 6	2.22	2.78*
AI178271	UBE2V2	ubiquitin-conjugating enzyme E2 variant 2	-1.92	-1.40*
AI176509	UBLE1B	ubiquitin-like 1 (sentrin) activating enzyme E1B	-1.69	-1.17*
AI101492	UBQLN1	ubiquilin 1	-1.50	1.01*
AI071606	USP1	ubiquitin specific protease 1	-1.87	-1.32*
AA851237	USP18	ubiquitin specific peptidase 18	6.02	6.60*
AI171345	USP48	ubiquitin specific protease 48	-1.71	-1.08*
AI059254	ZFP313	zinc finger protein 313	1.59	2.18*

Figure 2.7 Expression Estimates of Genes Involved in Proteolysis. a-e) Gene symbols and Accession numbers are plotted on the x-axis; the average of replicate normalized expression values for each treatment group (as described in Materials and Methods) is plotted on the y-axis. In some cases, a gene is represented on the microarray set more than once by different accession numbers. Fold change values for genes in a-e) are listed in Table 2.6.

a.

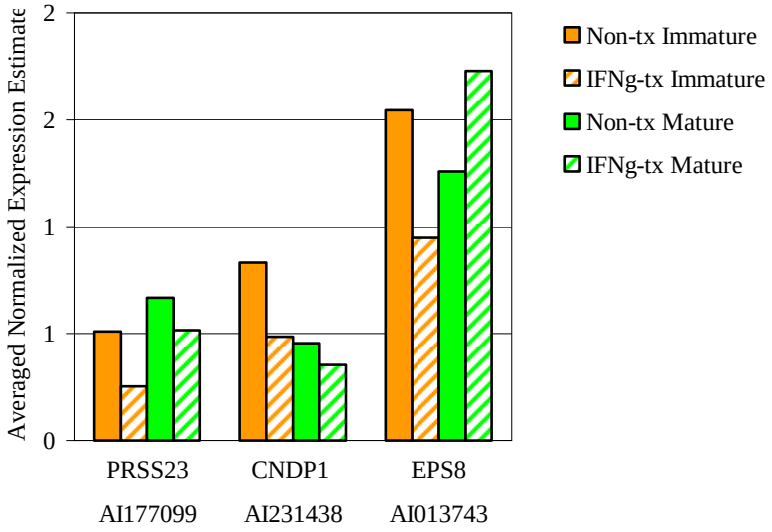

b.

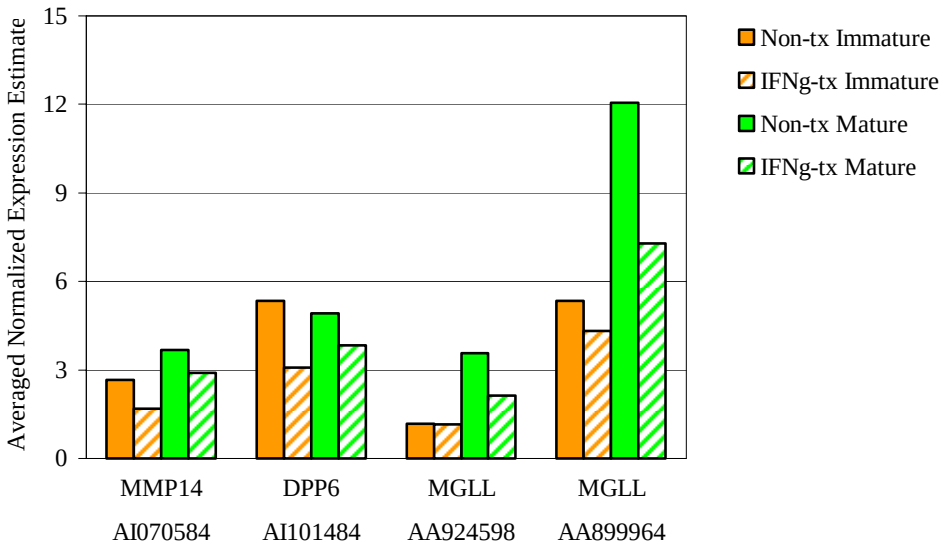

Figure 2.7 Expression Estimates of Genes Involved in Proteolysis.

c.

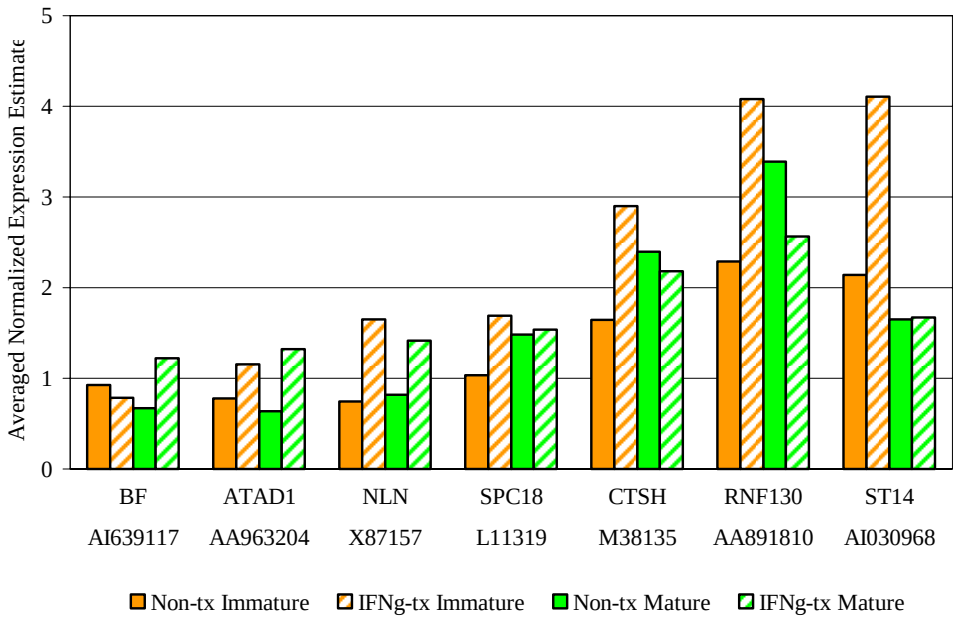

d.

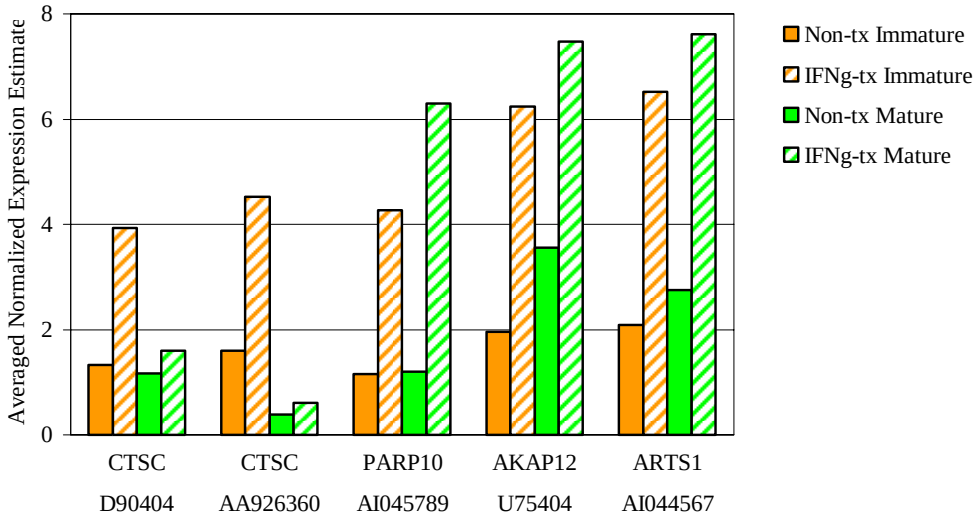

Figure 2.7 Expression Estimates of Genes Involved in Proteolysis.

e.

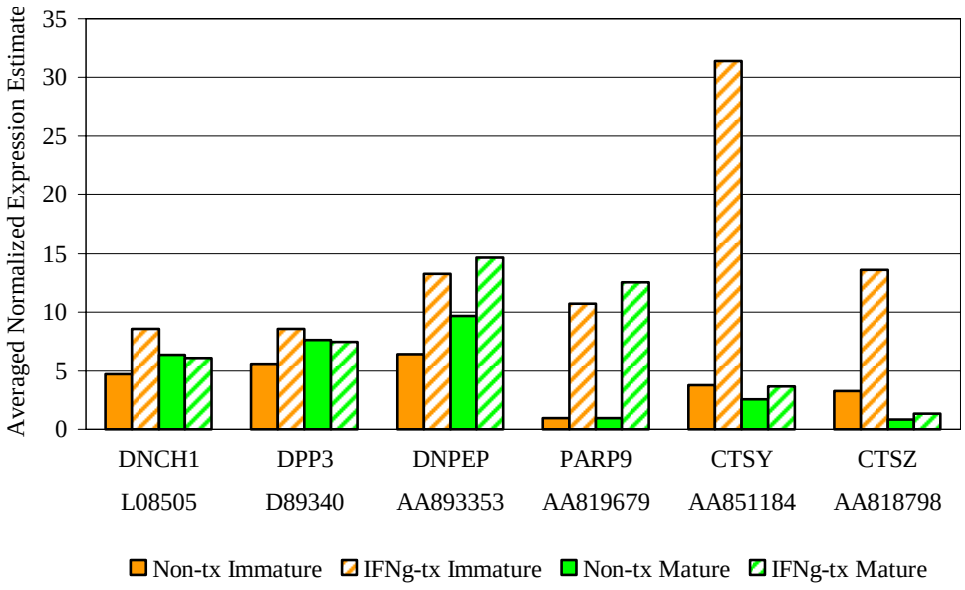

Table 2.6 Differential Expression of Genes Involved in Proteolysis. Replicate RNA samples from each treatment group were hybridized to separate arrays. The average of replicate normalized expression estimates for each sample group was used to calculate the fold change difference in expression for each gene in Figure 2.7. Positive fold change values indicate an increase, and negative values indicate a decrease in gene expression in the IFNγ-treated groups. The dagger indicates the Student's t-test p-value was greater than 0.1; the asterisk indicates there was one sample for each treatment.

			Fold Change (IFN-γ-tx OLs / Non-tx OLs)	
Accession No.	Gene Symbol	Gene Name	Immature	Mature
U75404	AKAP12	A kinase (PRKA) anchor protein (gravin) 12	3.18	2.10
AI044567	ARTS1	type 1 tumor necrosis factor receptor shedding aminopeptidase regulator	3.13	2.77*
AA963204	ATAD1	ATPase family, AAA domain containing 1	1.49	2.07*
AI639117	BF	B-factor, properdin	-1.18†	1.82
AI231438	CNDP1	carnosine dipeptidase 1	-1.73	-1.27*
AI008888	CSTB	cystatin B	2.84	-1.06
D90404	CTSC	cathepsin C	2.97	1.36†
AA926360	CTSC	cathepsin C	2.82	1.57*
M38135	CTSH	cathepsin H	1.77	-1.10†
AA851184	CTSY	cathepsin Y	8.36	1.44*
AA818798	CTSZ	cathepsin Z	4.15	1.64*
AA945915	DTX3	deltex3	9.21	10.2*
L08505	DNCH1	dynein, cytoplasmic, heavy chain 1	1.80	-1.05†
AA893353	DNPEP	aspartyl aminopeptidase	2.07	1.51†
D89340	DPP3	dipeptidylpeptidase 3	1.54	-1.02†
AI101484	DPP6	dipeptidylpeptidase 6	-1.73	-1.29*
AI013743	EPS8	epidermal growth factor receptor pathway substrate 8	-1.63	1.37*
AA924598	MGLL	monoglyceride lipase	-1.02†	-1.68*
AA899964	MGLL	monoglyceride lipase	-1.23	-1.65*
AI070584	MMP14	matrix metalloproteinase 14	-1.59	-1.27*

Accession No.	Gene Symbol	Gene Name	Fold Change (IFN-γ-tx OLs / Non-tx OLs) Immature	Mature
X87157	NLN	neurolysin	2.20	1.73
AI045789	PARP10	poly (ADP-ribose) polymerase family, member 10	3.70	5.24*
AA819679	PARP9	poly (ADP-ribose) polymerase family, member 9	11.3	13.4*
AI177099	PRSS23	protease, serine, 23	-2.01	-1.30*
AA891810	RNF130	ring finger protein 130, goliath	1.78	-1.32†
L11319	SPC18	signal peptidase complex 18kD	1.64	1.04†
AI030968	ST14	suppression of tumorigenicity 14	1.92	1.01*

Figure 2.8 Expression Estimates of Genes Involved in the Stress Response. a-c) Gene symbols and Accession numbers are plotted on the x-axis; the average of replicate normalized expression values for each treatment group (as described in Materials and Methods) is plotted on the y-axis. In some cases, a gene is represented on the microarray set more than once by different accession numbers. Fold change values for genes in a-c) are listed in Table 2.7.

a.

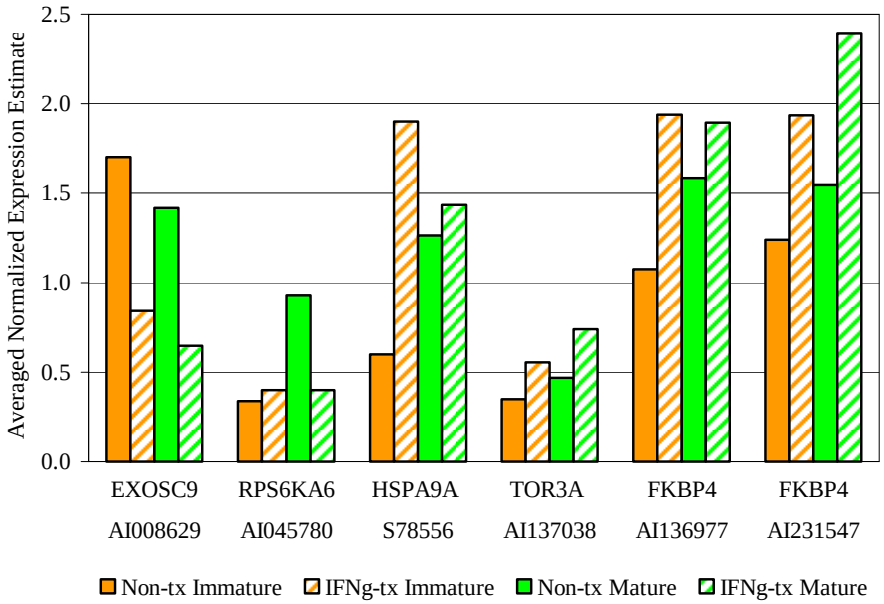

Figure 2.8 Expression Estimates of Genes Involved in the Stress Response.

b.

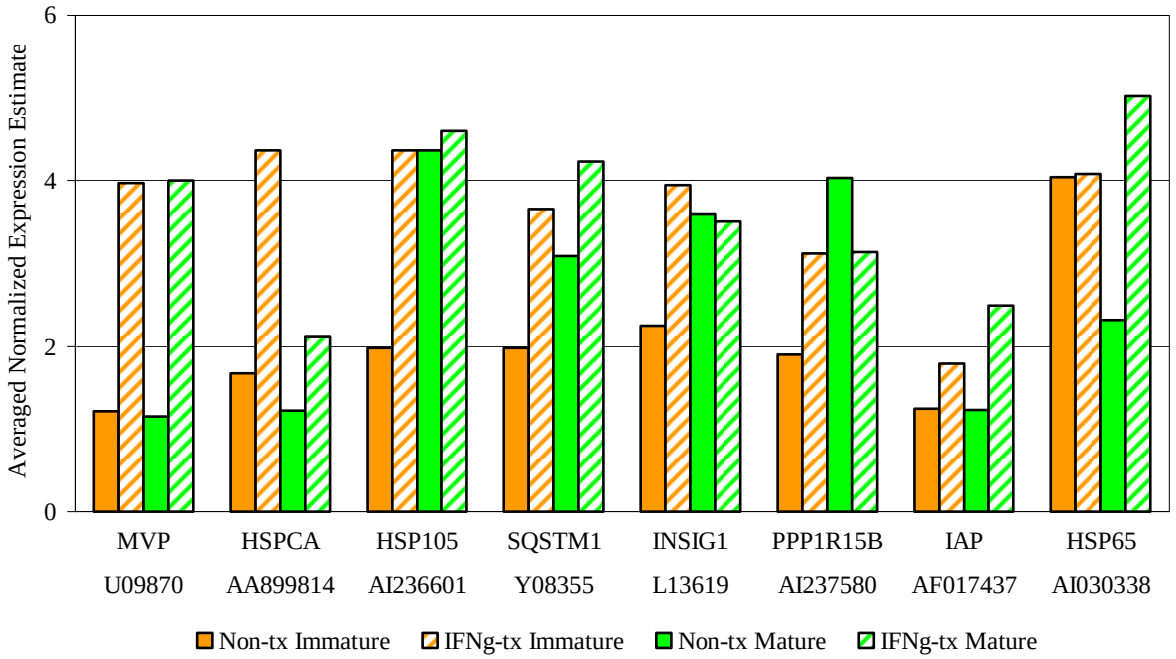

c.

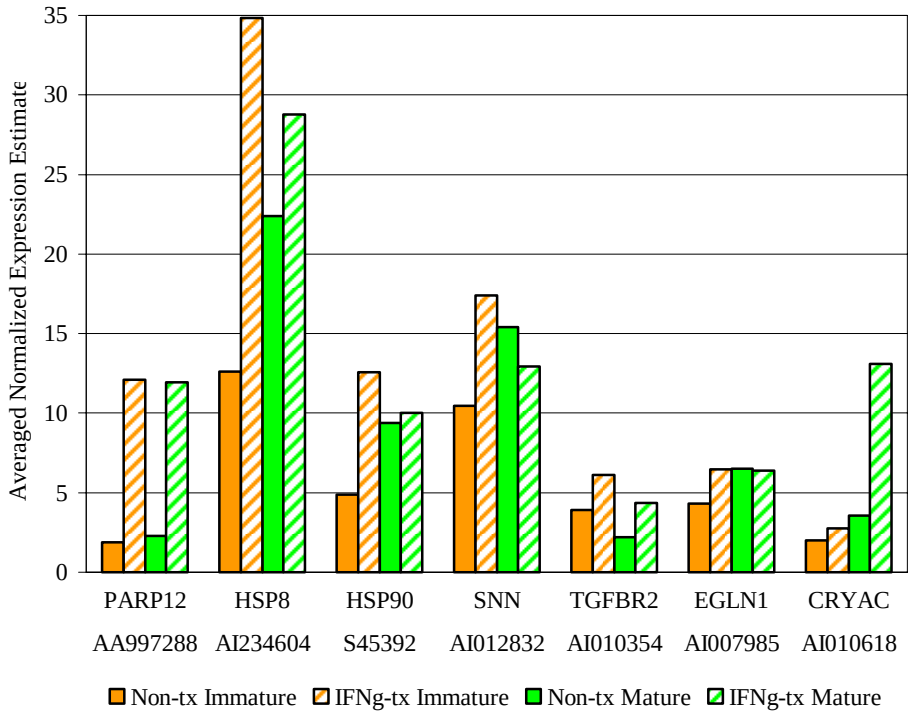

Table 2.7 Differential Expression of Genes Involved in the Stress Response. Replicate RNA samples from each treatment group were hybridized to separate arrays. The average of replicate normalized expression estimates for each sample group was used to calculate the fold change difference in expression for each gene in Figure 2.8. Positive fold change values indicate an increase, and negative values indicate a decrease in gene expression in the IFNγ-treated groups. The dagger indicates the Student's t-test p-value was greater than 0.1; the asterisk indicates there was one sample for each treatment.

			Fold Change (IFN-γ-tx OLs / Non-tx OLs)	
Accession No.	Gene Symbol	Gene Name	Immature	Mature
AI010618	CRYAC	crystallin, alpha C	1.37	3.70*
AI007985	EGLN1	EGL nine homolog 1	1.50	-1.02*
AI008629	EXOSC9	exosome component 9	-2.02	-2.19*
AI136977	FKBP4	FK506 binding protein 4	1.80	1.20†
AI231547	FKBP4	FK506 binding protein 4	1.56	1.55†
AI236601	HSP105	heat shock protein 105 kDa alpha	2.20	1.05†
AI030338	HSP65	heat shock protein 65	1.01†	2.17*
AI234604	HSP8	heat shock protein 8	2.76	1.29†
S45392	HSP90	heat shock protein 90	2.57	1.07†
S78556	HSPA9A	heat shock protein, A	3.17	1.14†
AA899814	HSPCA	heat shock protein 1a	2.62	1.74*
AF017437	IAP	integrin-associated protein form 4	1.44†	2.03
L13619	INSIG1	insulin induced gene 1	1.76	-1.03†
U09870	MVP	major vault protein	3.28†	3.48
AI237580	PPP1R15B	protein phosphatase 1, regulatory (inhibitor) subunit 15b	1.64	-1.29*
AA997288	PARP12	poly (ADP-ribose) polymerase family member 12	6.45	5.22*
AI045780	RPS6KA6	ribosomal protein S6 kinase, polypeptide 5	1.18	-2.33*
AI012832	SNN	stannin	1.66	-1.19*

Accession No.	Gene Symbol	Gene Name	Fold Change (IFN-γ-tx OLs / Non-tx OLs) Immature	Mature
Y08355	SQSTM1	sequestosome 1	1.85	1.37†
AI010354	TGFBR2	transforming growth factor, beta receptor II	1.56	2.00*
AI137038	TOR3A	torsin family 3, member A	1.59	1.58*

Figure 2.8 Expression Estimates of Genes Involved in Immune Response. a-j) Gene symbols and Accession numbers are plotted on the x-axis; the average of replicate normalized expression values for each treatment group (as described in Materials and Methods) is plotted on the y-axis. In some cases, a gene is represented on the microarray set more than once by different accession numbers. Fold change values for genes in a-j) are listed in Table 2.7.

a.

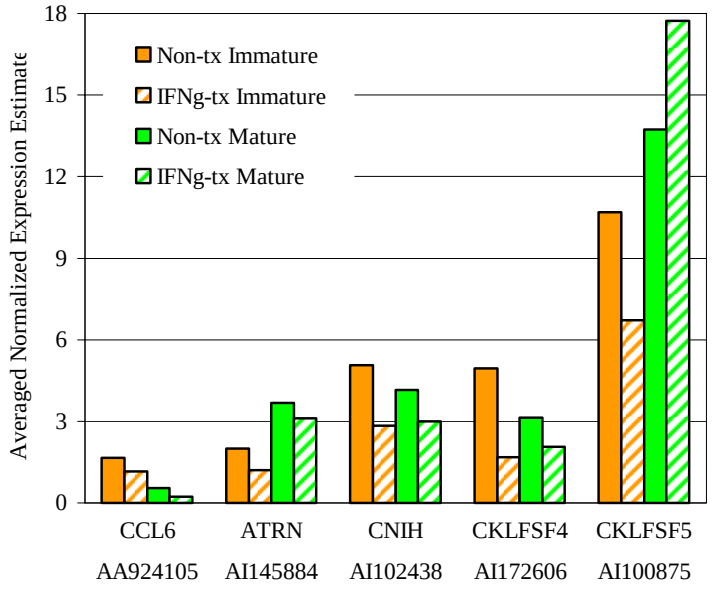

b.

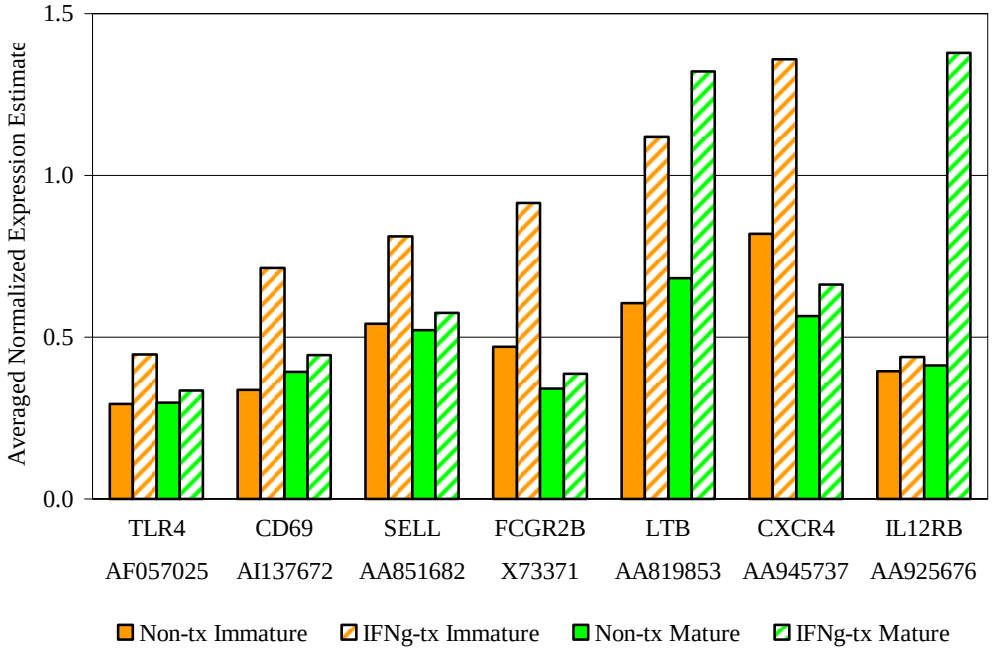

Figure 2.8 Expression Estimates of Genes Involved in Immune Response.

c.

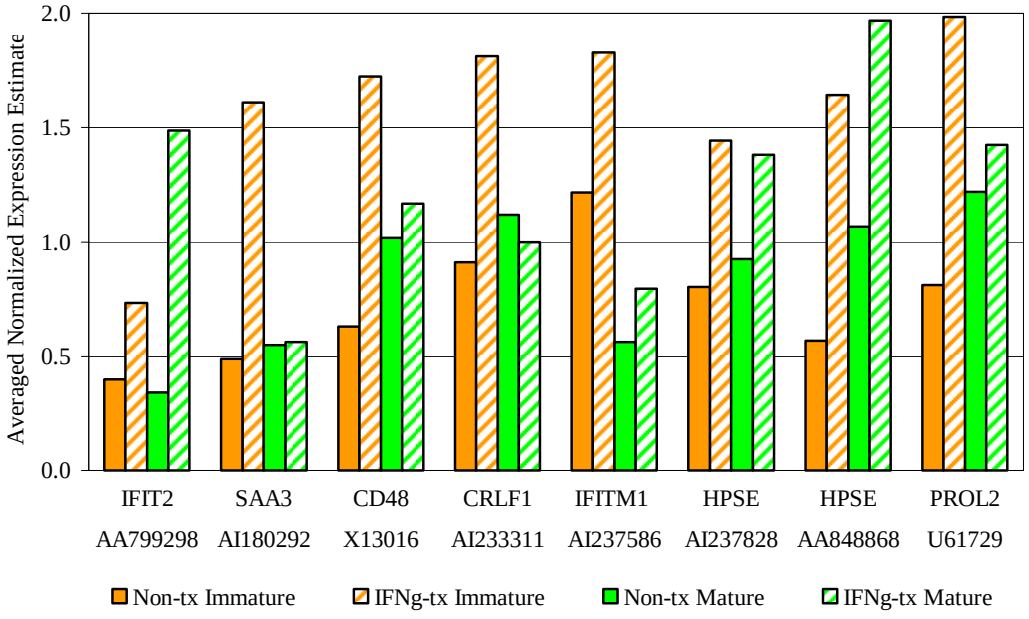

d.

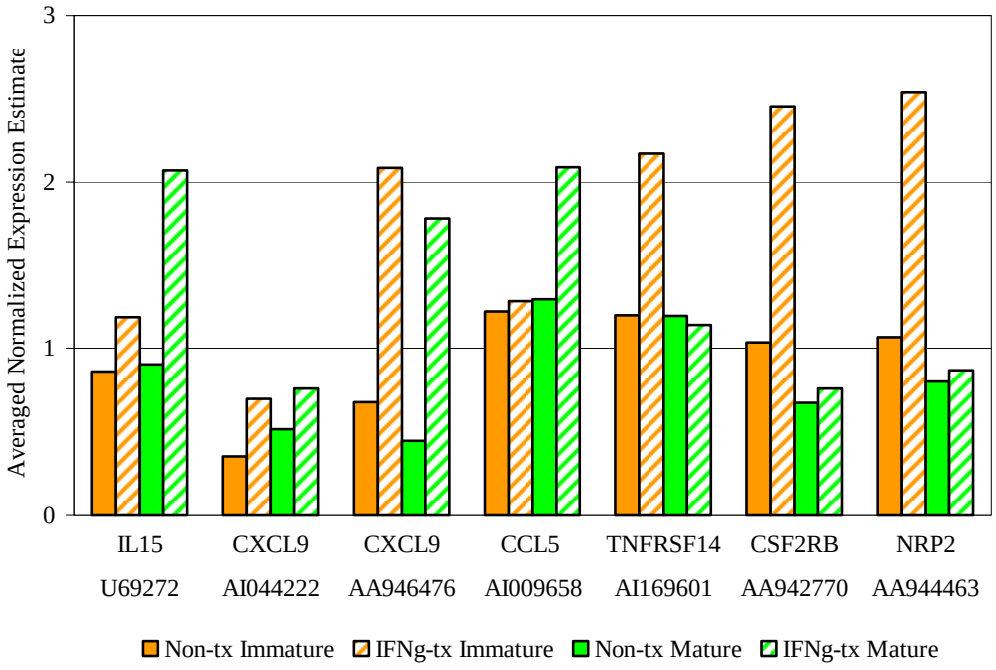

Figure 2.8 Expression Estimates of Genes Involved in Immune Response.

e.

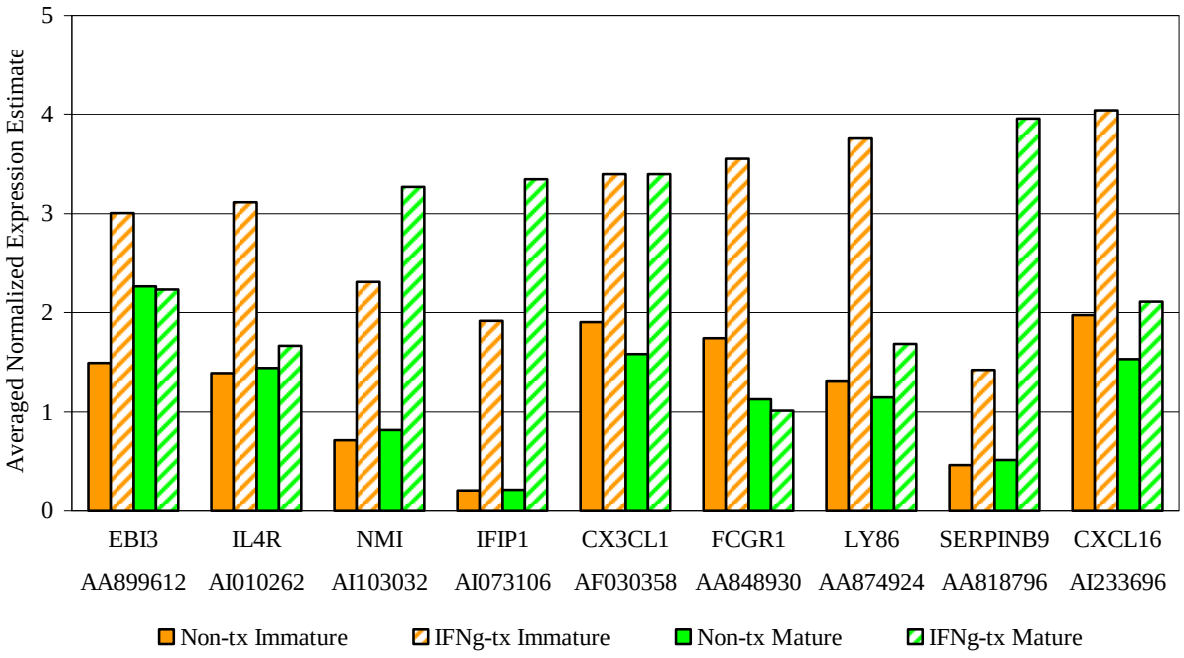

f.

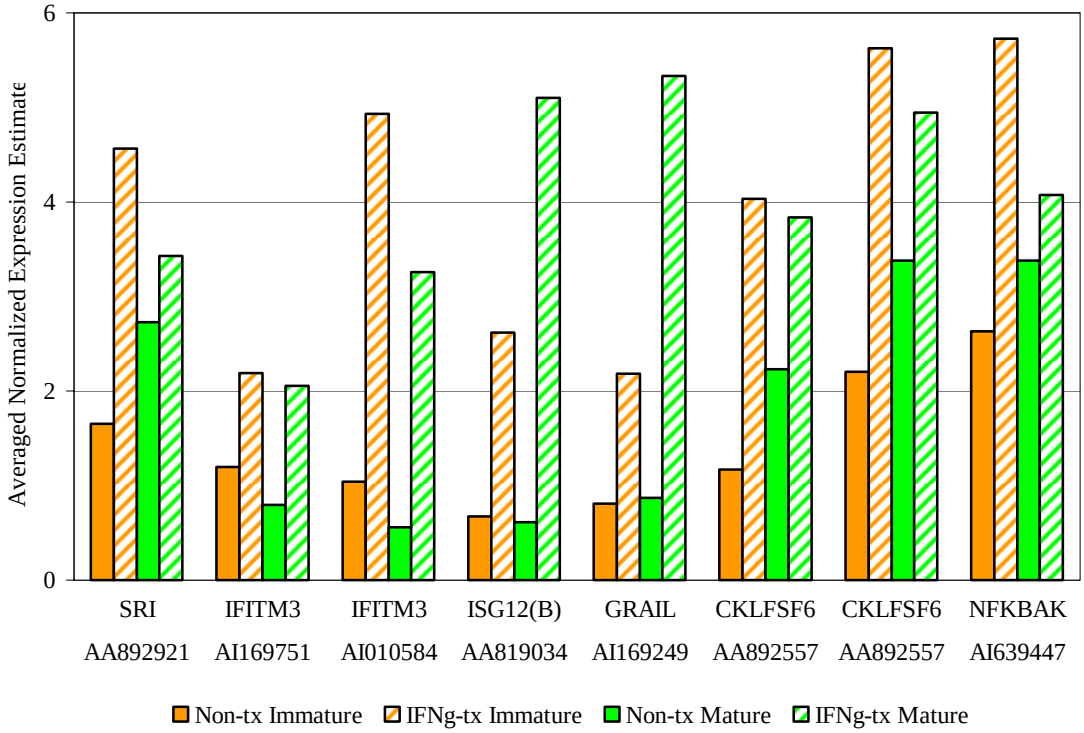

Figure 2.8 Expression Estimates of Genes Involved in Immune Response.

g.

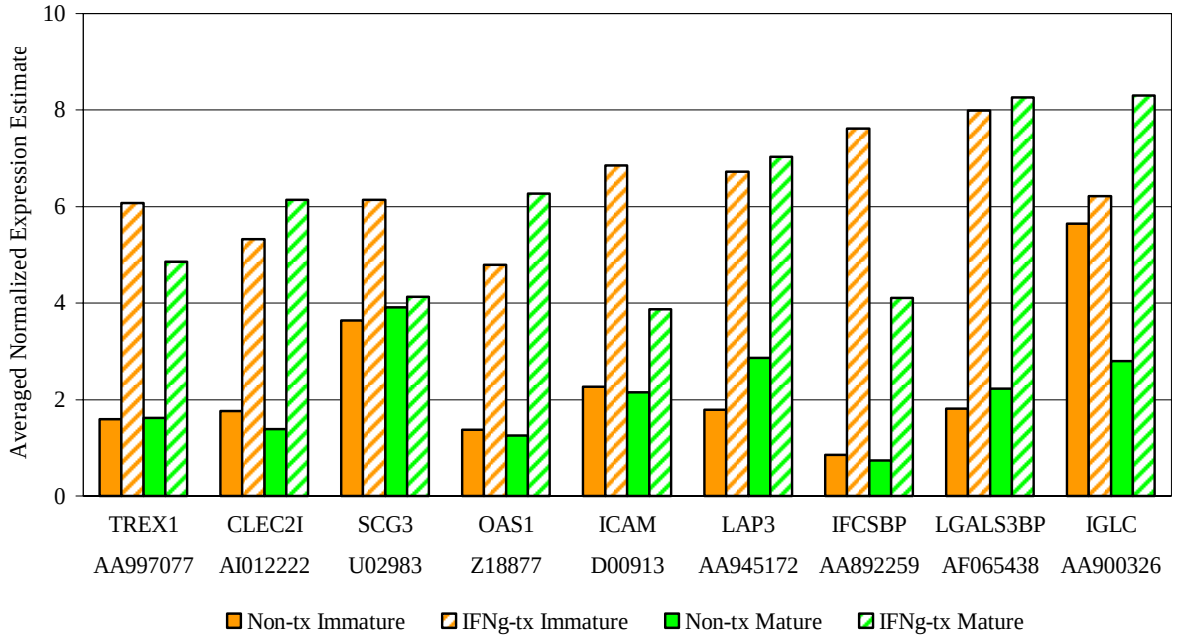

h.

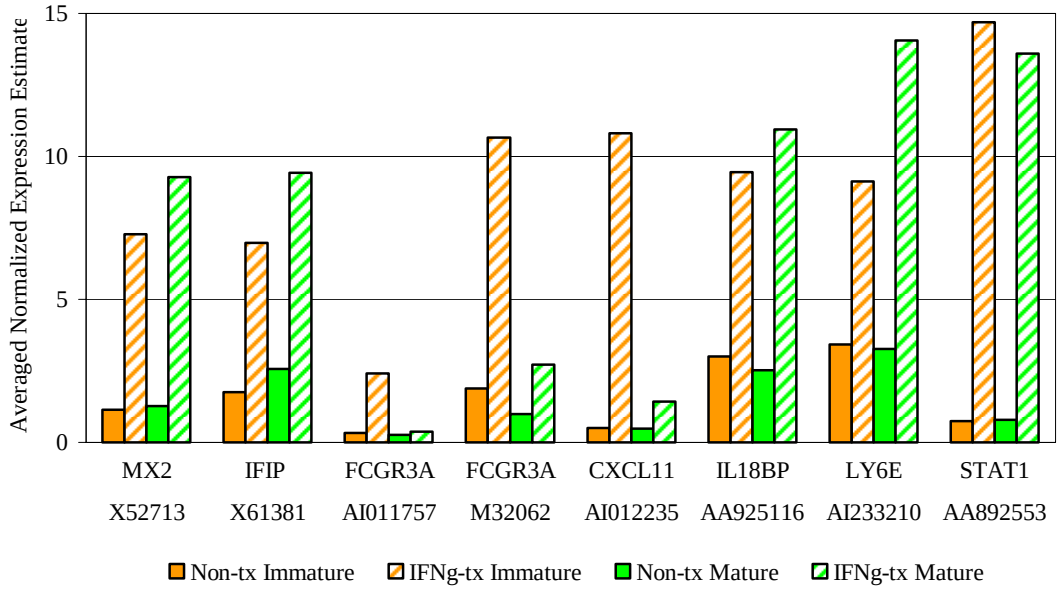

Figure 2.8 Expression Estimates of Genes Involved in Immune Response.

i.

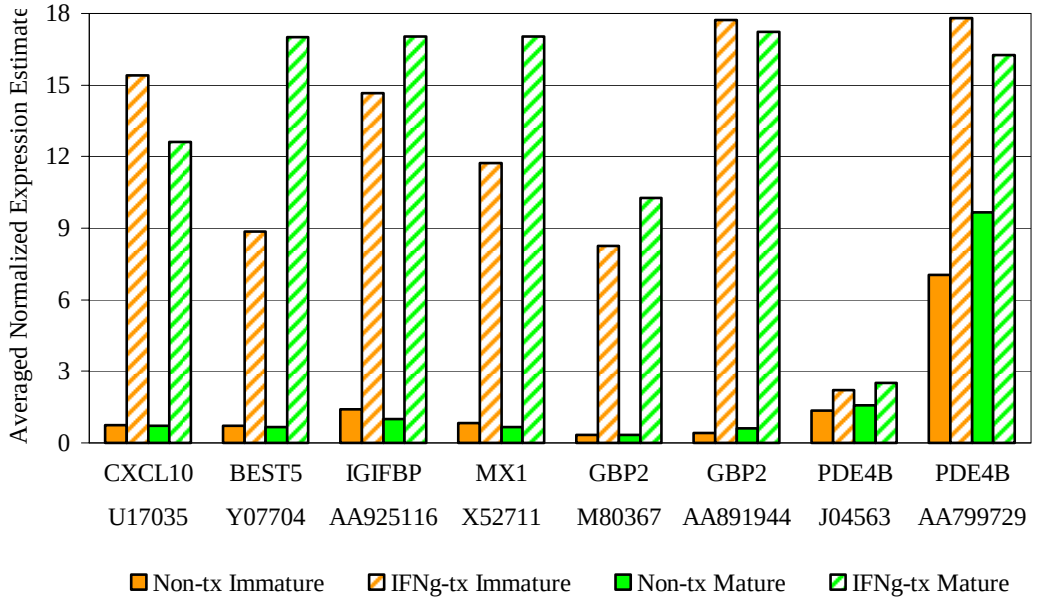

j.

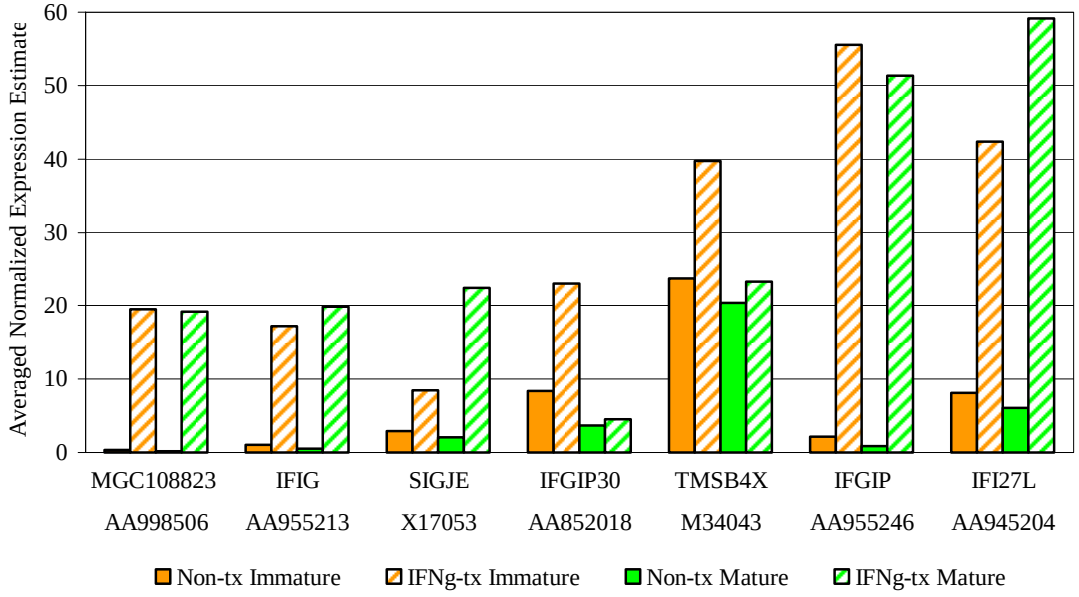

Table 2.7 Differential Expression of Genes Involved in the Immune Response. Replicate RNA samples from each treatment group were hybridized to separate arrays. The average of replicate normalized expression estimates for each sample group was used to calculate the fold change difference in expression for each gene in Figure 2.8. Positive fold change values indicate an increase, and negative values indicate a decrease in gene expression in the IFNγ-treated groups. The dagger indicates the Student's t-test p-value was greater than 0.1; the asterisk indicates there was one sample for each treatment.

			Fold Change (IFN-γ-tx OLs / Non-tx OLs)	
Accession No.	Gene Symbol	Gene Name	Immature	Mature
AI145884	ATRN	attractin	-1.65	-1.18*
Y07704	BEST5	Best5	12.4	25.7
AI009658	CCL5	chemokine (C-C motif) ligand 5	1.05†	1.61
AA924105	CCL6	chemokine (C-C motif) ligand 6	-1.44	-2.45*
X13016	CD48	CD48 antigen	2.74	1.15†
AI137672	CD69	CD69 antigen	2.11	1.13*
AI172606	CKLFSF4	chemokine-like factor superfamily 4	-2.93	-1.52*
AI100875	CKLFSF5	chemokine-like factor super family 5	-1.59	1.29*
AA892557	CKLFSF6	chemokine-like factor super family 6	2.55	1.46†
AA892557	CKLFSF6	chemokine-like factor superfamily 6	3.44	1.72†
AI012222	CLEC2I	c-type lectin 1	3.02	4.43*
AI102438	CNIH	cornichon homolog (Drosophila)	-1.79	-1.39*
AI233311	CRLF1	cytokine receptor-like factor 1	1.99	-1.12*
AA942770	CSF2RB	colony stimulating factor 2 receptor beta 1	2.37	1.13*
AF030358	CX3CL1	chemokine (C-X3-C motif) ligand 1	1.79†	2.15
AI044222	CXCL9	chemokine (C-X-C motif) ligand 9	1.99	1.47*
AA946476	CXCL9	chemokine (C-X-C motif) ligand 9	3.07	4.00*
U17035	CXCL10	chemokine (C-X-C motif) ligand 10	20.7	17.7
AI012235	CXCL11	chemokine (C-X-C motif) ligand 11	21.6	3.03*
AI233696	CXCL16	chemokine (C-X-C motif) ligand 16	2.05	1.38*

Accession No.	Gene Symbol	Gene Name	Fold Change (IFN-γ-tx OLs / Non-tx OLs) Immature	Mature
AA945737	CXCR4	chemokine (C-X-C motif) receptor 4	1.66	1.17
AA899612	EBI3	Epstein-Barr virus induced gene 3	2.02	-1.01*
AA848930	FCGR1	Fc IgG receptor I	2.04	-1.12*
X73371	FCGR2B	Fc IgG receptor II	1.95	1.14†
AI011757	FCGR3A	Fc IgG receptor III	7.25	1.47*
M32062	FCGR3A	Fc IgG receptor III	5.62	2.75†
AA891944	GBP2	guanylate nucleotide binding protein 2	42.1	29.0
M80367	GBP2	guanylate nucleotide binding protein 2	24.4	30.8
AI169249	GRAIL	ring finger protein 128 GRAIL	2.69	6.10*
AI237828	HPSE	heparanase	1.80	1.49*
AA848868	HPSE	heparanase	2.90	1.84*
D00913	ICAM	intercellular adhesion molecule-1	3.02	1.80
AA892259	IFCSBP	interferon consensus sequence binding protein	8.84	5.58
AA955246	IFGIP	interferon-gamma inducible protein	25.8	61.7*
AA852018	IFGIP30	interferon-gamma inducible protein 30	2.75	1.25*
AA945204	IFI27L	interferon-alpha inducible protein 27	5.21	9.79*
AA955213	IFIG	interferon inducible GTPase	17.0	37.6*
X61381	IFIP	interferon induced protein	3.97	3.67†
AI073106	IFIP1	interferon inducible protein 1	9.52†	15.9*
AA799298	IFIT2	interferon-induced protein with tetratricopeptide repeats 2	1.84	4.35*
AI237586	IFITM1	interferon induced transmembrane protein 1	1.50	1.41*
AI169751	IFITM3	interferon induced transmembrane protein 3	1.83	2.59*
AI010584	IFITM3	interferon induced transmembrane protein 3	4.74	5.81*
AA925116	IGIFBP	interferon-gamma inducing factor binding protein	10.3	17.1*
AA900326	IGLC	Ig light chain	1.10	2.96*

Accession No.	Gene Symbol	Gene Name	Fold Change (IFN-γ-tx OLs / Non-tx OLs) Immature	Mature
AA925676	IL12RB	interleukin-12 receptor beta	1.11	3.34*
U69272	IL15	interleukin-15	1.38	2.29
AA925116	IL18BP	interferon gamma inducing factor binding protein	3.13	4.36*
AI010262	IL4R	interleukin-4 receptor	2.24	1.16*
AA819034	ISG12(B)	putative ISG12(b) protein	3.89	8.38*
AA945172	LAP3	leucine aminopeptidase 3	3.77	2.45
AF065438	LGALS3BP	lectin, galactoside-binding, soluble, 3 binding protein	4.42	3.72
AA819853	LTB	lymphotoxin B	1.85	1.93*
AI233210	LY6E	lymphocyte antigen 6 complex, locus E	2.67	4.31*
AA874924	LY86	lymphocyte antigen 86	2.87	1.47†
AA998506	MGC108823	interferon-inducible GTPase	60.7	101*
X52711	MX1	myxovirus (influenza virus) resistance 1	14.1	26.0
X52713	MX2	myxovirus (influenza virus) resistance 2	6.42	7.30
AI639447	NFKBAK	nuclear factor kappa B activating kinase	2.17	1.21†
AI103032	NMI	N-myc (and STAT) interactor	3.26	4.03*
AA944463	NRP2	neuropilin 2	2.38	1.08*
Z18877	OAS1	2'-5' oligoadenylate synthetase	3.48	5.01
J04563	PDE4B	phosphodiesterase 4B	1.62	1.59
AA799729	PDE4B	phosphodiesterase 4b, cAMP-specific	2.53	1.68
U61729	PROL2	proline-rich protein 2	2.44	1.17†
AI180292	SAA3	serum amyloid A3	3.29	1.02*
U02983	SCG3	secretogranin III	1.69	1.06†
AA851682	SELL	selectin, lymphocyte	1.50	1.10*
AA818796	SERPINB9	serine (or cysteine) peptidase inhibitor, clade B, member 9, SPI6	3.10	7.72
X17053	SIGJE	small inducible cytokine A2, JE product	2.89†	10.9

			Fold Change (IFN-γ-tx OLs / Non-tx OLs)	
Accession No.	Gene Symbol	Gene Name	Immature	Mature
AA892921	SRI	sorcin	2.76	1.26†
AA892553	STAT1	signal transducer and activator of transcription 1	19.7	17.3
AF057025	TLR4	toll-like receptor 4	1.52	1.13†
M34043	TMSB4X	thymosin, beta 4	1.68	1.15†
AI169601	TNFRSF14	tumor necrosis factor receptor superfamily, member 14 (herpesvirus entry mediator)	1.81	-1.05*
AA997077	TREX1	3'-5' exonuclease TREX1	3.80	3.00*

Figure 2.9 Expression Estimates of Genes Involved in Oxidative Stress Response. a) Genes highlighted in yellow are upregulated in one or both IFN-γ-treated cultures. b-d) Gene symbols and Accession numbers are plotted on the x-axis; the average of replicate normalized expression values for each treatment group (as described in Materials and Methods) is plotted on the y-axis. In some cases, a gene is represented on the microarray set more than once by different accession numbers. Fold change values for genes in b-d) are listed in Table 2.8.

a.

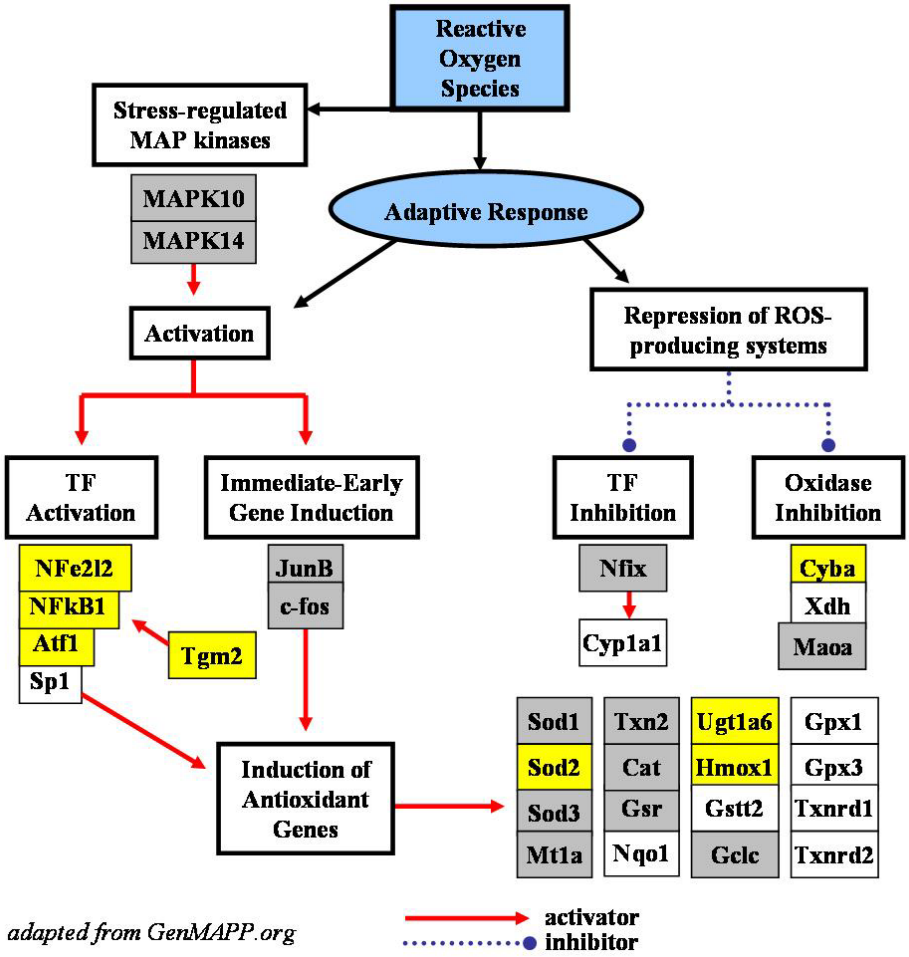

Figure 2.9 Expression Estimates of Genes Involved in Oxidative Stress Response.

b.

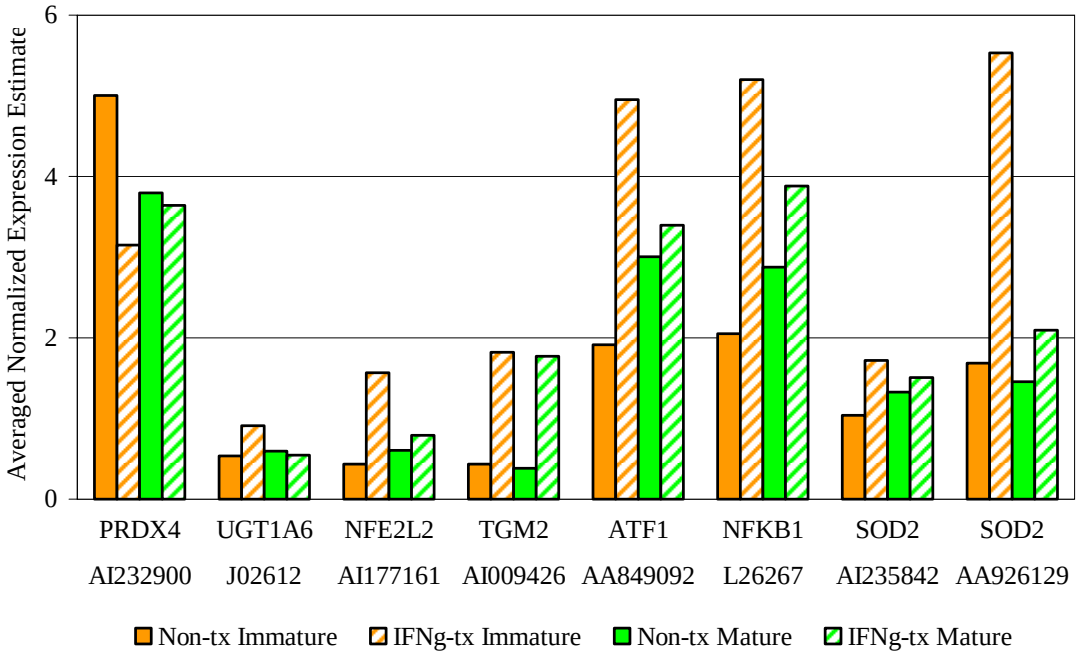

Figure 2.9 Expression Estimates of Genes Involved in Oxidative Stress Response.

c.

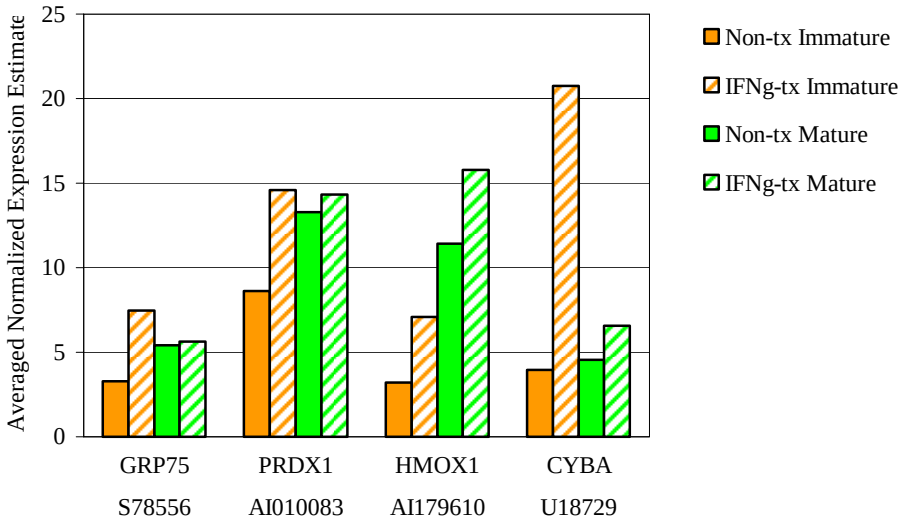

d.

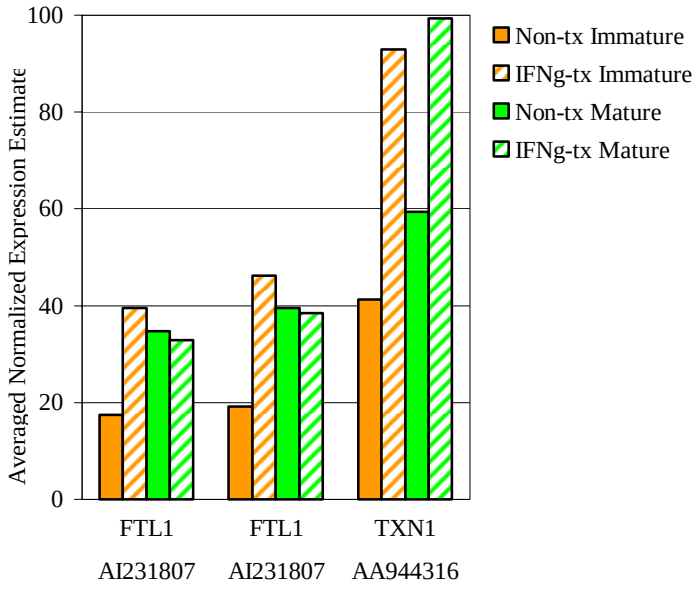

Table 2.8 Differential Expression of Genes Involved in the Oxidative Stress Response. Replicate RNA samples from each treatment group were hybridized to separate arrays. The average of replicate normalized expression estimates for each sample group was used to calculate the fold change difference in expression for each gene in Figure 2.9. Positive fold change values indicate an increase, and negative values indicate a decrease in gene expression in the IFNγ-treated groups. The dagger indicates the Student's t-test p-value was greater than 0.1; the asterisk indicates there was one sample for each treatment.

			Fold Change (IFN-γ-tx OLs / Non-tx OLs)	
Accession No.	Gene Symbol	Gene Name	Immature	Mature
AA849092	ATF1	activating transcription factor 1, cyclic-AMP-dependent	2.58	1.13*
U18729	CYBA	cytochrome b558 alpha-subunit	5.26	1.44†
AI231807	FTL1	ferritin light chain 1	2.28	-1.06†
AI231807	FTL1	ferritin light chain 1	2.42	-1.03†
S78556	GRP75	75-kDa glucose regulated protein	2.28	1.04†
J02722	HMOX1	heme oxygenase 1	1.92	1.92†
AI179610	HMOX1	heme oxygenase 1	2.22	1.38†
AI177161	NFE2L2	NF-E2-related factor 2	3.58	1.32†
L26267	NFKB1	nuclear factor kappa B p105 subunit , 3' end	2.53	1.35†
AI010083	PRDX1	peroxiredoxin 1	1.69	1.08†
AI232900	PRDX4	peroxiredoxin 4	-1.59	-1.04*
AI235842	SOD2	superoxide dismutase 2, mitochondrial	1.65	1.13*
AA926129	SOD2	superoxide dismutase 2, manganese-containing	3.28†	1.44†
AI009426	TGM2	tissue-type transglutaminase	4.23	4.65*
AA944316	TXN1	thioredoxin 1	2.25	1.67*
J02612	UGT1A6	UDP glycosyltransferase 1 family, polypeptide A6	1.70	-1.10†

Figure 2.11 Expression Estimates of Genes Involved in Apoptosis. a) Genes highlighted in yellow are upregulated and genes highlighted in green are downregulated in IFN-γ-treated immature and b) mature OL cultures. Gene symbols and Accession numbers for pro-apoptotic genes c-g) and survival genes h-i) are plotted on the x-axis; the average of replicate normalized expression values for each treatment group (as described in Materials and Methods) is plotted on the y-axis. In some cases, a gene is represented on the microarray set more than once by different accession numbers. Fold change values for genes in c-i) are listed in Table 2.10.

a. Apoptosis in IFN-γ-iOLs

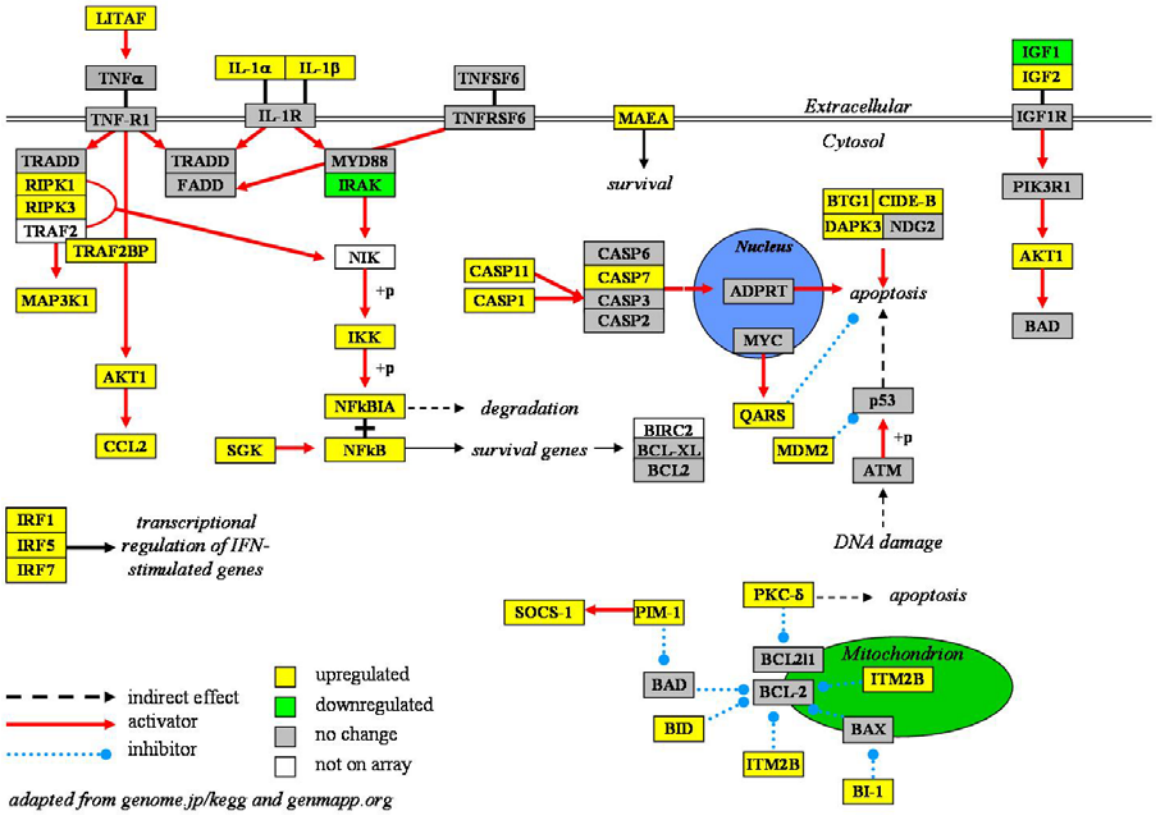

Figure 2.11 Expression Estimates of Genes Involved in Apoptosis.

b. Apoptosis in IFN-γ-mOLs

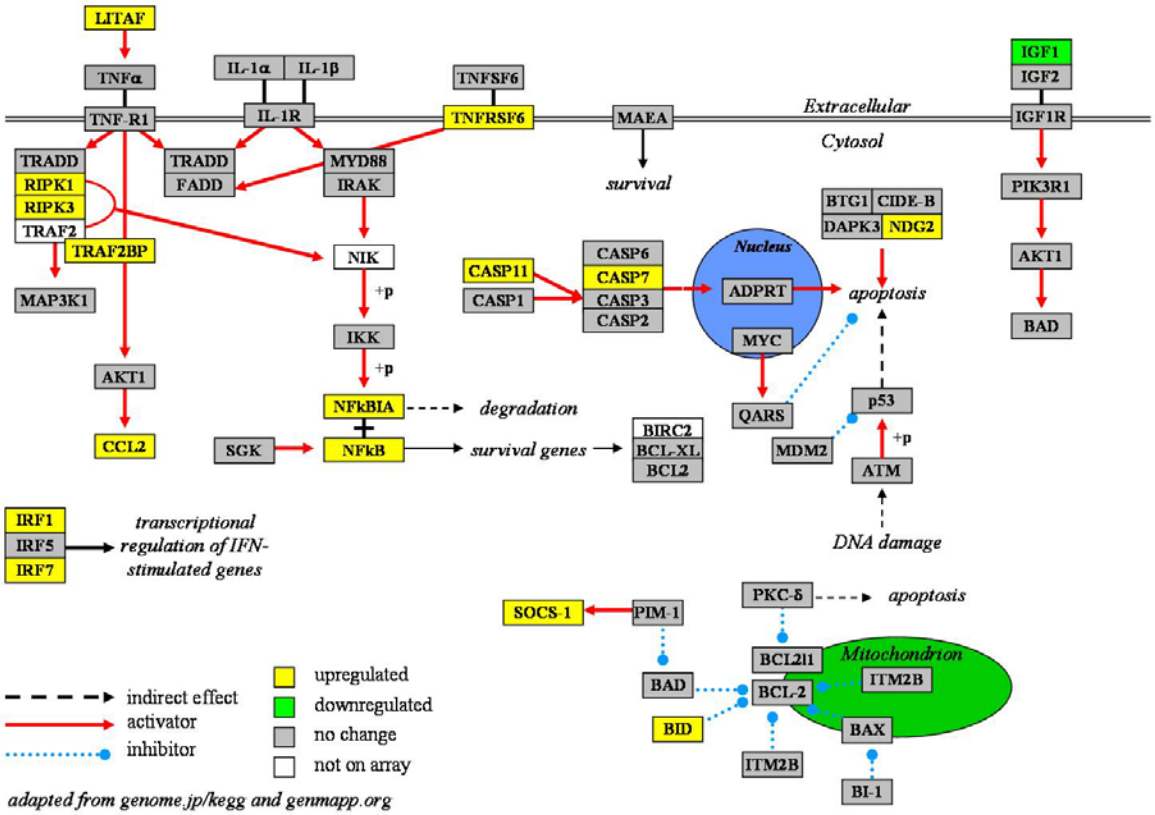

Figure 2.11 Expression Estimates of Genes Involved in Apoptosis.

c.

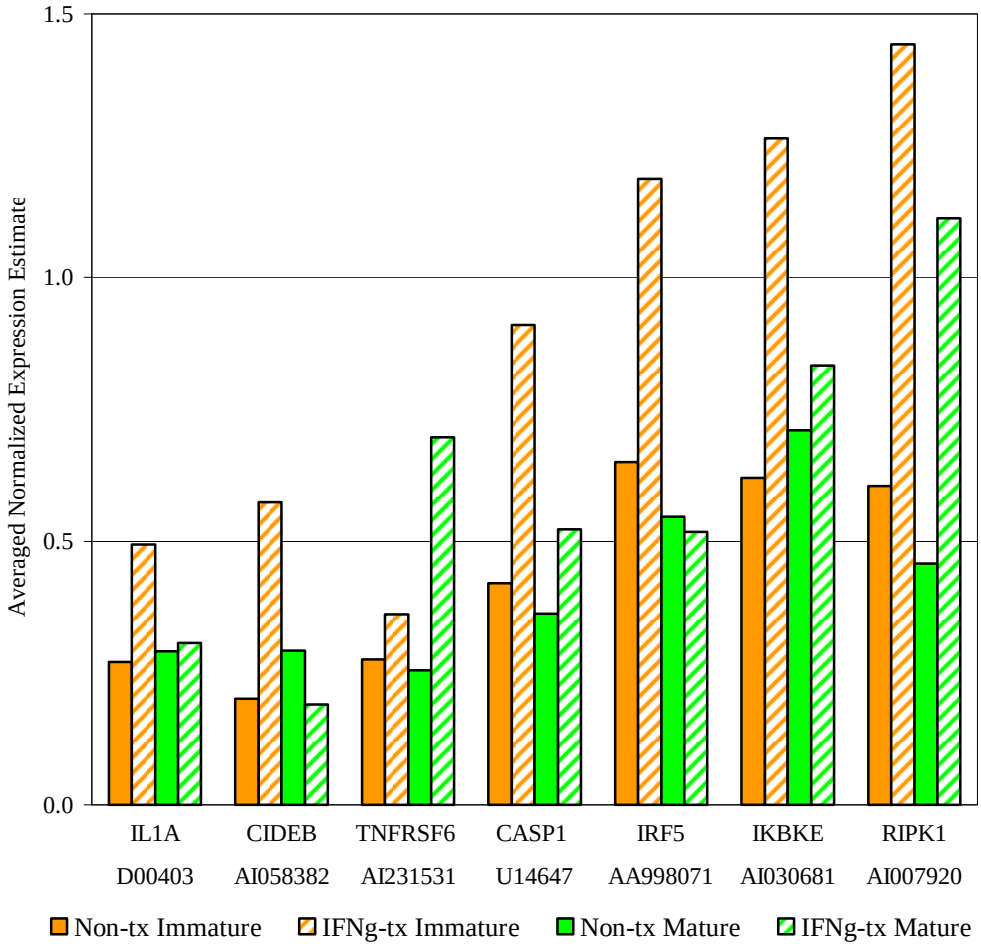

Figure 2.11 Expression Estimates of Genes Involved in Apoptosis.

d.

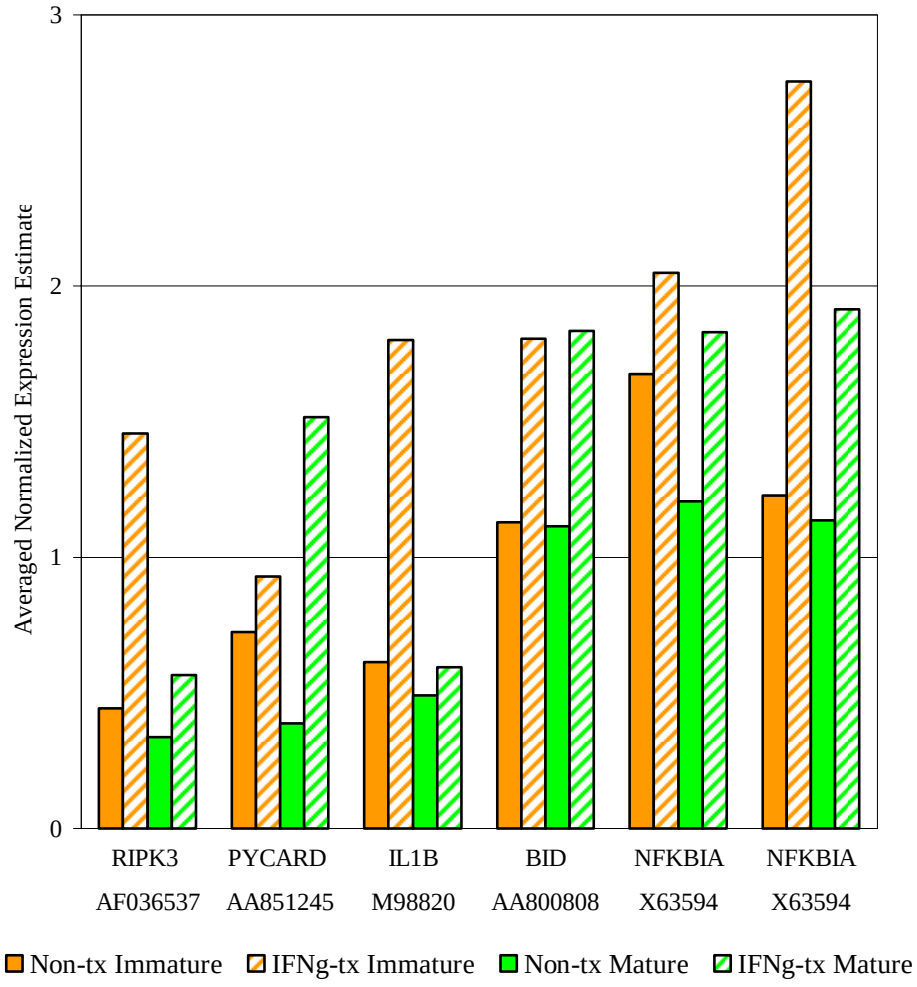

Figure 2.11 Expression Estimates of Genes Involved in Apoptosis.

e.

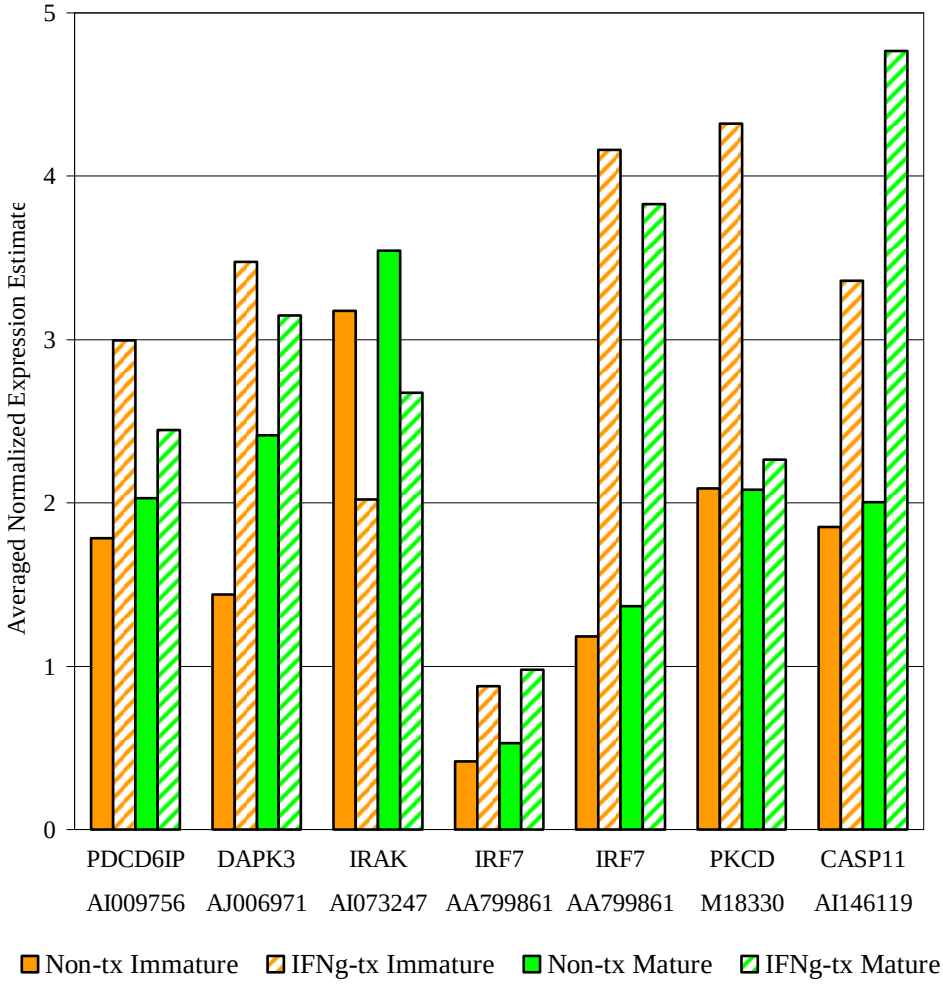

Figure 2.11 Expression Estimates of Genes Involved in Apoptosis.

f.

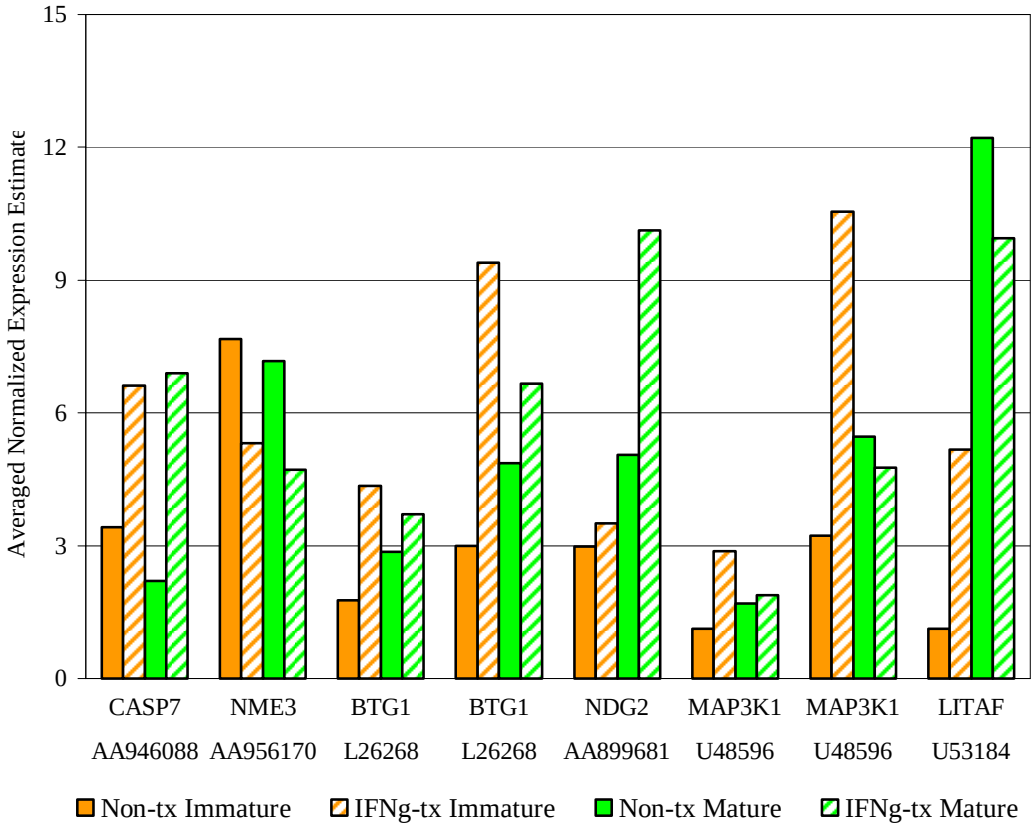

Figure 2.11 Expression Estimates of Genes Involved in Apoptosis.

g.

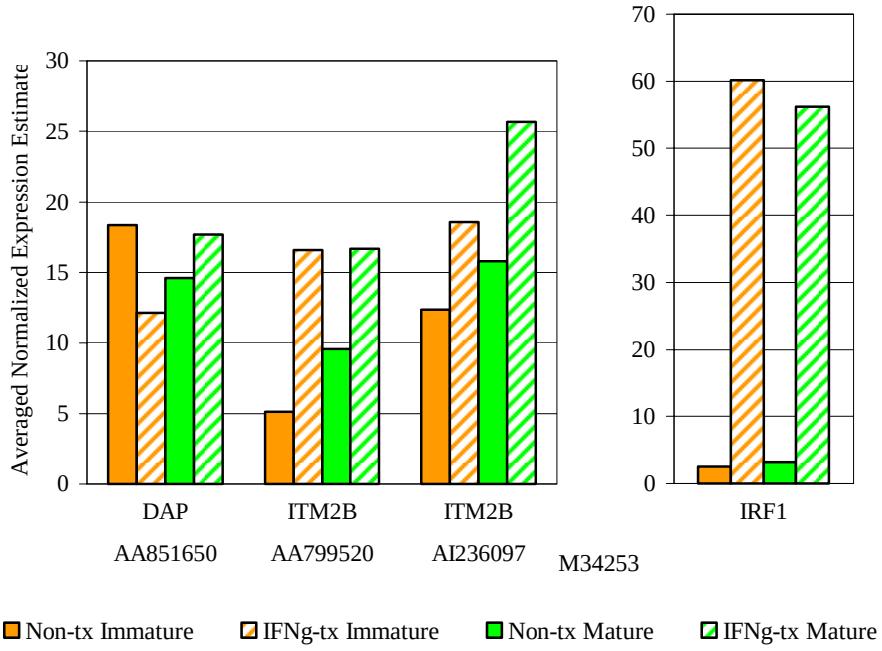

Figure 2.11 Expression Estimates of Genes Involved in Apoptosis.

h.

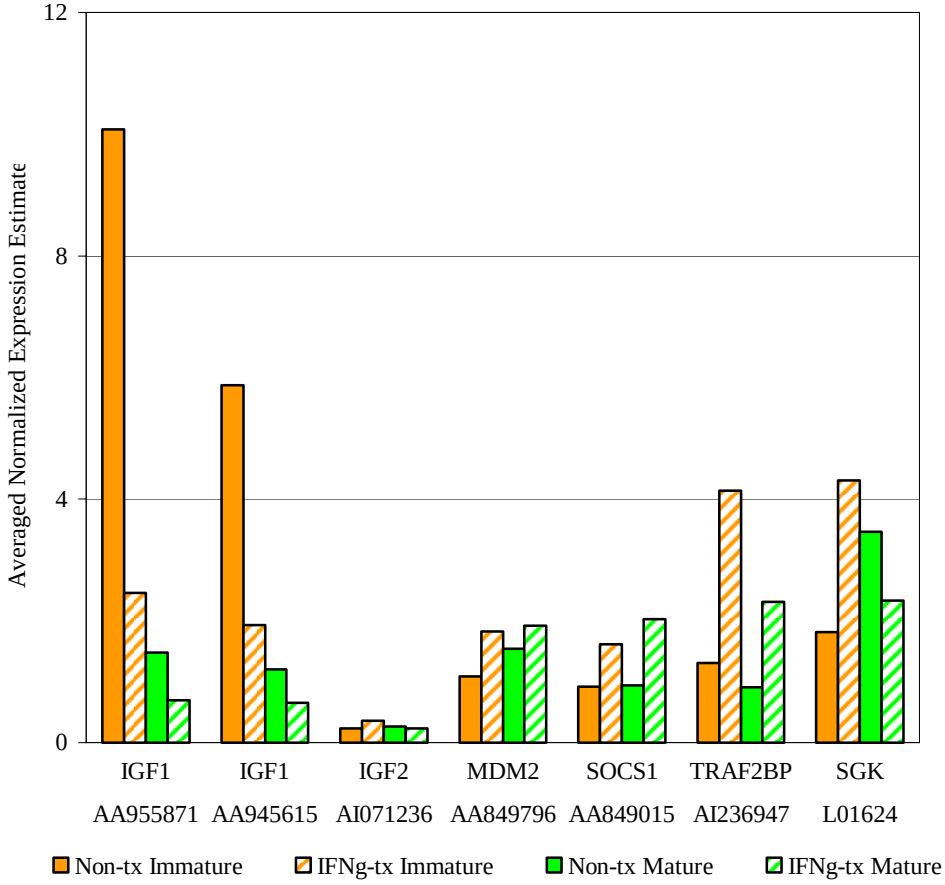

Figure 2.11 Expression Estimates of Genes Involved in Apoptosis.

i.

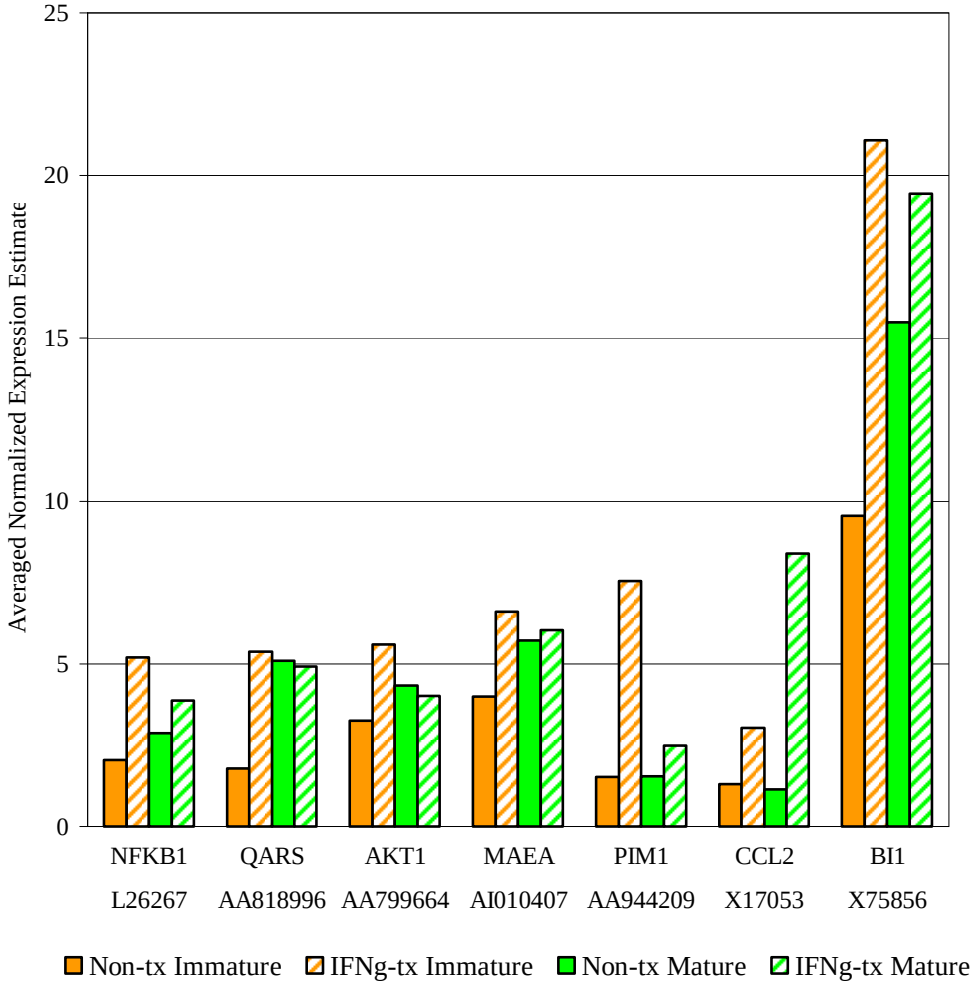

Table 2.10 Differential Expression of Genes Involved in Apoptosis. Replicate RNA samples from each treatment group were hybridized to separate arrays. The average of replicate normalized expression estimates for each sample group was used to calculate the fold change difference in expression for each gene in Figure 2.11. Positive fold change values indicate an increase, and negative values indicate a decrease in gene expression in the IFNγ-treated groups. The dagger indicates the Student's t-test p-value was greater than 0.1; the asterisk indicates there was one sample for each treatment.

			Fold Change (IFN-γ-tx OLs / Non-tx OLs)	
Accession No.	Gene Symbol	Gene Name	Immature	Mature
Pro-Apoptotic Genes				
AA800808	BID	BH3 interacting domain death agonist	1.60	1.64
L26268	BTG1	B-cell translocation gene 1	2.46	1.30†
L26268	BTG1	B-cell translocation gene 1	3.14	1.37†
U14647	CASP1	caspase 1	2.17†	1.44†
AA946088	CASP7	caspase 7	1.94	3.13*
AI146119	CASP11	caspase 11	1.81†	2.38*
AI058382	CIDE-B	cell death-inducing DNA fragmentation factor, alpha subunit-like effector B	2.85	-1.54*
AA851650	DAP	death-associated protein	-1.51	1.21*
AJ006971	DAPK3	death-associated protein kinase 3	2.41	1.30†
AI030681	IKBKE	inhibitor of kappaB kinase epsilon	2.04	1.17*
D00403	IL-1A	interleukin-1 alpha	1.82	1.05†
M98820	IL-1B	interleukin-1 beta	2.93	1.21†
AI073247	IRAK	interleukin-1 receptor-associated kinase 1 binding protein 1	-1.57	-1.33*
M34253	IRF1	interferon regulatory factor 1	24.1	17.9
AA998071	IRF5	interferon regulatory factor 5	1.83	-1.06*
AA799861	IRF7	interferon regulatory factor 7	2.10	1.86†
AA799861	IRF7	interferon regulatory factor 7	3.52†	2.80
AI043702	ITM2B	integral membrane protein 2b	2.09	1.26*
AA799520	ITM2B	integral membrane protein 2b	3.25	1.74†

			Fold Change (IFN-γ-tx OLs / Non-tx OLs)	
Accession No.	Gene Symbol	Gene Name	Immature	Mature
AI236097	ITM2B	integral membrane protein 2B	1.50	1.63*
U53184	LITAF	LPS-induced TNF-alpha factor	12.2†	2.36
U48596	MAP3K1	mitogen activated protein kinase kinase kinase 1	2.55	1.12†
U48596	MAP3K1	mitogen activated protein kinase kinase kinase 1	3.27	-1.15†
AA899681	NDG2	Nur77 downstream protein 2	1.18	2.00*
X63594	NFKBIA	nuclear factor of kappa light chain gene enhancer in B-cells inhibitor, alpha	1.22†	1.52
X63594	NFKBIA	nuclear factor of kappa light chain gene enhancer in B-cells inhibitor, alpha	2.24†	1.68
AA956170	NME3	non-metastatic cells 3	-1.44	-1.52*
AI009756	PDCD6IP	programmed cell death 6 interacting protein	1.68	1.21*
M18330	PKCD	protein kinase C, delta	2.07	1.09†
AA851245	PYCARD	apoptosis-associated speck-like protein containing a CARD	1.28	3.92*
AI007920	RIPK1	receptor (TNFRSF)-interacting serine-threonine kinase 1	2.38	2.43*
AF036537	RIPK3	homocysteine respondent protein HCYP2; receptor-interacting serine-threonine kinase 3	3.29†	1.67
AI231531	TNFRSF6	tumor necrosis factor receptor superfamily, member 6 (Fas)	1.31	2.73*
Survival Genes				
AA799664	AKT1	RAC protein kinase alpha; v-akt murine thymoma viral oncogene homolog 1	1.73	-1.08†
X75856	BI-1	Bax inhibitor 1	2.21	1.26†
X17053	CCL2	chemokine (C-C motif) ligand 2	2.33	7.33
AA955871	IGF1	insulin-like growth factor I, exon 6	-4.10	-2.14*
AA945615	IGF1	insulin-like growth factor I, exon 6	-3.04	-1.85*
AI071236	IGF2	insulin-like growth factor 2	1.55	-1.16*
AI010407	MAEA	macrophage erythroblast attacher (predicted)	1.65	1.06*
AA849796	MDM2	transformed mouse 3T3 cell double minute 2	1.68	1.25*
L26267	NFKB1	nuclear factor kappa B	2.53	1.35†

Accession No.	Gene Symbol	Gene Name	Fold Change (IFN-γ-tx OLs / Non-tx OLs) Immature	Mature
AA944209	PIM1	proviral integration site 1	4.94	1.60*
AA818996	QARS	glutaminyl-tRNA synthetase	3.02	-1.03*
L01624	SGK	serine/threonine protein kinase; serum/glucocorticoid regulated kinase	2.38	-1.48†
AA849015	SOCS-1	suppressor of cytokine signaling-1	1.75	2.15*
AI236947	TRAF2BP	TRAF2 binding protein	3.15	2.56*

Table 2.11 Differential Expression of Genes Involved in various cell functions important for cell growth, development and membrane synthesis. Replicate RNA samples from each treatment group were hybridized to separate arrays. The average of replicate normalized expression estimates (not shown) for each sample group was used to calculate the fold change difference in expression for each gene in the table. Positive fold change values indicate an increase, and negative values indicate a decrease in gene expression in the IFNγ-treated groups. The dagger indicates the Student's t-test p-value was greater than 0.1; the asterisk indicates there was one sample for each treatment group.

			Fold Change (IFN-γ-tx OLs / Non-tx OLs)	
Accession No.	Gene Symbol	Gene Name	Immature	Mature
Cell Adhesion				
AI044792	CD47	CD47 antigen	1.67	2.21*
AI230037	CDA08	T-cell immunomodulatory protein	-2.01	-1.40*
AI101443	COL1A2	procollagen, type I, alpha 2	-1.12†	2.43*
AA955974	COL9A1	collagen alpha 1(IX) chain, long form	-2.67	-1.93*
AA997447	ITGA4	integrin alpha 4	2.05	1.69*
AA858880	ITGAL	integrin alpha L	2.14	1.11*
L21711	LGALS5	galectin-5	2.51	3.75
AA859350	MCAM	melanoma cell adhesion molecule	1.20	2.26*
AI009843	NRP1	neuropilin 1	2.26	1.49*
AI059481	NRXN3	neurexin 3	-1.46	-3.06*
AA997710	PCDH19	protocadherin 19	-2.14	-1.14*
AA874848	THY1	thy-1 cell-surface glycoprotein	-1.32†	-2.42
Cell Cycle				
M80633	ADCY4	adenylyl cyclase type (IV)	2.75	1.11†
X13933	CALM1	calmodulin 1	1.59	1.03†
AA894330	CAMK2D	calcium/calmodulin-dependent protein kinase II, delta	1.83	1.35†
AA998516	CCNA2	cyclin A2	-2.22	-1.60*

Accession No.	Gene Symbol	Gene Name	Fold Change (IFN-γ-tx OLs / Non-tx OLs) Immature	Mature
AI008203	CCNB2	cyclin B2	-1.22	-2.27*
AI111344	CCNH	cyclin H	-1.70	1.05*
AI176278	CCNI	cyclin I	2.82	-1.19*
AI009652	CDC10	cell division cycle 10	1.94	-1.24*
AI009002	CDC25B	cell division cycle 25B	-2.00	-1.69*
AA956688	CDCA3	cell division cycle associated 3	-2.80	-2.21*
AI177871	CDK2AP1	cyclin-dependent kinase 2-associated protein 1	-1.53	-1.64*
AI230798	CDKN3	cyclin-dependent kinase inhibitor 3	-2.14	-2.31*
AI058854	CENPJ	centromere protein J	2.92	3.29*
U66471	CGR19	cell growth regulatory with ring finger domain	2.09	-1.01†
AI059345	CIT	citron	-1.51	-1.64*
AI103556	CKS1B	CDC28 protein kinase 1b	-1.72	-1.54*
AA944180	CKS2	CDC28 protein kinase 2	-3.36	-2.19*
AA943028	CSF1R	colony stimulating factor 1 receptor	1.89	-1.04*
AI010362	CUL1	cullin 1	1.92	-1.08*
AI072269	DNAJA2	DnaJ (Hsp40) homolog, subfamily A, member 2	-1.54	-1.15*
AA891884	ERBB3	v-erb-b2 erythroblastic leukemia viral oncogene homolog 3	1.13†	-1.51
AA893235	G0S2	G0/G1 switch gene 2	-1.39†	-2.37
L32591	GADD45A	growth arrest and DNA-damage-inducible 45 alpha	2.05	1.23
AI070068	GADD45B	growth arrest and DNA-damage-inducible 45 beta	1.59	1.84*
D38560	GAK	cyclin G-associated kinase	1.69	-1.09†
AA925012	GMNN	geminin	-2.04	-1.66*
AI177968	HIRA	histone cell cycle regulation defective homolog A isoform 1	-2.18	-1.15*
AI060200	KIF2C	kinesin family member 2C	-1.95	-1.54*
AI229508	MCM2	minichromosome maintenance deficient 2 mitotin	-1.65	-1.12*

Accession No.	Gene Symbol	Gene Name	Fold Change (IFN-γ-tx OLs / Non-tx OLs) Immature	Mature
AI178465	MDC1	mediator of DNA damage checkpoint 1	-1.54	-1.14*
AI178622	MDM1	transformed mouse 3T3 cell double minute 1	-1.81	-2.69*
AI227852	MGC112830	similar to transcription factor	-1.65	-1.44*
AI044253	MYBL1	myeloblastosis oncogene-like 1	-1.77	-1.36*
AI136733	NUCKS	nuclear ubiquitous casein kinase and cyclin-dependent kinase substrate	-1.68	-1.17*
AA964152	NUSAP1	nucleolar and spindle associated protein 1	-2.07	-1.69*
AI177755	PBEF1	pre-B-cell colony enhancing factor 1	6.99	6.33*
AI103682	POLA1	polymerase (DNA directed), alpha 1	-1.66	-1.22*
AA944231	POLD2	polymerase (DNA directed), delta 2	-1.56	-1.09*
AI070935	POLE2	polymerase (DNA directed), epsilon 2	-1.70	-1.21*
AI137747	POLG	polymerase (DNA directed), gamma	-1.52	-1.30*
AI233712	PPM1D	protein phosphatase 1D magnesium-dependent, delta	-1.57	-1.04*
AI043878	PPP6C	protein phosphatase V	1.56	-1.17*
AI113104	PRC1	protein regulator of cytokinesis 1	-1.82	-1.91*
AI177134	PRIM2	DNA primase, p58 subunit	-1.62	-1.48*
AI170807	RABGAP1	RAB GTPase activating protein 1	-1.62	-1.18*
M15427	RAF1	v-raf-1 murine leukemia viral oncogene homolog 1	1.85	1.12
U11681	RAFT1	rapamycin and FKBP12 target-1 protein	1.58	1.08†
AI236669	REV3L	REV3-like, catalytic subunit of DNA polymerase zeta RAD54 like	-1.75	-1.76*
AA899195	RFC2	replication factor C (activator 1) 2	-1.51	1.13*
AI103093	RFC3	replication factor C (activator 1) 3	-1.82	-1.16*
AI233728	RFC5	replication factor C (activator 1) 5	-1.71	-1.23*
AI011991	RHOG	ras homolog gene family, member G	1.83	1.27*
AI112987	RIS2	retroviral integration site 2	-1.75	-1.40*
AA899590	RRM2	ribonucleotide reductase M2	-3.05	-1.85*

Accession No.	Gene Symbol	Gene Name	Fold Change (IFN-γ-tx OLs / Non-tx OLs) Immature	Mature
AI008106	S100A6	S100 calcium binding protein A6	1.11	2.89*
AI137579	SESN1	sestrin 1	-1.57	-1.07*
AA924839	SKP2	S-phase kinase-associated protein 2 , isoform 2	-1.80	-1.67*
AA945656	SMC2L1	SMC2 structural maintenance of chromosomes 2-like 1	-2.35	-1.77*
U89282	TEP1	telomerase associated protein 1	1.78	1.50†
AA942706	TLK1	tousled-like kinase 1	1.62	1.14*
AA851739	TLK2	tousled-like kinase 2	2.10	1.03*
AI011321	XAB2	XPA binding protein 2	1.67	1.05*
Cell Growth				
AA901152	18S	18S ribosomal RNA	-1.48†	2.27*
AI146189	ANXA3	annexin A3	3.02	1.18*
AA925375	B3GAT1	beta-1,3-glucuronyltransferase 1	-1.52	-2.15*
AI230113	BZW2	basic leucine zipper and W2 domains 2	-1.60	-1.17*
M57276	CD53	CD53 antigen, leukocyte antigen MRC-OX44	4.52	1.34†
AI230215	CDCA8	cell division cycle associated 8	-2.70	-2.32*
AI233361	CHD6	chromodomain helicase DNA binding protein 6	-2.09	-2.56*
X59737	CKMT1	creatine kinase, mitochondrial 1, ubiquitous	-1.69	-1.32†
AA893683	CPSF3	cleavage and polyadenylation specificity factor 3	2.08	-1.11†
AI070318	CTGF	connective tissue growth factor	1.10†	1.68*
AA848813	DP1	deleted in polyposis 1	1.34	1.79*
AA848813	DP1	deleted in polyposis 1	1.23	1.90*
AI070336	EMP1	epithelial membrane protein 1	1.34	3.93*
AA818807	EMP2	epithelial membrane protein 2	1.06	2.12*
AA851618	EMP3	epithelial membrane protein 3	-1.24	2.88*
AA924460	EXOSC8	exosome component 8	-1.51	-1.29*

Accession No.	Gene Symbol	Gene Name	Fold Change (IFN-γ-tx OLs / Non-tx OLs) Immature	Mature
X08056	GAMT	guanidinoacetate methyltransferase	1.12†	-1.52
J03588	GAMT	guanidinoacetate methyltransferase	1.10†	-1.64
U07971	GATM	glycine amidinotransferase	1.09†	-1.88
AI177583	GLT	glycosyltransferase AD-017	-1.55	1.00*
AI180266	HGDF	hepatoma-derived growth factor	-2.57	-1.09*
AI137820	IGFBP10	insulin-like growth factor binding protein 10	-1.09†	4.66*
AI029920	IGFBP5	insulin-like growth factor binding protein 5	-2.28	-2.46†
AI176584	IGFBP5	insulin-like growth factor binding protein 5	-1.77	-3.61*
AI175647	KARS	lysyl-tRNA synthetase	1.43	1.93*
AA892250	KARS	lysyl-tRNA synthetase	3.22	1.96
AA800787	LAMP2	lysosomal membrane glycoprotein 2	2.18	-1.18†
AI177967	LTBP4	latent transforming growth factor beta binding protein 4	-2.31	-1.58*
AI230642	NUP160	nucleoporin 160	-1.53	1.00*
AA900364	ODF2	GLE1 RNA export mediator-like (yeast	-1.53	-1.22*
AI044795	OGFR	opioid growth factor receptor	1.75	1.35*
AI104536	PCBP2	poly(rC) binding protein 2	-1.53	-1.31*
AA819103	PFKL	phosphofructokinase, liver	-2.77	-1.92*
L25387	PFKP	phosphofructokinase, platelet	2.83	2.78
AI103465	POP4	processing of precursor 4	-1.79	1.11*
AA850679	PRPF39	PRP39 pre-mRNA processing factor 39 homolog	1.91	-1.14*
AI177921	PTDSS1	phosphatidylserine synthase 1	-1.50	-1.34*
AA875286	PTOV1	prostate tumor over expressed gene 1	1.74	-1.19†
AI060096	RASL11B	RAS-like family 11 member B	1.67	-1.55*
AI013541	RNASE T2	ribonuclease T2	2.56	1.44*
AI012859	RNASEL	ribonuclease L	1.94	1.43*

Accession No.	Gene Symbol	Gene Name	Fold Change (IFN-γ-tx OLs / Non-tx OLs) Immature	Mature
X62528	RNH	ribonuclease/angiogenin inhibitor	2.32	1.64†
AA800016	RNMT	RNA (guanine-7-) methyltransferase	1.82	1.17†
AI058889	RRS1	RRS1 ribosome biogenesis regulator homolog	-2.00	-1.38*
AI177256	SLFN5	schlafen 5	2.26	2.93†
AA899491	WARS	tryptophanyl-tRNA synthetase	2.69	3.41*
Electron Transport				
AA926200	AOX1	aldehyde oxidase 1	-1.20	2.60*
X54081	COX4A	cytochrome c oxidase 4a	2.24	-1.01†
AI170570	ENTPD5	ectonucleoside triphosphate diphosphohydrolase 5	-1.50	-1.23*
X12355	GRP58	glucose regulated protein 58 kDa	2.34	1.86†
AA925747	MCF2L	Mcf2 transforming sequence-like	-1.56	-1.40*
AA899520	RACGAP1	Rac GTPase-activating protein 1	-1.56	-1.13*
AA893860	TARS	threonyl-tRNA synthetase	1.64	-1.12†
AI171837	TXNL2	thioredoxin-like 2	-2.27	-1.03*
Nuclear mRNA Splicing				
AA819828	CUGBP1	CUG triplet repeat, RNA binding protein 1	-2.01	-1.62*
AI178706	CUGBP2	CUG triplet repeat,RNA-binding protein 2	-1.72	-1.12*
AI136376	HNRNPH1	heterogeneous nuclear ribonucleoprotein H1	-1.66	-1.01*
AI111877	HNRPC	heterogeneous nuclear ribonucleoprotein C	-2.06	-1.14*
AA945952	HNRPD	heterogeneous nuclear ribonucleoprotein D	1.59	1.03*
AI177016	LSM8	LSM8 homolog, U6 small nuclear RNA associated	-1.72	-1.05*
AI176497	MYEF2	myelin basic protein expression factor 2, repressor	-1.55	-1.65*
AI171535	PABPC4	poly A binding protein, cytoplasmic 4	-1.90	-1.58*

Accession No.	Gene Symbol	Gene Name	Fold Change (IFN-γ-tx OLs / Non-tx OLs) Immature	Mature
AI233870	PABPC4	poly A binding protein, cytoplasmic 4	-1.52	-1.21*
AA956626	RBMS3	RNA binding motif, single stranded interacting protein 3	1.02	2.58*
AI171267	SFRS7	splicing factor, arginine/serine-rich 7	-1.81	-1.29*
AI059437	SRRM1	serine/arginine repetitive matrix 1	-1.53	1.02*
AA851909	SYNCRIP	synaptotagmin binding, cytoplasmic RNA interacting protein	2.31	-1.14*
AI232957	TARDBP	TAR DNA binding protein	-1.83	-1.07*
Cell Metabolism				
AI009194	AK2	adenylate kinase 2	1.79	1.42*
AA799466	AK2	adenylate kinase 2	1.70	1.66†
J03190	ALAS1	aminolevulinic acid synthase 1	1.72	-1.12†
J03190	ALAS1	aminolevulinic acid synthase 1	1.50	-1.23†
M12919	ALDOA	aldolase A	2.58	1.10†
AI233343	ASRGL1	asparaginase-like sperm autoantigen	-1.71	-1.33*
AI145601	CAR14	carbonic anhydrase 14	1.08†	-2.55*
AI100768	CAR8	carbonic anhydrase 8	-1.75	-1.92*
AI177443	CERK	ceramide kinase	-1.21†	-2.05*
AI234151	CHST2	carbohydrate sulfotransferase 2	-1.59	1.20*
U52102	CRMP1	collapsin response mediator protein 1	1.52	1.06†
M64755	CSAD	cysteine sulfinic acid decarboxylase	-1.02†	-1.59
M95768	CTBS	chitobiase, di-N-acetyl-	1.60	1.00†
M38566	CYP27	cytochrome P450 27a1	2.17	2.35
U40004	CYP2J3	cytochrome P450 monooxygenase	1.84	3.24†
AA946300	CYP4F1	cytochrome P450-like protein	1.33	3.48*
AA848834	DHDDS	dehydrodolichyl diphosphate synthase	1.89	1.05*

Accession No.	Gene Symbol	Gene Name	Fold Change (IFN-γ-tx OLs / Non-tx OLs) Immature	Mature
AI030907	DHRS1	dehydrogenase/reductase (SDR family) member 1	-1.89	-1.13*
AI170606	DNASEX	deoxyribonuclease I-like 1	1.29†	2.01*
AA851921	ECHDC1	enoyl Coenzyme A hydratase domain containing 1	1.55	-1.15*
X16145	FUCA	fucosidase, alpha-L- 1, tissue	1.93	-1.04†
AI172253	GCSH	glycine cleavage system protein H	-1.81	-1.79*
AI103550	GCSH	glycine cleavage system protein H	-1.68	-1.70*
AA892086	GNS	glucosamine (N-acetyl)-6-sulfatase	2.32	1.21†
AA957007	GSTM5	glutathione S-transferase, mu 5	-1.51	1.00*
M13962	GUSB	glucuronidase, beta	1.22†	-1.57
AA848820	HPGD	NAD-dependent 15-hydroxyprostaglandin dehydrogenase	3.01	2.86*
AA891524	ISOC2	isochorismatase domain containing 2	1.43†	1.54
AI170294	MAN2A2	mannosidase 2 alpha 2	-2.28	-1.25*
AA891670	MAN2B1	mannosidase 2, alpha B1	1.52	-1.10†
Y09333	MTE1	mitochondrial very-long-chain acyl-CoA thioesterase	2.84†	2.32
AA945601	NADK	inorganic polyphosphate/ATP-NAD kinase	2.08	1.42*
AA945601	NADK	inorganic polyphosphate/ATP-NAD kinase	2.05	1.26*
AI059352	NT5	5 nucleotidase	1.40	-2.15*
D10706	OAZ1	ornithine decarboxylase antizyme 1	2.78	1.09†
D10706	OAZ1	ornithine decarboxylase antizyme 1	2.14	1.11†
AA893184	PDHX	pyruvate dehydrogenase complex, component X	1.74	1.19†
AA851370	PIP5K1A	phosphatidylinositol-4-phosphate 5-kinase, type 1 alpha	2.85	1.50*
AA891891	POLS	polymerase (DNA directed) sigma	1.64	1.03†
AI179986	PSPH	phosphoserine phosphatase	-1.60	-1.36*
AA851273	RARRES2	retinoic acid receptor responder 2	-1.04†	2.27*

Accession No.	Gene Symbol	Gene Name	Fold Change (IFN-γ-tx OLs / Non-tx OLs) Immature	Mature
M19257	RBP1	retinol binding protein 1	2.04	-1.32†
AI045256	RECQL	RecQ protein-like	-1.50	-1.26*
D10233	RENBP	renin binding protein	1.87	1.15†
AI236332	SAT	spermidine/spermine N1-acetyl transferase	2.22	1.28*
AI105184	SHMT1	serine hydroxymethyl transferase 1 (soluble)	-1.71	-1.48*
AA998234	SLC25A15	solute carrier family 25 (mitochondrial carrier; ornithine transporter) member 15	-1.78	-1.03*
AA850579	SUCLG2	succinate-Coenzyme A ligase, GDP-forming, beta subunit	2.11	-1.05*
AI011510	TAS1R2	aldehyde dehydrogenase 4 family member A1	1.83	3.60*
AI229638	TK1	thymidine kinase 1	-1.50	-1.43*
AI014130	TYKI	thymidylate kinase family LPS-inducible member	4.04	4.43*
AI111492	TYKI	thymidylate kinase family LPS-inducible member	5.09	8.63*
AI170679	UGP2	UDP-glucose pyrophosphorylase 2	-1.86	-1.18*
Protein Biosynthesis				
AI169284	ARL6IP1	ADP-ribosylation factor-like 6 interacting protein 1	-1.59	-1.18*
AA901245	BOLL	boule-like	-1.39	-1.53*
AI175100	BOLL	boule-like	-1.71	-1.66*
AA818804	BOLL	boule-like	-1.60	-1.33*
AA998690	ITGB4BP	integrin beta 4 binding protein	1.79	1.11*
AI175221	MRPL16	mitochondrial ribosomal protein L16	-1.68	-1.14*
AI104369	MRPL42	mitochondrial ribosomal protein L42	-1.72	-1.03*
AI178900	MRPS15	mitochondrial ribosomal protein S15	-1.52	-1.42*
AA945611	RPL10	ribosomal protein L10	2.04	1.03†
AI228624	RPL23	ribosomal protein L23	-1.77	-1.35*
AA686461	RPL30	ribosomal protein L30	-1.55	-1.32*

Accession No.	Gene Symbol	Gene Name	Fold Change (IFN-γ-tx OLs / Non-tx OLs) Immature	Mature
AI030000	RPL35	ribosomal protein L35	1.49	3.38*
AA850115	SARS2	seryl-tRNA synthetase 2	1.65	-1.04*
Protein Metabolism				
AA946474	CAST	calpastatin	1.56	2.48*
AI233209	CRYM	crystallin, mu	-1.81	-2.12*
S74141	HCTK	tyrosine kinase; hemopoietic cell kinase	2.53	1.42†
AI177543	PTPLA	protein tyrosine phosphatase-like, member a	-2.35	-2.69*
AI045021	TTC10	tetratricopeptide repeat domain 10	-1.44	-2.19*
AA963073	TTK	Ttk protein kinase	-2.20	-1.87*
D30740	YWHAZ	tyrosine 3-monooxygenase/tryptophan 5-monooxygenase activation protein, zeta polypeptide	2.47	1.06†
Protein Modification				
AI104393	ART3	ADP-ribosyltransferase 3	1.16	4.66*
AI177962	AXL	AXL receptor tyrosine kinase	1.29†	4.31*
AI177841	AXL	AXL receptor tyrosine kinase	1.35†	2.61*
M63333	CAMK4	calcium/calmodulin-dependent protein kinase IV	-1.58	1.02†
AA819816	CSNK1A1	casein kinase 1, alpha 1	-1.55	-1.25*
AI179878	GALNT10	UDP-N-acetyl-alpha-D-galactosamine: polypeptide N-acetylgalactosaminyltransferase 10	-1.50	-1.04*
AA924000	JAK1	janus kinase 1	1.52	1.35*
AA943886	PLK2	polo-like kinase 2	1.64	1.70*
AI170309	PPP3CB	protein phosphatase 3, catalytic subunit, beta	-1.71	-1.08*
AA964661	PPP4R2	protein phosphatase 4, regulatory subunit 2	1.50	-1.09*
L34262	PPT	palmitoyl-protein thioesterase	1.83	1.02†

Accession No.	Gene Symbol	Gene Name	Fold Change (IFN-γ-tx OLs / Non-tx OLs) Immature	Mature
AI102009	PRKRA	protein kinase, interferon inducible double stranded RNA dependent activator	-1.52	-1.17*
AI177910	PTPN18	protein tyrosine phosphatase, non-receptor type 18	1.82	1.10*
X58828	PTPN2	protein tyrosine phosphatase, non-receptor type 2	1.55	1.11†
S49400	PTPN5	protein tyrosine phosphatase, non-receptor type 5	1.28	2.26
U28938	PTPRO	protein tyrosine phosphatase, receptor type, O	1.92	-1.86
AI113338	PTPRT	protein tyrosine phosphatase, receptor type, T	-1.86	-1.84*
AI030254	RPS6KC1	ribosomal protein S6 kinase, polypeptide 1	-1.68	1.08*
AI011832	SNRK	SNF related kinase	1.98	1.24*
AI059722	SRPK2	serine/arginine-rich protein specific kinase 2	-1.98	-1.48*
AI102055	SRPK2	serine/arginine-rich protein specific kinase 2	-1.54	-1.22*
Cell Motility				
AI112954	ABI3	ABI gene family, member 3	1.55	-1.13*
AI070848	ACTB	actin, beta	1.62	1.12†
AF083269	ARPC1B	actin related protein 2/3 complex, subunit 1B	2.64	1.15†
AF083269	ARPC1B	actin related protein 2/3 complex, subunit 1B	2.19	1.18†
X76489	CD9	CD9 antigen	2.16	-1.59
AI229547	MARCKS	myristoylated alanine-rich C-kinase substrate	-1.99	1.01*
AI229547	MARCKS	myristoylated alanine-rich C-kinase substrate	-1.69	1.34*
AI010104	MSN	moesin	1.57	2.63*
Cytoskeletal				
AI014072	ADAMTS6	ADAMTS-6 precursor	-2.19	-1.02*
AA892332	ARPC4	actin related protein 2/3 complex, subunit 4	1.56	1.04†
H32978	ARPC5L	actin related protein 2/3 complex, subunit 5-like	-1.58	-1.24*

Accession No.	Gene Symbol	Gene Name	Fold Change (IFN-γ-tx OLs / Non-tx OLs) Immature	Mature
AA891724	BICD2	bicaudal D homolog 2	1.09†	-1.51
AA850040	CAP1	CAP, adenylate cyclase-associated protein 1	1.59	1.10*
AA894004	CAPG	capping protein (actin filament), gelsolin-like	3.02	1.17†
AA944422	CNN3	calponin 3, acidic	1.83	1.68
AA819207	COL1A2	procollagen, type I, alpha 2	-1.33	1.82*
AA859284	COL1A2	procollagen, type I, alpha 2	-1.44	1.82*
X70369	COL3A1	collagen, type III, alpha 1	1.85	-1.48†
AA892506	CORO1A	coronin, actin binding protein 1A	2.14	1.27†
AJ006064	CORO1B	coronin, actin-binding protein 1B	2.85	1.18†
AJ006064	CORO1B	coronin, actin-binding protein 1B	2.40	1.01†
AI232408	DAAM1	dishevelled associated activator of morphogenesis 1	-1.05†	1.82*
AA800743	DBNL	drebrin-like	2.03	1.88†
AI071800	DBNL	drebrin-like	1.45	2.27*
AI177125	DLC2	dynein light chain-2	-1.53	-1.77*
AI103774	DLC2	dynein light chain-2	-1.47	-1.58*
AI103370	FATH	fat tumor suppressor homolog	-1.86	-1.49*
AI176380	KIF2	kinesin heavy chain member 2	-1.69	-1.20*
AA851392	KIF22	kinesin family member 22	-1.83	-1.60*
AA851392	KIF22	kinesin family member 22	-1.78	-1.67*
AA892369	KIFC3	kinesin family member C3	1.20†	-1.70
AI030156	KLHL5	kelch-like 5	-1.78	-1.27*
AI111561	KRT9	keratin 9, type I, cytoskeletal	-1.03†	2.32*
U30938	MAP2	microtubule-associated protein 2	1.14†	-1.59
AI176721	MAPEB1	microtubule-associated protein EB1 (weakly similar)	1.87	2.84
AI227608	MAPT	microtubule-associated protein tau	1.84	-1.52†

			Fold Change (IFN-γ-tx OLs / Non-tx OLs)	
Accession No.	Gene Symbol	Gene Name	Immature	Mature
AI012030	MGP	matrix Gla protein	5.19	6.26
AA944935	MIG12	MID1 interacting G12-like protein	1.58	1.72*
AA924763	MIG12	MID1 interacting G12-like protein	-1.06†	1.86*
AA946377	MYH10	myosin heavy chain 10, non-muscle	-1.66	-1.13*
AI172178	MYH4	myosin, heavy polypeptide 4, skeletal muscle	-1.75	-1.17*
S77858	MYL6	myosin, light polypeptide 6, alkali, smooth muscle and non-muscle	2.39	1.10†
AI030684	NFL	neurofilament, light polypeptide	2.12	3.85*
AA964535	PARVA	parvin, alpha	1.02	1.52*
AA799323	PLEK	pleckstrin	3.36	1.36†
AA964601	PLEKHC1	pleckstrin homology domain containing, family C (with FERM domain) member 1	-1.56	1.37*
AI236227	PLS3	plastin 3 (T-isoform)	-1.05†	1.67*
AI012428	PSCDBP	pleckstrin homology, Sec7 and coiled-coil domains, binding protein	2.73	1.23*
AI144877	SSX2IP	synovial sarcoma, X breakpoint 2 interacting protein	-1.79	-1.23*
AA899649	STMN3	stathmin-like 3	1.01†	-2.42*
AI045848	SVIL	supervillin	1.25	1.67*
AI013247	TAGLN2	transgelin 2; SM22-alpha homolog	1.08†	2.75*
AI175566	TCTEX1	t-complex testis expressed 1	-1.40	-1.70*
AB010119	TCTEX1	t-complex testis expressed 1	1.54†	-1.69
AI169615	VAPA	vesicle-associated membrane protein, associated protein a	-1.59	-1.17*
AA956278	VASP	vasodilator-stimulated phosphoprotein	2.18	1.36*
AI176483	WASF2	WAS protein family, member 2	2.58	-1.01*
Development				
AI235611	ANXA4	annexin A4	1.46†	2.15*
U33553	CSPG5	chondroitin sulfate proteoglycan 5	2.02	-1.30†

			Fold Change (IFN-γ-tx OLs / Non-tx OLs)	
Accession No.	Gene Symbol	Gene Name	Immature	Mature
AI234146	CSRP1	cysteine and glycine-rich protein 1	1.54	1.56†
AI229304	DSCR1L1	Down syndrome critical region gene 1-like 1	-1.07†	-2.35*
AI043809	GAS7	growth arrest specific 7	1.57	1.86*
AA963891	GNAO	guanine nucleotide binding protein, alpha o	1.12†	-2.22*
AA875659	INEXA	internexin, alpha	-1.44†	-1.52
AI072817	LRRN6A	leucine rich repeat neuronal 6A	-2.05	-2.03*
U03414	OLFM1	olfactomedin 1	1.19†	1.55
AI030196	POGZ	pogo transposable element with ZNF domain	-1.56	-1.30*
AI102497	SERPINE2	serine (or cysteine) proteinase inhibitor, clade E, member 2	-1.52	-1.08*
AI229145	SERPINI1	serine (or cysteine) peptidase inhibitor, clade I, member 1	1.37†	-2.79*
AA900057	SNX27	PDZ protein Mrt1	-2.08	-1.01*
S72594	TIMP2	tissue inhibitor of metalloproteinase 2	1.75	1.06†
AI102578	TNFAIP2	TNF-alpha induced protein 2	5.40	7.45*
AI230716	TPM4	tropomyosin 4	-1.61	1.29*
Differentiation				
AA944481	ANGPTL4	angiopoietin-like protein 4	-1.36	2.00*
AI030028	CD34	CD34 antigen	-2.39	-1.28*
AA899893	DEPDC1B	DEP domain containing 1B	-2.19	-1.27*
AA859837	GDA	guanine deaminase	2.65	2.26
AA817826	GPC6	Gpc6 protein	-2.24	-1.18*
AI011448	NOTCH2	notch 2	3.15	-1.32*
AI177354	NUCB1	nucleobindin 1	3.11	4.07*
AA899410	SHC1	Src homology 2 domain-containing transforming protein 1	2.66	1.50*
AI231349	STMN2	stathmin-like 2	1.11†	-1.55*

Accession No.	Gene Symbol	Gene Name	Fold Change (IFN-γ-tx OLs / Non-tx OLs) Immature	Mature
AI228231	TSPAN2	tetraspan 2	-1.35	-2.13*
Proliferation				
AI013902	ANXA7	annexin A7	1.50	1.45*
AI229206	APRIN	androgen-induced proliferation inhibitor	-1.74	-1.24*
AA893621	ATP13A	ATPase type 13A	1.59	1.49
AI231017	BUB3	budding uninhibited by benzimidazoles 3 homolog	-1.58	1.29*
AI179620	CSNK2A1	casein kinase II, alpha 1 polypeptide	-1.81	-1.38*
AI030153	DDRF2	discoidin domain receptor family, member 2	1.27	2.72*
AA859593	EFP	estrogen-responsive finger protein	7.62	4.86
AI229178	FGFR2	fibroblast growth factor receptor 2	1.01†	-2.36*
AI145424	FGFR3	fibroblast growth factor receptor 3	-2.18	-2.14*
AI010226	FLI1	friend leukemia integration 1	2.02	-1.07*
AA851814	GPNMB	glycoprotein (transmembrane) nmb	1.65	2.59*
AA925692	HCLS1	hematopoietic cell specific Lyn substrate 1	1.80	1.00*
AI170366	HDGF	hepatoma-derived growth factor	-1.65	-1.20*
AA997800	KI-67	antigen KI-67	-2.43	-2.08*
AI103106	LMNB1	lamin B1	-3.02	-1.71*
AI013222	PDGFA	platelet derived growth factor alpha	1.46	3.47*
D82071	PTGDS2	prostaglandin D2 synthase 2	1.86	-1.02†
AI104090	RPS4X	40S ribosomal protein S4, X isoform	2.13	1.09*
AI170353	S100A11	S100 calcium binding protein A11	-1.07†	4.00*
AI010351	SCAP2	Src family associated phosphoprotein 2	2.57	1.14*
AI137491	SSR1	signal sequence receptor, alpha	-1.53	-1.07*
AA996959	VDUP1	vitamin D3 up-regulated protein 1	-2.35	-2.04*

Accession No.	Gene Symbol	Gene Name	Fold Change (IFN-γ-tx OLs / Non-tx OLs) Immature	Mature
AA997302	ZFP36	zinc finger protein 36	2.22	-1.01*
Signal Transduction				
AI072842	AKAP11	A-kinase anchor protein 11	-1.69	-1.33*
AA926354	ARL11	ADP-ribosylation factor-like 11	-1.64	-1.66*
AI228929	BAI3	brain-specific angiogenesis inhibitor 3	-1.84	-1.11*
AI045319	BAIAP1	BAI1-associated protein 1	-1.82	-1.41*
AI031002	CDC42EP4	CDC42 effector protein (Rho GTPase binding) 4	-1.78	1.18*
AA851938	CDC42EP4	CDC42 effector protein (Rho GTPase binding) 4	-1.67	-1.29*
AA892496	CHN2	chimerin 2	1.58†	-1.62
X55812	CNR1	cannabinoid receptor 1 (brain)	1.71	-1.13†
AI146166	DLGAP1	PSD-95 binding protein	-1.84	-1.10*
AA943737	EDG1	endothelial differentiation sphingolipid G-protein-coupled receptor 1	-1.87	1.15*
AI112149	EDG2	endothelial differentiation, lysophosphatidic acid G-protein-coupled receptor, 2	1.02†	2.26*
AI112097	FGF13	fibroblast growth factor 13	-1.69	-2.69*
AI179953	GJB2	gap junction membrane channel protein beta 2	-1.41	-3.25*
AI059426	GJB6	gap junction membrane channel protein beta 6	1.76	1.00*
AI228557	GNAI1	guanine nucleotide binding protein, alpha inhibiting 1	-1.10†	-2.76*
AA817892	GNB2	guanine nucleotide binding protein, beta 2	2.03	1.01†
AI232477	GNG5	guanine nucleotide binding protein, gamma 5	1.42†	-1.54
S61973	GRINA	NMDA receptor glutamate-binding subunit	2.48	1.38†
AI058957	HOMER2	homer homolog 2	1.27†	-2.65*
AI009602	IL13RA1	interleukin 13 receptor, alpha 1	2.19	1.88*
AI010211	IQGAP3	IQ motif containing GTPase activating protein 3	-1.51	-1.35*

Accession No.	Gene Symbol	Gene Name	Fold Change (IFN-γ-tx OLs / Non-tx OLs) Immature	Mature
AI060017	LCP2	lymphocyte cytosolic protein 2	4.01	-1.22*
M17412	LOC360721	growth and transformation-dependent protein	1.31†	-1.68
AA893357	MAGI1	membrane associated guanylate kinase interacting protein-like 1	1.55	1.35†
AI102732	MGC109340	microsomal signal peptidase, 23kDa	-2.47	-2.30*
L09119	NRGN	neurogranin	-1.54	-1.01†
AA998124	NUDT3	nudix (nucleotide diphosphate linked moiety X)-type motif 3	-1.84	1.09*
AI030619	PAK4	P21 (CDKN1A)-activated kinase 4	-1.66	-1.04*
AI168973	PDCL3	phosducin-like 3	-1.57	-1.12*
AI102252	PHPT1	phosphohistidine phosphatase 1	-1.55	-1.11*
D83538	PIK4CA	phosphatidylinositol 4-kinase, catalytic, alpha	1.64	1.01†
AI144586	PLEKHB1	evectin-1	-2.04	-1.43*
AI044747	PPP1R14C	protein phosphatase 1, regulatory (inhibitor) subunit 14c	-1.58	-1.12*
AI029941	PPP2R2D	protein phosphatase 2, regulatory subunit B, delta isoform	-1.53	-1.41*
AA925328	RAB40B	Rab40b, member RAS oncogene family	-1.82	-1.41*
AA946057	RAB7	Rab7, member RAS oncogene family	1.55	1.14*
L07925	RALGDS	ral guanine nucleotide dissociation stimulator	1.55	-1.04†
AA944856	RAP1B	Ras-related protein 1b	2.89	1.14†
AI170661	RASA3	Ras p21 protein activator 3	-1.50	1.00*
AA946457	RASGRP3	Ras, guanyl releasing protein 3	-2.07	-1.22*
AI227769	RASSF4	Ras association (RalGDS/AF-6) domain family 4	1.59	4.27*
AI010253	RGD1309362	similar to interferon-inducible GTPase	6.51	10.6*
AA851185	SOCS2	suppressor of cytokine signaling 2	2.14	2.16*
AA899068	TGFBR3	transforming growth factor, beta receptor 3	1.64	-1.09*
AA850542	TRAF4	Tnf receptor associated factor 4	-2.03	-1.24*
AI072698	TRAF4AF1	TRAF4 associated factor 1	-2.01	-2.08*

Accession No.	Gene Symbol	Gene Name	Fold Change (IFN-γ-tx OLs / Non-tx OLs) Immature	Mature
AI145007	TSPAN12	tetraspannin 12, transmembrane 4 superfamily member 12	-2.71	-1.55*
Transcription Regulation				
AI171503	ARTS1	type 1 tumor necrosis factor receptor shedding aminopeptidase regulator	2.29	4.20*
AI072945	CBX6	chromobox homolog 6	-1.51	-1.22*
AI176486	CDKN2B	cyclin-dependent kinase inhibitor 2B (p15, inhibits CDK4)	-1.58	1.03*
AI169557	CDKN2C	cyclin-dependent kinase inhibitor 2C (p18, inhibits CDK4)	-1.83	-1.31*
AA893193	CHD2	chromodomain helicase DNA binding protein 2	1.51	1.02†
AA891829	CIAO1	WD40 protein Ciao1	1.53	1.00†
AI014091	CITED2	Cbp/p300-interacting transactivator, with Glu/Asp-rich carboxy-terminal domain, 2	1.40†	1.54
AI045762	CNOT6L	CCR4-NOT transcription complex, subunit 6-like	1.57	1.12*
AA944413	COPEB	core promoter element binding protein	2.10	2.14*
AI070020	CREB3L4	cAMP responsive element binding protein 3-like 4	2.36	1.19*
AA946461	CREG	cellular repressor of E1A-stimulated genes	2.79	1.07*
AI010116	CRSP6	cofactor required for Sp1 transcriptional activation, subunit 6	1.51	1.07*
AI227592	CSEN	calsenilin, presenilin binding protein, EF hand transcription factor	-1.68	1.00*
AI008205	DATF1	death associated transcription factor 1	2.17	-1.22*
AA799481	EED	embryonic ectoderm development	1.75	-1.02†
AA899415	ELF2	E74-like factor 2	2.34	1.30*
AI101323	ETV5	ets variant gene 5	-2.35	-1.28*
AI175569	FALZ	fetal Alzheimer antigen	-2.11	-1.15*
AI231201	FOXR1	forkhead box R1	-1.55	-1.06*
AI178672	FUSIP1	FUS interacting protein (serine-arginine rich) 1	-1.81	-1.27*
AA892637	ELL3	elongation factor RNA polymerase II-like 3	1.80	1.31†

Accession No.	Gene Symbol	Gene Name	Fold Change (IFN-γ-tx OLs / Non-tx OLs) Immature	Mature
X65948	GTF2B	alpha initiation factor.; general transcription factor IIB	2.05	1.25†
U09551	HBP1	high mobility group box transcription factor 1	1.50	-1.39
AI101116	HERC3	Hect domain and RLD 3	-1.58	-1.37*
AI179857	HIP2	huntingtin interacting protein 2	-2.01	-1.20*
X54250	HIVEP1	human immunodeficiency virus type I enhancer binding protein 1	1.62	1.36†
D37951	HIVEP2	human immunodeficiency virus type I enhancer binding protein 2	2.25	1.11†
AI179987	HMG17	high mobility group protein 17	-1.71	-2.18*
AA996401	HMGB2	high mobility group box 2	-1.72	-1.39†
AI072957	HMGB3	high mobility group box 3	-1.39†	-2.03*
AI178675	HMGN3	high mobility group nucleosomal binding domain 3	-2.12	-1.35*
AI171983	HN1L	HN1-like protein	-1.50	-1.15*
AI178441	HNRPR	heterogeneous nuclear ribonucleoprotein R	-1.70	-1.67*
AA925304	HNRPUL1	heterogeneous nuclear ribonucleoprotein U-like 1	-1.53	-1.10*
AI102887	HOD	homeobox only domain	1.53	-1.29*
AI102739	HOD	homeobox only domain	1.34†	-2.14*
AF000942	ID3	inhibitor of DNA binding 3	1.53	1.40†
AA818860	IDB4	inhibitor of DNA binding 4	1.05†	2.05*
AA819390	ING1	inhibitor of growth family, member 1	-1.59	-1.25*
AI102643	ISGF3G	interferon stimulated gene factor 3, gamma	2.53	3.42*
AA799539	IVNS1ABP	influenza virus NS1A binding protein	1.14†	-2.10
AA858982	LMO4	LIM domain only 4	-1.10†	2.04*
AI177103	MADH3	MAD homolog 3	-1.83	-1.07*
AI231450	MEF2A	myocyte enhancer factor 2C	-1.51	-1.23*
AI231313	MGC116373	similar to HR21spA	-1.68	-1.27*

Accession No.	Gene Symbol	Gene Name	Fold Change (IFN-γ-tx OLs / Non-tx OLs) Immature	Mature
AI071279	MLL5	myeloid/lymphoid or mixed-lineage leukemia 5	-1.63	-1.22*
AI010147	MLLT1	myeloid/lymphoid or mixed lineage-leukemia translocation to 6	1.58	1.00*
AI170291	MTPN	myotrophin	-1.71	-1.30*
AI228667	MTPN	myotrophin	-1.63	-1.47*
AI045608	NFIA	nuclear factor I/A	-1.59	-1.18*
AI171842	NFIB	nuclear factor I/B	-2.36	-1.21*
U14533	NR1H2	nuclear receptor subfamily 1, group H, member 2	1.76	1.14†
AA850038	NR2F2	nuclear receptor subfamily 2, group F, member 2	1.24†	2.20*
AF003926	NR2F6	nuclear receptor subfamily 2, group F, member 6	1.55	1.60†
AA998981	PEG3	paternally expressed 3	-1.71	-1.04*
AI009219	PLEKHA5	pleckstrin homology domain containing, family A member 5	1.55	1.17*
AA894282	PNRC2	proline-rich nuclear receptor coactivator 2	1.13†	-1.52
AA942959	PPP1R1B	protein phosphatase 1, regulatory (inhibitor) subunit 1B	-1.46	-3.21*
AA924754	PRRX1	paired related homeobox 1	-1.53	1.00*
AA851793	PURB	pur-beta	-2.42	-1.79*
AI045231	RUNX1	runt related transcription factor 1	1.59	1.09*
AI227638	SATB1	special AT-rich sequence binding protein 1	-1.97	-1.37*
AA799614	SIRT2	sirtuin (silent mating type information regulation 2 homolog) 2	2.18	-1.35†
AA957591	SMARCA4	SWI/SNF related, matrix associated, actin dependent regulator of chromatin, subfamily a, member 4	-1.82	-1.23*
AA957591	SMARCA4	SWI/SNF related, matrix associated, actin dependent regulator of chromatin, subfamily a, member 4	-1.71	-1.23*
AI177058	SNAPC2	small nuclear RNA activating complex, polypeptide 2	-1.55	-1.08*
U83883	SND1	staphylococcal nuclease domain containing 1	1.80	1.07†

Accession No.	Gene Symbol	Gene Name	Fold Change (IFN-γ-tx OLs / Non-tx OLs) Immature	Mature
AA900619	SNRPB	similar to small nuclear ribonucleoprotein B	2.45	-1.07*
AA963855	SOX11	SRY-box containing gene 11	1.66	1.71*
AI137765	SOX4	SRY-box containing gene 4	-1.72	-1.09*
AI073207	SOX6	SRY-box containing gene 6	-1.55	-1.03*
AI070313	SP110	SP110 nuclear body protein	7.05	7.44*
AI178187	SP140	SP140 nuclear body protein isoform 1	2.24	1.32*
AA892553	STAT1	signal transducer and activator of transcription 1	19.7	17.3
AA799569	STAT2	signal transducer and activator of transcription 2	7.77	5.03
AI236828	STAT3	signal transducer and activator of transcription 3	1.74	2.21*
AI008865	STAT3	signal transducer and activator of transcription 3	1.61	2.20*
AI230912	TAF13	TAF13 RNA polymerase II, TATA box binding protein (Tbp)-associated factor	-1.52	-1.52*
AI009780	TAF1A	TATA box binding protein (Tbp)-associated factor, RNA polymerase I, A	2.28	3.55*
AA964863	TAF4	Tbp-associated factor 4	-1.99	-2.26*
AI231172	TCERG1	transcription elongation regulator 1	-1.55	-1.52*
AI008415	TCF4	transcription factor 4	-1.79	-1.50*
AA849929	TCF4	transcription factor 4	-1.52	-1.24*
L25785	TGFB1I4	transforming growth factor beta 1 induced transcript 4	1.24†	-1.62
AA850509	TRIP13	thyroid hormone receptor interactor 13	-2.01	-1.66*
AA956638	UHRF1	ubiquitin-like, containing PHD and RING finger domains, 1	-1.79	-1.69*
AA891717	USF1	upstream transcription factor 1	1.50	1.07†
AA819367	VEZF1	vascular endothelial zinc finger 1	-1.58	-1.58*
AI175794	XPO1	exportin 1, CRM1 homolog	-1.62	-1.58*
AA924380	ZFP131	zinc finger protein 131	-1.55	1.01*

Accession No.	Gene Symbol	Gene Name	Fold Change (IFN-γ-tx OLs / Non-tx OLs) Immature	Mature
AI010795	ZFP276	zinc finger protein 276	1.52	1.03*
AI175753	ZFP307	zinc finger protein 307	-1.58	1.03*
AI231074	ZNF541	zinc finger protein 541	-1.28	-2.29*
Translation Initiation				
L29281	EIF2A	eukaryotic translation initiation factor 2A	4.01	3.10
AI031019	EIF2B1	eukaryotic translation initiation factor 2B, subunit 1 alpha	1.15†	-1.53
AI031019	EIF2B1	eukaryotic translation initiation factor 2B, subunit 1 alpha	1.36†	-1.67
AI175938	EIF2C1	eukaryotic translation initiation factor 2C, 1	-1.93	-1.13*
AI172206	EIF4B	eukaryotic translation initiation factor 4B	-1.61	-1.28*
AI178816	EIF4E	eukaryotic translation initiation factor 4E	-1.89	-1.37*
AI101338	EIF4E3	eukaryotic translation initiation factor 4E member 3	1.11†	2.32*
AA926205	EIF4EBP2	eukaryotic translation initiation factor 4E binding protein 2	-2.36	-1.12*
Transport				
AA848829	ABCA1	ATP-binding cassette, sub-family A member 1	2.53	1.36*
M60322	ALDR1	aldose reductase	2.31	1.43†
M60322	ALDR1	aldose reductase	1.56	1.30†
U75917	AP2S1	adaptor-related protein complex 2, sigma 1 subunit	1.77	1.04†
U75917	AP2S1	adaptor-related protein complex 2, sigma 1 subunit	1.86	-1.02†
AI235942	AQP4	aquaporin 4	-1.63	-1.43*
AA850290	ATP10D	ATPase, class V, type 10D	4.17	1.10*
AI176376	ATP1B1	ATPase Na+/K+ transporting beta 1	1.33	-2.34*
AA817814	ATP1B2	ATPase, Na+/K+ transporting, beta 2	-1.61	1.08*

Accession No.	Gene Symbol	Gene Name	Fold Change (IFN-γ-tx OLs / Non-tx OLs) Immature	Mature
Y12635	ATP6B2	ATPase, H+ transporting, lysosomal (vacuolar proton pump), beta 56/58 kDa, isoform 2	1.88	1.18†
AI013039	ATP6K	vacuolar proton-ATPase subunit M9.2	1.88	1.44*
AI172204	BCAP29	B-cell receptor-associated protein 29	-1.79	-1.09*
AI175027	BET1	blocked early in transport 1 homolog	-1.59	-1.24*
J05122	BZRP	benzodiazepin receptor	1.66	1.31†
M86621	CACNA2D1	calcium channel, voltage-dependent, alpha2/delta subunit 1	-1.53	-1.20†
AA956900	CBR3	NADPH-dependent carbonyl reductase, carbonyl reductase 3	-1.57	1.00*
X66494	CHOT1	choline transporter	-1.12†	-2.15
AI012221	CLIC1	chloride intracellular channel 1	1.43	2.72*
AA851229	CLIC2	chloride intracellular channel 2	1.90	1.47*
AI168975	CNDP2	cytosolic nonspecific dipeptidase (glutamate carboxypeptidase-like protein 1)	1.56	1.13*
L33869	CP	ceruloplasmin	2.69	1.98†
AI010470	CP	ceruloplasmin	2.36	5.65*
AF007107	CYB5	soluble cytochrome b5	1.61	-1.19†
D00568	CYP11B2	cytochrome P450, subfamily 11B, polypeptide 2	1.60	-1.07†
J02852	CYP2A3A	cytochrome P450, subfamily IIA	1.72	-1.08†
AA945571	CYP2C6	cytochrome P450, subfamily IIC6	1.70	-1.09†
D85035	DPYD	dihydropyrimidine dehydrogenase	1.68	2.03†
D63772	EAAC1	neuronal high affinity glutamate transporter; solute carrier family 1, member 1	1.16†	-1.75
AA957585	EHD3	EH-domain containing 3	1.71	1.29*
AI176596	ENTH	enthoprotin	-1.50	-1.17*
AI059566	EPB4.1L4B	erythrocyte protein band 4.1-like 4b	-1.54	1.05*
AI009344	FXYD1	FXYD domain-containing ion transport regulator 1	1.13	4.02*
U38379	GGH	gamma-glutamyl hydrolase precursor	-1.08†	-1.53

Accession No.	Gene Symbol	Gene Name	Fold Change (IFN-γ-tx OLs / Non-tx OLs) Immature	Mature
X54656	GLURK3	glutamate receptor, ionotropic, AMPA3 (alpha 3)	-1.76†	-1.72
AA924630	GRHPR	glyoxylate reductase/hydroxypyruvate reductase	-1.65	-1.02*
D16478	HADHA	mitochondrial long-chain enoyl-CoA hydratase/3-hydroxyacyl-CoA dehydrogenase alpha-subunit of mitochondrial trifunctional protein	1.61	1.26†
AA851497	HBA-A1	hemoglobin alpha, adult chain 1	1.64	1.04*
AA899367	HSD17B2	hydroxysteroid dehydrogenase 17 beta, type 2	-1.76	1.01*
AI236145	HSD17B7	hydroxysteroid dehydrogenase 17 beta, type 7	1.30	-1.52
AA891785	IDH2	isocitrate dehydrogenase 2 (NADP+), mitochondrial	1.68	1.12†
AI011824	IDH3B	NAD+-specific isocitrate dehydrogenase b subunit	1.53	1.01*
AI111872	IMP9	importin 9	-1.81	-1.74*
AA848315	IMPDH2	inosine monophosphate dehydrogenase 2	-1.57	1.04*
AA849817	KCNAB1	potassium voltage-gated channel, shaker-related subfamily, beta member 1	-1.85	-1.69*
AI007861	KCNAB3	potassium voltage gated channel, shaker related subfamily, beta member 3	1.70	-1.02*
AA818016	KIF20A	kinesin family member 20A , rabkinesin-6	-3.32	-2.24*
AI231497	KPNA2	karyopherin (importin) alpha 2	-1.87	-1.39*
AA851873	KPNB1	karyopherin (importin) beta 1	-1.52	-1.01*
AA945166	MCFD2	multiple coagulation factor deficiency 2	1.62	1.06*
AI009678	MYRIP	myosin VIIA and Rab interacting protein	-1.57	1.01*
AA875268	NDUFS7	NADH dehydrogenase (ubiquinone) Fe-S protein 7	1.87	1.05†
AA799609	NUP98	nucleoporin 98	1.62	-1.18
AA901035	OSBPL6	oxysterol binding protein-like 6	-1.52	1.05*
U47031	P2RX4	purinergic receptor P2X, ligand-gated ion channel, 4	3.01	1.49†
X02918	P4HB	prolyl 4-hydroxylase, beta polypeptide	2.04	-1.06†
AI231465	PDK3	pyruvate dehydrogenase kinase, isoenzyme 3	-1.72	-1.48*

Accession No.	Gene Symbol	Gene Name	Fold Change (IFN-γ-tx OLs / Non-tx OLs) Immature	Mature
AA946250	PR	voltage-dependent calcium channel gamma subunit-like protein	3.15	1.08*
AI171526	PRICKLE1	prickle-like 1	-1.09	-2.05*
AA799616	PTTG1IP	pituitary tumor-transforming 1 interacting protein	1.85	-1.09†
D79221	RA410	vesicle transport-related protein	1.73	1.19†
AI179939	RAB2	Rab2, RAS oncogene family-like	6.67	9.12*
M83678	RAB13	Rab13	1.95	2.84
AI007905	RAB6B	Rab6b, member RAS oncogene family	-1.56	-1.61*
AA866460	RNP24	coated vesicle membrane protein	1.80	-1.23†
AA956992	SCAMP3	secretory carrier membrane protein 3	-1.62	1.02*
AI146177	SFXN5	sideroflexin 5	-1.66	1.08*
AI104173	SLC11A1	solute carrier family 11 (proton-coupled divalent metal ion transporters), member 1	2.71	-1.05*
AA892390	SLC11A2	solute carrier family 11 (proton-coupled divalent metal ion transporters), member 2	1.18†	-1.57
AA925961	SLC12A2	solute carrier family 12, member	-1.43	-2.28*
U75395	SLC12A4	solute carrier family 12, member 4	2.05	1.49†
AA799691	SLC12A7	solute carrier family 12 (potassium/chloride transporters), member 7	1.76	1.84†
AB000280	SLC15A4	peptide/histidine transporter	1.93	-1.56
AI112459	SLC21A14	solute carrier family 21 (organic anion transporter), member 14	-1.99	-1.76*
AA998949	SLC24A6	solute carrier family 24 (sodium/ potassium/calcium exchanger), member 6	2.84	1.43*
AA925662	SLC32A2	solute carrier family 31, member 2	1.83	1.30*
AA957643	SLC40A1	solute carrier family 39 (iron-regulated transporter), member 1	-1.08†	1.56*
AI229664	SLC40A1	solute carrier family 39 (iron-regulated transporter), member 1	-1.03†	1.62*
AA943700	SLC6A11	solute carrier family 6 (neurotransmitter transporter, GABA), member 11	1.51	-1.18*
AA899235	SLC7A8	solute carrier family 8 (cationic amino acid transporter, Y+ system) member 7	1.76	-1.59*

Accession No.	Gene Symbol	Gene Name	Fold Change (IFN-γ-tx OLs / Non-tx OLs) Immature	Mature
AA999064	SMOX	spermine oxidase	1.59	-1.02*
AA892759	SNAP23	synaptosomal-associated protein 23	1.63	-1.02†
AA943153	SNAP25	synaptosomal-associated protein 25	1.45†	-3.73*
AI030877	SNX10	sorting nexin 10	1.69	2.41*
L20821	STX4A	syntaxin 4	2.39	1.44†
AI102079	STXBP1	syntaxin binding protein 1	1.53	1.49
AA859088	SYT4	synaptotagmin 4	-1.09†	-2.29*
AI228125	SYT4	synaptotagmin 4	1.05†	-2.09*
AI237645	TFRC	transferrin receptor	-1.40†	-2.27*
AI146033	TIMM9	translocase of inner mitochondrial membrane 9 homolog	-1.56	-1.24*
AI013157	TMED3	transmembrane emp24 domain containing 3	1.66	1.10*
AI008536	TRAPPC4	trafficking protein particle complex 4	1.74	1.03*
AA899079	TTYH1	tweety homolog 1	1.01†	-1.50*
AI227624	TTYH1	tweety homolog 1	-2.09	-1.51*
AI012433	UA20	ATPase, class VI, type 11A	1.75	-1.26*
AI007981	UCRC	ubiquinol-cytochrome c reductase complex 7.2kDa protein isoform a	1.54	-1.12*
AB013732	UGDH	UDP-glucose dehydrogeanse	1.09†	-1.57
AI234533	UNC93B	Unc93 homolog B	2.07	1.09*
AI010239	UQCRC1	ubiquinol-cytochrome c reductase core protein 1	1.75	1.00*
AF054826	VAMP5	vesicle-associated membrane protein 5	1.79	3.43
AA848348	VDAC1	voltage-dependent anion channel 1	1.83	-1.05*
AI045409	XKR5	XK-related protein 5	-2.13	-1.78*
AI233182	XPOT	exportin, tRNA	-1.64	-1.31*

Table 2.12 Differential expression of genes of unknown function. Replicate RNA samples from each treatment group were hybridized to separate arrays. The average of replicate normalized expression estimates (not shown) for each sample group was used to calculate the fold change difference in expression for each gene in the table. Positive fold change values indicate an increase, and negative values indicate a decrease in gene expression in the IFNγ-treated groups. The dagger indicates the Student's t-test p-value was greater than 0.1; the asterisk indicates there was one sample for each treatment group.

			Fold Change (IFN-γ-tx OLs / Non-tx OLs)	
Accession No.	Gene Symbol	Gene Name	Immature	Mature
AI136833	DUFD1	DUF729 domain containing 1	-2.49	-2.06*
AI030494	KCTD2	potassium channel tetramerisation domain containing protein 2	-2.12	-1.19*
AI237713	NS5ATP9	NS5A (hepatitis C virus) transactivated protein 9	-2.10	-1.92*
AI137337	RGD1308877	similar to CGI-09 protein	-2.05	-1.25*
AI012208	CAV	caveolin	-2.01	-1.47*
AI029608	IBRDC3	IBR domain containing 3	4.93	4.27*
AA850577	NCOR1	nuclear receptor co-repressor 1	2.55	-1.04*
AI009752	LOC367314	similar to FLI-LRR associated protein-1	2.44	1.20*
AI030755	FBXW17	F-box and WD-40 domain protein 17	2.36	3.08*
AA850112	SURF4	surfeit protein 4	2.30	-1.05*
AI010974	COMMD4	COMM domain containing 4	2.22	1.04*
AI030921	LOC501065	similar to LNV	2.22	1.53*
AI059844	FLN29	FLN29 gene product	2.09	1.84*
AI058667	LOC289181	similar to IQ motif and WD repeats 1	2.00	-1.27*

Table 2.13 Differential Expression of ESTs. ESTs were unidentifiable by BLAST algorithm against the Genbank database. Replicate RNA samples from each treatment group were hybridized to separate arrays. The average of replicate normalized expression estimates (not shown) for each sample group was used to calculate the fold change difference in expression for each gene in the table. Positive fold change values indicate an increase, and negative values indicate a decrease in gene expression in the IFNγ-treated groups. The dagger indicates the Student's t-test p-value was greater than 0.1; the asterisk indicates there was one sample for each treatment group.

	Fold Change (IFN-γ-tx OLs / Non-tx OLs)	
Accession No.	Immature	Mature
AA925743	-3.65	-1.51*
AA925824	-3.29	-1.44*
AA849714	-3.18	-1.62*
AI175283	-2.92	-1.24*
AI071227	-2.61	-1.63*
AI101818	-2.48	-1.20*
AI144771	-2.44	-2.03*
AI171307	-2.34	-1.21*
AI104521	-2.33	-1.23*
AA945100	-2.28	1.02*
AI111551	-2.26	-1.72*
AA957836	-2.22	-1.34*
AI136871	-2.21	-1.53*
AI175590	-2.19	-1.52*
AI144824	-2.19	-1.08*
AI171367	-2.17	-1.36*
AI176490	-2.15	-1.27*
AA946046	-2.14	-1.04*
AI230370	-2.09	-1.75*

	Fold Change (IFN-γ-tx OLs / Non-tx OLs)	
Accession No.	Immature	Mature
AI029480	2.24	1.74*
AI058761	2.24	-1.09*
AI233121	2.24	1.63*
AI059875	2.23	-1.11*
AI059735	2.19	-1.05*
AI010719	2.19	-1.05*
AA997460	2.18	-2.15*
AA901178	2.12	1.02*
AA800224	2.09	1.55
AI007721	2.09	-1.18*
AI233164	2.09	-1.49*
AI011183	2.08	1.24*
AI045042	2.08	1.07*
AA924764	2.07	2.82*
AI043759	2.06	2.10*
AI059740	2.05	-1.06*
AI227669	2.03	2.68*
AA800199	2.00	1.07†
AI070107	1.95	2.96*

Accession No.	Fold Change (IFN-γ-tx OLs / Non-tx OLs) Immature	Mature
AI229198	-2.04	-1.82*
AI176172	-2.03	-1.42*
AI168940	-2.02	-1.67*
AI008246	-2.01	-1.35*
AI112043	-2.00	-1.58*
AA964426	-1.94	-2.14*
AI043985	-1.92	2.06*
AI232128	-1.73	-2.31*
AA997109	-1.73	-1.55*
AI234914	-1.65	-2.15*
AI011639	-1.63	-1.14*
AA818158	-1.62	-2.98*
AI071973	-1.60	-2.11*
AI070585	-1.57	-1.95*
AI171800	-1.50	-2.01*
AA997015	41.4	49.7*
AI044983	26.3	29.7*
AA819788	16.1	31.2*
AA998964	12.5	12.1*
AA899109	11.0	5.97*
AI058707	8.40	1.46*
AA818937	7.56	18.6*
AA891220	7.47	5.00
AA924350	5.34	6.07*
AI071166	5.32	3.79*
AI060183	4.93	-1.02*

Accession No.	Fold Change (IFN-γ-tx OLs / Non-tx OLs) Immature	Mature
AA998677	1.92	-2.21*
AI009713	1.90	2.25*
AA944289	1.87	2.13*
AI029829	1.70	2.12*
R46931	1.70	2.24*
AA851040	1.70	2.54*
AA801255	1.63	-1.12*
AI232924	1.62	2.94*
AA964627	1.62	8.44*
AI010179	1.51	2.19*
AA925101	-1.18	-4.98*
AA965107	1.20†	-3.91*
AI043990	-1.17†	-3.35*
AA925994	1.28	-3.07*
AI070905	-1.37	-3.03*
AI101500	-1.05†	-2.89*
AI045330	1.07†	-2.76*
AI101016	1.22†	-2.64*
AA998650	1.13	-2.60*
AI102037	-1.49	-2.53*
AI045116	-1.45	-2.49*
AA998732	-1.20	-2.49*
AI071467	-1.04	-2.46*
AA997945	1.08	-2.46*
AI172541	-1.03†	-2.39*
AI008647	1.05	-2.35*

Accession No.	Fold Change (IFN-γ-tx OLs / Non-tx OLs) Immature	Mature
AA998576	4.92	6.72
AI012648	4.81	1.36*
AI009770	4.50	3.54*
AI234162	4.44	4.27*
AI231805	4.10	1.67*
AI059652	3.96	-1.10*
AI112362	3.95	5.09*
AI012552	3.78	4.16*
AA858505	3.77	5.41*
AA998169	3.58	-1.07*
AA799804	3.48	-1.07†
AA963279	3.32	10.2*
AI030026	3.29	2.64*
AA849519	3.08	-1.14*
AA851065	3.06	2.97*
H31418	2.85	1.42†
AA924573	2.81	2.72*
AI138040	2.66	2.28*
AI029790	2.65	1.52*
AA849042	2.61	1.25*
AI059078	2.58	2.45*
AA851364	2.47	1.11*
AA849720	2.42	1.27*
AA892284	2.40	-1.03†
AI176136	2.33	-1.82*
AA801051	2.33	1.18*

Accession No.	Fold Change (IFN-γ-tx OLs / Non-tx OLs) Immature	Mature
AI235186	1.09†	-2.26*
AI059568	-1.03†	-2.22*
AI070118	-1.21†	-2.16*
AI071504	-1.19†	-2.16*
AA963228	-1.24	-2.16*
AI069939	1.27	-2.15*
AI101009	-1.08†	-2.11*
AA944926	-1.38	-2.11*
AI112807	1.32†	-2.11*
AI175668	-1.18†	-2.10*
AI233181	1.27†	-2.08*
AI009142	1.30	5.49*
AI029264	1.30	3.90*
AI137286	1.17	3.89*
AA944162	-1.08	3.46*
AI072476	-1.02†	3.44*
AA818801	1.43	3.39*
AA997849	1.46	3.11*
AI071755	2.13†	3.08*
AA850916	-1.08	2.92*
AA925256	-1.02	2.77*
AA924660	1.05†	2.64*
AI043958	1.44	2.62*
AI175045	-1.04	2.55*
AA956304	1.35	2.51*
AA926036	1.25	2.50*

Accession No.	Fold Change (IFN-γ-tx OLs / Non-tx OLs) Immature	Mature
AA893869	2.33	1.58
AI177415	2.33	1.76*
AA998356	2.31	1.64*
AA817708	2.31	1.03*
AI045343	2.30	-1.12*
AA851361	2.30	1.27*
AA850686	2.29	-1.13*
AI059095	2.28	4.23*
AI176599	2.25	1.04*
AI013657	2.25	3.01*
AI045577	2.25	-1.09*

Accession No.	Fold Change (IFN-γ-tx OLs / Non-tx OLs) Immature	Mature
AI059241	1.30	2.49*
AI102833	-1.35†	2.48*
AI236053	1.10†	2.25*
AI008019	-1.10	2.20*
AA944838	-1.32	2.17*
AA925074	1.31	2.13*
AA963192	1.43	2.07*
AI012475	-1.02	2.06*
AI058995	1.44	2.04*
AI144865	-1.05†	2.02*

CHAPTER THREE

EFFECTS OF INTERFERON-GAMMA ON DEMYELINATION AND REMYELINATION IN CUPRIZONE-TREATED MICE

INTRODUCTION

Interferon-gamma (IFN-γ) is a pleiotropic cytokine secreted by activated T lymphocytes and natural killer cells with receptors on all cell types except erythrocytes. This cytokine is an important modulator of the immune system and has been implicated in playing a deleterious role in immune-mediated diseases of the central nervous system (CNS) including multiple sclerosis (MS) in humans and experimental autoimmune encephalomyelitis (EAE) in rodents (reviewed in Popko et al., 1997; Baerwald et al., 1999; reviewed in Steinman, 2001). IFN-γ is not normally present in the CNS; however, it has been found in the cerebral spinal fluid and demyelinating lesions of MS patients (Panitch, 1992; Miller et al., 1995; reviewed in Roland and McFarland, 1995). Furthermore, administration of the cytokine to MS patients exacerbated the disease (Panitch et al., 1987), and IFN-γ antibodies slowed its progression (Skurkovich et al., 2001).

In some types of EAE and in cuprizone-induced demyelination, there is a relapsing-remitting cycle whereby demyelination is followed by periods of recovery (Franklin, 2002; Bruck et al., 2003). A similar situation occurs in 85% of MS cases with exacerbations lasting several weeks followed by sometimes long periods of partial recovery. Over time, the number of partially remyelinated and irreparable lesions increases to the point that patients enter a secondary progressive phase of the disease (Trapp et al., 1999).

MS is the most common demyelinating disease of the CNS, affecting approximately 2.5 million people world-wide, most often in the second to forth decade of life and with Northern American/Northern European and female bias (Compston and Coles, 2002; reviewed in Noseworthy, 1999). The etiology and contributing factors of MS remain elusive, in part due to the extreme variability of symptoms and rate of progression, but it is now widely accepted that MS is an autoimmune inflammatory disorder with both environmental and genetic elements influencing its course (Raine, 1994; Noseworthy, 1999).

During exacerbations, demyelinated axons are unable to properly propagate electrical signals due to the loss of demarcated nodes of Ranvier, the short spaces between myelin sheath internodes at which sodium channels cluster and provide the depolarization/ repolarization necessary for rapid, salutatory conduction. In periods of remission, oligodendrocyte progenitor cells (OPCs) migrate to lesion sites where they differentiate into mature oligodendrocytes (OLs) and extend membrane processes, which become sheaths of myelin that wrap bare axons and nearly fully restore signal conduction (Mason et al., 2000; Matsushima and Morell, 2001). A single OL can extend up to ~50 myelin processes, which requires enormous amounts of plasma membrane lipid and protein synthesis (Smith, 1996).

While T cells and macrophages infiltrate the CNS and secrete cytokines in EAE, cuprizone-induced demyelination is largely non-immune-mediated, making it an excellent model for studying the effect of a single cytokine on demyelination and remyelination. In this study, we have combined the cuprizone model of demyelination/remyelination (Matsushima and Morell, 2001) with a transgenic line of mice in which astrocytes, under the tetracycline-inducible system, ectopically express and secrete IFN-γ in the CNS (Lin et al., 2004). This system allows for both spatial and temporal control of IFN-γ expression.

MATERIALS AND METHODS

Transgenic Animals and Cuprizone Treatment (Figures 3.1-3.3)

Two single transgenic lines of mice on the C57BL/6 background were exploited to create a double transgenic line expressing IFN-γ as previously described (Lin et al., 2004; Lin et al., 2006). Briefly, line 110 GFAP/tTA was crossed to line 184 TRE/IFN-γ to produce double transgenic GFAP/tTA x TRE/IFN-γ mice. These animals express the tetracycline transactivator protein (tTA), which binds to a modified CMV/TRE promoter containing tTA binding sites to drive IFN-γ expression. The transgene was suppressed from conception by adding 0.05mg/ml of doxycycline (dox) to the drinking water until either 6- or 8wks of age. Cuprizone treatment of male double transgenic mice receiving dox began at 6wks of age by incorporating 0.2% cuprizone (Sigma-Aldrich, St. Louis, MO) into milled chow. Animals were returned to normal chow after 6wks of treatment (12wks of age).

All animal procedures were conducted in the laboratory of Brian Popko at the University of Chicago in complete compliance with the NIH *Guide for the Care and Use of Laboratory Animals* and were approved by the Institutional Animal Care and Use Committee of The University of Chicago.

RNA Isolation, Amplification, and Microarray Hybridization

RNA was isolated according to previously-described methods (Lin et al., 2006). Briefly, mice were perfused with ice-cold phosphate-buffered saline (PBS), and RNA was isolated from the corpus collosum (Jurevics et al., 2002) using Trizol Reagent (Invitrogen, Carlsbad, CA) followed by DNAseI (Invitrogen, Carlsbad, CA) treatment to eliminate genomic DNA.

100ng of total RNA from each corpus collosum was used to synthesize cDNA according to the GeneChip® Eukaryotic Small Sample Target Labeling Protocol (Affymetrix). Two rounds of amplification were conducted using T7-$(dT)_{24}$ primer (Life Technologies). Biotinylated cRNA was then generated using the BioArray High Yield RNA Transcription Kit (Life Technologies), then subsequently fragmented in 5X fragmentation buffer (200mM Tris-acetate pH 8.1, 500mM KOAc and 150mM MgOAc) at 94°C for 35 min. 15μg of fragmented cRNA was added to hybridization cocktail (50pM control oligonucleotide [B2, *BioB*, *BioC*, *BioD* and *Cre*], 0.01mg/ml herring sperm DNA, 0.5mg/ml acetylated BSA, 100mM MES, 1M [Na^+], 20mM EDTA and 0.01% Tween 20). 10μg of cRNA in cocktail was hybridized to each array for 16 hours at 45°C in the GeneChip® Hybridization Oven 640 (Affymetrix). Microarrays were then washed, stained with R-phycoerythrin streptavidin in the GeneChip® Fluidics Station 400 (Affymetrix), and scanned in the Hewlett Packard GeneChip® Scanner 3000 7G 4C using GeneChip® Operating Software (Affymetrix). cRNA quality was assessed by examining the intensity ratio of 5':3' probe pair binding of control genes.

Microarray Analysis

The mouse genome MOE 430 2.0 GeneChip® (Affymetrix) containing probe sets representing over 45,000 genes and expressed sequence tags (ESTs) was used for all hybridization reactions, and three independent hybridizations were performed for each treatment group. Hybridization intensities were summarized with the Robust MultiArray Analysis (RMA) algorithm (Irizarry et al., 2003) to generate an expression estimate for each probe set (gene). Expression estimates were normalized using GeneSpring® software

(Agilent Technologies) as follows: 1) negative expression estimates were floored to 0.01, 2) the top 90% of expression estimates was used to calculate the 50th percentile for each array, and 3) expression estimates were normalized to the 50th percentile value of the corresponding array. Normalized expression estimates were averaged across replicate samples and significance of difference between treatment groups was determined by Student's t-test (p-value<0.1). We report here differential mRNA expression as the fold change between IFN-γ-expressing and non-expressing sample groups. Gene function information and probe set annotations were obtained from GeneSpring GX (Agilent Technologies), Netaffx™ (Affymetrix; www.affymetrix.com), the National Center for Biotechnology Information (NCBI; www.nbci.nlm.nih.gov) and literature review. ESTs were identified, when possible, by BLAST search of the nucleotide database (www.ncbi.nlm.nih.gov/BLAST). Pathway information was obtained from the Gene Map Annotator and Pathway Profiler (GenMAPP; Gladstone Institutes, University of California at San Francisco; www.genmapp.org), PathArt© (Jubilent Biosys), NetAffx™ (Affymetrix), and primary literature.

RESULTS AND DISCUSSION

In order to examine the effects of a single cytokine, IFN-γ, on demyelination and remyelination, we used the tetracycline-inducible system to ectopically express IFN-γ in astrocytes at two different time points (Lin et al., 2004) and used the neurotoxicant cuprizone (bis-cyclohexanone oxaldihydrazone) to induce demyelination (Matsushima and Morell, 2001). The tetracycline transactivator protein (tTA) was under the transcriptional control of the astrocyte-specific glial fibrillary acidic protein (GFAP) promoter in one line of mice (110, GFAP/tTA), and in a second line, IFN-γ was under the control of the cytomegalovirus

(CMV) promoter than had been modified to contain tetracycline response element (TRE) sequences (184, TRE/IFN-γ). These two lines were crossed to produce double transgenic animals (GFAP/tTA x TRE/IFN-γ) in which the tTA molecule binds the TRE sites on the CMV promoter allowing transcription of IFN-γ (Fig. 3.1). Doxycycline (dox) is a tetracycline analog that binds tTA, preventing it from attaching to the CMV/TRE promoter, which effectively suppresses IFN-γ expression (Lin et al, 2004; Lin et al., 2006). Cuprizone was incorporated at 0.2% into milled chow beginning at 6wks of age to induce demyelination in male double transgenic animals receiving dox.

There are considerable data that suggest IFN-γ both contributes to and protects against EAE and oligodendrocyte survival. Given the controversial nature of this cytokine, IFN-γ was induced at two different time points to determine whether the timing of IFN-γ induction influences its effect on demyelination and/or remyelination. One control group and two treatment groups were created, and the corpus collosa were harvested at either 11wks when demyelination was at maximum, or at 14wks when active remyelination was robust (Lin et al., 2006). In all three groups, animals were given dox from conception, and cuprizone treatment began at 6wks of age and ended at 12wks of age. In the control group, the animals remained on dox throughout the entire experiment. In the first treatment group, dox was removed at the same time cuprizone treatment began (6wks of age) resulting in significant IFN-γ protein levels approximately two weeks later when demyelination was evident (Lin et al., 2004, 2005, 2006). In the second treatment group, dox was removed two weeks after the initiation of cuprizone treatment (8wks of age), and measurable IFN-γ levels again occurred approximately two weeks later, when demyelination was at maximum. Table 3.1 describes

the samples and comparisons used in this experiment, and the sample abbreviations in the table will be used throughout this paper.

Table 3.1 Description of Samples, Abbreviations, and Expression Comparisons.

Sample Abbreviation	Sample Description	Fold Change Comparison
11wk-C	Corpus collosum harvested at 11wks from control group.	----------
11wk-E	Corpus collosum harvested at 11wks; IFN-γ induced at 6wks of age.	11wk-E / 11wk-C
11wk-L	Corpus collosum harvested at 11wks; IFN-γ induced at 8wks of age.	11wk-L / 11wk-C
14wk-C	Corpus collosum harvested at 14wks from control group.	----------
14wk-E	Corpus collosum harvested at 14wks; IFN-γ induced at 6wks of age.	14wk-E / 14wk-C
14wk-L	Corpus collosum harvested at 14wks; IFN-γ induced at 8wks of age.	14wk-L / 14wk-C

Quantitative expression of 44,998 genes and ESTs plus 65 control genes from each of the sample groups described above was measured on MOE 430 2.0 GeneChips® (Affymetrix). We found 552 genes of interest based on significant difference (+/- 1.5-fold and Student's t-test p-value<0.1). A statistical cutoff of $p<0.1$ was selected because of the natural variability that exists between animals, particularly for robustly expressed genes. Using a lower p-value cutoff would likely result in too numerous false negatives. Of the 552 significantly changing genes, 7 (1.2%) were upregulated and 117 (21%) were downregulated in the 11wk samples. At 14wks, 311 (56%) were upregulated and 124 (22%) were downregulated.

The hybridization cocktail contained poly-A (*Trp*, *Thr*, *Phe*, *Lys*, and *Dap*) and hybridization (*BioB, BioC, BioD,* and *Cre*) control genes. The ratios of 5':3' probe pair binding for the poly-A controls ranged from 1:1 to 1:1.8, indicating that the RNA was of excellent quality. Expression estimates of the hybridization controls were also normal, demonstrating that the hybridization reactions worked properly.

Differential Expression of Genes Involved in Myelin Formation
(Figure 3.4; Table 3.2)

In 11-wk-old non-IFN-γ-expressing mice, the corpus collosum was severely demyelinated after 5 weeks of cuprizone treatment, and there were significantly fewer $CC1^+$ mature oligodendrocytes than in non-treated mice (Lin et al., 2006). At 14wks, after 2 weeks of recovery in the absence of cuprizone, there was considerable evidence of remyelination as measured by MBP immunostaining and EM analysis of remyelinated axons. At 14wk-E, there was less remyelination (Lin et al., 2006); however, at 14wk-L remyelination was slightly enhanced (Lin and Popko, unpublished data). There was no change in myelin gene expression at either 11wk-E or 11wk-L, but QK was upregulated at 14wk-E and TRFR, MAL, MBP, and QK were upregulated at 14wk-L.

The transferrin receptor (TRFR) has a high affinity for iron-bound transferrin (hTf) and administration of hTf has been shown to increase the rate of differentiation and myelination in cultured OLs (Paez et al., 2004; Garcia et al., 2003, 2004; Marta et al., 2003; Moos and Morgan 2000) as well as increase transcription of MBP, CNP, and several microtubule and actin genes (Marta et al., 2002). Moreover, these actions are enhanced by IGF-1 (Espinosa-Jeffrey et al., 2002). In controls, TRFR was expressed at high levels (> 8 times the average expression on the array) and increased by 50% at 14wk-L. Following a cuprizone-induced

demyelinating insult, OPCs repopulate the corpus collosum and differentiate into mature, myelinating OLs (Matsushima and Morell, 2001; Mason et al., 2000). In the non-IFN-γ-expressing animals, $CC1^+$ oligodendrocytes began appearing in the corpus collosum after 6wks of cuprizone treatment, and 2 weeks later their numbers had increased more than 5-fold (Lin et al., 2006; Lin and Popko, unpublished data). At 14wk-E, however, there were significantly fewer $CC1^+$ cells and more OPCs than at either 14wk-C or 14wk-L (Lin et al., 2006; Lin and Popko, unpublished data) . Perhaps, therefore, the upregulation of TRFR at 14wk-L is a reflection of an increased number of mature, myelinating OLs, and thus a higher demand for iron.

Myelin and lymphocyte protein (MAL) is a component of myelin rafts and is found in the non-compact paranode regions of myelin where it is involved in maintaining proper axo-paranode adhesion (Schaeren-Wiemers et al., 2004; Erne et al., 2002). Myelin basic protein (MBP) is also a structural component of myelin, important for the stabilization of compact lamellar domains and for forming the intraperiod- and major dense lines. The observed upregulation of MAL and MBP at 14wk-L may be indicative of increased paranode adhesion and myelin wrapping by mature OLs.

Quaking (QK) is an RNA-binding protein that regulates MAG splicing and stabilizes MBP mRNA (Wu et al., 2002; Lu et al., 2004). In the control groups, QK expression was twice as robust during demyelination (11wk-C) than remyelination (14wk-C). QK expression did not change in the presence of IFN-γ at 11wks, but increased more than 2-fold at 14wk-E and more then 3-fold at 14wk-L, further evidence for an effort to maintain myelin message levels during remyelination, particularly when IFN-γ is induced later.

Several myelin-related genes, including MOBP, MAG, CNP, MOG, and PLP, did not show a difference in expression between the control and IFN-γ-expressing groups, but did show higher expression at 14wks than 11wks, which is consistent with a larger population of mature, myelinating OLs during the recovery phase. Taken together, these data suggest that IFN-γ may promote myelin gene expression in remyelinating OLs, especially when induced at the peak of the demyelinating insult.

Differential Expression of Genes Involved in Cholesterol and Lipid Biosynthesis and Metabolism
(Figures 3.5 and 3.6; Table 3.3)

Cholesterol is synthesized locally in the brain and constitutes approximately 30% of the total lipid in myelin (Morell, 1996). Cholesterol and fatty acid synthesis do not always correlate with the rate of myelination (Muse et al., 2001); however, they are necessary for generating plasma membrane and myelin sheath. Few cholesterol and lipid synthesis genes were significantly differentially regulated. At 11wk-E, SQLE, SC4MOL, HSD17B7 and VLDLR were moderately downregulated, but did not show significant difference in regulation at 11wk-L. At 14wks there was a mixed response in both IFN-γ-expressing groups. FDFT1, an enzyme involved in cholesterol synthesis, was modestly downregulated at 14wk-E and 14wk-L. Other genes involved in fatty acid metabolism, peroxisomal organization and steroid synthesis were both up- and downregulated to some degree. The most significant difference was a decrease in the peroxisomal biogenesis factor PEX6 message at both 14wk-E and 14wk-L.

Differential Expression of Genes Involved in the Immune Response
(Figures 3.7 and 3.8; Table 3.4)

We observed very little transcriptional change in immune response gene during the demyelination phase at 11wks, but saw a much greater response at 14wks that was dependent on the time of IFN-γ induction. Strongly upregulated genes included PDE4B, which is induced by LPS stimulation and results in TNF-α upregulation (Jin and Conti, 2002); CD48 and CD83, antigens involved in T cell and NK cell activation; interleukin receptors IL-6RA and IL-13RA1; and macrophage activation protein 2 (MPA2). With few exceptions, immune response genes were more robustly upregulated at 14wk-E than 14wk-L. Interestingly, JAK was upregulated in both 14wk-E and 14wk-L, but STAT-1 and STAT-2 were upregulated only in 14wk-E. The JAK-STAT pathway is a major downstream event of IFN-γ signaling that elicits the upregulation of additional cytokine and immunoregulatory genes. The difference in expression between 14wk-E and 14wk-L is suggestive of a protective role for IFN-γ during remyelination when induced at the peak of demyelination.

Differential Expression of Genes Involved in Antigen Processing and Presentation, and ER Stress
(Figures 3.9 - 3.14; Tables 3.5 - 3.8)

A hallmark of IFN-γ exposure to OLs is the robust upregulation of MHC class I and II (Baerwald et al., 1999; Benveniste and Benos, 1995). Peptide antigens for MHC class I are cleaved by the proteasome, which is a conglomeration of many peptides that form a 26S or 20S structure (Coux et al., 1996). Alpha subunits encoded by PSMA genes and beta subunits encoded by PSMB genes make up the 20S proteasome. The addition of RPN and RPT subunits encoded by PSMD and PSMC genes, respectively, constitutes the 26S proteasome.

It is the 20S proteasome that degrades most peptides destined for antigen presentation; and in response to IFN-γ, TNF-α, and IFN-α, certain proteasome subunits are induced to form "immunoproteasomes" (Yamano et al., 2002). Most of the antigens presented by MHC class I are processed in this manner. Immunoproteasome subunits are encoded by PSMB8 (LMP7), PSMB9 (LMP2), and PSME1/2 (PA28α/β), all of which were significantly upregulated at 14wk-E, but not 14wk-L, 11wk-E, or 11wk-L (Figs. 3.9b and 3.10g; Table 3.5). Peptides that have been broken down by the immunoproteasome are transferred to the endoplasmic reticulum (ER) via the transporter TAP1/2. Inside the ER, MHC class I forms a dimer with β_2 microglobulin (β_2M) and associates with TAP until it binds a peptide antigen. The MHC-β2M-antigen complex is then released from the ER, processed through the Golgi, and transported to the cell surface where the antigen is presented to circulating T cells. Like the proteasome genes, TAP1 and β_2M were also upregulated at 14wk-E, but at no other time point (Fig. 3.10a,d; Table 3.5). In addition, several MHC class I genes were robustly upregulated at 14wk-E, and to a lesser degree at 14wk-L (Figs. 3.9 and 3.10; Table 3.5). There was little change in transcriptional regulation of MHC class I at 11wks with only a few genes downregulated at 11wk-E (Fig. 3.9 and Table 3.5). MHC class II antigen complexes are processed via endosomes by several accessory proteins including cathepsin S (CTSS) and CD74 invariant chain. As observed with MHC class I expression, MHC class II genes, along with CTSS and CD74, were upregulated at 14wk-E, but not at any other time point (Figs. 3.10e,f; Table 3.5). These data are further evidence that when introduced late in the process of demyelination / early remyelination, IFN-γ results in a diminished immune response during the recovery period.

Some peptides are targeted for degradation by ubiquination, then broken down by the 26S proteasome and transported into the ER for antigen presentation. The process of ubiquination begins with the conjugation of ubiquitin to a ubiquitin-activating enzyme (E1), after which ubiquitin is transferred to a ubiquitin-conjugating enzyme (E2), and then ubiquitin ligase (E3) transfers the ubiquitin to a protein targeted for degradation (Hershko and Ciechanover, 1992; Ciechanover, 1994). Data for these events are more difficult to interpret, as there was both increased and decreased expression of genes related to ubiquitin and 26S proteasome-mediated protein degradation. Perhaps there are competing mechanisms for the degradation and preservation of proteins, or possibly the data represent a shift toward the use of certain ubiquitin genes over others.

At 11wk-L, the ubiquitin ligase UBE3A was slightly upregulated and the only ubiquitin gene differentially expressed at that time point (Fig. 3.9c, Table 3.5). At 11wk-E, the ubiquitin-conjugating enzyme UBE2R2, the ubiquitin carboxy-terminal hydrolase UCHL1, and two deubiquinating enzymes, USP3 and USP11, were downregulated (Fig. 3.9c, Table 3.5). At 14wk-E and 14wk-L, the E2 enzyme UBE2D2 along with RNF122 and MARCH7 were upregulated, while two E3 enzymes, NEDD4L and UBE3C, were downregulated Fig. 3.10i; Table 3.5). UBE3A was upregulated at 14wk-L; the E1-like enzyme UBE1L and deubiquinating enzyme USP18 were downregulated at 14wk-E and USP14 was downregulated at both 14wk-E and 14wk-L (Fig. 3.10h; Table 3.5). Two 26S subunits were differentially regulated; PSMD10 was downregulated at 14wk-E and 14wk-L, and PSMD13 was upregulated at 14wk-E (Fig. 3.10g; Table 3.5).

In addition to antigen processing, the 26S proteasome also degrades aggregated, mal-folded or accumulated unfolded proteins. Since the ER in OLs is already producing large

amounts of membrane components for myelination, the additional requirement for MHC antigen in response to IFN-γ could likely tax the ER such that unfolded proteins accumulate and a stress response is initiated (Lin et al., 2004, 2005). Such a response involves the upregulation of protein folding chaperones, retrograde transport of mal-folded proteins out of the ER for degradation by the 26S proteasome, and decreased protein translation (Rutkowski and Kaufman, 2004; Rao et al., 2004; Ma and Hendershot, 2001). Protein folding chaperones were slightly downregulated at 11wk-E, but not at any other time point (Fig. 3.12; Table 3.7). At both 14wk-E and 14wk-L there was upregulation of protein degradation genes, (Fig. 3.11; Table 3.6), and at 14wk-L there was an additional overall decrease in protein synthesis genes (Figs. 3.13 and 3.14; Table 3.8). Together, these data provide some evidence of an ER stress response during remyelination, with the later-IFN-γ-expressers perhaps more able to mount a response.

Differential Expression of Genes Involved in the Oxidative Stress Response
(Figures 3.15 and 3.16; Table 3.9)

Cells initiate an oxidative stress response to combat damaging accumulation of reactive oxygen species (ROS), and evidence of such a response has been found in EAE and MS (Espejo et al., 2005; Gilgun-Sherki et al., 2004). At 11wk-E there was a slight decrease in redox genes and at 11wk-L a slight increase. At 14wk-E the oxidase inhibitor CYBA was upregulated, and at 14wk-L the antioxidant CAT was upregulated. Other reducing genes had slight and varied regulation at both 14wk-E and 14wk-L. It is unclear from these data exactly what role IFN-γ may play on oxidative stress during demyelination and remyelination in this system, but perhaps there is some increased response to ROS during the recovery phase.

Differential Expression of Genes Involved in Cell Death
(Figures 3.17 and 3.18; Table 3.10)

Considerable evidence indicates developing OLs exposed to IFN-γ in culture undergo apoptosis (Baerwald and Popko, 1998; Agresti et al., 1996; Vartanian et al., 1995). In our array analysis, we found only minor differential regulation of genes involved in cell death, and the timing of IFN-γ induction seemed to play a role in their expression. Overall, there was a general decrease in apoptotic genes at 11wk-E, but not at 11wk-L. The most significantly downregulated gene was TRB-3 at 11wk-E, which in addition to being pro-apoptotic, also responds to ER stress (Corcoran et al., 2005).

At 14wks, differential regulation of minor cell death genes was varied in both 14wk-E and 14wk-L. Most notably, the pro-apoptotic DNA fragmentation gene CIDE-B was upregulated at 14wk-E, but downregulated at 14wk-L. IGF-1, which has been shown to have a protective effect on OL survival (Ye et al., 1995; Mason et al., 2000; Gao et al., 2002), was robustly expressed in non-treated immature OLs, at ~10 times the average expression of the array and ~ 6 times higher than non-treated mature OLs. In both immature and mature populations, IFN-γ treatment resulted in a decrease in IGF-1; however, the decrease was considerably less in the mature cells, which may point to their resistance against the injurious effects of IFN-γ.

Differential Expression of Genes Involved in Cell Cycle Regulation, Differentiation and Development
(Figures 3.19 -3.23; Tables 3.11-3.13)

During peak demyelination, there was a decrease in expression of genes that promote withdrawal from proliferation, and this effect was more dramatic at 11wk-E than 11wk-L. Moreover, there was a decrease in differentiation-promoting genes at 11wk-E, but not 11wk-L, and these genes were also increased at both 14wk-E and 14wk-L. There was an

upregulation of cell cycle genes preferential to differentiation and these were more robustly upregulated at 14wk-L than 14wk-E. Furthermore, development-associated genes were increased at 14wk-L and to a lesser extent at 14wk-E, but not in either 11-wk condition. Together, these data suggest that early IFN-γ expression may promote proliferation during demyelination, and that later IFN-γ expression may promote differentiation during remyelination. Likewise, previous data have demonstrated a greater number of progenitor cells at 10wk-E than 10wk-C and fewer progenitors at 12wk-E and 12wk-L than 12wk-C (Lin et al., 2006; Lin and Popko, unpublished data). Our measurements were taken between the time of the observed increase and decrease in OPCs; therefore, it is reasonable to presume that there would still be a number of proliferating OPCs at 11wks. Lin et al. also reported that at 14wks there were fewer mature OLs in the early IFN-γ expressers (2005), but the same number in the late expressers (unpublished data) compared to controls. Our data indicating some increased expression of differentiation and developmental genes at 14wk-L and less expression of the same at 14wk-E are consistent with these observations.

Differential Expression of Genes Involved in Various Other Cell Functions
(Figures 3.24 - 3.40 and Tables 3.14 - 3.22)

Clearly, IFN-γ expression during the beginning or peak of demyelination elicits diverse transcriptional responses. Figures 3.24-3.40 and Tables 3.14-3.22 illustrate differential expression of genes involved in cell growth, cell metabolism, cytoskeleton organization, cell adhesion, protein modification, nucleic acid binding, transcription regulation, signal transduction, and transport. Selected genes are discussed below.

Several myosin and kinesin motor proteins were upregulated in both 14wk-E and 14wk-L, and may play a role in extending membrane processes in mature OLs. Contactin-1

(CNTN1), which takes part in axo-glial adhesion; the cell surface protein CD44, which may play a role in T cell attachment; and the cell-cell adhesion molecule cadherin-11 (CDN11) were also upregulated in both 14wk-E and 14wk-L. Nucleic acid binding zinc finger proteins ZCCHC6 and ZDHHC2 were upregulated at 14wk-L and more so at 14wk-E. In addition, numerous genes for mitochondrial ATPases, potassium channels, and solute carrier family transporters as well as several signal transduction genes were differentially regulated.

A number of genes of unknown function and many ESTs were differentially regulated in response to IFN-γ. For reference, these genes and ESTs are listed in Tables 3.23 and 3.24, respectively.

CONCLUSION

Transgenic mice expressing IFN-γ in astrocytes in a temporally-controlled system were treated with the demyelination-inducing toxicant cuprizone. IFN-γ was induced either simultaneously with the start of cuprizone treatment or two weeks into treatment. Transcriptional regulation was measured from the corpus collosum either at the peak of demyelination or during robust remyelination and was quantitated using microarray analysis. Numerous genes were differentially regulated in response to IFN-γ, but interestingly, the degree of transcriptional regulation among several groups of genes was influenced by the timing of IFN-γ induction, particularly during active remyelination.

At 11wks, very few OLs still remain in the corpus collosum after cuprizone treatment (Lin et al., 2006; Matsushima and Morell, 2001; Mason et al., 2000). The changes in gene expression measured here, therefore, may have occurred in the many infiltrating astrocytes

present in lesion sites and/or in new $NG2^+$ progenitors, which begin to appear in the corpus collosum at 10wks (after 4wks of cuprizone treatment).

In the early expressers at 11wks, there was a greater induction of MHC and a decrease in protein synthesis and cell metabolism genes; whereas, in the late expressers, only MHC class I showed appreciable differential regulation. Consistent with other work in our lab that measured an initial increase in progenitors at 10wk-E, but a decrease at 12wk-E (Lin et al., 2006; Lin and Popko, unpublished data), the decrease in protein synthesis and metabolism genes may reflect a shut down of progenitor cells, and this also supports the observed decrease in remyelination in the early expressers (Lin et al., 2006).

After 6 weeks of cuprizone treatment followed by 2 weeks of recovery, non-IFN-γ-expressing animals displayed an increase in myelin gene expression and the number of mature OLs, with a proportionate decrease in progenitor cells, as well as a ~48% recovery of remyelinated axons (Lin et al., 2006). In contrast, the early IFN-γ expressers showed a decrease in myelin gene expression, fewer mature OLs, an increase in the number of astrocytes and macrophages, and only ~27% recovery of remyelinated axons (Lin et al., 2006).

In the early expressers during remyelination, our analysis indicated an upregulation of both JAK and a STAT1, which are downstream modulators of IFN-γ signaling. Concordantly, we observed robust upregulation of both MHC class I and class II along with their processing and assembly genes. The processing of class I occurs in the ER, and several recent experiments have indicated that robust upregulation of MHC class I by IFN-γ in OLs, particularly actively myelinating OLs, leads to ER stress, which may contribute to OL cell death during remyelination (Lin et al, 2005, 2006; Lin and Popko, unpublished data). In

addition to the large induction of MHC and protein processing genes, we also observed an increase in genes involved in protein ubiquination and degradation. We did not, however, find appreciable upregulation of apoptotic genes.

In contrast to the early expressers, late expressers during remyelination showed an increase in myelin gene expression, fewer macrophages, and remarkably, an increase in the number of remyelinated axons compared even to control animals (55% vs. 48% in controls, $p<0.05$) (Lin and Popko, unpublished data). Concordantly in our array experiments, we observed an increase in myelin gene expression, including MBP, MAL, and QK, and found only a slight upregulation in STAT1 with much weaker induction of downstream IFN-γ signaling genes.

Consistent with diminished IFN-γ intracellular signal transduction, we also observed reduced induction of MHC class I and II and very little upregulation of MHC processing and transport genes compared to early expressers. Furthermore, there was no increase, or only a slight increase, in expression of IFN-γ-sensitive genes that were found to be upregulated in the early expressers, including interferon-inducible protein 1, interleukin 6 receptor alpha, interleukin 13 receptor alpha 1, macrophage activation 2, and IFN-γ-induced GTPase.

Taken together, these data strongly suggest that IFN-γ induction prior to the completion of demyelination results in decreased remyelination and fewer mature OLs, which may be due, at least in part, to ER stress induced by robust induction of MHC and protein processing genes. When expressed later, however, our data point toward a possible beneficial role for IFN-γ in reparative remyelination.

Figure 3.1 Tetracycline-Inducible Expression of IFN-γ. Two transgenic lines of mice were crossed to produce a double transgenic line expressing IFN-γ in the absence of doxycycline: a) the tetracycline operon repressor (tTA) and eukaryotic transcription activity domain fusion construct (VP16) are under the control of astrocyte-specific promoter for glial fibrillary acidic protein (GFAP); b) IFN-γ is driven by the CMV promoter modified to contain a binding site for tTA

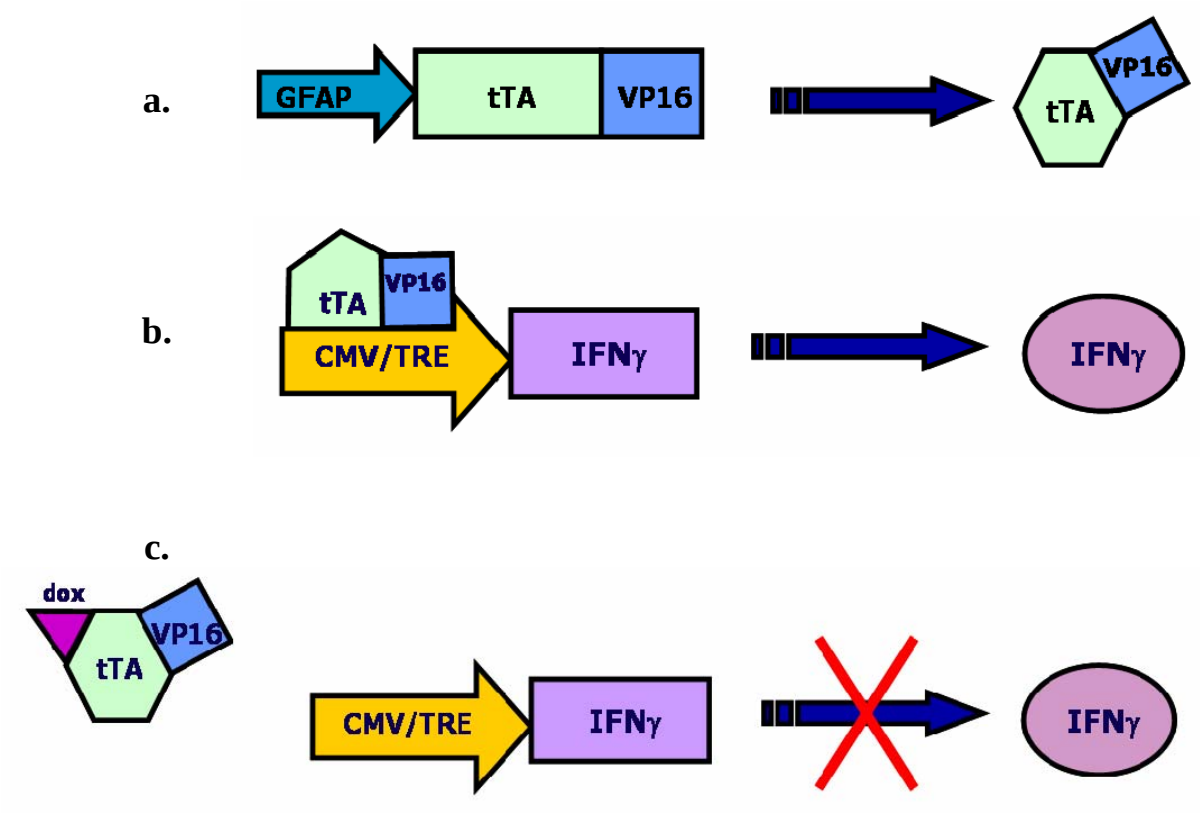

Figure 3.2 Cuprizone Model of Demyelination in C57BL/6J Wild-type Mice. Six-week-old male mice were fed milled chow containing 0.02% Cuprizone for either 6wks or 16wks. By the fifth week of treatment, nearly all axons were demyelinated. Animals taken off Cuprizone after 6wks remyelinated nearly completely. Animals treated with Cuprizone continuously for 16wks experienced partial remyelination in the sixth week followed by a second period of demyelination in weeks nine and ten. Animals remyelinated only minimally in the twelfth week and were again nearly completely demyelinated from 14wks-16wks (Matsushima and Morell, 2001).

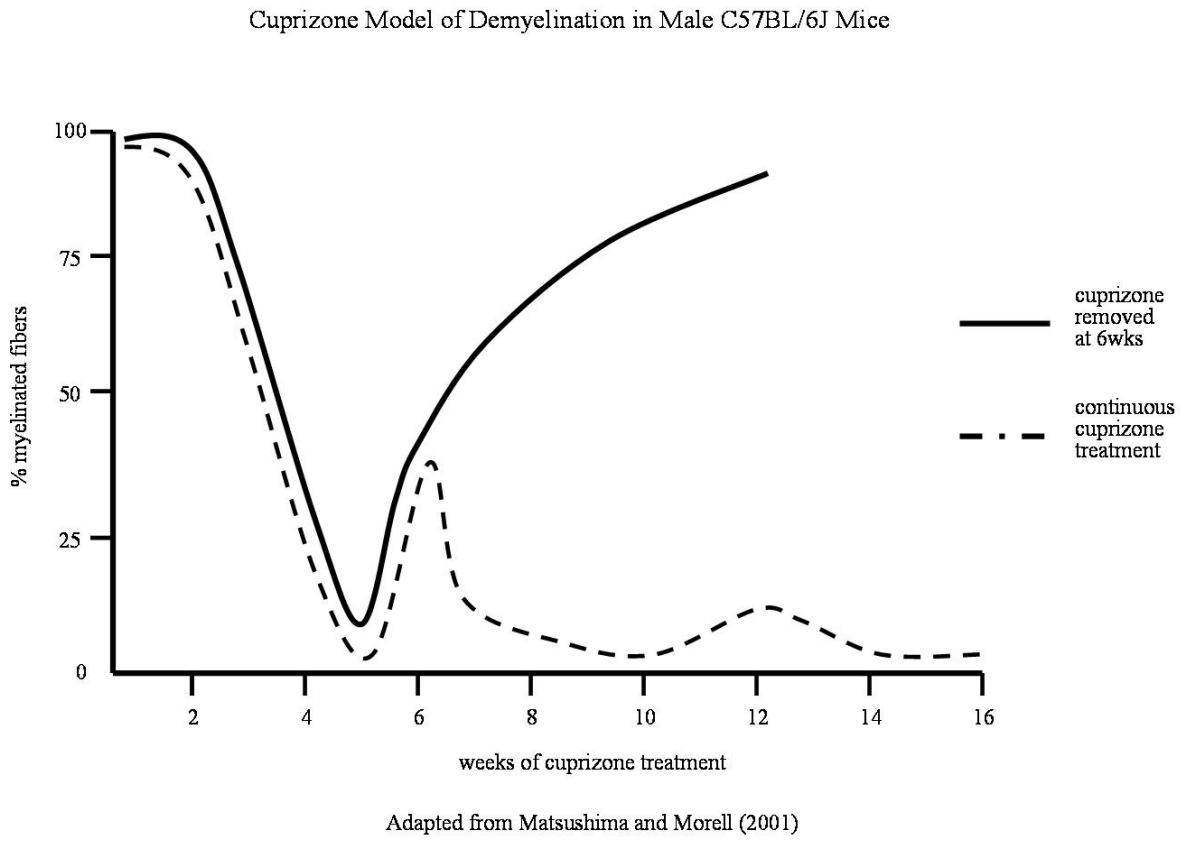

Figure 3.3 Cuprizone Treatment and IFN-γ Induction in Male GFAP/tTA x TRE/IFN-γ Transgenic Mice.

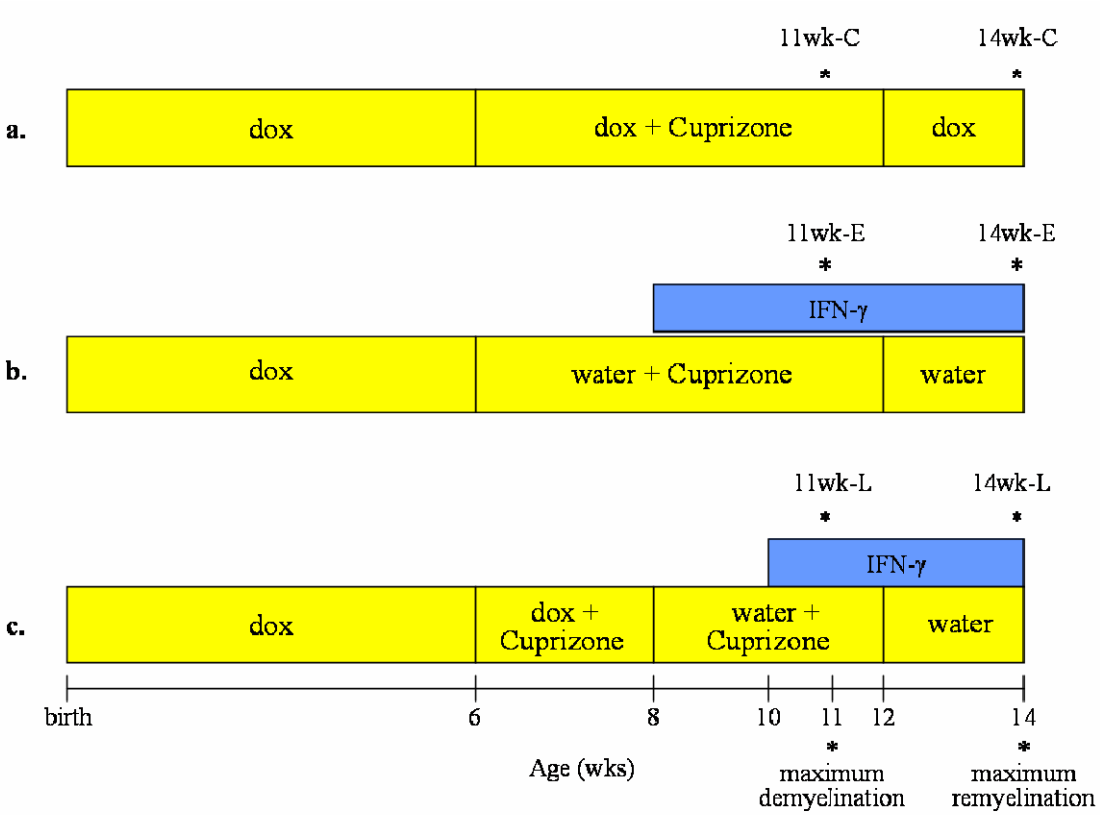

Figure 3.4 Expression Estimates of Genes Involved in Myelin Formation at 14wks. Gene symbols and Accession numbers are plotted on the x-axis; the average of replicate normalized expression values for each treatment group (as described in Materials and Methods) is plotted on the y-axis. In some cases, a gene is represented on the microarray set more than once by different accession numbers. Fold change values are listed in Table 3.2.

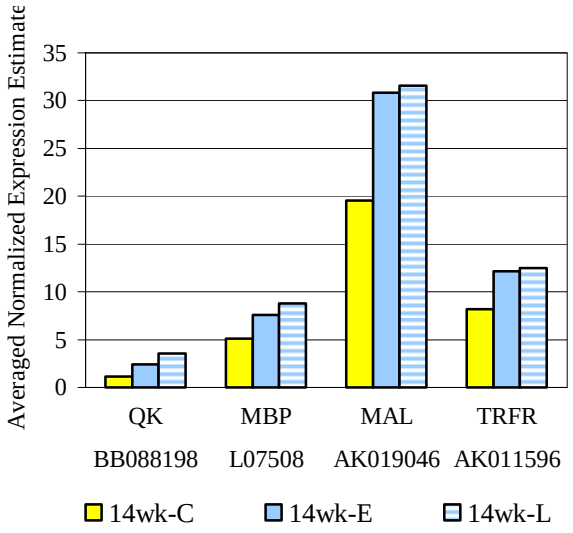

Table 3.2 Differential Expression of Genes Involved in Myelin Formation. Replicate RNA samples from each treatment group were hybridized to separate arrays. The average of replicate normalized expression estimates for each sample group was used to calculate the fold change difference in expression for each gene in Figure 3.4. Positive fold change values indicate an increase, and negative values indicate a decrease in gene expression in the IFNγ-expressing groups. Values in grey indicate the Student's t-test p-value was greater than 0.1.

			Fold Change (IFN-γ-expressing / non-expressing)			
Accession No.	Gene Symbol	Gene Name	11wk-E	11wk-L	14wk-E	14wk-L
AK019046	MAL	myelin and lymphocyte protein	1.27	1.38	1.58	**1.61**
L07508	MBP	myelin basic protein	1.49	1.28	1.49	**1.73**
BB088198	QK	quaking	1.17	1.15	**2.14**	**3.13**
AK011596	TRFR	transferrin receptor	-1.21	1.06	1.48	**1.52**

Figure 3.5 Expression Estimates of Genes Involved in Cholesterol and Lipid Biosynthesis and Metabolism at 11wks. Gene symbols and Accession numbers are plotted on the x-axis; the average of replicate normalized expression values for each treatment group (as described in Materials and Methods) is plotted on the y-axis. In some cases, a gene is represented on the microarray set more than once by different accession numbers. Fold change values are listed in Table 3.3.

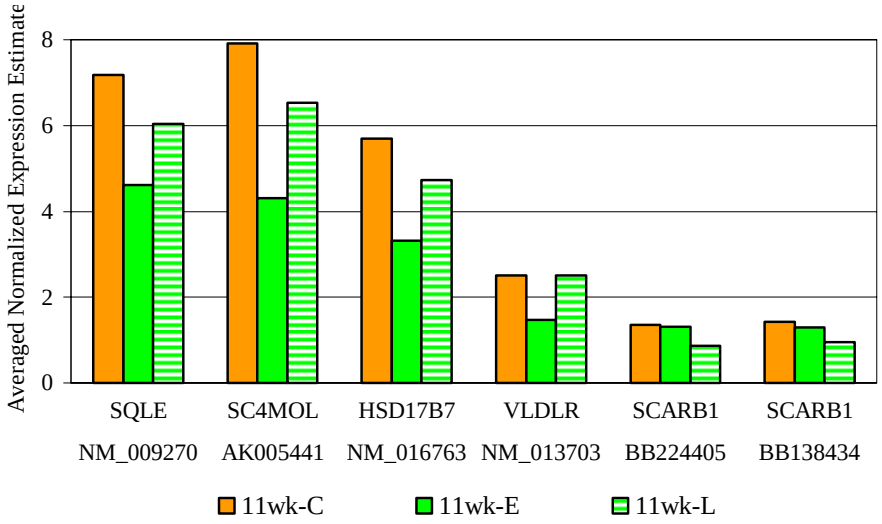

Figure 3.6 Expression Estimates of Genes Involved in Cholesterol and Lipid Biosynthesis and Metabolism at 14wks. a-c) Gene symbols and Accession numbers are plotted on the x-axis; the average of replicate normalized expression values for each treatment group (as described in Materials and Methods) is plotted on the y-axis. In some cases, a gene is represented on the microarray set more than once by different accession numbers. Fold change values are listed in Table 3.3.

a.

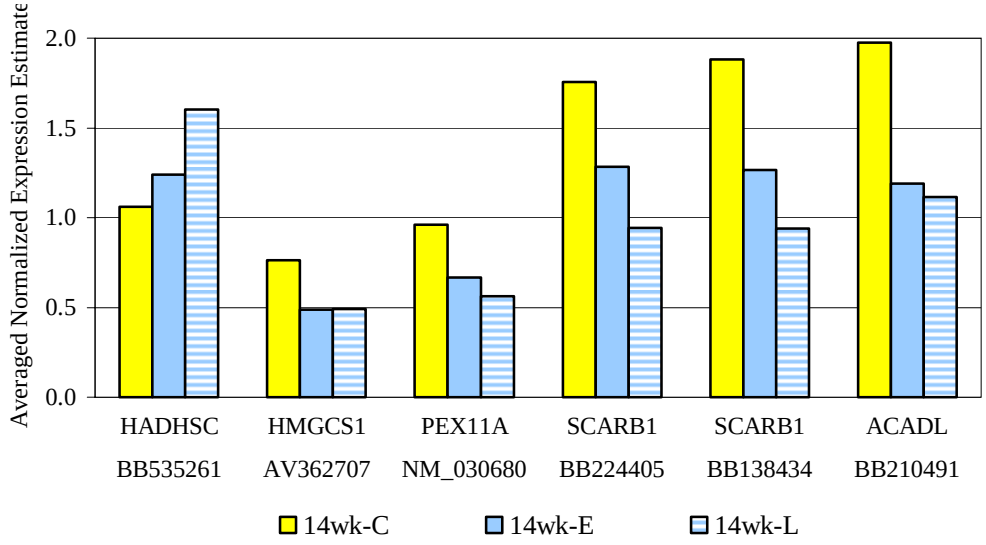

b.

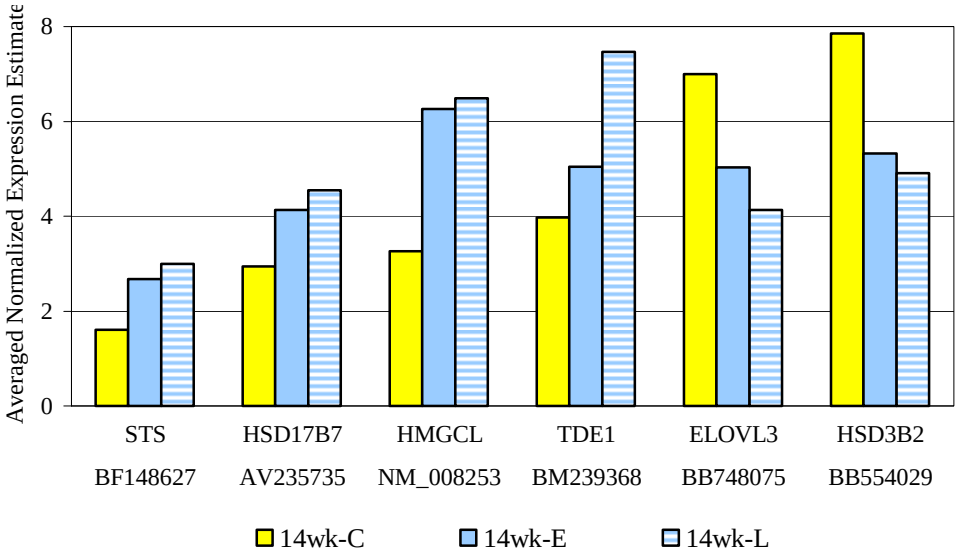

Figure 3.6 Expression Estimates of Genes Involved in Cholesterol and Lipid Biosynthesis and Metabolism at 14wks.

c.

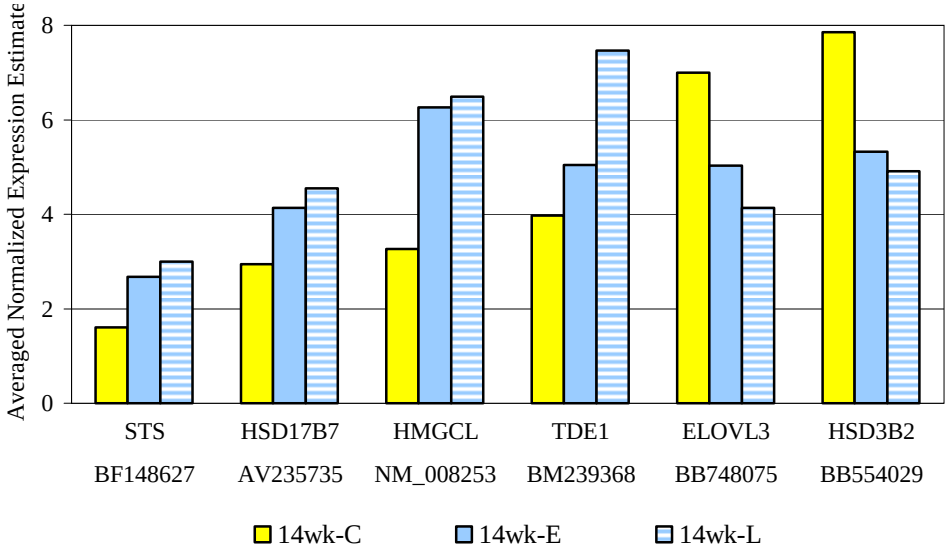

Table 3.3 Differential Expression of Genes Involved in Cholesterol and Lipid Biosynthesis and Metabolism. Replicate RNA samples from each treatment group were hybridized to separate arrays. The average of replicate normalized expression estimates for each sample group was used to calculate the fold change difference in expression for each gene in Figures 3.5 and 3.6. Positive fold change values indicate an increase, and negative values indicate a decrease in gene expression in the IFNγ-expressing groups. Values in grey indicate the Student's t-test p-value was greater than 0.1.

			Fold Change (IFN-γ-expressing / non-expressing)			
Accession No.	Gene Symbol	Gene Name	11wk-E	11wk-L	14wk-E	14wk-L
BB210491	ACADL	acetyl-Coenzyme A dehydrogenase, long-chain	1.06	-1.19	**-1.66**	**-1.77**
AW493391	DGKD	diacylglycerol kinase, delta	**-1.58**	-1.06	1.53	1.19
BB748075	ELOVL3	elongation of very long chain fatty acids (FEN1/Elo2, SUR4/Elo3, yeast)-like 3	1.16	-1.20	-1.39	**-1.69**
BB028312	FDFT1	farnesyl diphosphate farnesyl transferase 1	-1.10	-1.12	**-1.62**	**-1.88**
BB535261	HADHSC	L-3-hydroxyacyl-Coenzyme A dehydrogenase, short chain	1.04	1.18	1.17	**1.51**
NM_008253	HMGCL	3-hydroxy-3-methylglutaryl-Coenzyme A lyase	-1.30	1.10	1.92	**1.99**
AV362707	HMGCS1	3-hydroxy-3-methylglutaryl-Coenzyme A synthase 1	1.03	-1.01	**-1.57**	-1.55
NM_016763	HSD17B7	hydroxysteroid (17-beta) dehydrogenase 7	**-1.72**	-1.21	1.57	1.38
AV235735	HSD17B7	hydroxysteroid (17-beta) dehydrogenase 7	-1.12	1.06	1.41	**1.55**
BB554029	HSD3B2	hydroxysteroid dehydrogenase-2, delta<5>-3-beta	-1.01	-1.04	-1.48	**-1.60**
NM_030680	PEX11A	peroxisomal biogenesis factor 11a	**-1.18**	-1.14	**-1.44**	**-1.71**
BB315077	PEX5	peroxisome biogenesis factor 5	1.21	1.10	1.24	**1.79**
BG971031	PEX6	peroxisomal biogenesis factor 6	1.00	**-1.36**	**-2.03**	**-2.49**
AK005441	SC4MOL	sterol-C4-methyl oxidase-like	**-1.84**	-1.21	2.21	2.01
BB224405	SCARB1	scavenger receptor class B, member 1	-1.03	**-1.56**	-1.37	**-1.86**
BB138434	SCARB1	scavenger receptor class B, member 1	-1.10	**-1.50**	-1.48	**-2.00**
NM_009270	SQLE	squalene epoxidase	**-1.56**	-1.19	1.76	1.87

Accession No.	Gene Symbol	Gene Name	Fold Change (IFN-γ-expressing / non-expressing) 11wk-E	11wk-L	14wk-E	14wk-L
BF148627	STS	steroid sulfatase	-1.28	1.11	1.66	**1.86**
BM239368	TDE1	tumor differentially expressed 1	-1.07	1.21	1.27	**1.88**
AK005203	TDE1L	tumor differentially expressed 1, like	-1.28	1.21	1.64	**1.81**
NM_013703	VLDLR	very low density lipoprotein receptor	**-1.69**	1.00	1.53	1.74

Figure 3.7 Expression Estimates of Genes Involved in the Immune Response at 11wks. Gene symbols and Accession numbers are plotted on the x-axis; the average of replicate normalized expression values for each treatment group (as described in Materials and Methods) is plotted on the y-axis. In some cases, a gene is represented on the microarray set more than once by different accession numbers. Fold change values are listed in Table 3.4.

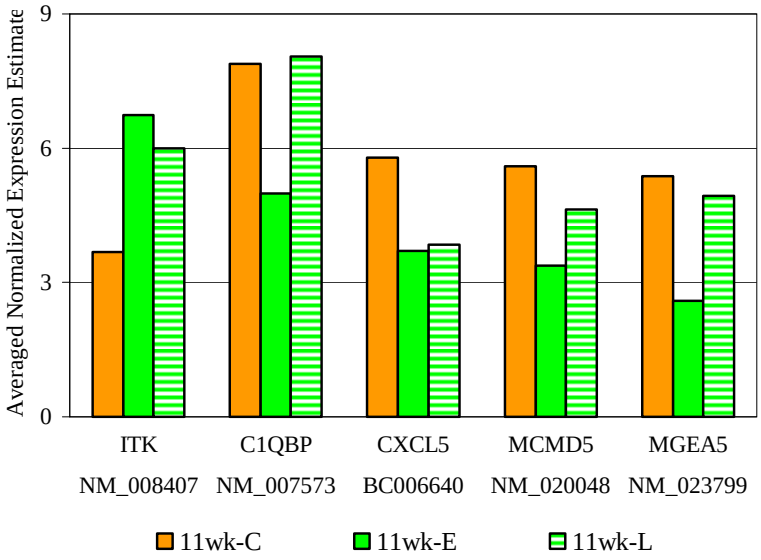

Figure 3.8 Expression Estimates of Genes Involved in the Immune Response at 14wks. a-e) Gene symbols and Accession numbers are plotted on the x-axis; the average of replicate normalized expression values for each treatment group (as described in Materials and Methods) is plotted on the y-axis. In some cases, a gene is represented on the microarray set more than once by different accession numbers. Fold change values are listed in Table 3.4.

a.

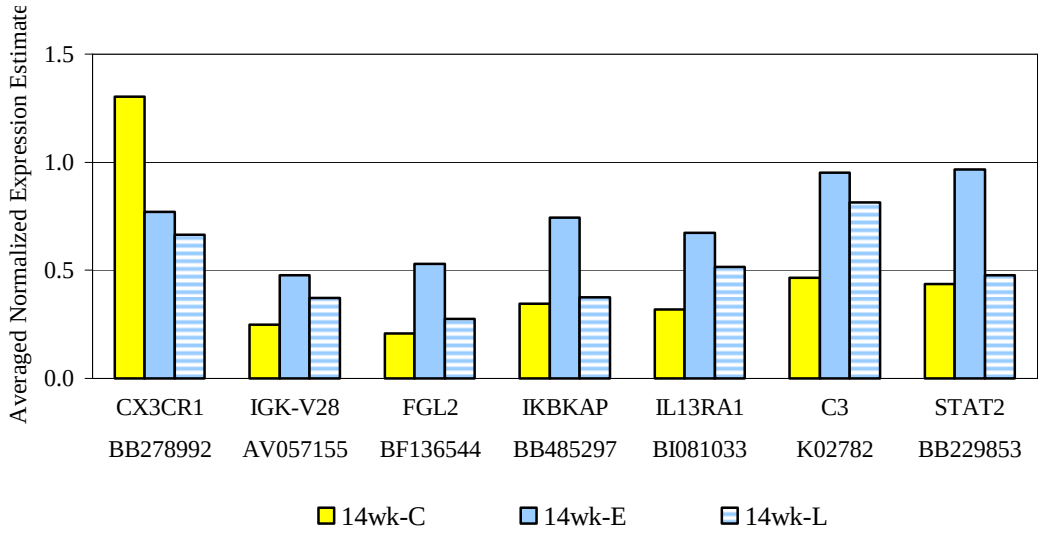

b.

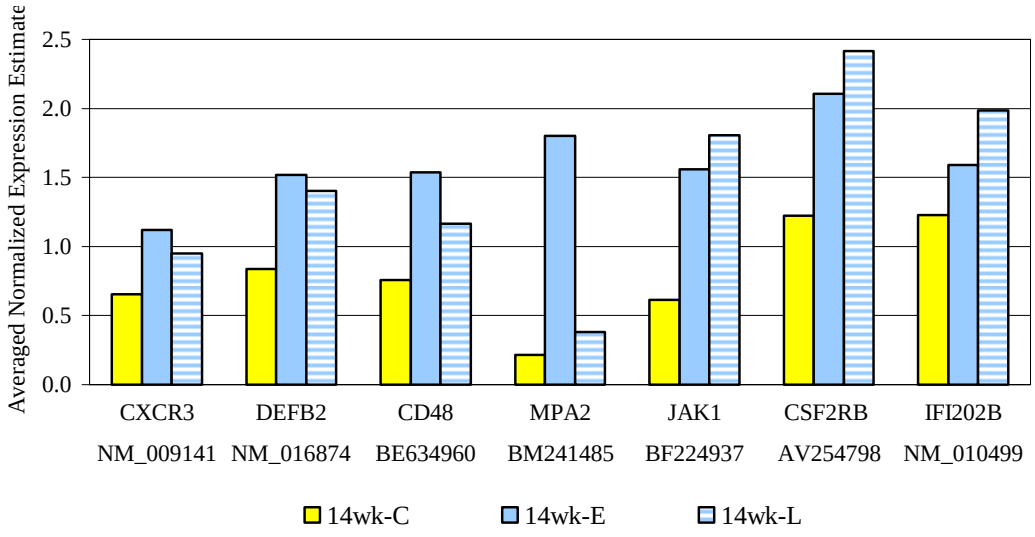

Figure 3.8 Expression Estimates of Genes Involved in the Immune Response at 14wks.

c.

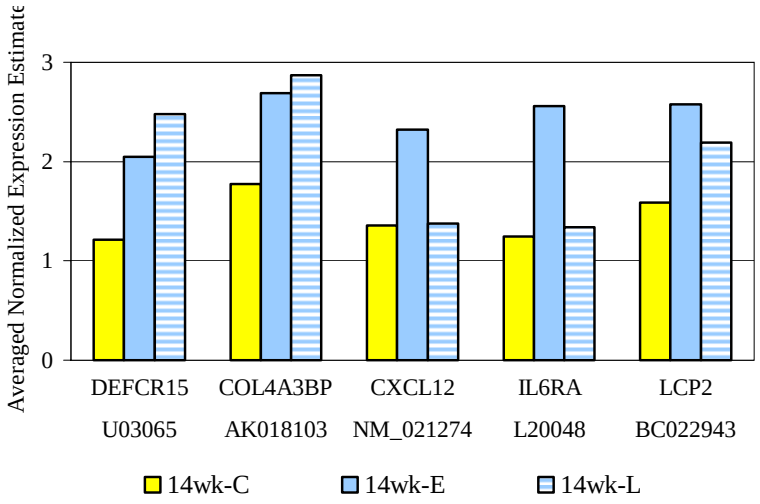

d.

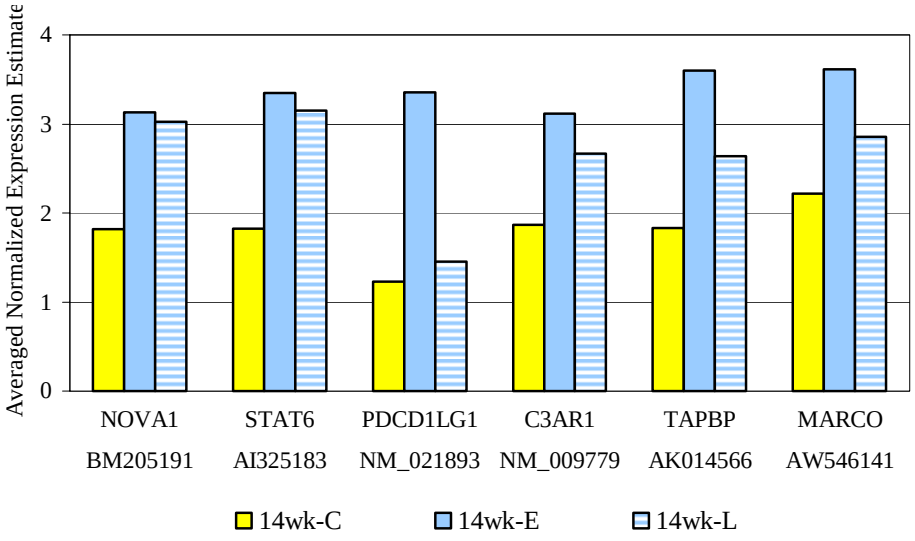

Figure 3.8 Expression Estimates of Genes Involved in the Immune Response at 14wks.

e.

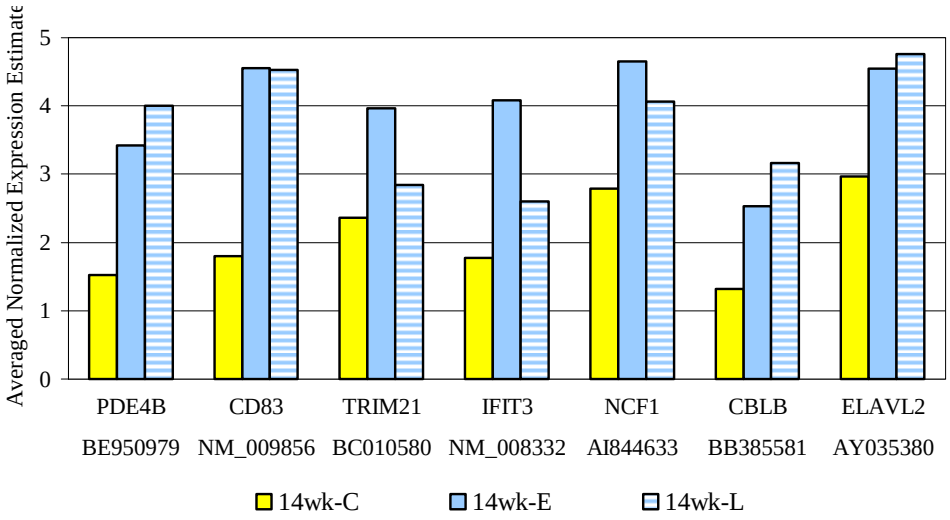

f.

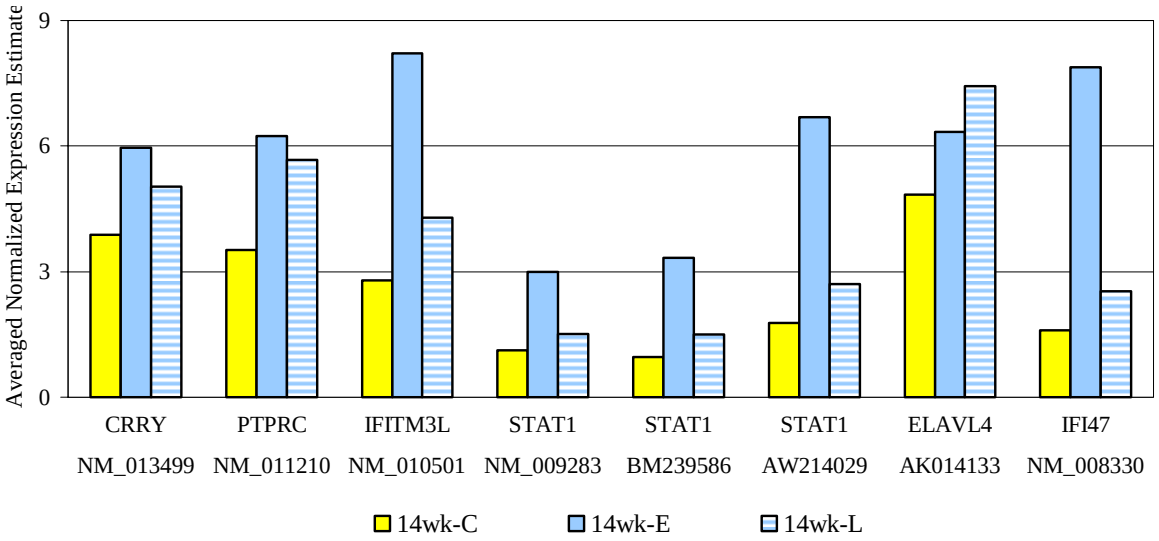

Figure 3.8 Expression Estimates of Genes Involved in the Immune Response at 14wks.

g.

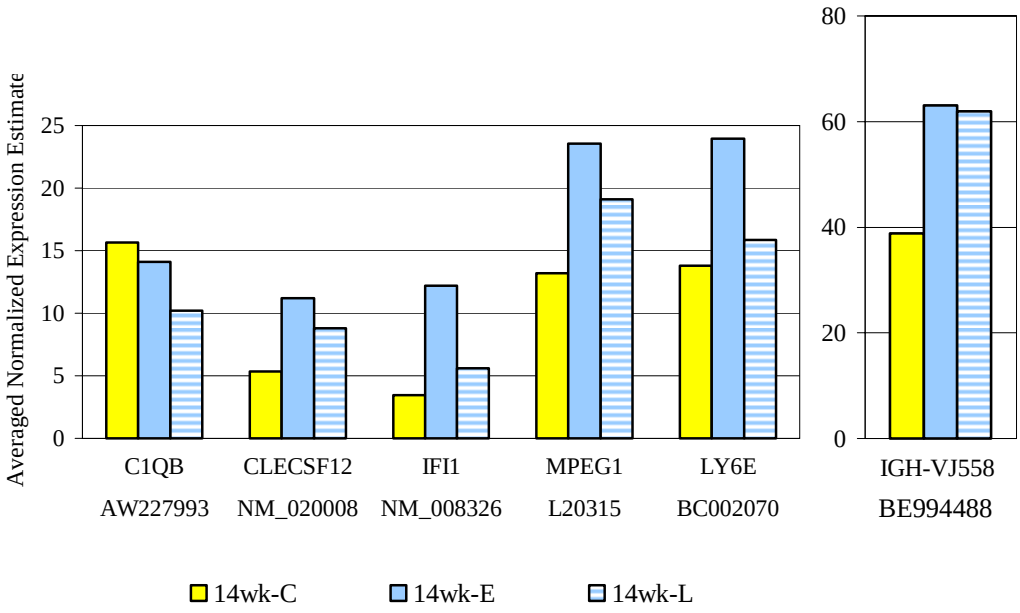

Table 3.4 Differential Expression of Genes Involved in the Immune Response. Replicate RNA samples from each treatment group were hybridized to separate arrays. The average of replicate normalized expression estimates for each sample group was used to calculate the fold change difference in expression for each gene in Figures 3.7 and 3.8. Positive fold change values indicate an increase, and negative values indicate a decrease in gene expression in the IFNγ-expressing groups. Values in grey indicate the Student's t-test p-value was greater than 0.1.

			Fold Change (IFN-γ-expressing / non-expressing)			
Accession No.	Gene Symbol	Gene Name	11wk-E	11wk-L	14wk-E	14wk-L
AW227993	C1QB	complement component 1, q subcomponent, beta polypeptide	-1.07	-1.40	-1.11	**-1.54**
NM_007573	C1QBP	complement C1q binding protein	**-1.58**	1.02	1.57	1.72
K02782	C3	complement C3	-1.09	-1.18	**2.05**	1.75
NM_009779	C3AR1	complement C3a receptor 1	-1.04	-1.14	**1.67**	1.43
BB385581	CBLB	casitas B-lineage lymphoma b	-1.11	-1.09	1.92	**2.40**
BE634960	CD48	CD48 antigen	1.09	-1.01	**2.03**	1.54
NM_009856	CD83	CD83 antigen	-1.12	-1.12	**2.53**	**2.52**
NM_020008	CLECSF12	C-type (calcium dependent, carbohydrate recognition domain) lectin, superfamily member 12	1.20	-1.12	**2.08**	**1.64**
AK018103	COL4A3BP	collagen, type IV, alpha 3 binding protein	1.13	1.12	**1.52**	**1.62**
NM_013499	CRRY	complement receptor related protein	-1.33	-1.13	**1.53**	1.29
AV254798	CSF2RB	colony stimulating factor 2 receptor, beta 1, low-affinity	-1.50	-1.04	1.72	**1.97**
BB278992	CX3CR1	chemokine (C-X3-C) receptor 1	1.08	-1.08	**-1.69**	**-1.96**
NM_021274	CXCL12	chemokine (C-X-C motif) ligand 12	-2.00	-2.15	**1.71**	1.01
BC006640	CXCL5	chemokine (C-X-C motif) ligand 5	**-1.56**	**-1.50**	-1.22	-1.26
NM_009141	CXCR3	chemokine (C-X-C motif) receptor 3	-2.12	-1.80	**1.70**	**1.45**
NM_016874	DEFB2	defensin beta 2	1.07	1.05	**1.81**	1.68
U03065	DEFCR15	defensin related cryptdin 15	1.15	**1.26**	**1.69**	**2.04**

Accession No.	Gene Symbol	Gene Name	Fold Change (IFN-γ-expressing / non-expressing) 11wk-E	11wk-L	14wk-L	14wk-E
AY035380	ELAVL2	ELAV (embryonic lethal, abnormal vision, Drosophila)-like 2	1.09	1.07	1.53	**1.61**
AK014133	ELAVL4	ELAV (embryonic lethal, abnormal vision, Drosophila)-like 4	-1.05	1.20	1.31	**1.53**
BF136544	FGL2	fibrinogen-like protein 2	-1.06	-1.15	**2.54**	1.31
NM_008326	IFI1	interferon inducible protein 1	1.23	1.10	**3.56**	1.64
NM_010499	IFI202B	interferon activated gene 202B	-1.18	-1.09	1.30	**1.62**
NM_008330	IFI47	interferon gamma inducible protein	1.11	-1.08	4.94	**1.58**
NM_008332	IFIT3	interferon-induced protein with tetratricopeptide repeats 3	-1.21	-1.21	**2.30**	1.47
NM_010501	IFITM3L	interferon induced transmembrane protein 3-like	-1.40	-1.62	**2.94**	1.53
BE994488	IGH-VJ558	immunoglobulin heavy chain, (J558 family)	-1.01	-1.02	**1.63**	1.59
AV057155	IGK-V28	immunoglobulin kappa chain variable 8	**1.30**	1.14	**1.92**	1.50
BB485297	IKBKAP	inhibitor of kappa light polypeptide enhancer in B-cells, kinase complex-associated protein	**1.34**	1.11	**2.15**	1.08
BI081033	IL13RA1	interleukin 13 receptor, alpha 1	-1.23	-1.27	**2.11**	1.61
L20048	IL6RA	interleukin 6 receptor, alpha	1.06	-1.82	**2.05**	1.07
NM_008407	ITK	IL2-inducible T-cell kinase	**1.83**	**1.63**	1.37	1.36
BF224937	JAK1	Janus kinase 1	1.06	-1.29	**2.54**	**2.94**
BC022943	LCP2	lymphocyte cytosolic protein 2	-1.13	-1.36	**1.62**	1.38
BC002070	LY6E	lymphocyte antigen 6 complex, locus E	1.00	1.00	**1.73**	1.15
AW546141	MARCO	macrophage receptor with collagenous structure	-1.12	-1.35	**1.63**	1.29
NM_020048	MCMD5	mini chromosome maintenance deficient 5	**-1.66**	**-1.21**	1.98	1.88
NM_023799	MGEA5	meningioma expressed antigen 5 (hyaluronidase)	**-2.08**	-1.09	1.57	1.85
BM241485	MPA2	macrophage activation 2	-1.45	-2.30	**8.41**	1.77

Accession No.	Gene Symbol	Gene Name	Fold Change (IFN-γ-expressing / non-expressing) 11wk-E	11wk-L	14wk-L	14wk-E
L20315	MPEG1	macrophage expressed gene 1	-1.05	-1.14	**1.78**	**1.45**
BM124348	MRG2	myeloid ecotropic viral integration site-related gene 2	**-1.71**	-1.10	1.17	1.15
AI844633	NCF1	neutrophil cytosolic factor 1	-1.06	-1.13	**1.67**	1.46
BM205191	NOVA1	neurooncological ventral antigen 1	-1.07	1.07	**1.73**	**1.67**
NM_021893	PDCD1LG1	programmed cell death 1 ligand 1	1.28	1.01	**2.73**	1.18
BE950979	PDE4B	phosphodiesterase 4B	1.28	1.05	**2.25**	**2.63**
NM_011210	PTPRC	protein tyrosine phosphatase, receptor type, C	1.15	-1.13	**1.77**	1.62
NM_009283	STAT1	signal transducer and activator of transcription 1	1.09	-1.12	**2.68**	1.35
BM239586	STAT1	signal transducer and activator of transcription 1	-1.21	-1.55	**3.50**	1.57
AW214029	STAT1	signal transducer and activator of transcription 1	-1.04	-1.63	**3.77**	1.53
BB229853	STAT2	signal transducer and activator of transcription 2	-1.01	-1.41	**2.22**	1.10
AI325183	STAT6	signal transducer and activator of transcription 6	-1.48	-1.19	**1.83**	**1.73**
AK014566	TAPBP	TAP binding protein	-1.23	-1.35	**1.97**	1.44
BC010580	TRIM21	tripartite motif protein 21	-1.06	-1.17	**1.68**	**1.21**

Figure 3.9 Expression Estimates of Genes Involved in Antigen Processing and Presentation at 11wks. Gene symbols and Accession numbers for genes involved in a) MHC class I presentation, b) the 20S proteasome, and c) the ubiquitin pathway are plotted on the x-axis; the average of replicate normalized expression values for each treatment group (as described in Materials and Methods) is plotted on the y-axis. In some cases, a gene is represented on the microarray set more than once by different accession numbers. Fold change values are listed in Table 3.5.

a.

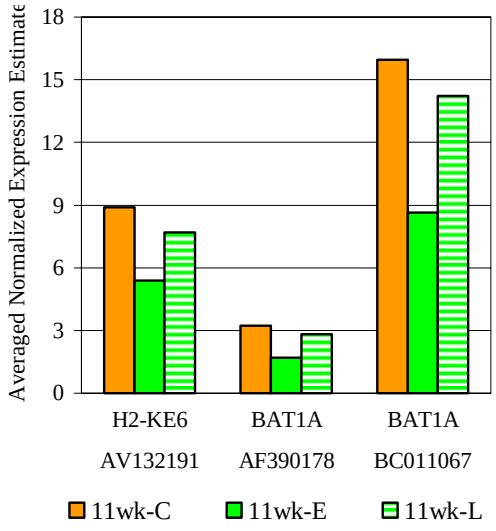

b.

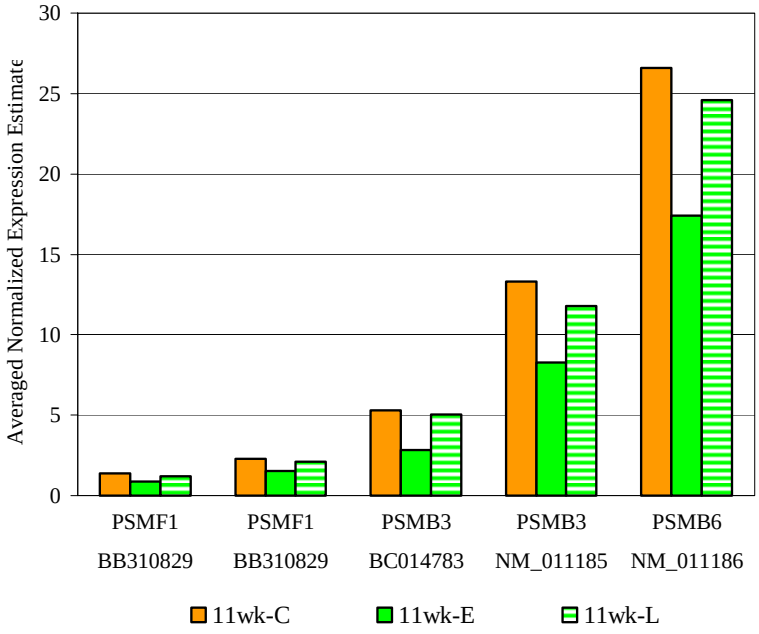

Figure 3.9 Expression Estimates of Genes Involved in Antigen Processing and Presentation at 11wks.

c.

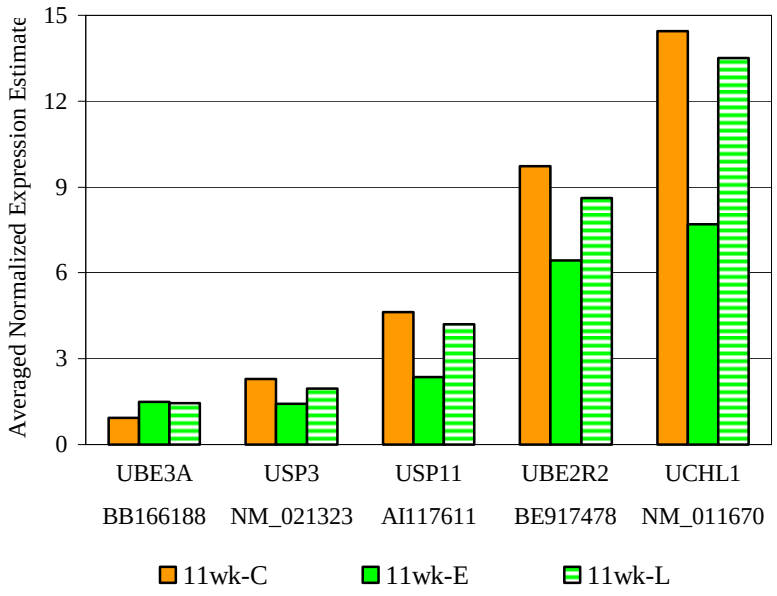

Figure 3.10 Expression Estimates of Genes Involved in Antigen Processing and Presentation at 14wks. Gene symbols and Accession numbers for genes involved in a-d) MHC class I presentation, e-f) MHC class II presentation, g) the 20S and 26S proteasomes, and h-i) the ubiquitin pathway are plotted on the x-axis; the average of replicate normalized expression values for each treatment group (as described in Materials and Methods) is plotted on the y-axis. In some cases, a gene is represented on the microarray set more than once by different accession numbers. Fold change values are listed in Table 3.5.

a.

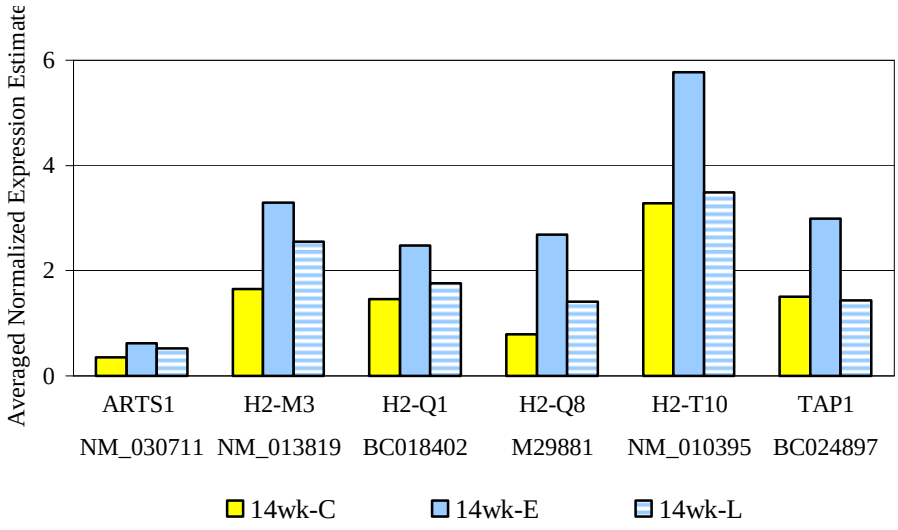

b.

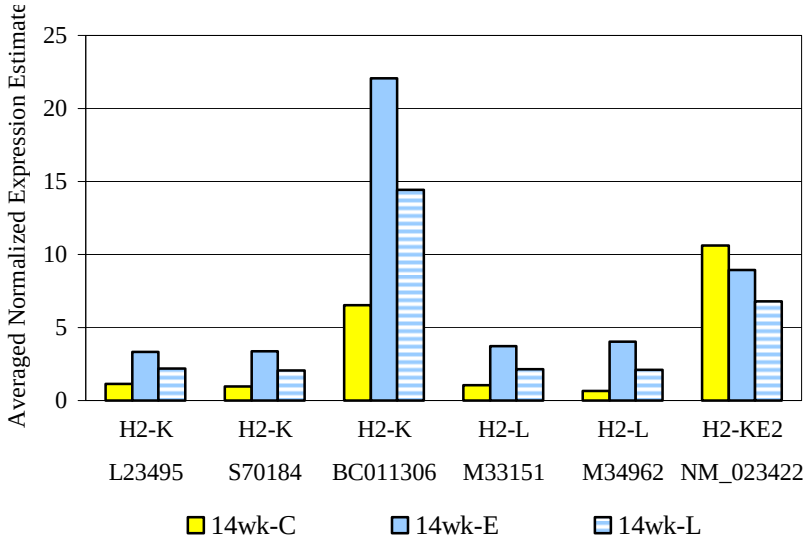

Figure 3.10 Expression Estimates of Genes Involved in Antigen Processing and Presentation at 14wks.

c.

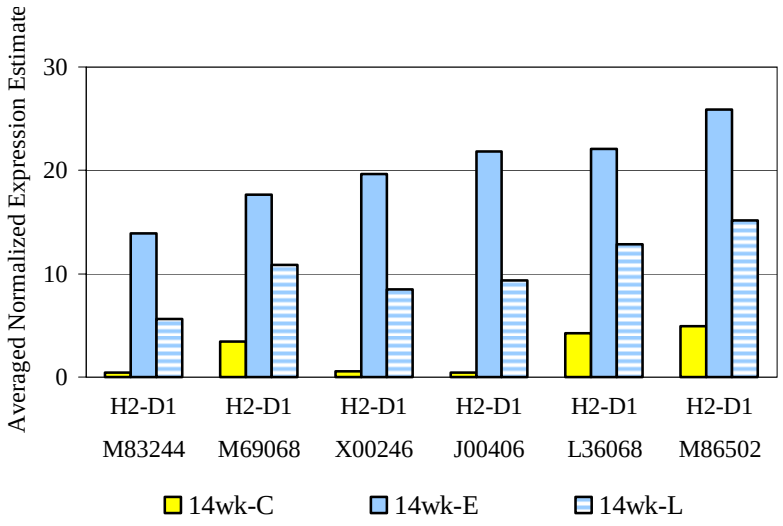

d.

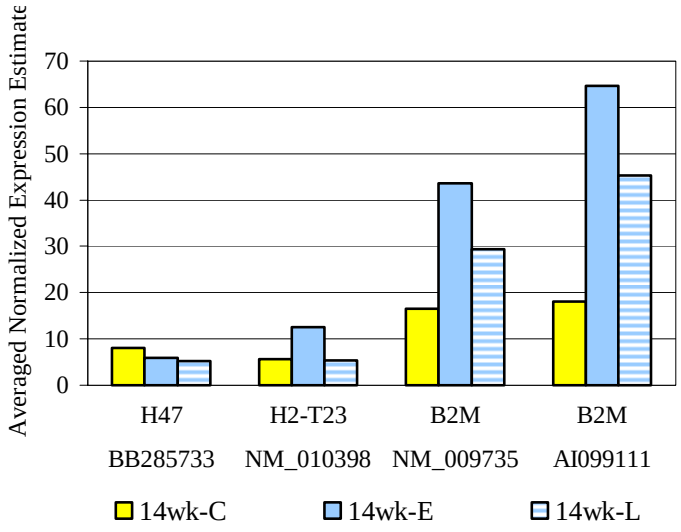

Figure 3.10 Expression Estimates of Genes Involved in Antigen Processing and Presentation at 14wks.

e.

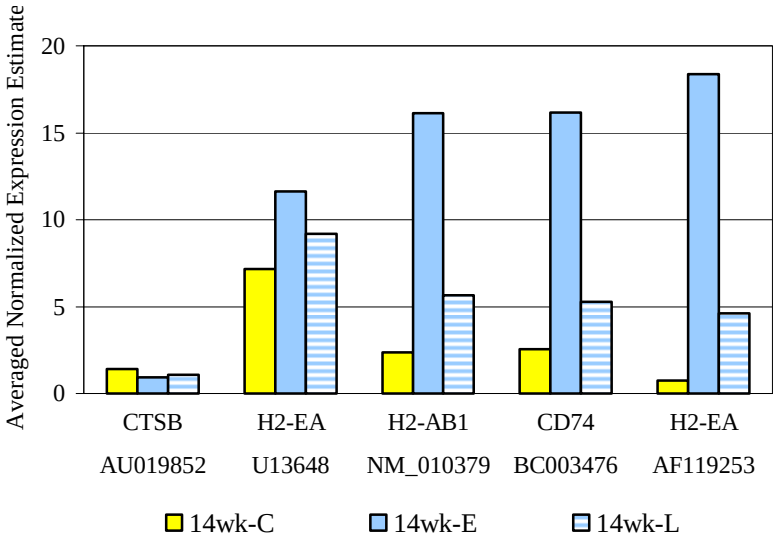

f.

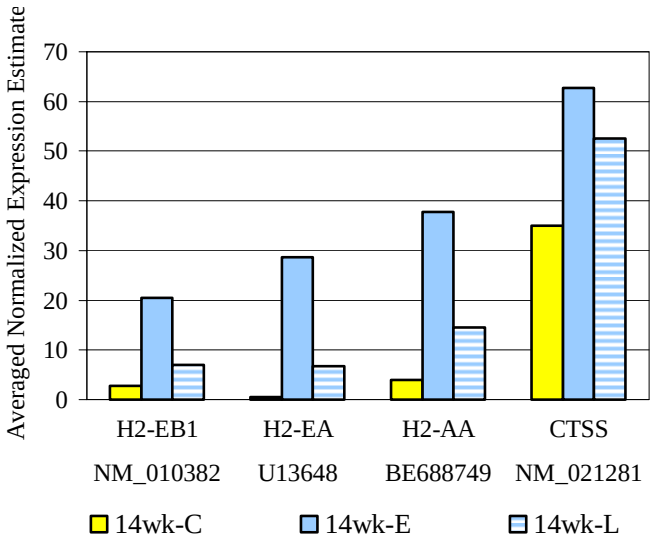

Figure 3.10 Expression Estimates of Genes Involved in Antigen Processing and Presentation at 14wks.

g.

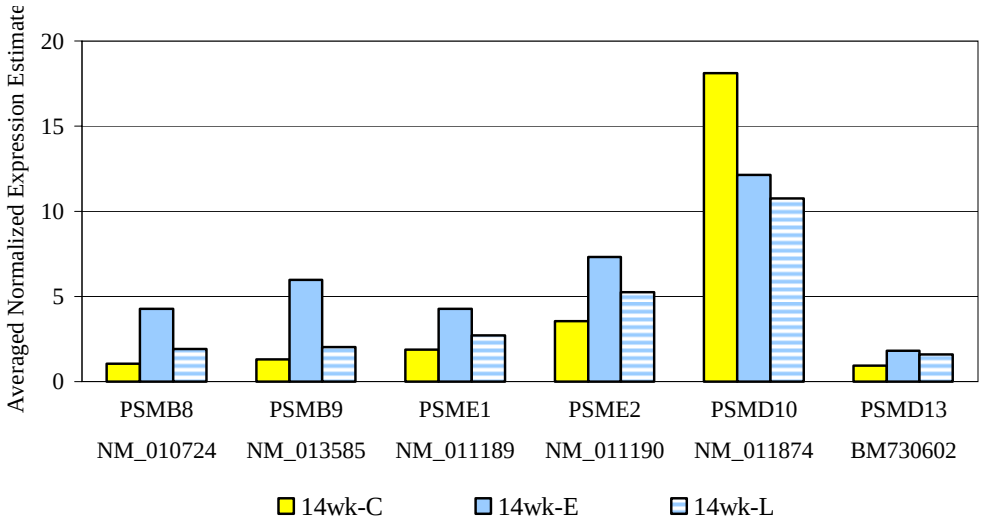

h.

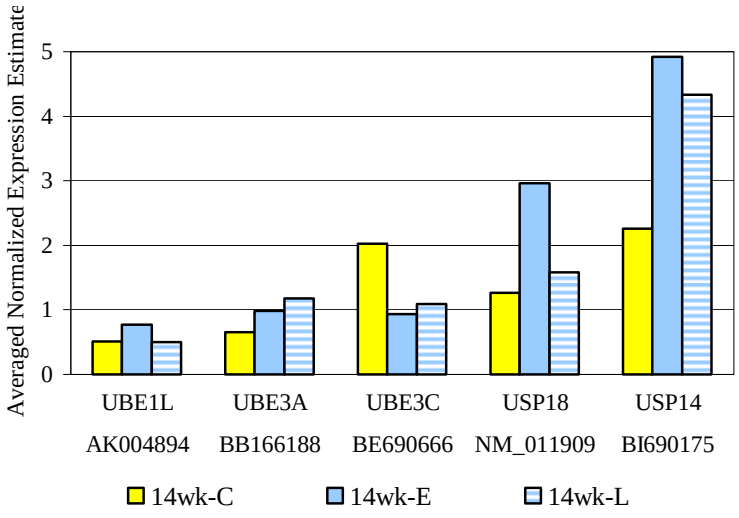

Figure 3.10 Expression Estimates of Genes Involved in Antigen Processing and Presentation at 14wks.

i.

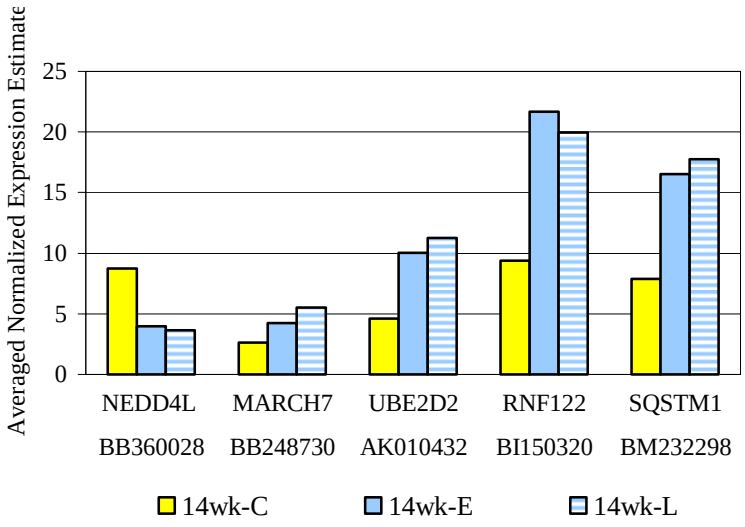

Table 3.5 Differential Expression of Genes Involved in Antigen Processing and Presentation. Replicate RNA samples from each treatment group were hybridized to separate arrays. The average of replicate normalized expression estimates for each sample group was used to calculate the fold change difference in expression for each gene in Figures 3.9 and 3.10. Positive fold change values indicate an increase, and negative values indicate a decrease in gene expression in the IFNγ-expressing groups. Values in grey indicate the Student's t-test p-value was greater than 0.1.

			Fold Change (IFN-γ-expressing / non-expressing)			
Accession No.	Gene Symbol	Gene Name	11wk-E	11wk-L	14wk-L	14wk-E
MHC Class I Presentation						
NM_030711	ARTS1	type 1 tumor necrosis factor receptor shedding aminopeptidase regulator	-1.30	-1.27	1.76	**1.50**
AA170322	B2M	beta-2 microglobulin	1.16	1.04	**1.74**	1.41
NM_009735	B2M	beta-2 microglobulin	-1.24	-1.20	**2.65**	1.79
AI099111	B2M	beta-2 microglobulin	-1.28	-1.15	**3.59**	**2.51**
AF390178	BAT1A	HLA-B-associated transcript 1A	**-1.89**	-1.15	1.22	1.10
BC011067	BAT1A	HLA-B-associated transcript 1A	**-1.85**	**-1.12**	1.63	1.46
M69068	H2-D1	histocompatibility 2, D region locus 1	-1.14	-1.19	**5.14**	**3.15**
L36068	H2-D1	histocompatibility 2, D region locus 1	-1.13	-1.14	**5.18**	**3.02**
M86502	H2-D1	histocompatibility 2, D region locus 1	-1.16	-1.17	**5.26**	**3.08**
M83244	H2-D1	histocompatibility 2, D region locus 1	9.42	3.07	**31.7**	12.7
X00246	H2-D1	histocompatibility 2, D region locus 1	10.18	3.36	**35.3**	**15.2**
J00406	H2-D1	histocompatibility 2, D region locus 1	13.22	4.44	**51.0**	**21.9**
L23495	H2-K	histocompatibility 2, K region	-1.33	-1.38	**2.94**	1.93
BC011306	H2-K	histocompatibility 2, K region	-1.44	-1.33	**3.37**	2.20
S70184	H2-K	histocompatibility 2, K region	-1.29	-1.20	**3.42**	2.08
NM_023422	H2-KE2	H2-K region expressed gene 2	-1.02	-1.17	-1.18	**-1.56**
AV132191	H2-KE6	H2-K region expressed gene 6	**-1.65**	-1.16	1.40	1.21
M33151	H2-L	histocompatibility 2, D region locus 1	-1.20	-1.16	**3.51**	2.02

Accession No.	Gene Symbol	Gene Name	Fold Change (IFN-γ-expressing / non-expressing) 11wk-E	11wk-L	14wk-E	14wk-L
M34962	H2-L	histocompatibility 2, L region	-1.13	-1.20	**6.00**	**3.09**
NM_013819	H2-M3	histocompatibility 2, M region locus 3	1.03	1.01	**1.99**	**1.54**
BC018402	H2-Q1	histocompatibility 2, Q region locus 1	**1.71**	**1.29**	1.29	1.18
M29881	H2-Q8	histocompatibility 2, Q region locus 7	1.12	-1.20	**3.38**	1.77
NM_010395	H2-T10	histocompatibility 2, T region locus 10	-1.12	-1.20	**1.76**	1.06
NM_010398	H2-T23	histocompatibility 2, T region locus 23	1.05	-1.25	**2.26**	-1.03
BB285733	H47	histocompatibility 47	-1.02	-1.10	-1.35	**-1.53**
BC024897	TAP1	transporter 1, ATP-binding cassette, sub-family B, MDR/TAP	1.15	-1.16	**1.98**	-1.06
MHC Class II Presentation						
BC003476	CD74	CD74	3.24	1.83	**6.36**	2.07
AU019852	CTSB	cathepsin B	1.02	-1.01	**-1.51**	**-1.31**
NM_021281	CTSS	cathepsin S	1.01	-1.07	**1.79**	1.50
BE688749	H2-AA	histocompatibility 2, class II antigen A, alpha	6.48	2.91	**9.59**	3.67
NM_010379	H2-AB1	histocompatibility 2, class II antigen A, beta 1	3.04	1.52	**6.84**	2.39
U13648	H2-EA	histocompatibility 2, class II antigen E alpha	1.24	1.11	**1.62**	**1.28**
AF119253	H2-EA	histocompatibility 2, class II antigen E alpha	5.97	1.83	**25.0**	6.26
U13648	H2-EA	histocompatibility 2, class II antigen E alpha	10.83	1.19	**53.9**	12.6
NM_010382	H2-EB1	histocompatibility 2, class II antigen E beta	3.13	1.78	**7.34**	2.49
20S Proteasome						
BC014783	PSMB3	proteasome (prosome, macropain) subunit, beta type 3	**-1.86**	-1.05	2.00	1.76
NM_011185	PSMB3	proteasome (prosome, macropain) subunit, beta type 3	**-1.61**	**-1.13**	1.55	1.33
NM_011186	PSMB6	proteasome (prosome, macropain) subunit, beta type 6	**-1.53**	-1.08	1.34	1.27

Accession No.	Gene Symbol	Gene Name	Fold Change (IFN-γ-expressing / non-expressing) 11wk-E	11wk-L	14wk-E	14wk-L
NM_010724	PSMB8	proteosome (prosome, macropain) subunit, beta type 8 (large multi-functional peptidase 7 - LMP7)	-1.29	-1.43	**4.07**	1.84
NM_013585	PSMB9	proteosome (prosome, macropain) subunit, beta type 9 (large multi-functional peptidase 2, LMP2)	1.04	-1.18	**4.62**	1.57
NM_011189	PSME1	proteasome (prosome, macropain) 28 subunit, alpha	**-1.43**	**-1.42**	**2.28**	1.46
NM_011190	PSME2	proteasome (prosome, macropain) 28 subunit, beta	-1.35	-1.20	**2.07**	1.48
BB310829	PSMF1	proteasome (prosome, macropain) inhibitor subunit 1	**-1.57**	-1.16	1.63	1.53
BB310829	PSMF1	proteasome (prosome, macropain) inhibitor subunit 1	**-1.50**	-1.08	1.47	1.27
26S Proteasome						
NM_011874	PSMD10	proteasome (prosome, macropain) 26S subunit, non-ATPase, 10	-1.23	-1.06	**-1.49**	**-1.68**
BM730602	PSMD13	proteasome (prosome, macropain) 26S subunit, non-ATPase, 13	-1.64	-1.13	**1.96**	1.71
Ubiquitin Pathway						
BB248730	MARCH7	membrane-associated RING-CH protein VII	1.18	1.02	**1.61**	**2.11**
BB360028	NEDD4L	developmentally down-regulated gene 4-like, neural precursor cell expressed	-1.15	-1.27	**-2.18**	**-2.40**
BI150320	RNF122	ring finger protein 122	-1.13	1.04	**2.32**	**2.13**
BM232298	SQSTM1	sequestosome 1	-1.46	-1.04	2.10	**2.26**
AK004894	UBE1L	ubiquitin-activating enzyme E1-like	-1.06	-1.18	**1.51**	-1.01
AK010432	UBE2D2	ubiquitin-conjugating enzyme E2D 2	-1.23	1.11	**2.17**	**2.42**
BE917478	UBE2R2	ubiquitin-conjugating enzyme E2R 2	**-1.51**	-1.13	1.33	1.11
BB166188	UBE3A	ubiquitin protein ligase E3A	1.58	**1.55**	1.51	**1.80**
BE690666	UBE3C	ubiquitin protein ligase E3C	1.21	**-1.25**	**-2.17**	**-1.86**
NM_011670	UCHL1	ubiquitin carboxy-terminal hydrolase L1	**-1.88**	-1.07	1.57	1.34
AI117611	USP11	ubiquitin specific protease 11	**-1.96**	-1.10	1.57	1.58
BI690175	USP14	ubiquitin specific protease 14	-1.22	-1.18	**2.18**	**1.92**

Accession No.	Gene Symbol	Gene Name	Fold Change (IFN-γ-expressing / non-expressing) 11wk-E	11wk-L	14wk-E	14wk-L
NM_011909	USP18	ubiquitin specific protease 18	-1.53	-1.96	**2.34**	1.25
NM_021323	USP3	ubiquitin specific protease 3	**-1.60**	-1.18	1.28	1.20

Figure 3.11 Expression Estimates of Genes Involved in Proteolysis at 14wks. Gene symbols and Accession numbers are plotted on the x-axis; the average of replicate normalized expression values for each treatment group (as described in Materials and Methods) is plotted on the y-axis. In some cases, a gene is represented on the microarray set more than once by different accession numbers. Fold change values are listed in Table 3.6.

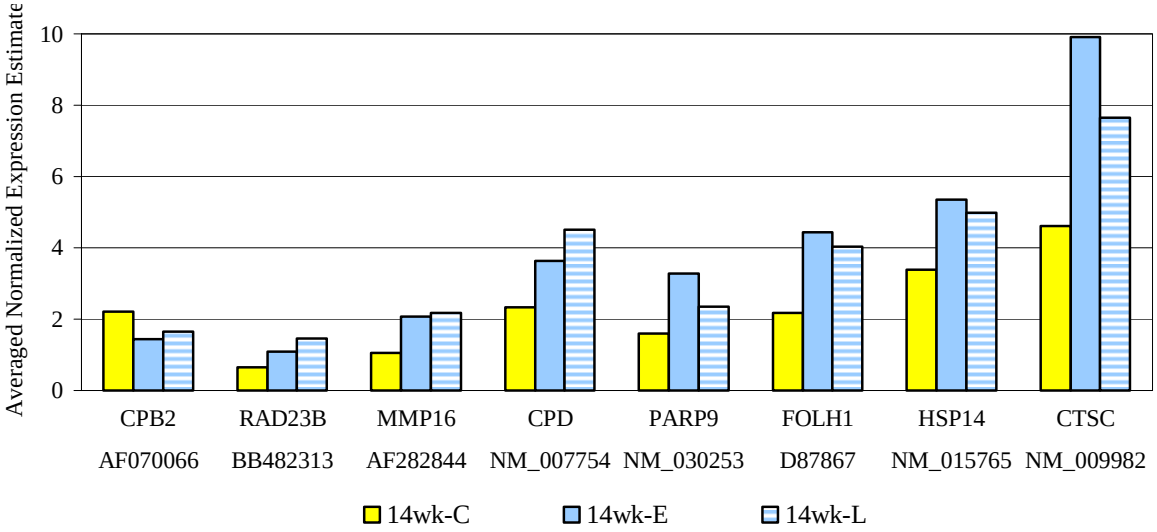

Table 3.6 Differential Expression of Genes Involved in Proteolysis. Replicate RNA samples from each treatment group were hybridized to separate arrays. The average of replicate normalized expression estimates for each sample group was used to calculate the fold change difference in expression for each gene in Figure 3.11. Positive fold change values indicate an increase, and negative values indicate a decrease in gene expression in the IFNγ-expressing groups. Values in grey indicate the Student's t-test p-value was greater than 0.1.

			Fold Change (IFN-γ-expressing / non-expressing)			
Accession No.	Gene Symbol	Gene Name	11wk-E	11wk-L	14wk-E	14wk-L
BE952331	APBA2BP	amyloid beta (A4) precursor protein-binding, family A, member 1 binding protein	**-2.18**	-1.09	1.14	-1.02
AF070066	CPB2	carboxypeptidase B2 (plasma)	1.00	1.10	**-1.53**	**-1.33**
NM_007754	CPD	carboxypeptidase D	-1.28	-1.05	1.56	**1.94**
NM_009982	CTSC	cathepsin C	-1.17	-1.39	**2.15**	1.66
D87867	FOLH1	folate hydrolase	-1.72	-1.21	**2.04**	1.85
NM_015765	HSP14	heat shock protein 4	-1.43	-1.12	**1.58**	1.47
AF282844	MMP16	matrix metalloproteinase 16	1.24	1.06	**1.97**	**2.08**
NM_030253	PARP9	poly (ADP-ribose) polymerase family, member 9	-1.11	-1.28	**2.06**	1.48
BB482313	RAD23B	RAD23b homolog	1.03	-1.01	**1.69**	**2.26**
NM_009112	S100A10	S100 calcium binding protein A10 (calpactin)	**-2.01**	-1.66	1.06	1.68
AV295650	S100A10	S100 calcium binding protein A10 (calpactin)	**-1.68**	**-1.81**	-1.47	1.11

Figure 3.12 Expression Estimates of Genes Involved in the Stress Response at 11wks. Gene symbols and Accession numbers are plotted on the x-axis; the average of replicate normalized expression values for each treatment group (as described in Materials and Methods) is plotted on the y-axis. In some cases, a gene is represented on the microarray set more than once by different accession numbers. Fold change values are listed in Table 3.7.

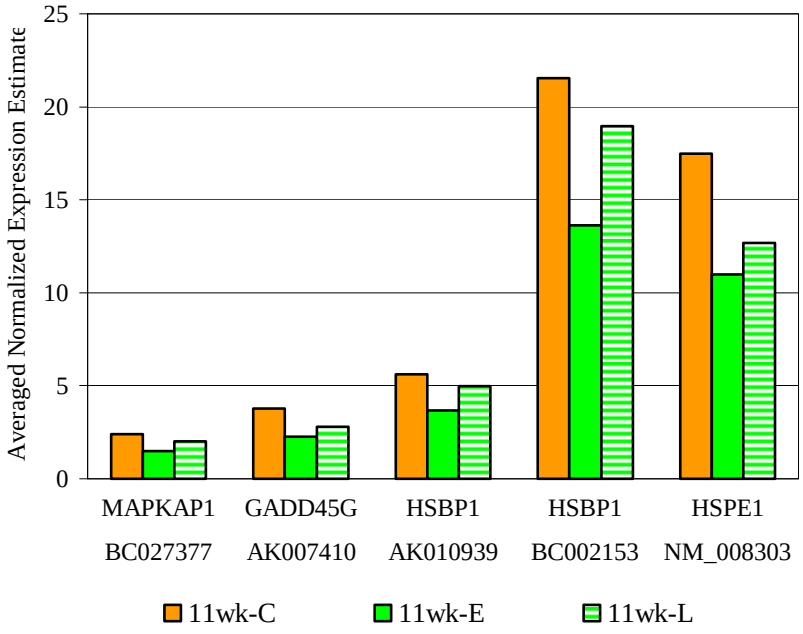

Table 3.7 Differential Expression of Genes Involved in the Stress Response. Replicate RNA samples from each treatment group were hybridized to separate arrays. The average of replicate normalized expression estimates for each sample group was used to calculate the fold change difference in expression for each gene in Figure 3.12. Positive fold change values indicate an increase, and negative values indicate a decrease in gene expression in the IFNγ-expressing groups. Values in grey indicate the Student's t-test p-value was greater than 0.1.

			Fold Change (IFN-γ-expressing / non-expressing)			
Accession No.	Gene Symbol	Gene Name	11wk-E	11wk-L	14wk-E	14wk-L
AK006478	DNAJB4	DnaJ (Hsp40) homolog, subfamily B, member 4	-1.07	**1.29**	1.20	**1.50**
AK007410	GADD45G	growth arrest and DNA-damage-inducible 45 gamma	**-1.67**	-1.36	1.02	-1.27
AK010939	HSBP1	heat shock factor binding protein 1	**-1.53**	**-1.13**	1.34	1.05
BC002153	HSBP1	heat shock factor binding protein 1	**-1.58**	-1.14	1.50	1.46
NM_008303	HSPE1	heat shock protein 1	**-1.59**	**-1.38**	1.28	1.00
BC027377	MAPKAP1	MAP kinase interacting protein 1	**-1.63**	-1.19	1.04	1.10

Figure 3.13 Expression Estimates of Genes Involved in Protein Biosynthesis at 11wks. a-c) Gene symbols and Accession numbers are plotted on the x-axis; the average of replicate normalized expression values for each treatment group (as described in Materials and Methods) is plotted on the y-axis. In some cases, a gene is represented on the microarray set more than once by different accession numbers. Fold change values are listed in Table 3.8.

a.

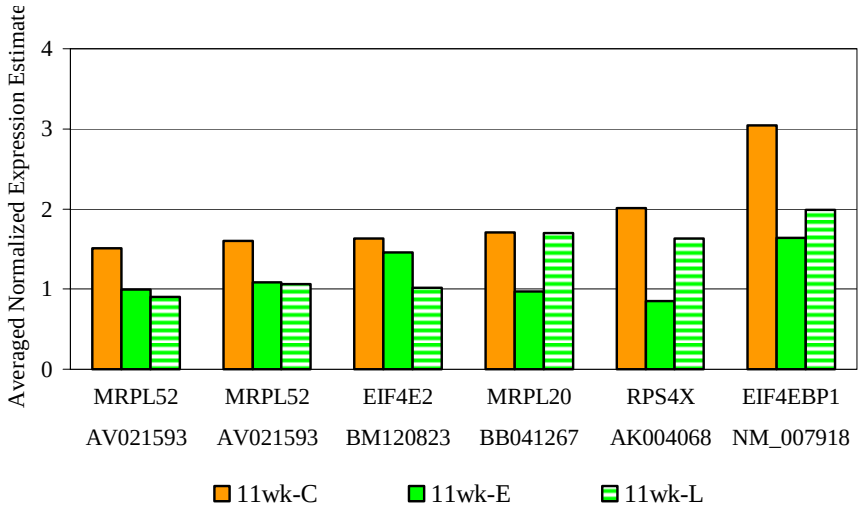

b.

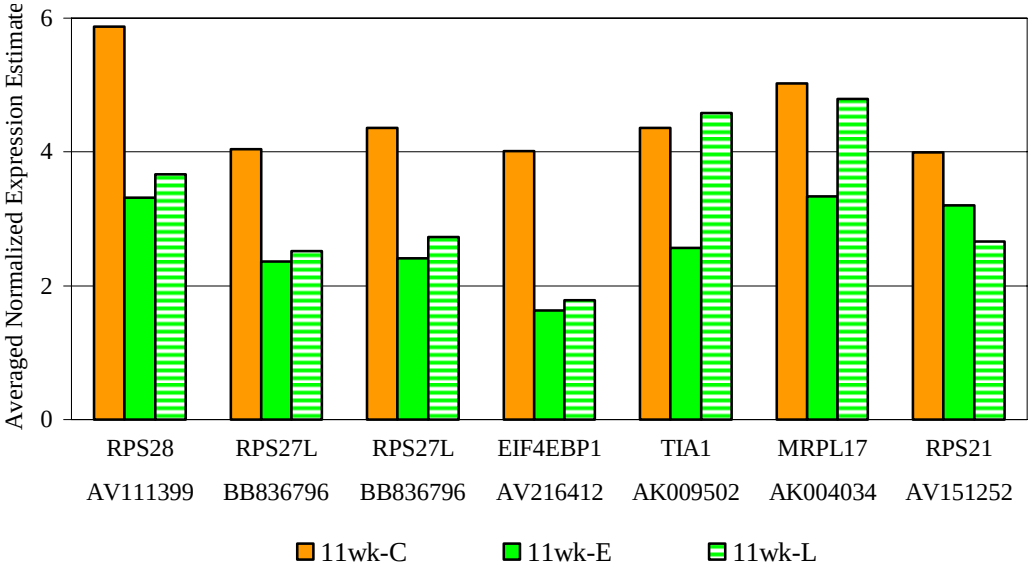

Figure 3.13 Expression Estimates of Genes Involved in Protein Biosynthesis at 11wks.

c.

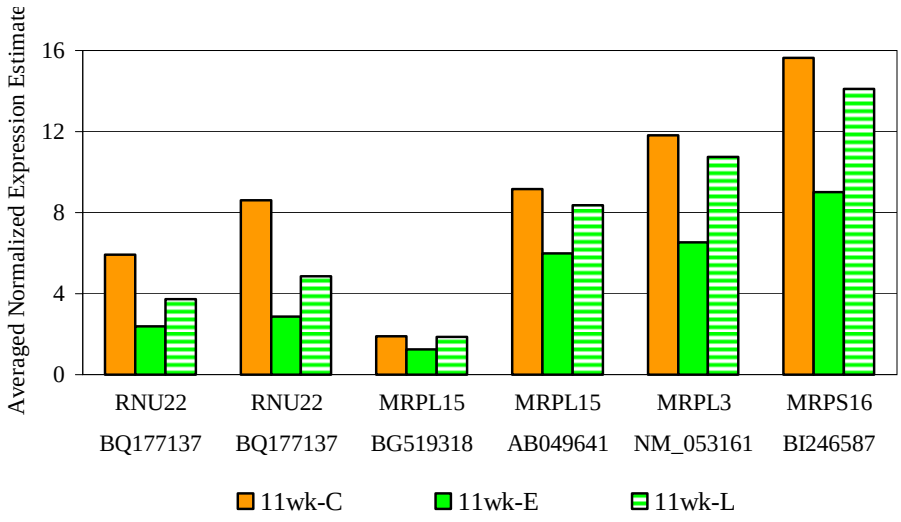

Figure 3.14 Expression Estimates of Genes Involved in Protein Biosynthesis at 14wks. a-c) Gene symbols and Accession numbers are plotted on the x-axis; the average of replicate normalized expression values for each treatment group (as described in Materials and Methods) is plotted on the y-axis. In some cases, a gene is represented on the microarray set more than once by different accession numbers. Fold change values are listed in Table 3.8.

a.

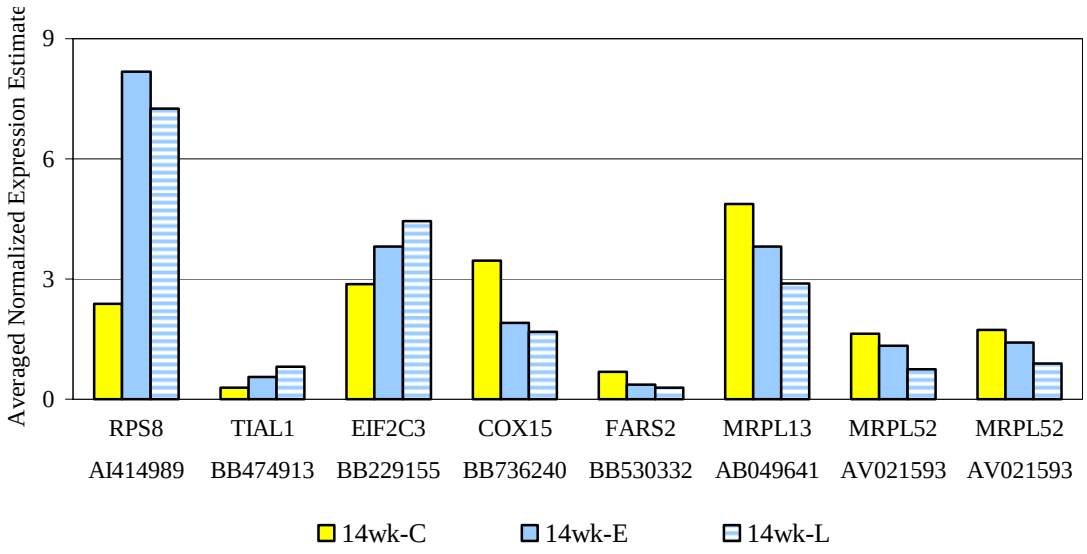

b.

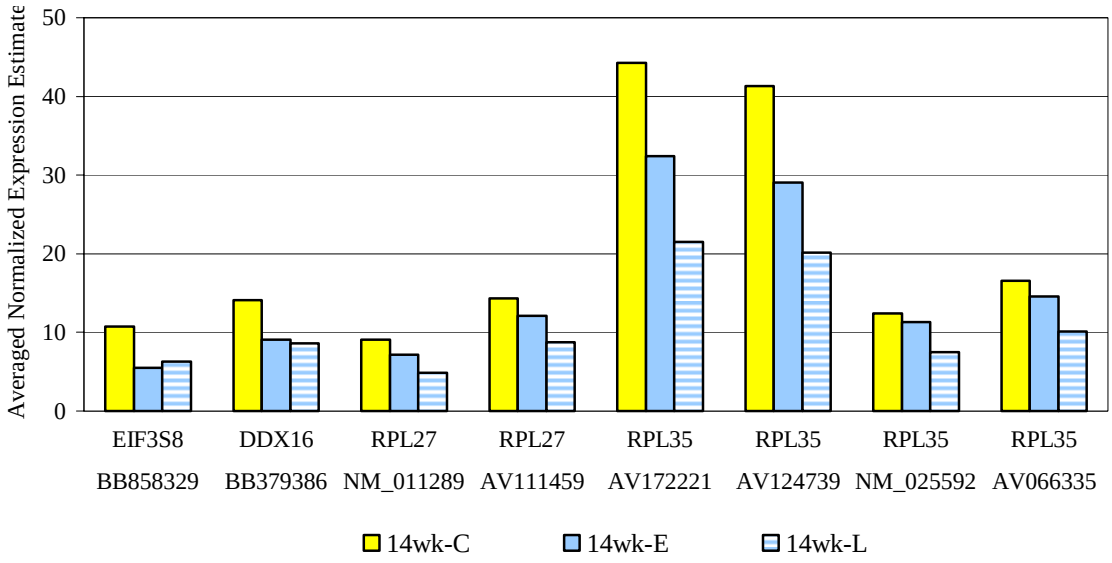

Figure 3.14 Expression Estimates of Genes Involved in Protein Biosynthesis at 14wks.

c.

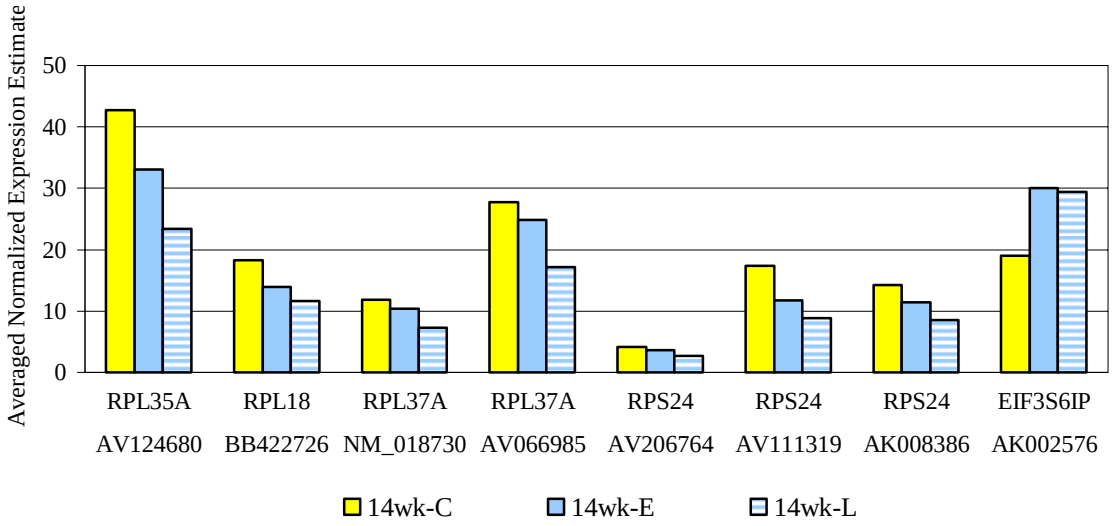

Table 3.8 Differential Expression of Genes Involved in Protein Biosynthesis. Replicate RNA samples from each treatment group were hybridized to separate arrays. The average of replicate normalized expression estimates for each sample group was used to calculate the fold change difference in expression for each gene in Figures 3.13 and 3.14. Positive fold change values indicate an increase, and negative values indicate a decrease in gene expression in the IFNγ-expressing groups. Values in grey indicate the Student's t-test p-value was greater than 0.1.

			Fold Change (IFN-γ-expressing / non-expressing)			
Accession No.	Gene Symbol	Gene Name	11wk-E	11wk-L	14wk-E	14wk-L
BB736240	COX15	cytochrome c oxidase assembly protein	-1.08	-1.27	-1.81	**-2.05**
BB379386	DDX16	DEAD/H (Asp-Glu-Ala-Asp/His) box polypeptide 16	1.05	-1.13	**-1.55**	**-1.64**
BB229155	EIF2C3	eukaryotic translation initiation factor 2C, 3	1.20	-1.23	**1.33**	**1.55**
AK002576	EIF3S6IP	eukaryotic translation initiation factor 3, subunit 6 interacting protein	-1.17	1.22	**1.58**	1.54
BB858329	EIF3S8	eukaryotic translation initiation factor 3, subunit 8	-1.61	-1.34	**-1.95**	**-1.71**
BM120823	EIF4E2	eukaryotic translation initiation factor 4E member 2	-1.12	**-1.60**	-1.52	-2.06
AV216412	EIF4EBP1	eukaryotic translation initiation factor 4E binding protein 1	**-2.47**	-2.25	-1.12	**-1.37**
NM_007918	EIF4EBP1	eukaryotic translation initiation factor 4E binding protein 1	**-1.85**	-1.53	-1.07	-1.22
BB530332	FARS2	phenylalanine-tRNA synthetase 2, mitochondrial	-1.02	-1.31	-1.84	**-2.46**
AB049641	MRPL13	mitochondrial ribosomal protein L13	-1.30	-1.24	-1.28	**-1.69**
AB049641	MRPL15	mitochondrial ribosomal protein L15	**-1.53**	-1.10	1.23	1.09
BG519318	MRPL15	mitochondrial ribosomal protein L15	**-1.53**	-1.02	1.43	1.45
AK004034	MRPL17	mitochondrial ribosomal protein L17	**-1.50**	-1.05	1.38	1.19
BB041267	MRPL20	mitochondrial ribosomal protein L20	**-1.76**	1.00	1.49	1.65
NM_053161	MRPL3	mitochondrial ribosomal protein L3	**-1.81**	-1.10	1.65	1.51
AV021593	MRPL52	mitochondrial ribosomal protein L52	**-1.52**	**-1.67**	-1.23	**-2.18**

Accession No.	Gene Symbol	Gene Name	Fold Change (IFN-γ-expressing / non-expressing) 11wk-E	11wk-L	14wk-E	14wk-L
AV021593	MRPL52	mitochondrial ribosomal protein L52	**-1.47**	**-1.51**	-1.21	**-1.95**
BI246587	MRPS16	mitochondrial ribosomal protein S16	**-1.74**	**-1.11**	1.69	1.38
BQ177137	RNU22	RNA, U22 small nucleolar	**-3.02**	-1.78	1.66	1.16
BQ177137	RNU22	RNA, U22 small nucleolar	**-2.50**	-1.59	1.56	1.31
BB422726	RPL18	ribosomal protein L18	**-1.24**	**-1.31**	-1.32	**-1.58**
NM_011289	RPL27	ribosomal protein L27	**-1.32**	**-1.32**	-1.26	**-1.86**
AV111459	RPL27	ribosomal protein L27	**-1.29**	**-1.26**	-1.19	**-1.63**
AV066335	RPL35	ribosomal protein L35	**-1.28**	**-1.32**	-1.14	**-1.63**
NM_025592	RPL35	ribosomal protein L35	**-1.41**	**-1.31**	-1.10	**-1.67**
AV172221	RPL35	ribosomal protein L35	**-1.17**	**-1.29**	-1.37	**-2.06**
AV124739	RPL35	ribosomal protein L35	-1.10	**-1.27**	-1.42	**-2.05**
AV124680	RPL35A	ribosomal protein L35a	**-1.14**	**-1.23**	-1.29	**-1.83**
NM_018730	RPL37A	ribosomal protein L37a	-1.18	**-1.38**	-1.13	**-1.63**
AV066985	RPL37A	ribosomal protein L37a	-1.09	**-1.31**	-1.12	**-1.62**
AV151252	RPS21	ribosomal protein S21	**-1.25**	**-1.50**	-2.03	-2.72
AK008386	RPS24	ribosomal protein S24	**-1.37**	**-1.21**	-1.25	**-1.68**
AV111319	RPS24	ribosomal protein S24	**-1.33**	**-1.20**	**-1.48**	**-1.96**
AV206764	RPS24	ribosomal protein S24	-1.29	**-1.17**	-1.11	**-1.52**
BB836796	RPS27L	ribosomal protein S27-like	**-1.81**	-1.60	1.69	1.13
BB836796	RPS27L	ribosomal protein S27-like	**-1.71**	**-1.61**	1.32	-1.11
AV111399	RPS28	ribosomal protein S28	**-1.77**	**-1.60**	1.45	1.03
AK004068	RPS4X	ribosomal protein S4, X-linked	**-2.36**	-1.23	1.23	1.11
AI414989	RPS8	ribosomal protein S8	-1.71	-1.05	**3.44**	**3.05**
AK009502	TIA1	cytotoxic granule-associated RNA binding protein 1	**-1.70**	1.05	1.12	1.13
BB474913	TIAL1	Tial1 cytotoxic granule-associated RNA binding protein-like 1	-1.14	1.29	1.93	**2.78**

Figure 3.15 Expression Estimates of Genes Involved in the Oxidative Stress Response at 11wks. Gene symbols and Accession numbers are plotted on the x-axis; the average of replicate normalized expression values for each treatment group (as described in Materials and Methods) is plotted on the y-axis. In some cases, a gene is represented on the microarray set more than once by different accession numbers. Fold change values are listed in Table 3.9.

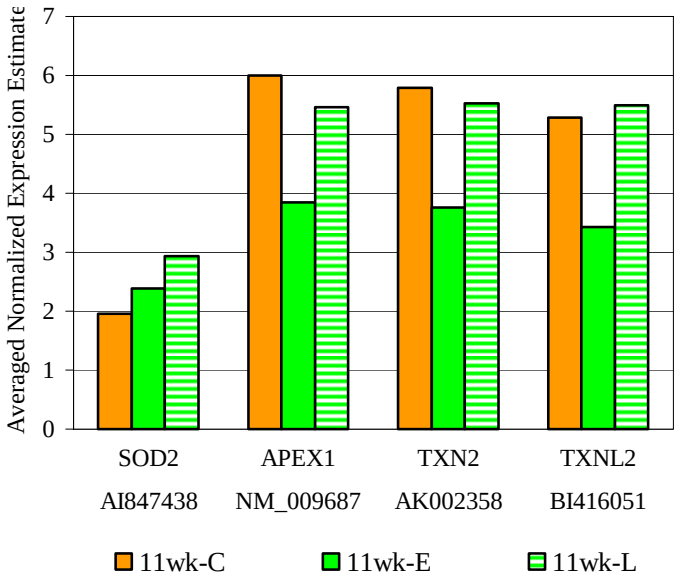

Figure 3.16 Expression Estimates of Genes Involved in the Oxidative Stress Response at 14wks. a-b) Gene symbols and Accession numbers are plotted on the x-axis; the average of replicate normalized expression values for each treatment group (as described in Materials and Methods) is plotted on the y-axis. In some cases, a gene is represented on the microarray set more than once by different accession numbers. Fold change values are listed in Table 3.9.

a.

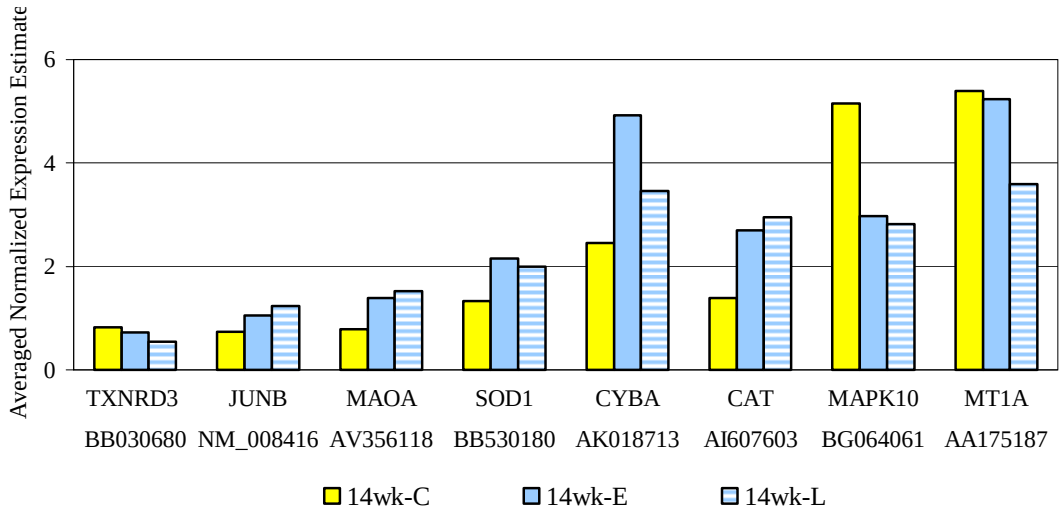

b.

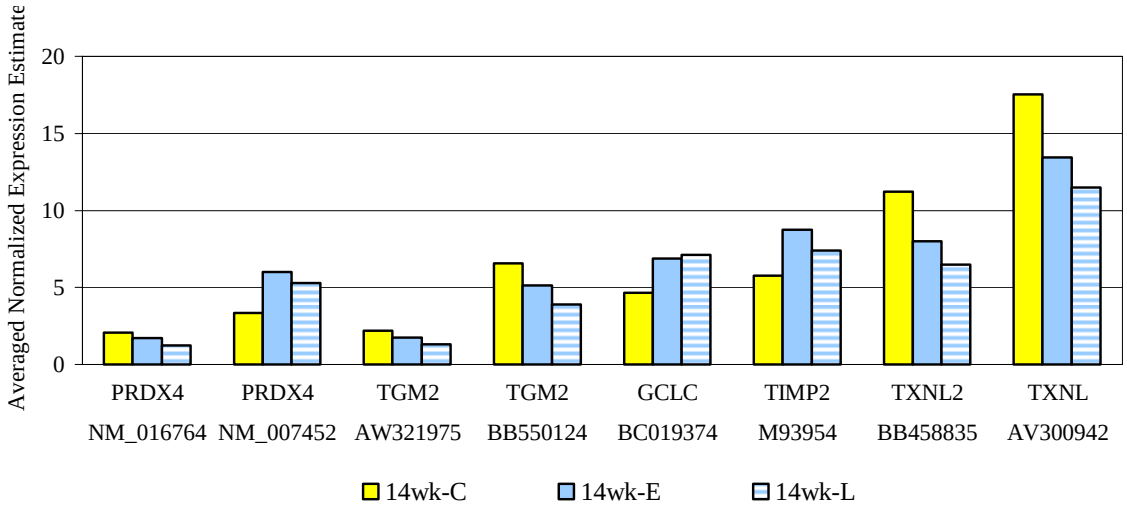

Table 3.9 Differential Expression of Genes Involved in the Oxidative Stress Response. Replicate RNA samples from each treatment group were hybridized to separate arrays. The average of replicate normalized expression estimates for each sample group was used to calculate the fold change difference in expression for each gene in Figures 3.15 and 3.16. Positive fold change values indicate an increase, and negative values indicate a decrease in gene expression in the IFNγ-expressing groups. Values in grey indicate the Student's t-test p-value was greater than 0.1.

			Fold Change (IFN-γ-expressing / non-expressing)			
Accession No.	Gene Symbol	Gene Name	11wk-E	11wk-L	14wk-E	14wk-L
NM_009687	APEX1	apurinic/apyrimidinic endonuclease 1	**-1.56**	**-1.10**	1.43	1.27
AI607603	CAT	catalase	-1.11	1.01	1.94	**2.12**
AK018713	CYBA	cytochrome b-245, alpha	-1.41	-1.45	**2.01**	1.41
BC019374	GCLC	glutamate-cysteine ligase, catalytic	-1.03	1.13	**1.49**	**1.54**
NM_008416	JUNB	Jun-B oncogene	1.01	-1.11	1.43	**1.68**
AV356118	MAOA	monoamine oxidase A	1.05	1.06	**1.75**	**1.92**
BG064061	MAPK10	mitogen activated protein kinase 10	1.09	-1.27	**-1.73**	**-1.83**
AA175187	MT1A	metallothionein-I activator	**-1.45**	**-1.22**	-1.03	**-1.50**
NM_016764	PRDX4	peroxiredoxin 4	**-1.32**	**-1.33**	-1.20	**-1.65**
NM_007452	PRDX4	peroxiredoxin 4	-1.42	-1.06	**1.81**	1.59
BB530180	SOD1	superoxide dismutase 1	1.14	1.02	**1.61**	**1.49**
AI847438	SOD2	superoxide dismutase 2, mitochondrial	1.22	**1.50**	1.23	1.39
BB550124	TGM2	transglutaminase 2, C polypeptide	1.24	-1.27	-1.28	**-1.68**
AW321975	TGM2	transglutaminase 2, C polypeptide	1.22	**-1.27**	-1.24	**-1.65**
M93954	TIMP2	tissue inhibitor of metalloproteinase 2	-1.04	-1.26	**1.51**	1.28
AK002358	TXN2	thioredoxin 2	**-1.54**	-1.05	1.20	1.16
AV300942	TXNL	thioredoxin-like (32kD)	1.02	-1.08	-1.31	**-1.52**
BI416051	TXNL2	thioredoxin-like 2	**-1.54**	1.04	1.70	1.79
BB458835	TXNL2	thioredoxin-like 2	-1.29	-1.21	**-1.41**	**-1.73**
BB030680	TXNRD3	thioredoxin reductase 3	-1.27	-1.18	-1.13	**-1.52**

Figure 3.17 Expression Estimates of Genes Involved in Cell Death at 11wks. a-b) Gene symbols and Accession numbers are plotted on the x-axis; the average of replicate normalized expression values for each treatment group (as described in Materials and Methods) is plotted on the y-axis. In some cases, a gene is represented on the microarray set more than once by different accession numbers. Fold change values are listed in Table 3.10.

a.

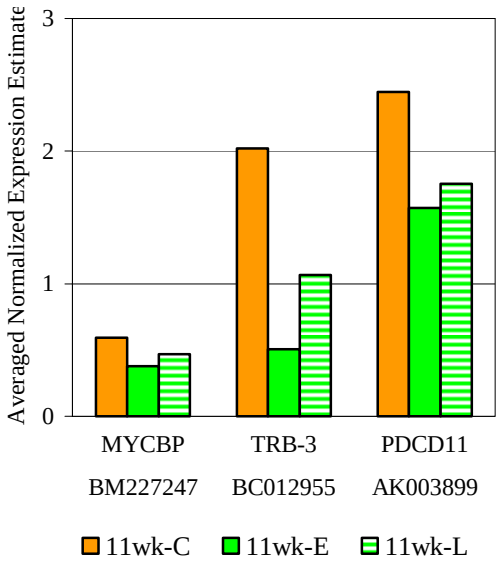

b.

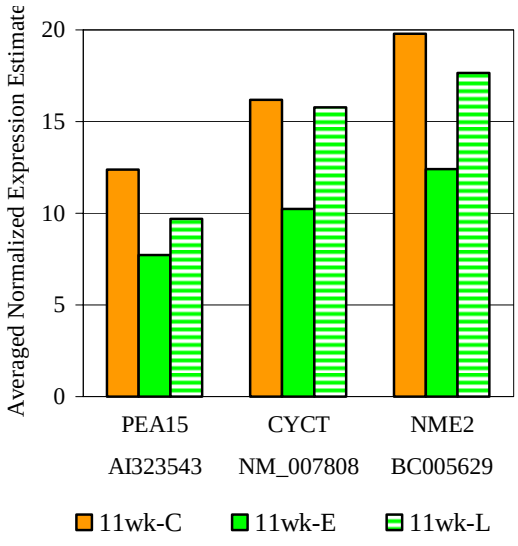

Figure 3.18 Expression Estimates of Genes Involved in Cell Death at 14wks. a-c) Gene symbols and Accession numbers are plotted on the x-axis; the average of replicate normalized expression values for each treatment group (as described in Materials and Methods) is plotted on the y-axis. In some cases, a gene is represented on the microarray set more than once by different accession numbers. Fold change values are listed in Table 3.10.

a.

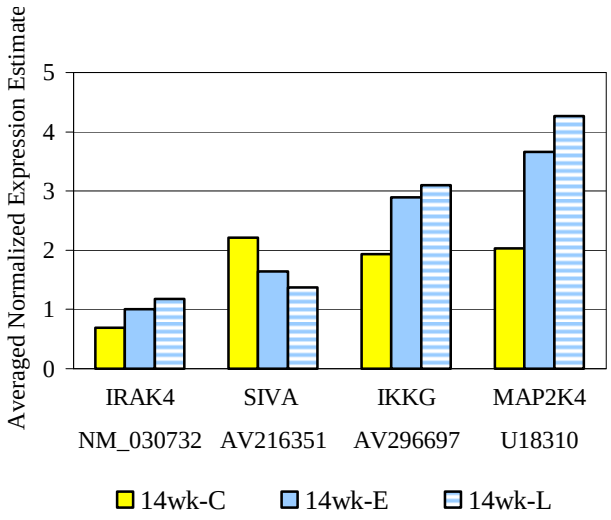

b.

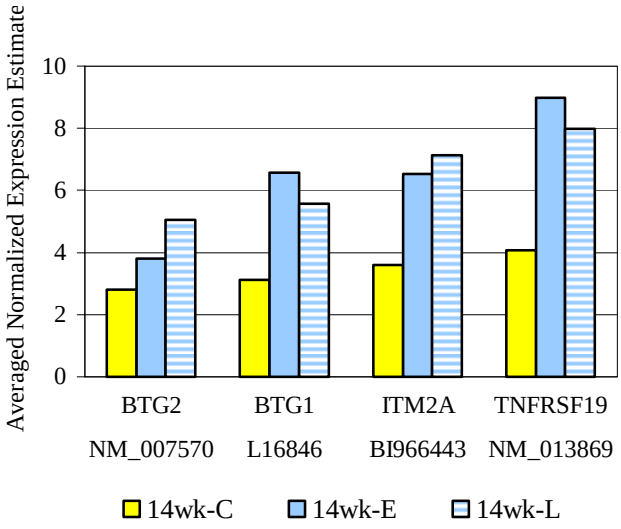

Figure 3.18 Expression Estimates of Genes Involved in Cell Death at 14wks.

c.

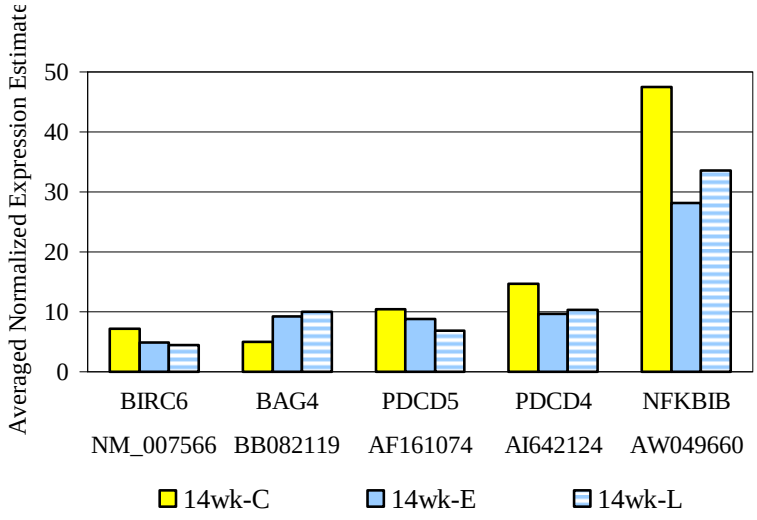

Table 3.10 Differential Expression of Genes Involved in Cell Death. Replicate RNA samples from each treatment group were hybridized to separate arrays. The average of replicate normalized expression estimates for each sample group was used to calculate the fold change difference in expression for each gene in Figures 3.17 and 3.18. Positive fold change values indicate an increase, and negative values indicate a decrease in gene expression in the IFNγ-expressing groups. Values in grey indicate the Student's t-test p-value was greater than 0.1.

			Fold Change (IFN-γ-expressing / non-expressing)			
Accession No.	Gene Symbol	Gene Name	11wk-E	11wk-L	14wk-E	14wk-L
Pro-Apoptotic Genes						
L16846	BTG1	B-cell translocation gene 1, anti-proliferative	**-1.46**	-1.21	**2.11**	1.79
NM_007570	BTG2	B-cell translocation gene 2, anti-proliferative	-1.44	1.09	1.36	**1.81**
NM_007808	CYCT	cytochrome c, testis	**-1.58**	-1.03	1.23	1.10
NM_030732	IRAK4	interleukin-1 receptor-associated kinase 4	-1.05	1.06	**1.44**	**1.69**
BI966443	ITM2A	integral membrane protein 2A	-1.10	1.15	**1.82**	**1.98**
U18310	MAP2K4	mitogen activated protein kinase kinase 4	-1.07	1.11	1.80	**2.10**
BM227247	MYCBP	c-myc binding protein	**-1.58**	-1.27	1.06	1.05
AW049660	NFKBIB	nuclear factor of kappa light chain gene enhancer in B-cells inhibitor, beta	1.12	-1.07	**-1.69**	**-1.42**
AK003899	PDCD11	programmed cell death protein 11	**-1.55**	-1.39	-1.08	-1.08
AI642124	PDCD4	programmed cell death 4	-1.23	1.06	**-1.52**	**-1.42**
AF161074	PDCD5	programmed cell death 5	**-1.14**	**-1.09**	-1.19	**-1.52**
AI323543	PEA15	phosphoprotein enriched in astrocytes 15	**-1.60**	**-1.28**	1.61	1.49
AV216351	SIVA	Cd27 binding protein (Hindu God of destruction)	1.02	-1.15	**-1.35**	**-1.62**
NM_013869	TNFRSF19	tumor necrosis factor receptor superfamily, member 19	-1.52	-1.22	**2.21**	1.96
BC012955	TRB-3	Tribbles 3 homolog	**-4.00**	-1.90	-1.15	**-1.18**

Accession No.	Gene Symbol	Gene Name	Fold Change (IFN-γ-expressing / non-expressing) 11wk-E	11wk-L	14wk-E	14wk-L
Survival Genes						
BB082119	BAG4	BCL2-associated athanogene 4	-1.24	1.09	**1.85**	**2.01**
NM_007566	BIRC6	baculoviral IAP repeat-containing 6	1.06	-1.07	**-1.45**	**-1.59**
AV296697	IKKG	inhibitor of kappaB kinase gamma	1.10	-1.03	1.49	**1.60**
BC005629	NME2	expressed in non-metastatic cells 2, protein (NM23B) (nucleoside diphosphate kinase)	**-1.59**	-1.12	1.53	1.44

Figure 3.19 Expression Estimates of Genes Involved in Cell Cycle at 11wks. Gene symbols and Accession numbers are plotted on the x-axis; the average of replicate normalized expression values for each treatment group (as described in Materials and Methods) is plotted on the y-axis. In some cases, a gene is represented on the microarray set more than once by different accession numbers. Fold change values are listed in Table 3.11.

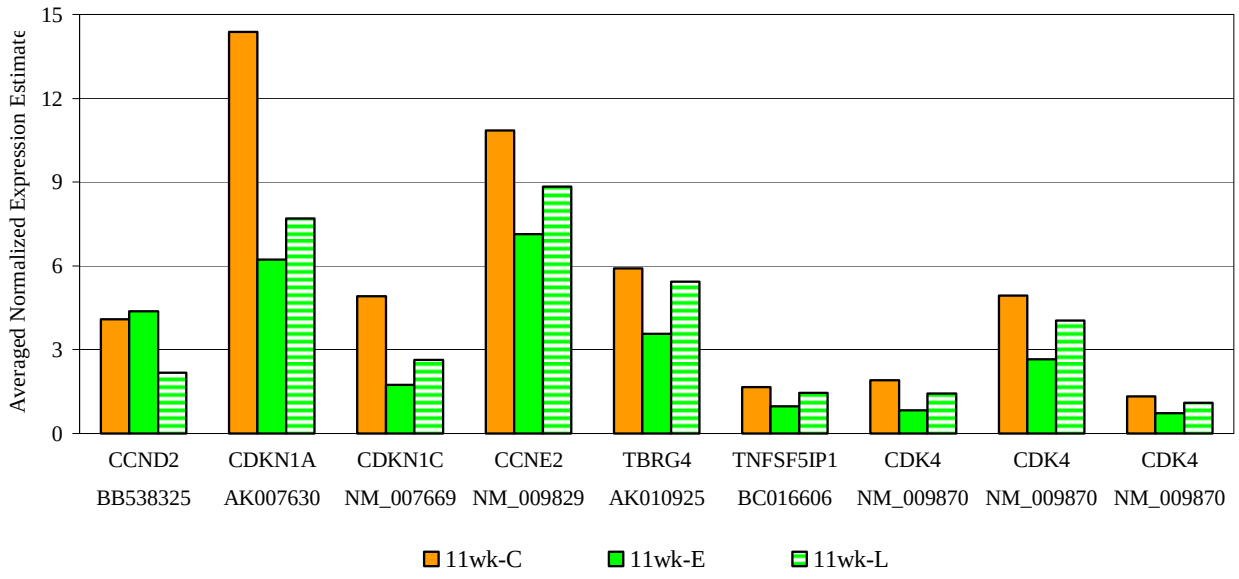

Figure 3.20 Expression Estimates of Genes Involved in Cell Cycle at 14wks. a-b) Gene symbols and Accession numbers are plotted on the x-axis; the average of replicate normalized expression values for each treatment group (as described in Materials and Methods) is plotted on the y-axis. In some cases, a gene is represented on the microarray set more than once by different accession numbers. Fold change values are listed in Table 3.11.

a.

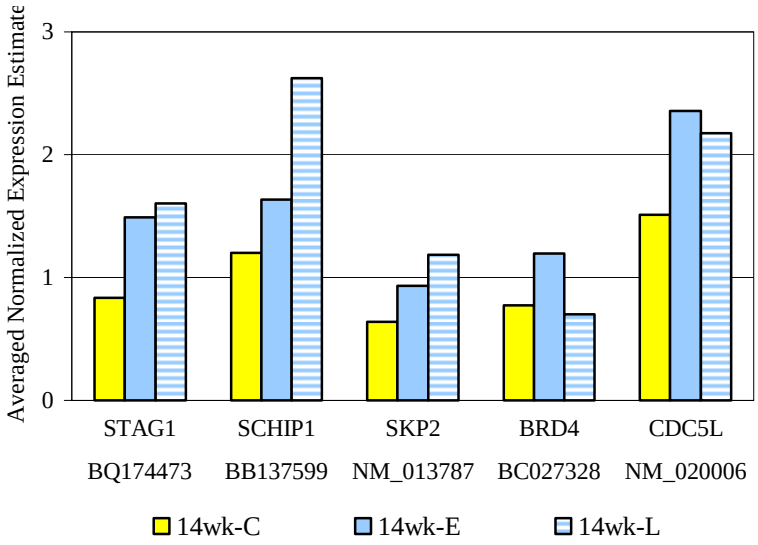

b.

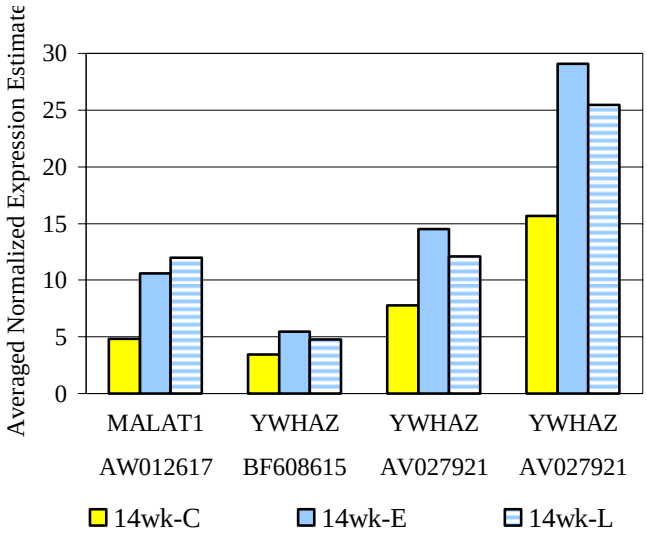

Table 3.11 Differential Expression of Genes Involved in Cell Cycle. Replicate RNA samples from each treatment group were hybridized to separate arrays. The average of replicate normalized expression estimates for each sample group was used to calculate the fold change difference in expression for each gene in Figures 3.19 and 3.20. Positive fold change values indicate an increase, and negative values indicate a decrease in gene expression in the IFNγ-expressing groups. Values in grey indicate the Student's t-test p-value was greater than 0.1.

			Fold Change (IFN-γ-expressing / non-expressing)			
Accession No.	Gene Symbol	Gene Name	11wk-E	11wk-L	14wk-E	14wk-L
BC027328	BRD4	bromodomain containing 4	-2.41	-2.25	**1.55**	-1.10
BB538325	CCND2	cyclin D2	1.07	**-1.88**	1.30	1.14
NM_009829	CCNE2	cyclin E2	**-1.52**	-1.23	1.48	1.46
NM_020006	CDC5L	cell division cycle 5-like	-1.10	-1.11	**1.56**	**1.44**
NM_009870	CDK4	cyclin-dependent kinase 4	**-2.31**	**-1.33**	1.98	1.53
NM_009870	CDK4	cyclin-dependent kinase 4	**-1.85**	-1.22	1.32	1.16
NM_009870	CDK4	cyclin-dependent kinase 4	**-1.80**	**-1.21**	1.19	-1.10
AK007630	CDKN1A	cyclin-dependent kinase inhibitor 1A (P21)	**-2.31**	**-1.87**	-1.35	-1.85
NM_007669	CDKN1C	cyclin-dependent kinase inhibitor 1C (P57)	**-2.81**	-1.87	-1.44	-1.76
AW012617	MALAT1	metastasis associated lung adenocarcinoma transcript 1	1.08	-1.17	**2.18**	**2.47**
BB137599	SCHIP1	schwannomin interacting protein 1	1.16	1.12	1.36	**2.18**
NM_013787	SKP2	S-phase kinase-associated protein 2 (p45)	-1.06	1.00	1.46	**1.86**
BQ174473	STAG1	stromal antigen 1	-1.07	1.05	**1.78**	**1.92**
AK010925	TBRG4	cell cycle progression 2 protein	**-1.65**	-1.09	1.37	1.22
BC016606	TNFSF5IP1	tumor necrosis factor superfamily, member 5-induced protein 1	**-1.71**	-1.15	1.55	1.58
BF608615	YWHAZ	tyrosine 3-monooxygenase/ tryptophan 5-monooxygenase activation protein, zeta polypeptide	-1.03	1.02	**1.58**	1.39
AV027921	YWHAZ	tyrosine 3-monooxygenase/ tryptophan 5-monooxygenase activation protein, zeta polypeptide	-1.29	1.01	**1.87**	1.56
AV027921	YWHAZ	tyrosine 3-monooxygenase/ tryptophan 5-monooxygenase activation protein, zeta polypeptide	-1.25	1.02	**1.86**	1.63

Figure 3.21 Expression Estimates of Genes Involved in Differentiation at 11wks. Gene symbols and Accession numbers are plotted on the x-axis; the average of replicate normalized expression values for each treatment group (as described in Materials and Methods) is plotted on the y-axis. In some cases, a gene is represented on the microarray set more than once by different accession numbers. Fold change values are listed in Table 3.12.

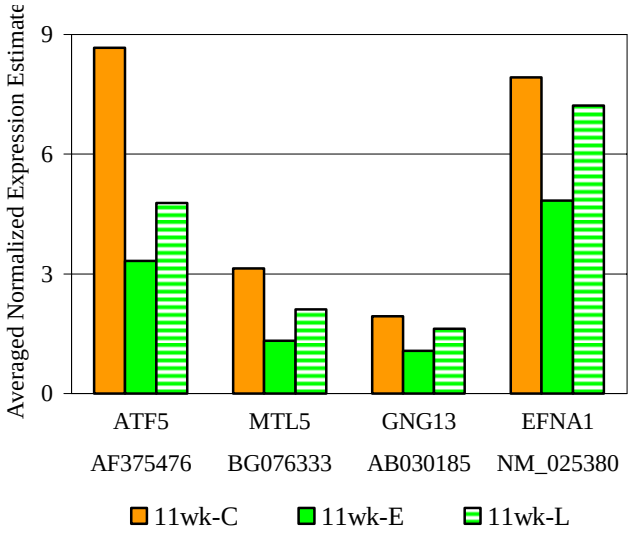

Figure 3.22 Expression Estimates of Genes Involved in Differentiation at 14wks. a-b) Gene symbols and Accession numbers are plotted on the x-axis; the average of replicate normalized expression values for each treatment group (as described in Materials and Methods) is plotted on the y-axis. In some cases, a gene is represented on the microarray set more than once by different accession numbers. Fold change values are listed in Table 3.12.

a.

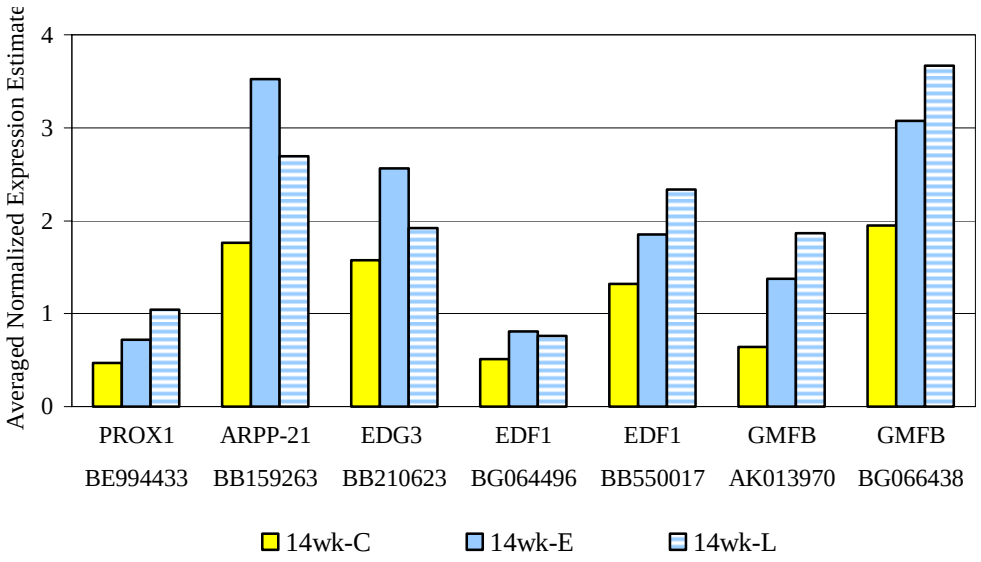

b.

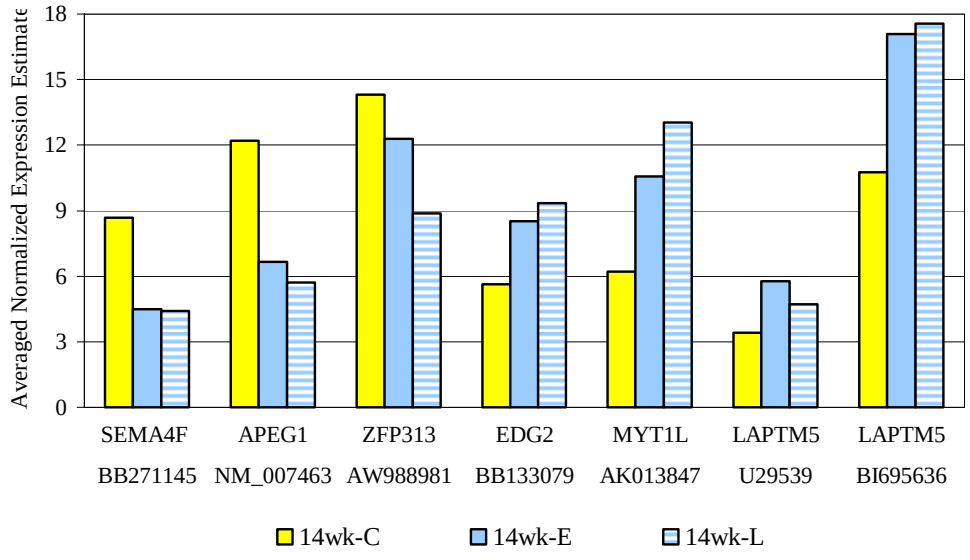

Table 3.12 Differential Expression of Genes Involved in Differentiation. Replicate RNA samples from each treatment group were hybridized to separate arrays. The average of replicate normalized expression estimates for each sample group was used to calculate the fold change difference in expression for each gene in Figures 3.21 and 3.22. Positive fold change values indicate an increase, and negative values indicate a decrease in gene expression in the IFNγ-expressing groups. Values in grey indicate the Student's t-test p-value was greater than 0.1.

			Fold Change (IFN-γ-expressing / non-expressing)			
Accession No.	Gene Symbol	Gene Name	11wk-E	11wk-L	14wk-E	14wk-L
NM_007463	APEG1	aortic preferentially expressed gene 1	1.19	-1.10	**-1.83**	**-2.13**
BB159263	ARPP-21	cyclic AMP-regulated phosphoprotein, 21	-1.48	1.09	**2.00**	**1.53**
AF375476	ATF5	activating transcription factor 5	**-2.60**	-1.82	-1.08	**-1.20**
BG064496	EDF1	endothelial differentiation-related factor 1	-1.50	-1.60	**1.58**	1.49
BB550017	EDF1	endothelial differentiation-related factor 1	1.15	1.05	1.41	**1.77**
BB133079	EDG2	endothelial differentiation, lysophosphatidic acid G-protein-coupled receptor, 2	-1.27	1.03	**1.51**	**1.66**
BB210623	EDG3	endothelial differentiation, sphingolipid G-protein-coupled receptor, 3	-1.29	-1.28	**1.62**	1.22
NM_025380	EFNA1	ephrin A1	**-1.64**	-1.10	1.57	1.42
BG066438	GMFB	glia maturation factor, beta	-1.08	-1.08	1.58	**1.88**
AK013970	GMFB	glia maturation factor, beta	-1.33	-1.05	2.14	**2.91**
AB030185	GNG13	guanine nucleotide binding protein 13, gamma	**-1.80**	-1.20	1.11	-1.13
U29539	LAPTM5	lysosomal-associated protein transmembrane 5	1.02	-1.32	**1.69**	1.38
BI695636	LAPTM5	lysosomal-associated protein transmembrane 5	-1.38	-1.09	**1.59**	**1.63**
BG076333	MTL5	metallothionein-like 5	**-2.35**	**-1.48**	1.06	1.11
BE994433	PROX1	prospero-related homeobox 1	1.20	1.07	**1.53**	**2.21**
BB271145	SEMA4F	sema domain, immunoglobulin domain (Ig), TM domain, and short cytoplasmic domain	-1.01	-1.07	**-1.94**	**-1.97**
AW988981	ZFP313	zinc finger protein 313	**-1.35**	**-1.33**	-1.16	**-1.61**

Figure 3.23 Expression Estimates of Genes Involved in Development at 14wks. a-b) Gene symbols and Accession numbers are plotted on the x-axis; the average of replicate normalized expression values for each treatment group (as described in Materials and Methods) is plotted on the y-axis. In some cases, a gene is represented on the microarray set more than once by different accession numbers. Fold change values are listed in Table 3.13.

a.

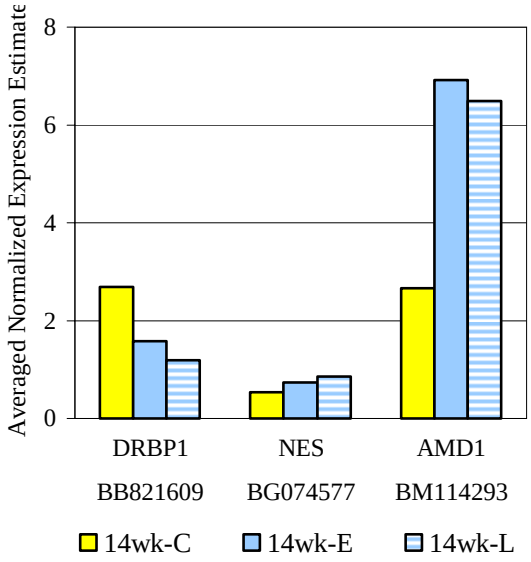

b.

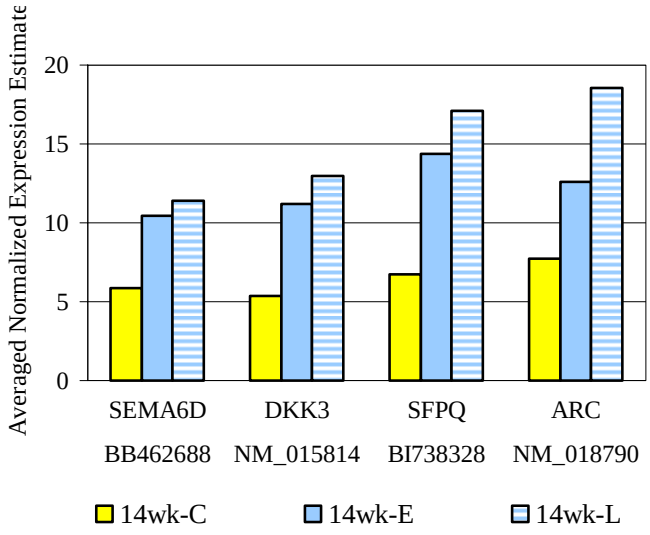

Table 3.13 Differential Expression of Genes Involved in Development. Replicate RNA samples from each treatment group were hybridized to separate arrays. The average of replicate normalized expression estimates for each sample group was used to calculate the fold change difference in expression for each gene in Figure 3.23. Positive fold change values indicate an increase, and negative values indicate a decrease in gene expression in the IFNγ-expressing groups. Values in grey indicate the Student's t-test p-value was greater than 0.1.

			Fold Change (IFN-γ-expressing / non-expressing)			
Accession No.	Gene Symbol	Gene Name	11wk-E	11wk-L	14wk-E	14wk-L
BM114293	AMD1	S-adenosylmethionine decarboxylase 1	1.09	1.12	**2.60**	**2.43**
NM_018790	ARC	activity regulated cytoskeletal-associated protein	1.47	1.11	1.63	**2.40**
NM_015814	DKK3	dickkopf homolog 3	-1.06	1.18	**2.08**	**2.41**
BB821609	DRBP1	developmentally regulated RNA binding protein 1	1.04	-1.12	-1.71	**-2.27**
BG074577	NES	nestin	1.14	1.06	**1.37**	**1.59**
BB462688	SEMA6D	sema domain, transmembrane domain (TM), and cytoplasmic domain, (semaphorin) 6D	-1.29	-1.07	1.79	**1.94**
BI738328	SFPQ	splicing factor proline/glutamine rich (polypyrimidine tract binding protein associated)	1.18	1.06	**2.13**	**2.55**

Figure 3.24 Expression Estimates of Genes Involved in Cell Growth at 11wks. Gene symbols and Accession numbers are plotted on the x-axis; the average of replicate normalized expression values for each treatment group (as described in Materials and Methods) is plotted on the y-axis. In some cases, a gene is represented on the microarray set more than once by different accession numbers. Fold change values are listed in Table 3.14.

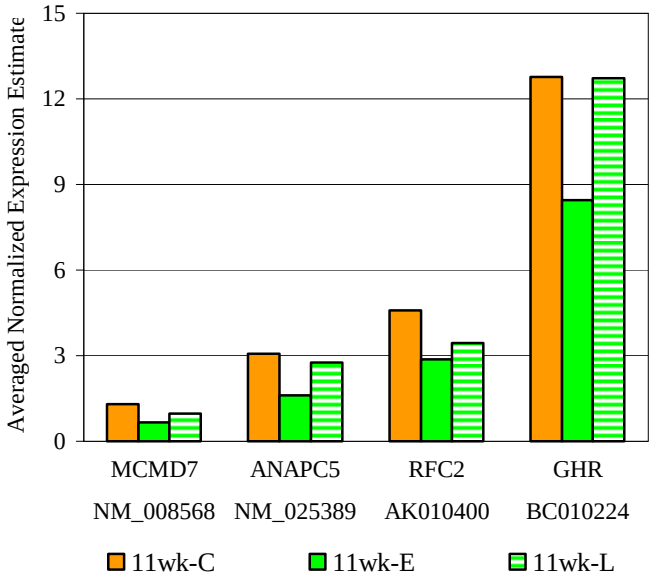

Figure 3.25 Expression Estimates of Genes Involved in Cell Growth at 14wks. a-b) Gene symbols and Accession numbers are plotted on the x-axis; the average of replicate normalized expression values for each treatment group (as described in Materials and Methods) is plotted on the y-axis. In some cases, a gene is represented on the microarray set more than once by different accession numbers. Fold change values are listed in Table 3.14.

a.

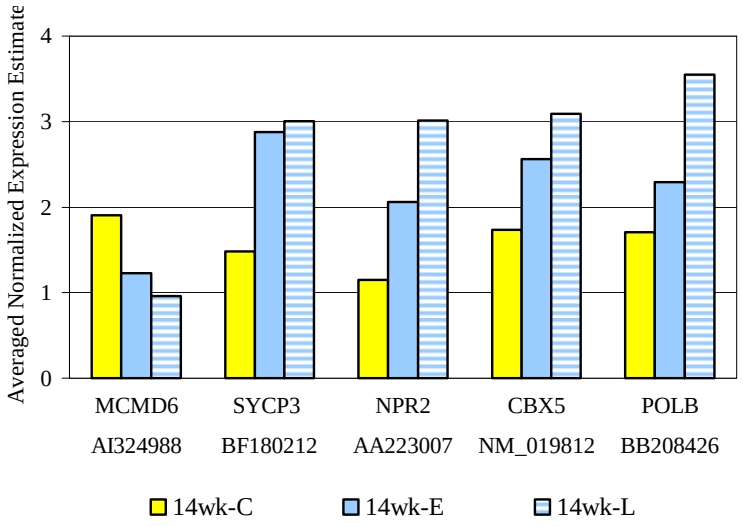

b.

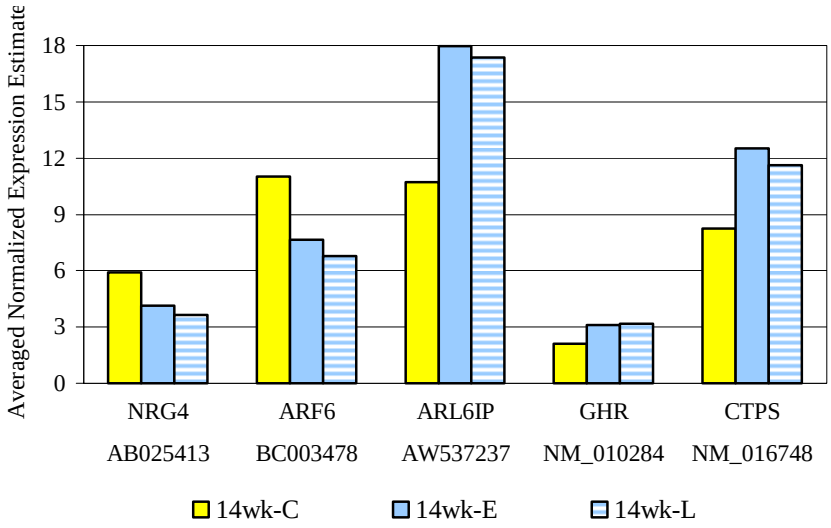

Table 3.14 Differential Expression of Genes Involved in Cell Growth. Replicate RNA samples from each treatment group were hybridized to separate arrays. The average of replicate normalized expression estimates for each sample group was used to calculate the fold change difference in expression for each gene in Figures 3.24 and 3.25. Positive fold change values indicate an increase, and negative values indicate a decrease in gene expression in the IFNγ-expressing groups. Values in grey indicate the Student's t-test p-value was greater than 0.1.

			Fold Change (IFN-γ-expressing / non-expressing)			
Accession No.	Gene Symbol	Gene Name	11wk-E	11wk-L	14wk-E	14wk-L
NM_025389	ANAPC5	anaphase-promoting complex subunit 5	**-1.89**	-1.11	1.46	1.14
BC003478	ARF6	ADP-ribosylation factor 6	-1.06	**-1.28**	-1.44	**-1.63**
AW537237	ARL6IP	ADP-ribosylation-like factor 6 interacting protein	-1.17	-1.01	**1.67**	**1.62**
NM_019812	CBX5	chromobox homolog 5	-1.03	1.09	1.47	**1.78**
NM_016748	CTPS	cytidine 5'-triphosphate synthase	-1.19	1.06	**1.52**	1.41
BC010224	GHR	growth hormone receptor	**-1.51**	1.00	1.19	1.17
NM_010284	GHR	growth hormone receptor	-1.11	-1.14	**1.47**	**1.50**
AI324988	MCMD6	mini chromosome maintenance deficient 6	-1.22	-1.38	-1.55	**-1.99**
NM_008568	MCMD7	mini chromosome maintenance deficient 7	**-1.95**	-1.33	-1.16	-1.23
AA223007	NPR2	natriuretic peptide receptor 2	-1.10	1.27	1.79	**2.62**
AB025413	NRG4	neuregulin 4	-1.62	-1.75	-1.43	**-1.62**
BB208426	POLB	DNA polymerase B1	1.19	1.19	1.34	**2.08**
AK010400	RFC2	replication factor C (activator 1) 2 (40kD)	**-1.60**	**-1.34**	-1.11	**-1.40**
BF180212	SYCP3	synaptonemal complex protein 3	1.00	1.23	**1.94**	**2.03**

Figure 3.26 Expression Estimates of Genes Involved in Metabolism at 11wks. Gene symbols and Accession numbers are plotted on the x-axis; the average of replicate normalized expression values for each treatment group (as described in Materials and Methods) is plotted on the y-axis. In some cases, a gene is represented on the microarray set more than once by different accession numbers. Fold change values are listed in Table 3.15.

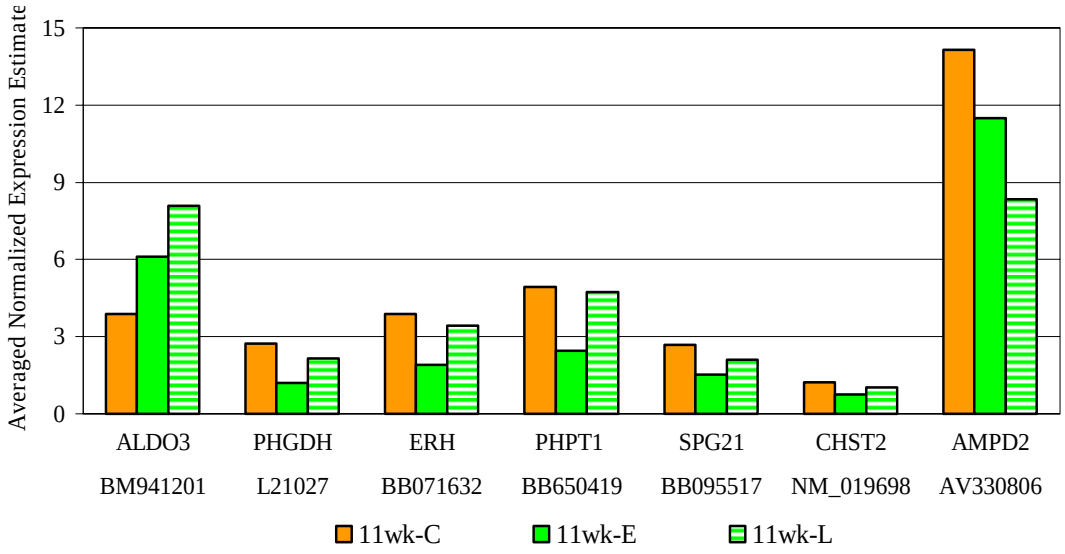

Figure 3.27 Expression Estimates of Genes Involved in Metabolism at 14wks. a-b) Gene symbols and Accession numbers are plotted on the x-axis; the average of replicate normalized expression values for each treatment group (as described in Materials and Methods) is plotted on the y-axis. In some cases, a gene is represented on the microarray set more than once by different accession numbers. Fold change values are listed in Table 3.15.

a.

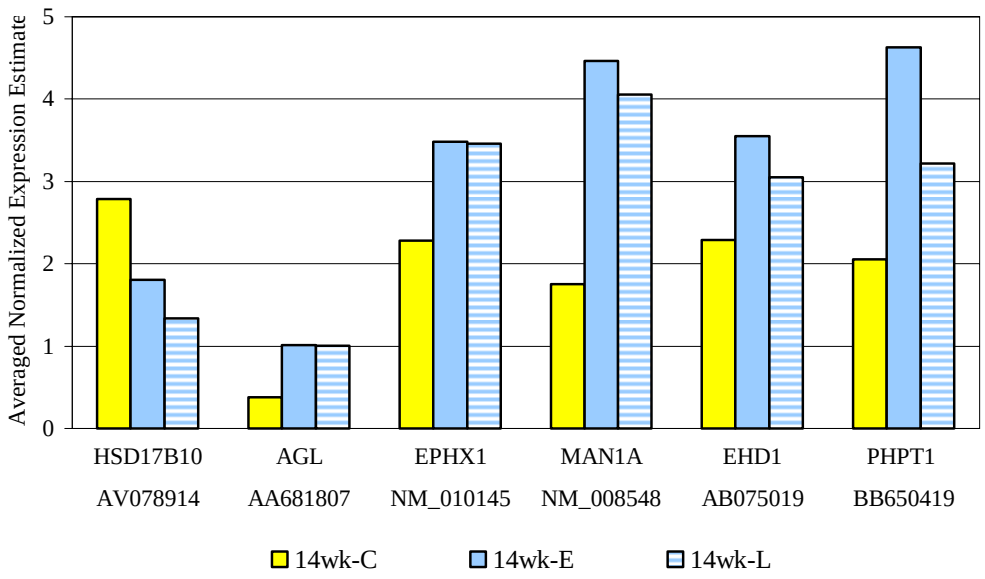

b.

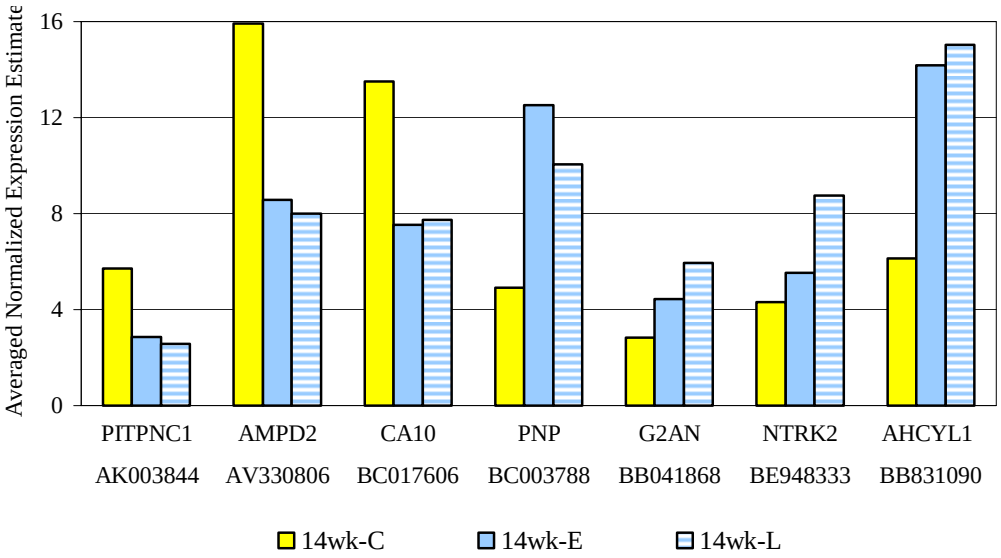

Table 3.15 Differential Expression of Genes Involved in Metabolism. Replicate RNA samples from each treatment group were hybridized to separate arrays. The average of replicate normalized expression estimates for each sample group was used to calculate the fold change difference in expression for each gene in Figures 3.26 and 3.27. Positive fold change values indicate an increase, and negative values indicate a decrease in gene expression in the IFNγ-expressing groups. Values in grey indicate the Student's t-test p-value was greater than 0.1.

			Fold Change (IFN-γ-expressing / non-expressing)			
Accession No.	Gene Symbol	Gene Name	11wk-E	11wk-L	14wk-E	14wk-L
AA681807	AGL	amylo-1,6-glucosidase, 4-alpha-glucanotransferase	1.34	1.53	**2.66**	**2.64**
BB831090	AHCYL1	S-adenosylhomocysteine hydrolase-like 1	-1.03	1.16	2.31	**2.45**
BM941201	ALDO3	aldolase 3, C isoform	**1.58**	**2.08**	1.17	1.25
AV330806	AMPD2	adenosine monophosphate deaminase 2 (isoform L)	-1.23	**-1.70**	**-1.86**	**-1.99**
BC017606	CA10	carbonic anhydrase-related protein 10	-1.05	-1.11	-1.79	**-1.74**
NM_019698	CHST2	carbohydrate sulfotransferase 2	**-1.62**	-1.20	1.34	1.22
AB075019	EHD1	EH-domain containing 1	-1.08	1.06	**1.55**	1.33
NM_010145	EPHX1	epoxide hydrolase 1, microsomal	-1.20	-1.14	**1.53**	**1.52**
BB071632	ERH	enhancer of rudimentary	**-2.03**	-1.13	1.91	1.62
BB041868	G2AN	alpha glucosidase 2, alpha neutral subunit	**1.31**	1.03	1.57	**2.10**
AV078914	HSD17B10	hydroxyacyl-CoA dehydrogenase type II	**-1.33**	**-1.22**	-1.54	**-2.09**
NM_008548	MAN1A	mannosidase 1, alpha	-1.10	-1.08	**2.55**	**2.31**
BE948333	NTRK2	neurotrophic tyrosine kinase, receptor, type 2	1.24	**-1.13**	1.28	**2.03**
L21027	PHGDH	3-phosphoglycerate dehydrogenase	**-2.25**	-1.26	2.15	2.03
BB650419	PHPT1	phosphohistidine phosphatase 1	**-2.01**	-1.05	**2.25**	1.56
AK003844	PITPNC1	phosphatidylinositol transfer protein, cytoplasmic 1	1.21	-1.15	**-2.01**	**-2.23**
BC003788	PNP	purine-nucleoside phosphorylase	-1.05	1.08	**2.55**	**2.05**
BB095517	SPG21	spastic paraplegia 21 homolog (human)	**-1.77**	**-1.27**	1.92	1.71

Figure 3.28 Expression Estimates of Genes Involved in Cytoskeleton Organization at 11wks. Gene symbols and Accession numbers are plotted on the x-axis; the average of replicate normalized expression values for each treatment group (as described in Materials and Methods) is plotted on the y-axis. In some cases, a gene is represented on the microarray set more than once by different accession numbers. Fold change values are listed in Table 3.16.

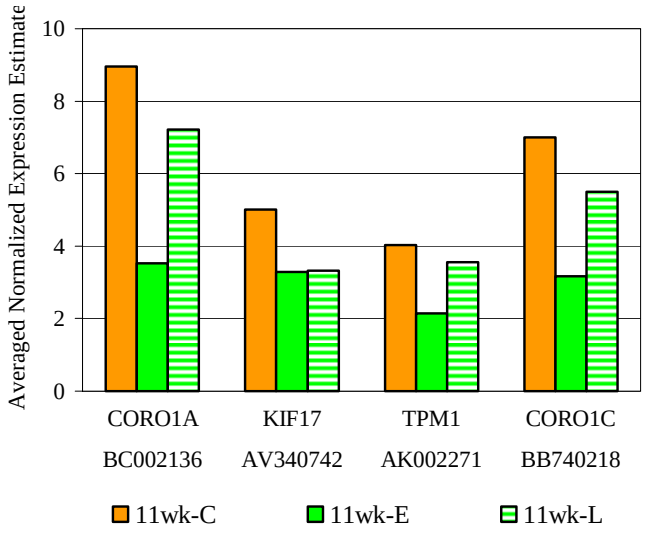

Figure 3.29 Expression Estimates of Genes Involved in Cytoskeleton Organization at 14wks. a-b) Gene symbols and Accession numbers are plotted on the x-axis; the average of replicate normalized expression values for each treatment group (as described in Materials and Methods) is plotted on the y-axis. In some cases, a gene is represented on the microarray set more than once by different accession numbers. Fold change values are listed in Table 3.16.

a.

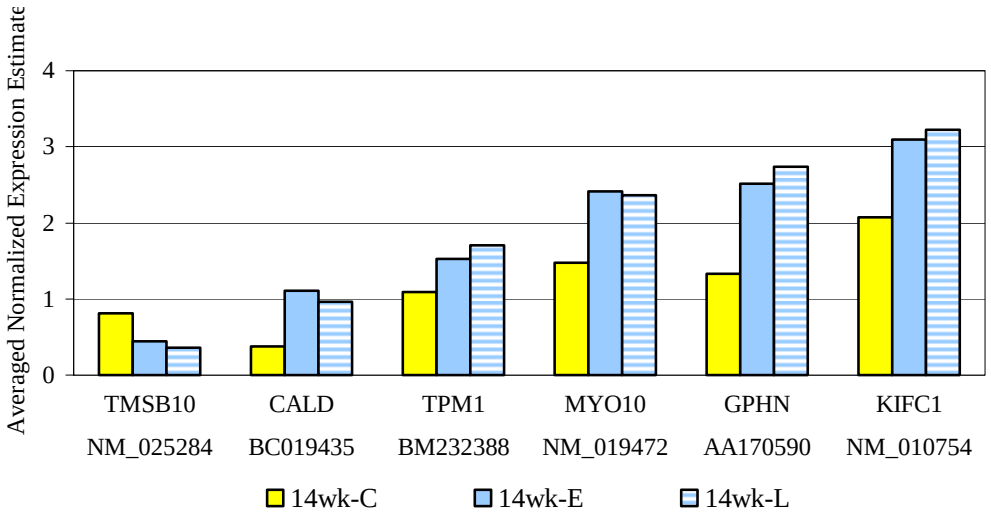

b.

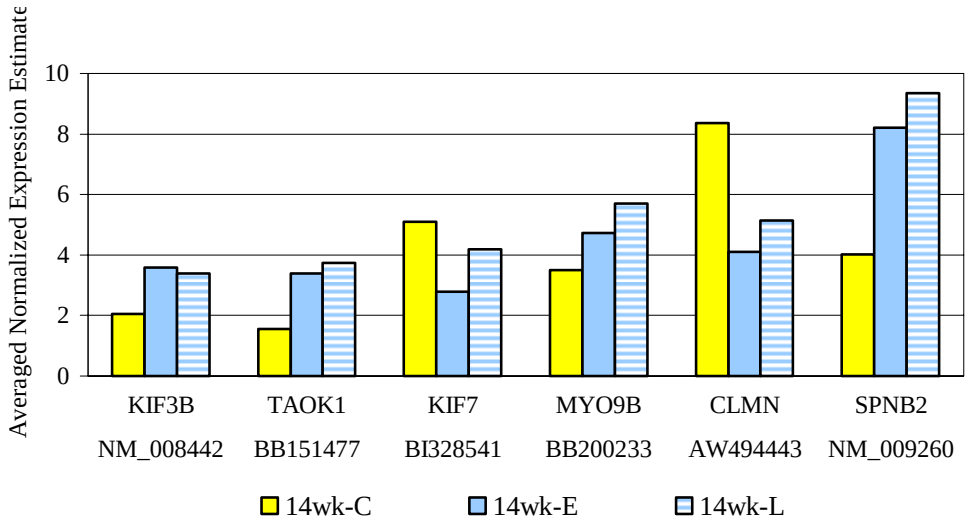

Figure 3.29 Expression Estimates of Genes Involved in Cytoskeleton Organization at 14wks.

c.

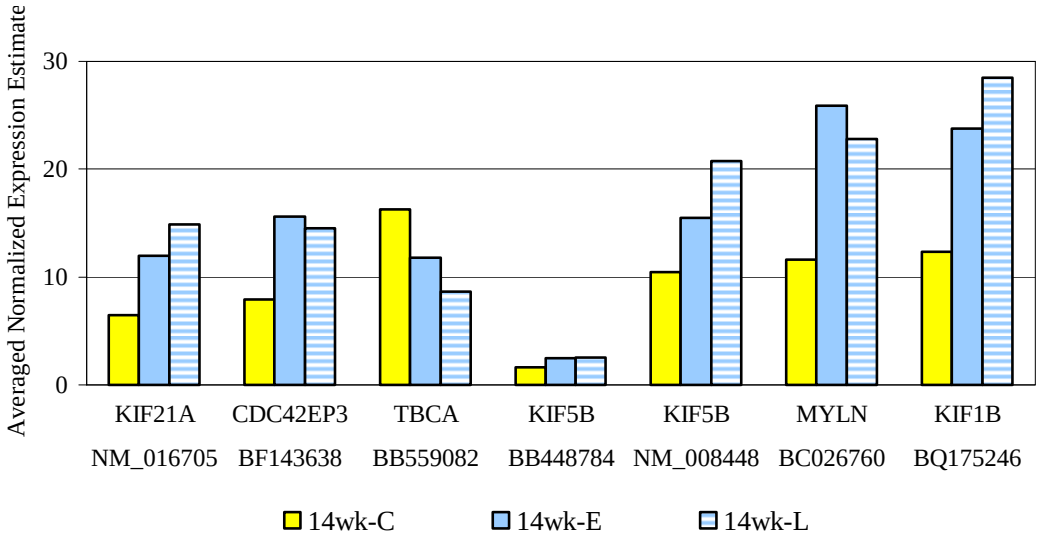

Table 3.16 Differential Expression of Genes Involved in Cytoskeleton Organization. Replicate RNA samples from each treatment group were hybridized to separate arrays. The average of replicate normalized expression estimates for each sample group was used to calculate the fold change difference in expression for each gene in Figures 3.28 and 3.29. Positive fold change values indicate an increase, and negative values indicate a decrease in gene expression in the IFNγ-expressing groups. Values in grey indicate the Student's t-test p-value was greater than 0.1.

			Fold Change (IFN-γ-expressing / non-expressing)			
Accession No.	Gene Symbol	Gene Name	11wk-E	11wk-L	14wk-E	14wk-L
BC019435	CALD	caldesmon, non-muscle	-1.11	-1.43	**2.92**	**2.55**
BF143638	CDC42EP3	CDC42 effector protein (Rho GTPase binding) 3	-1.43	1.05	**1.97**	1.84
AW494443	CLMN	calmin	1.26	1.14	**-2.04**	-1.62
BC002136	CORO1A	coronin, actin binding protein 1A	**-2.53**	-1.24	1.57	1.20
BB740218	CORO1C	coronin, actin binding protein 1C	**-2.20**	-1.27	1.01	-1.37
AA170590	GPHN	gephyrin	1.08	1.43	**1.89**	**2.06**
AV340742	KIF17	kinesin family member 17	**-1.53**	**-1.51**	1.08	-1.01
BQ175246	KIF1B	kinesin family member 1B	1.11	1.08	**1.92**	**2.31**
NM_016705	KIF21A	kinesin family member 21A	1.01	1.22	**1.85**	**2.30**
NM_008442	KIF3B	kinesin family member 3B	-1.02	1.01	**1.75**	1.66
BB448784	KIF5B	kinesin family member 5B	-1.11	-1.12	**1.52**	**1.56**
NM_008448	KIF5B	kinesin family member 5B	-1.06	1.11	1.48	**1.99**
BI328541	KIF7	kinesin family member 7	-1.10	**-1.33**	**-1.84**	-1.22
NM_010754	KIFC1	kinesin family member C1	-1.38	1.07	**1.49**	**1.55**
BC026760	MYLN	myosin light chain, alkali, nonmuscle	-1.50	-1.07	**2.22**	1.96
NM_019472	MYO10	myosin X	-1.08	-1.29	1.64	**1.60**
BB200233	MYO9B	myosin IXb	1.13	**1.20**	1.35	**1.63**
NM_009260	SPNB2	spectrin beta 2, non-erythrocytic	1.11	-1.03	**2.04**	**2.33**
BB151477	TAOK1	TAO kinase 1	-1.05	-1.08	**2.17**	**2.38**
BB559082	TBCA	tubulin cofactor a	**-1.27**	**-1.29**	-1.38	**-1.88**

Accession No.	Gene Symbol	Gene Name	Fold Change (IFN-γ-expressing / non-expressing) 11wk-E	11wk-L	14wk-E	14wk-L
NM_025284	TMSB10	thymosin, beta 10	-1.39	-1.33	**-1.83**	**-2.26**
AK002271	TPM1	tropomyosin 1, alpha	**-1.89**	-1.13	1.54	1.30
BM232388	TPM1	tropomyosin 1, alpha	1.00	-1.16	**1.40**	**1.56**

Figure 3.30 Expression Estimates of Genes Involved in Cell Adhesion at 11wks. Gene symbols and Accession numbers are plotted on the x-axis; the average of replicate normalized expression values for each treatment group (as described in Materials and Methods) is plotted on the y-axis. In some cases, a gene is represented on the microarray set more than once by different accession numbers. Fold change values are listed in Table 3.17.

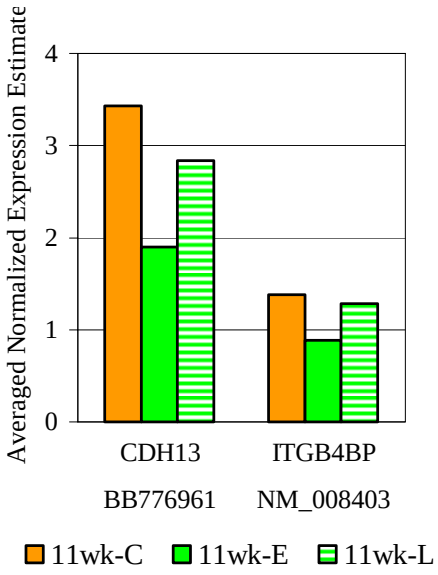

Figure 3.31 Expression Estimates of Genes Involved in Cell Adhesion at 14wks. a-c) Gene symbols and Accession numbers are plotted on the x-axis; the average of replicate normalized expression values for each treatment group (as described in Materials and Methods) is plotted on the y-axis. In some cases, a gene is represented on the microarray set more than once by different accession numbers. Fold change values are listed in Table 3.27.

a.

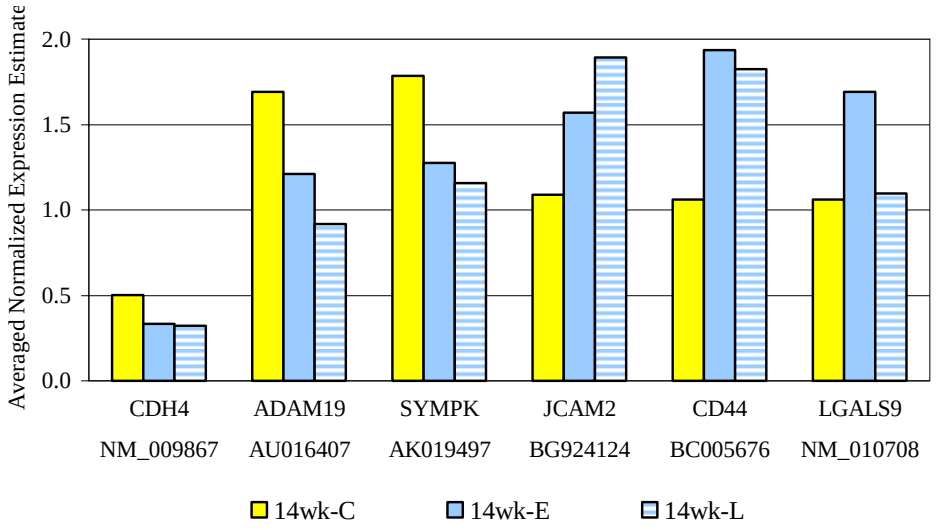

b.

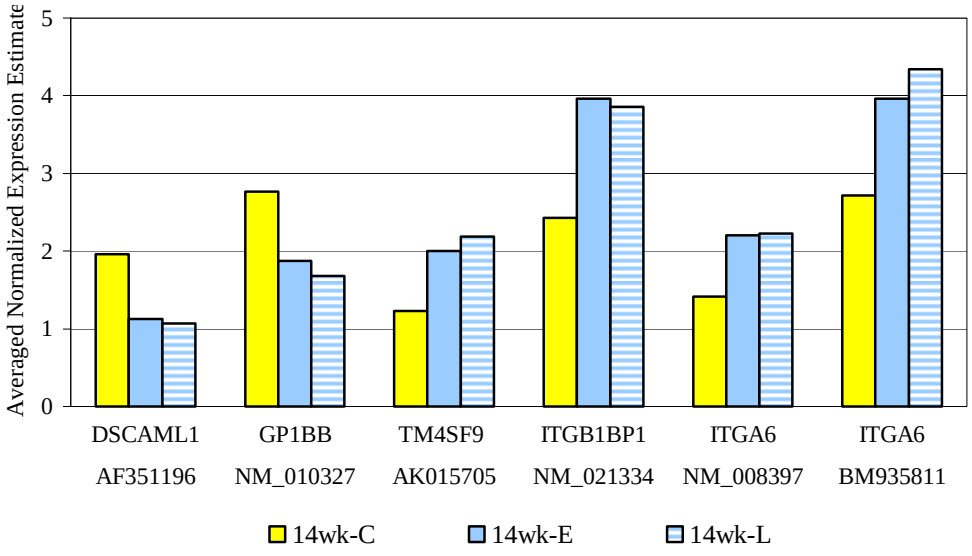

Figure 3.31 Expression Estimates of Genes Involved in Cell Adhesion at 14wks.

c.

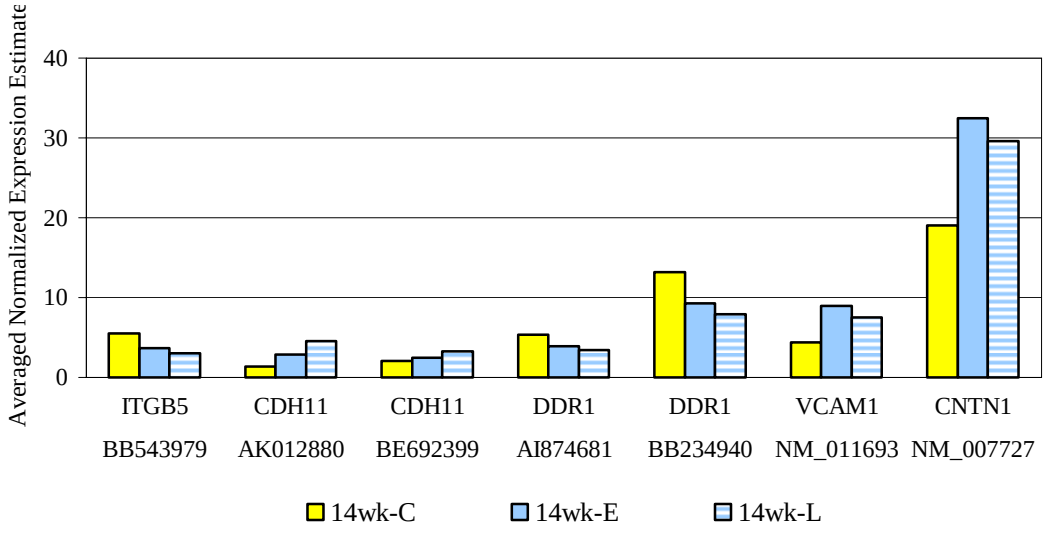

Table 3.17 Differential Expression of Genes Involved in Cell Adhesion. Replicate RNA samples from each treatment group were hybridized to separate arrays. The average of replicate normalized expression estimates for each sample group was used to calculate the fold change difference in expression for each gene in Figures 3.30 and 3.31. Positive fold change values indicate an increase, and negative values indicate a decrease in gene expression in the IFNγ-expressing groups. Values in grey indicate the Student's t-test p-value was greater than 0.1.

			Fold Change (IFN-γ-expressing / non-expressing)			
Accession No.	Gene Symbol	Gene Name	11wk-E	11wk-L	14wk-E	14wk-L
AU016407	ADAM19	a disintegrin and metalloproteinase domain 19	1.03	**-1.43**	-1.40	**-1.84**
BC005676	CD44	CD44 antigen	-1.75	-1.84	**1.82**	**1.72**
AK012880	CDH11	cadherin 11	1.94	1.71	**2.06**	**3.29**
BE692399	CDH11	cadherin 11	1.33	1.02	1.21	**1.60**
BB776961	CDH13	cadherin 13	**-1.81**	-1.21	1.28	1.20
NM_009867	CDH4	cadherin 4	-1.15	-1.25	**-1.51**	**-1.56**
NM_007727	CNTN1	contactin 1	1.07	1.03	**1.70**	**1.55**
BB234940	DDR1	discoidin domain receptor family, member 1	1.36	1.00	-1.43	**-1.66**
AI874681	DDR1	discoidin domain receptor family, member 1	1.28	-1.04	-1.37	**-1.56**
BB378700	DDR1	discoidin domain receptor family, member 1	1.07	-1.14	**-1.38**	**-1.53**
AF351196	DSCAML1	Down syndrome cell adhesion molecule-like 1	1.26	1.02	-1.73	**-1.83**
NM_010327	GP1BB	glycoprotein Ib, beta polypeptide	1.04	-1.15	-1.47	**-1.64**
NM_008397	ITGA6	integrin alpha 6	1.07	-1.15	1.56	**1.57**
BM935811	ITGA6	integrin alpha 6	-1.14	-1.14	1.46	**1.60**
NM_021334	ITGB1BP1	integrin beta 1 binding protein 1	1.61	-1.07	**1.63**	**1.59**
NM_008403	ITGB4BP	integrin beta 4 binding protein	**-1.56**	-1.07	1.52	1.20
BB543979	ITGB5	integrin beta 5	1.14	-1.48	-1.51	**-1.84**
BG924124	JCAM2	junction cell adhesion molecule 2	1.03	1.11	1.44	**1.73**
NM_010708	LGALS9	lectin, galactose binding, soluble 9	-1.50	-1.48	**1.59**	1.03

Accession No.	Gene Symbol	Gene Name	Fold Change (IFN-γ-expressing / non-expressing) 11wk-E	11wk-L	14wk-E	14wk-L
AK019497	SYMPK	symplekin	-1.05	-1.13	-1.40	**-1.54**
AK015705	TM4SF9	transmembrane 4 superfamily member 9	1.03	-1.02	**1.63**	**1.79**
NM_011693	VCAM1	vascular cell adhesion molecule 1	-1.57	-1.64	**2.06**	**1.72**

Figure 3.32 Expression Estimates of Genes Involved in Protein Modification at 14wks. Gene symbols and Accession numbers are plotted on the x-axis; the average of replicate normalized expression values for each treatment group (as described in Materials and Methods) is plotted on the y-axis. In some cases, a gene is represented on the microarray set more than once by different accession numbers. Fold change values are listed in Table 3.18.

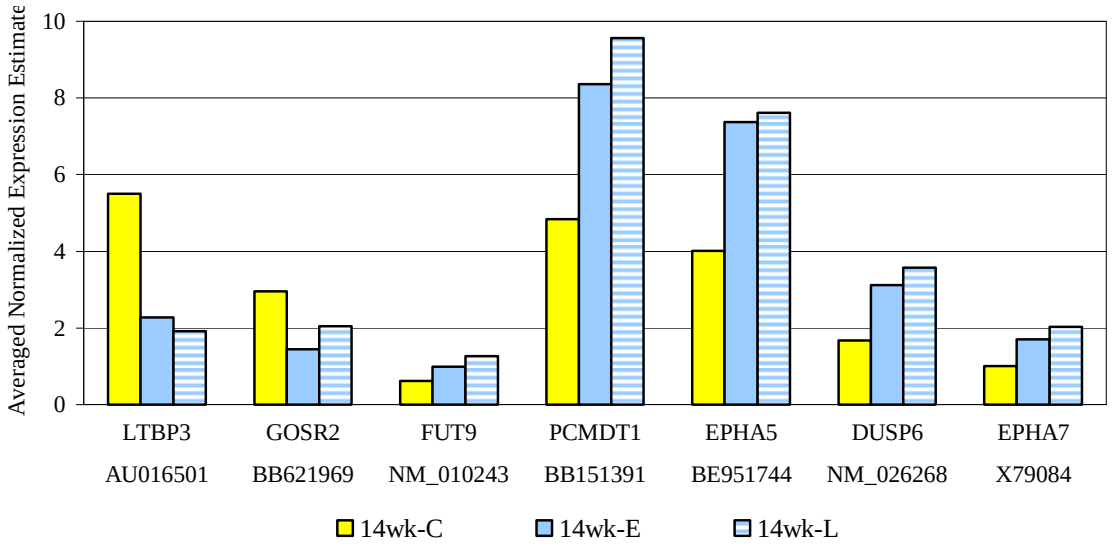

Table 3.18 Differential Expression of Genes Involved in Protein Modification. Replicate RNA samples from each treatment group were hybridized to separate arrays. The average of replicate normalized expression estimates for each sample group was used to calculate the fold change difference in expression for each gene in Figure 3.32. Positive fold change values indicate an increase, and negative values indicate a decrease in gene expression in the IFNγ-expressing groups. Values in grey indicate the Student's t-test p-value was greater than 0.1.

			Fold Change (IFN-γ-expressing / non-expressing)			
Accession No.	Gene Symbol	Gene Name	11wk-E	11wk-L	14wk-E	14wk-L
NM_026268	DUSP6	dual specificity phosphatase 6	-1.24	-1.07	**1.86**	**2.13**
AK013481	EPHA4	Eph receptor A4	**-1.57**	1.08	1.63	1.78
BE951744	EPHA5	Eph receptor A5	**-1.24**	-1.04	**1.83**	**1.90**
X79084	EPHA7	Eph receptor A7	-1.36	1.22	**1.69**	2.02
NM_010243	FUT9	fucosyltransferase 9	1.14	1.53	**1.58**	**2.04**
BB621969	GOSR2	golgi SNAP receptor complex member 2	-1.22	-1.16	**-2.05**	-1.44
AU016501	LTBP3	latent TGF-beta binding protein 3	1.13	-1.12	**-2.42**	**-2.87**
BB151391	PCMDT1	protein-L-isoaspartate (D-aspartate) O-methyltransferase domain containing 1	-1.09	1.29	**1.73**	**1.98**

Figure 3.33 Expression Estimates of Genes Involved in Nucleic Acid Binding at 11wks. a-b) Gene symbols and Accession numbers are plotted on the x-axis; the average of replicate normalized expression values for each treatment group (as described in Materials and Methods) is plotted on the y-axis. In some cases, a gene is represented on the microarray set more than once by different accession numbers. Fold change values are listed in Table 3.19.

a.

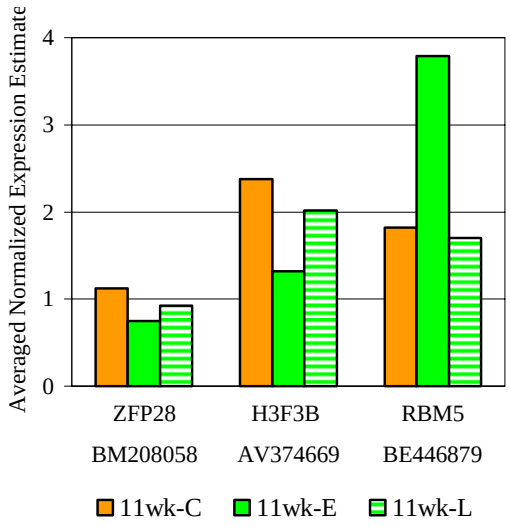

b.

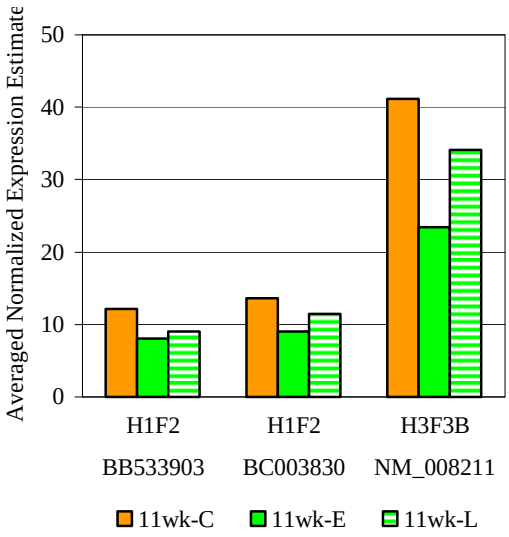

Figure 3.34 Expression Estimates of Genes Involved in Nucleic Acid Binding at 14wks. a-c) Gene symbols and Accession numbers are plotted on the x-axis; the average of replicate normalized expression values for each treatment group (as described in Materials and Methods) is plotted on the y-axis. In some cases, a gene is represented on the microarray set more than once by different accession numbers. Fold change values are listed in Table 3.19.

a.

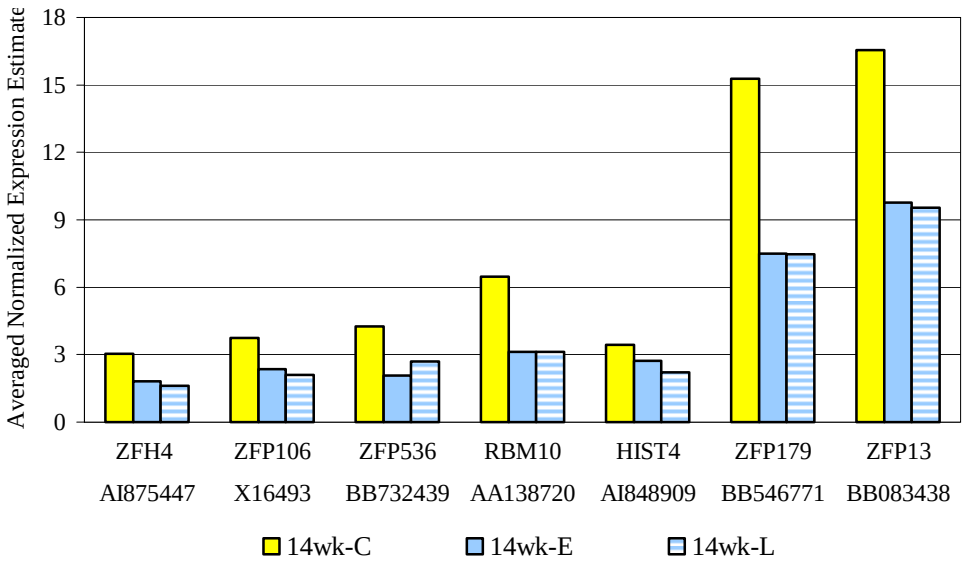

b.

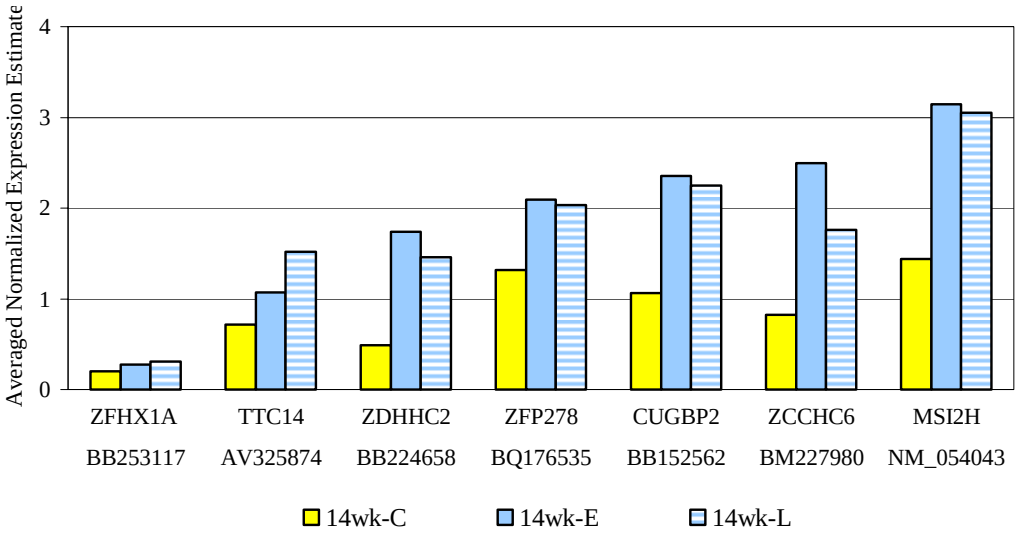

Figure 3.34 Expression Estimates of Genes Involved in Nucleic Acid Binding at 14wks.

c.

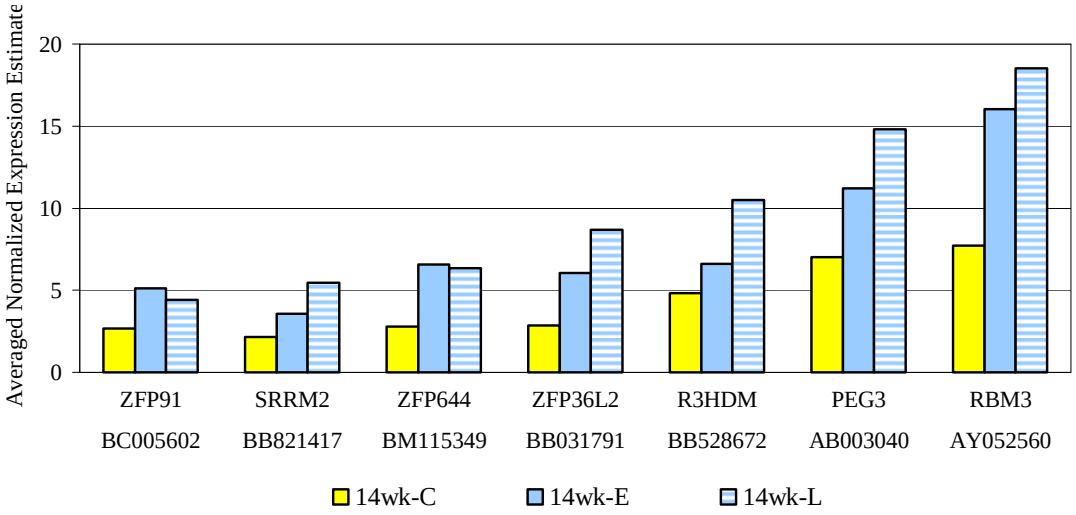

Table 3.19 Differential Expression of Genes Involved in Nucleic Acid Binding. Replicate RNA samples from each treatment group were hybridized to separate arrays. The average of replicate normalized expression estimates for each sample group was used to calculate the fold change difference in expression for each gene in Figures 3.33 and 3.34. Positive fold change values indicate an increase, and negative values indicate a decrease in gene expression in the IFNγ-expressing groups. Values in grey indicate the Student's t-test p-value was greater than 0.1.

			Fold Change (IFN-γ-expressing / non-expressing)			
Accession No.	Gene Symbol	Gene Name	11wk-E	11wk-L	14wk-E	14wk-L
BB152562	CUGBP2	CUG triplet repeat, RNA binding protein 2	1.22	-1.16	**2.22**	**2.11**
BC003830	H1F2	histone 1, H1c	**-1.51**	-1.19	1.66	1.58
BB533903	H1F2	histone 1, H1c	**-1.50**	**-1.35**	1.06	-1.35
NM_008211	H3F3B	H3 histone, family 3B	**-1.76**	-1.21	1.62	1.63
AV374669	H3F3B	H3 histone, family 3B	**-1.81**	-1.18	1.47	1.67
AI848909	HIST4	histone 1, H3a	-1.18	-1.35	**-1.25**	**-1.54**
NM_054043	MSI2H	Musashi homolog 2	1.21	1.09	**2.19**	**2.12**
AB003040	PEG3	paternally expressed 3	-1.01	1.19	**1.59**	**2.11**
BB528672	R3HDM	R3H domain	1.27	1.00	1.37	**2.18**
AA138720	RBM10	RNA binding motif protein 10	1.04	-1.11	**-2.07**	**-2.06**
AY052560	RBM3	RNA binding motif protein 3	-1.25	1.26	**2.08**	**2.40**
BE446879	RBM5	RNA binding motif protein 5	**2.08**	-1.07	-1.29	-1.22
BB821417	SRRM2	serine/arginine repetitive matrix 2	1.36	1.28	1.67	**2.55**
AV325874	TTC14	tetratricopeptide repeat domain 14	1.10	1.13	1.50	**2.12**
BM227980	ZCCHC6	zinc finger, CCHC domain containing 6	-1.62	-1.52	**3.04**	2.14
BB224658	ZDHHC2	zinc finger, DHHC domain containing 2	1.07	1.05	**3.58**	**2.99**
AI875447	ZFH4	zinc finger homeodomain 4	1.13	-1.15	**-1.66**	**-1.88**
BB253117	ZFHX1A	zinc finger homeobox 1a	1.12	1.09	**1.36**	**1.55**
X16493	ZFP106	zinc finger protein 106	-1.01	-1.05	**-1.58**	**-1.78**

Accession No.	Gene Symbol	Gene Name	Fold Change (IFN-γ-expressing / non-expressing) 11wk-E	11wk-L	14wk-E	14wk-L
BB083438	ZFP13	zinc finger protein 13	-1.14	-1.16	**-1.69**	**-1.74**
BB546771	ZFP179	zinc finger protein 179	1.34	1.03	**-2.04**	**-2.05**
BQ176535	ZFP278	zinc finger protein 278	1.09	1.36	1.59	**1.55**
BM208058	ZFP28	zinc finger protein 28	**-1.50**	**-1.22**	-1.01	-1.18
BB031791	ZFP36L2	zinc finger protein 36 like 2	-1.05	1.07	2.11	**3.03**
BB732439	ZFP536	zinc finger protein 536	1.12	-1.05	**-2.06**	**-1.58**
BM115349	ZFP644	zinc finger protein 644	1.00	1.28	**2.34**	**2.27**
BC005602	ZFP91	zinc finger protein 91	1.05	1.04	**1.92**	**1.64**

Figure 3.35 Expression Estimates of Genes Involved in Transcription Regulation at 11wks. Gene symbols and Accession numbers are plotted on the x-axis; the average of replicate normalized expression values for each treatment group (as described in Materials and Methods) is plotted on the y-axis. In some cases, a gene is represented on the microarray set more than once by different accession numbers. Fold change values are listed in Table 3.20.

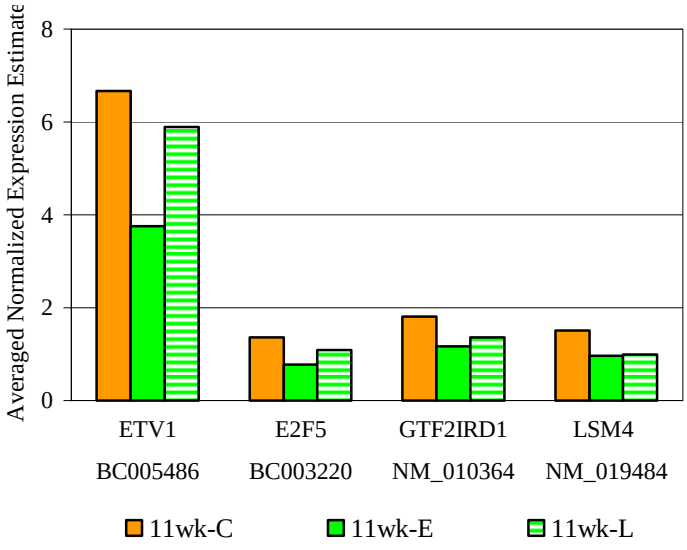

Figure 3.36 Expression Estimates of Genes Involved in Transcription Regulation at 14wks. a-h) Gene symbols and Accession numbers are plotted on the x-axis; the average of replicate normalized expression values for each treatment group (as described in Materials and Methods) is plotted on the y-axis. In some cases, a gene is represented on the microarray set more than once by different accession numbers. Fold change values are listed in Table 3.20.

a.

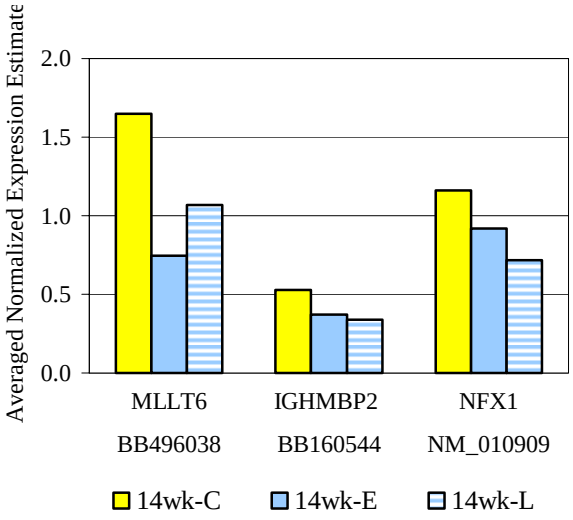

b.

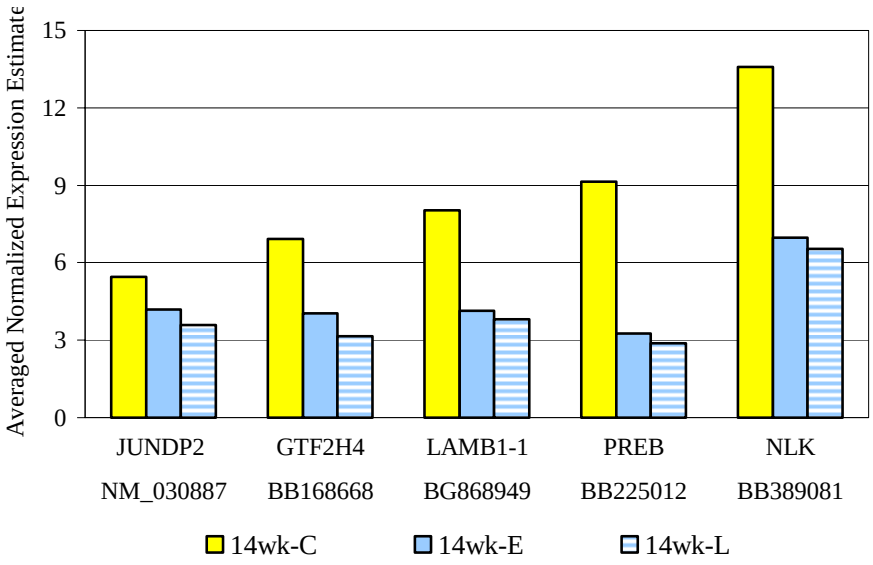

Figure 3.36 Expression Estimates of Genes Involved in Transcription Regulation at 14wks.

c.

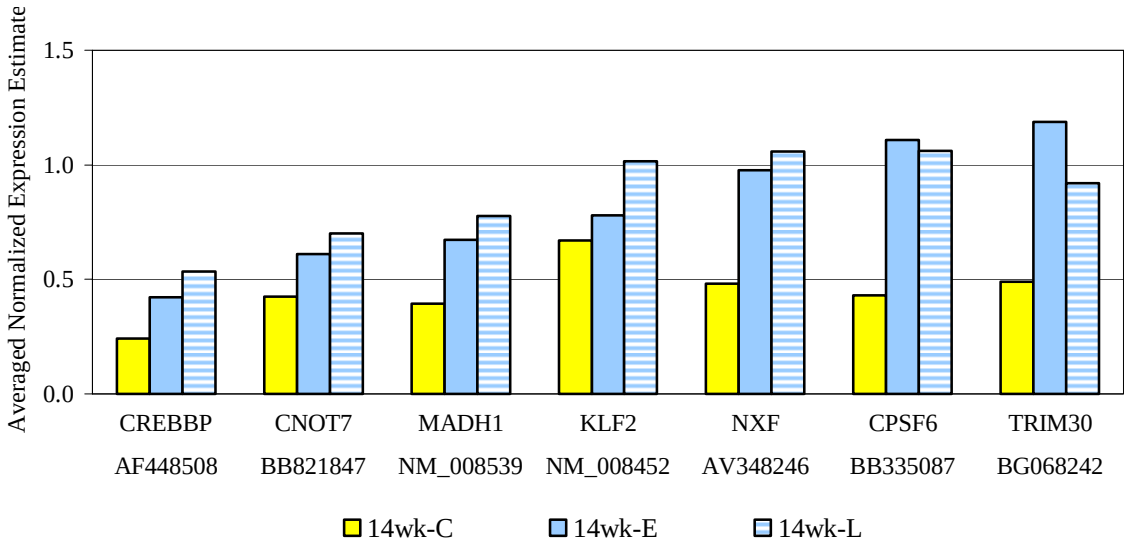

d.

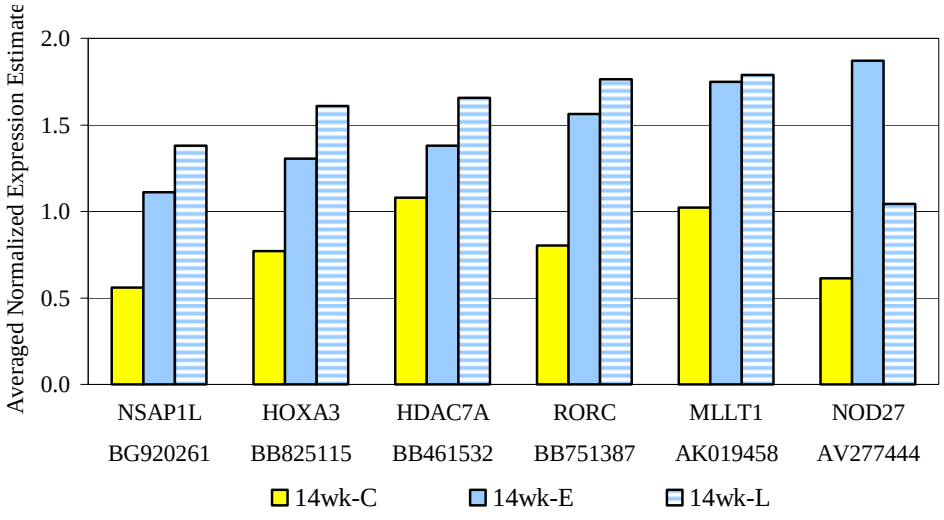

Figure 3.36 Expression Estimates of Genes Involved in Transcription Regulation at 14wks.

e.

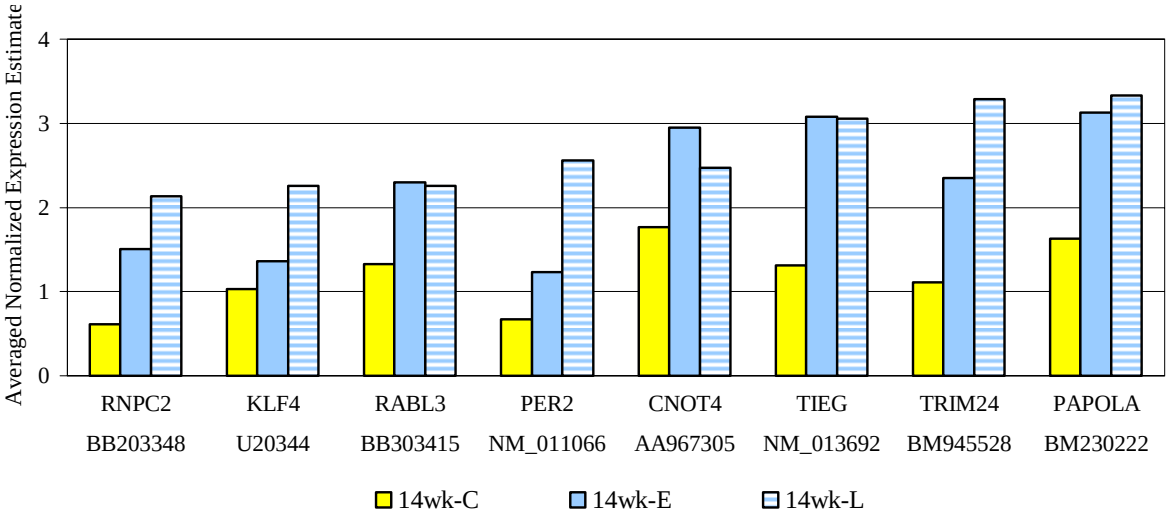

f.

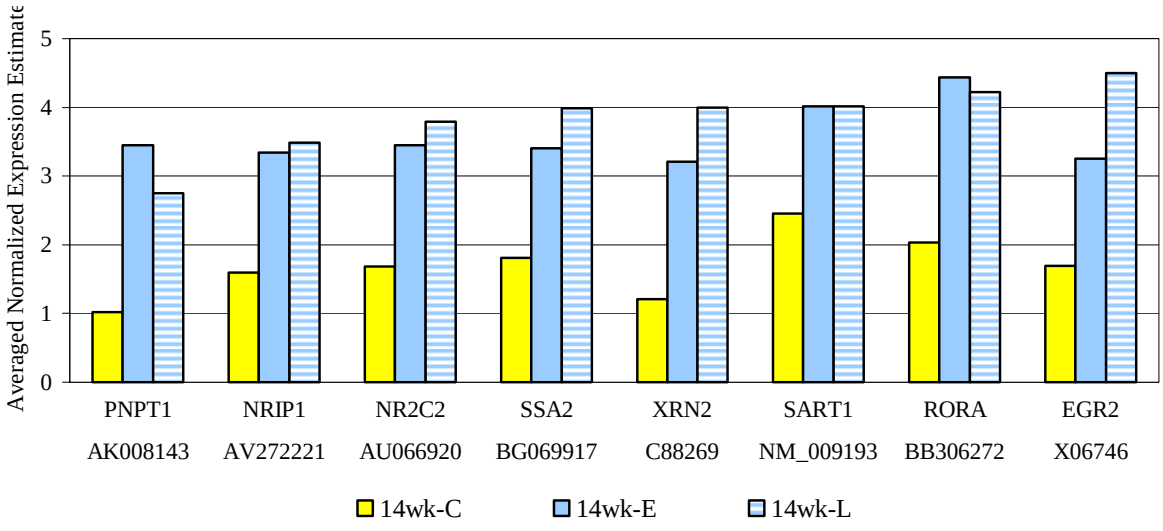

Figure 3.36 Expression Estimates of Genes Involved in Transcription Regulation at 14wks.

g.

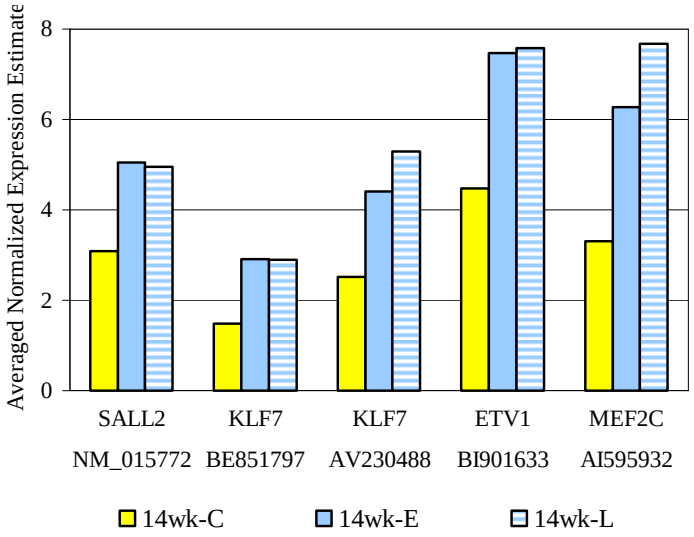

h.

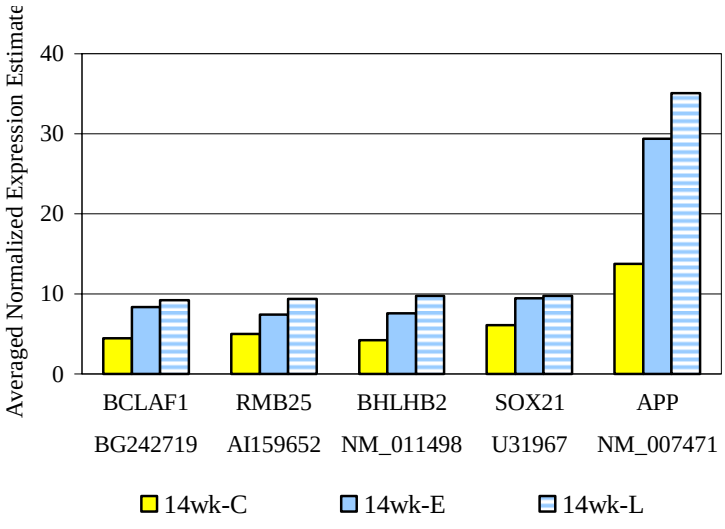

Table 3.20 Differential Expression of Genes Involved in Transcription Regulation. Replicate RNA samples from each treatment group were hybridized to separate arrays. The average of replicate normalized expression estimates for each sample group was used to calculate the fold change difference in expression for each gene in Figures 3.35 and 3.36. Positive fold change values indicate an increase, and negative values indicate a decrease in gene expression in the IFNγ-expressing groups. Values in grey indicate the Student's t-test p-value was greater than 0.1.

			Fold Change (IFN-γ-expressing / non-expressing)			
Accession No.	Gene Symbol	Gene Name	11wk-E	11wk-L	14wk-E	14wk-L
NM_007471	APP	amyloid beta (A4) precursor protein	-1.12	**1.18**	**2.14**	**2.55**
NM_023502	APP	amyloid beta (A4) precursor protein	-1.25	1.00	1.75	**2.05**
BG242719	BCLAF1	Bcl2-associated transcription factor 1	-1.13	1.17	**1.89**	**2.08**
NM_011498	BHLHB2	basic helix-loop-helix domain containing, class B2	-1.03	**1.31**	**1.79**	**2.31**
AA967305	CNOT4	CCR4-NOT transcription complex, subunit 4	-1.02	-1.09	**1.67**	1.40
BB821847	CNOT7	CCR4-NOT transcription complex, subunit 7	-1.46	1.15	**1.44**	**1.66**
BB335087	CPSF6	cleavage and polyadenylation specific factor 6	1.34	1.14	**2.57**	**2.46**
AF448508	CREBBP	CREB binding protein	**1.32**	1.15	**1.74**	**2.21**
BC003220	E2F5	E2F transcription factor 5	**-1.77**	**-1.25**	1.96	2.08
X06746	EGR2	early growth response 2	-1.09	-1.41	1.92	**2.65**
BC005486	ETV1	ets variant gene 1	**-1.78**	-1.13	1.69	1.89
BI901633	ETV1	ets variant gene 1	-1.01	1.15	**1.67**	**1.69**
BB168668	GTF2H4	general transcription factor II H, polypeptide 4	-1.14	**-1.35**	**-1.71**	**-2.19**
NM_010364	GTF2IRD1	general transcription factor II I repeat domain-containing 1	**-1.55**	-1.33	-1.11	-1.20
BB461532	HDAC7A	histone deacetylase 7A	1.08	1.21	1.28	**1.54**
BB825115	HOXA3	homeo box A3	1.28	1.08	**1.69**	**2.09**
BB160544	IGHMBP2	immunoglobulin mu binding protein 2	1.09	1.06	-1.42	**-1.55**
NM_030887	JUNDP2	Jun dimerization protein 2	1.12	-1.03	**-1.30**	**-1.51**

Accession No.	Gene Symbol	Gene Name	Fold Change (IFN-γ-expressing / non-expressing) 11wk-E	11wk-L	14wk-E	14wk-L
NM_008452	KLF2	Kruppel-like factor 2 (lung)	1.05	1.11	1.16	**1.51**
U20344	KLF4	Kruppel-like factor 4 (gut)	-1.19	-1.31	1.32	**2.19**
AV230488	KLF7	Kruppel-like factor 7 (ubiquitous)	-1.36	-1.20	1.76	**2.10**
BE851797	KLF7	Kruppel-like factor 7	1.00	-1.07	1.96	**1.95**
BG868949	LAMB1-1	laminin B1 subunit 1	1.58	-1.03	**-1.94**	**-2.11**
NM_019484	LSM4	U6 snRNA-associated SM-like protein 4	**-1.55**	**-1.52**	1.59	1.05
NM_008539	MADH1	MAD homolog 1	-1.25	-1.17	**1.71**	**1.97**
AI595932	MEF2C	myocyte enhancer factor 2C	-1.18	1.21	**1.90**	**2.32**
AK019458	MLLT1	myeloid/lymphoid or mixed lineage-leukemia translocation to 3 homolog	-1.11	1.01	**1.72**	**1.75**
BB496038	MLLT6	myeloid/lymphoid or mixed lineage-leukemia translocation to 6 homolog	-1.06	1.07	**-2.21**	-1.55
AK013847	MYT1L	myelin transcription factor 1-like	1.00	**1.31**	**1.70**	**2.10**
NM_010909	NFX1	nuclear transcription factor, X-box binding 1	-1.02	-1.01	-1.26	**-1.61**
BB389081	NLK	nemo like kinase	-1.04	1.05	**-1.95**	**-2.07**
AV277444	NOD27	nucleotide-binding oligomerization domains 27	1.44	1.06	**3.05**	**1.70**
AU066920	NR2C2	nuclear receptor subfamily 2, group C, member 2	1.02	1.08	**2.05**	**2.25**
AV272221	NRIP1	nuclear receptor interacting protein 1	1.16	1.07	**2.09**	**2.18**
BG920261	NSAP1L	NS1-associated protein 1-like	1.20	1.06	1.98	**2.46**
AV348246	NXF	bHLH-PAS type transcription factor NXF	-1.50	1.00	2.03	**2.20**
BM230222	PAPOLA	poly (A) polymerase alpha	1.01	1.03	1.92	**2.05**
NM_011066	PER2	period homolog 2	1.18	1.22	1.85	**3.83**
AK008143	PNPT1	polyribonucleotide nucleotidyltransferase 1	-1.20	1.05	**3.37**	**2.69**
BB225012	PREB	prolactin regulatory element binding	1.05	-1.15	**-2.81**	**-3.17**

Accession No.	Gene Symbol	Gene Name	Fold Change (IFN-γ-expressing / non-expressing) 11wk-E	11wk-L	14wk-E	14wk-L
BB303415	RABL3	RAB, member of RAS oncogene family-like 3	-1.03	-1.26	**1.74**	**1.70**
AI159652	RMB25	RNA binding motif protein 25	1.01	**-1.14**	1.49	**1.88**
BB203348	RNPC2	RNA-binding region containing protein 2, coactivator of AP-1 and estrogen receptors	1.10	1.17	**2.45**	**3.47**
BB306272	RORA	RAR-related orphan receptor alpha	**1.48**	1.38	**2.19**	**2.08**
BB751387	RORC	RAR-related orphan receptor gamma	1.04	-1.28	**1.95**	**2.20**
NM_015772	SALL2	sal-like 2 (Drosophila)	-1.11	-1.02	1.63	**1.60**
NM_009193	SART1	squamous cell carcinoma antigen recognized by T-cells 1	-1.12	1.18	**1.63**	**1.64**
U31967	SOX21	DNA-binding protein SOX21	-1.28	-1.30	1.55	**1.60**
BG069917	SSA2	Sjogren syndrome antigen A2	-1.07	**1.30**	1.88	**2.21**
NM_013692	TIEG	TGFB inducible early growth response	1.13	-1.16	**2.35**	**2.33**
BM945528	TRIM24	tripartite motif protein 24	-1.42	1.27	2.11	**2.95**
BG068242	TRIM30	tripartite motif protein 30	-1.12	-1.44	2.43	**1.88**
C88269	XRN2	5'-3' exoribonuclease 2	-1.05	1.19	2.65	**3.31**

Figure 3.37 Expression Estimates of Genes Involved in Signal Transduction at 11wks. a-b) Gene symbols and Accession numbers are plotted on the x-axis; the average of replicate normalized expression values for each treatment group (as described in Materials and Methods) is plotted on the y-axis. In some cases, a gene is represented on the microarray set more than once by different accession numbers. Fold change values are listed in Table 3.21.

a.

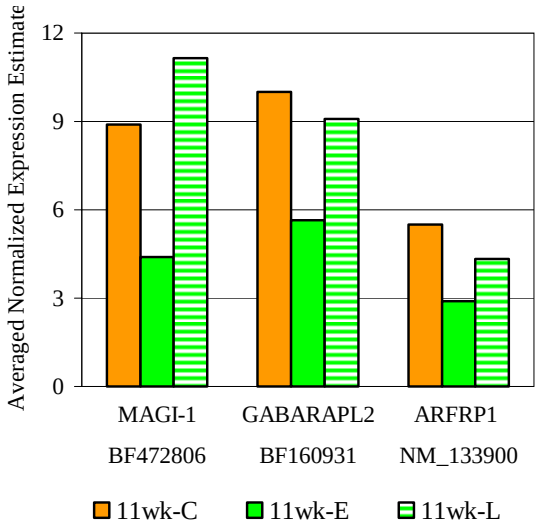

b.

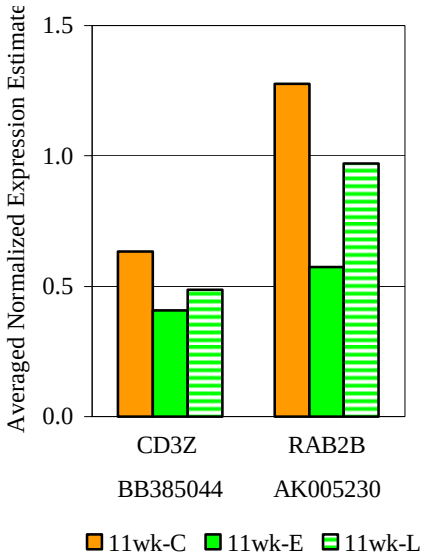

Figure 3.38 Expression Estimates of Genes Involved in Signal Transduction at 14wks. a-g) Gene symbols and Accession numbers are plotted on the x-axis; the average of replicate normalized expression values for each treatment group (as described in Materials and Methods) is plotted on the y-axis. In some cases, a gene is represented on the microarray set more than once by different accession numbers. Fold change values are listed in Table 3.21.

a.

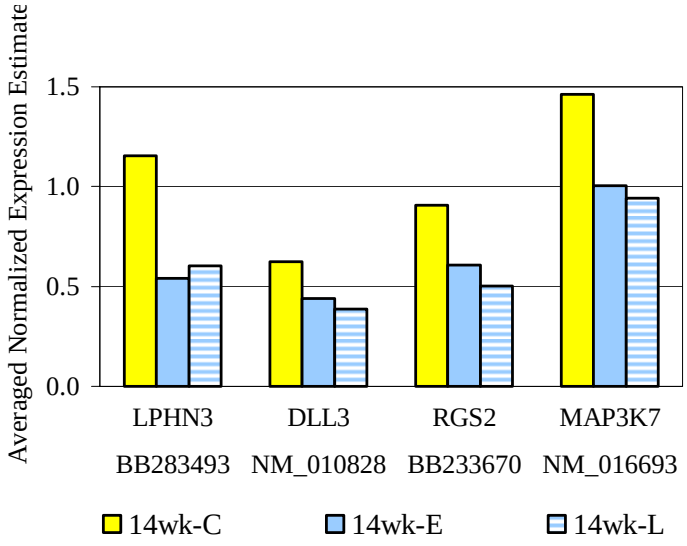

b.

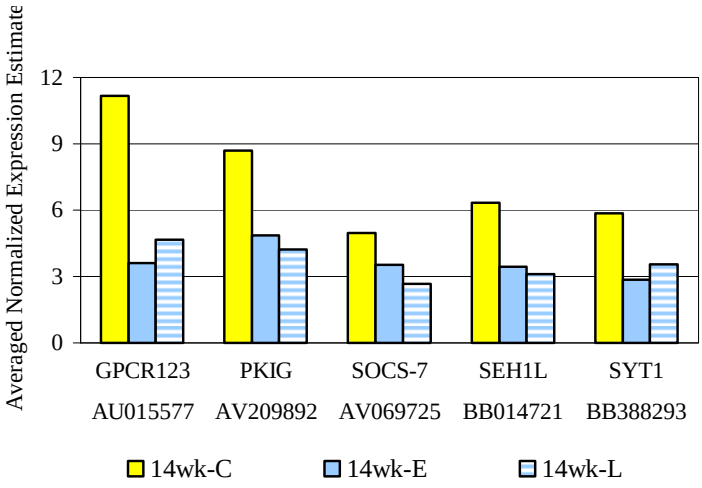

Figure 3.38 Expression Estimates of Genes Involved in Signal Transduction at 14wks.

c.

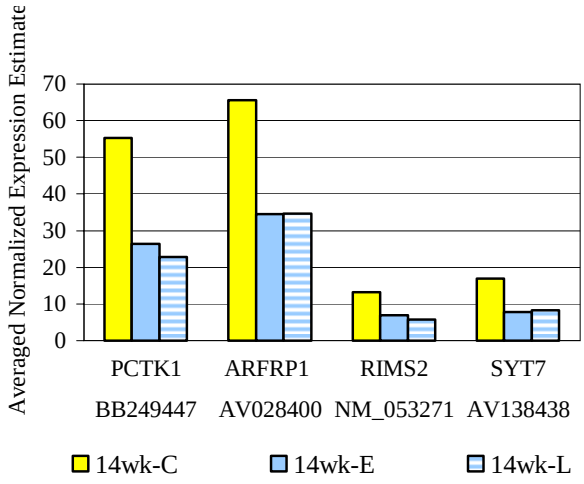

d.

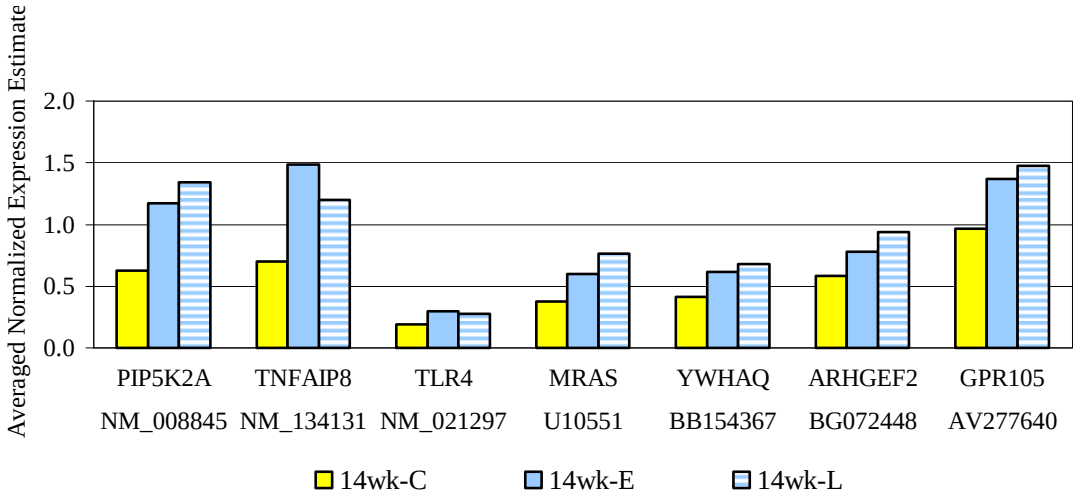

Figure 3.38 Expression Estimates of Genes Involved in Signal Transduction at 14wks.

e.

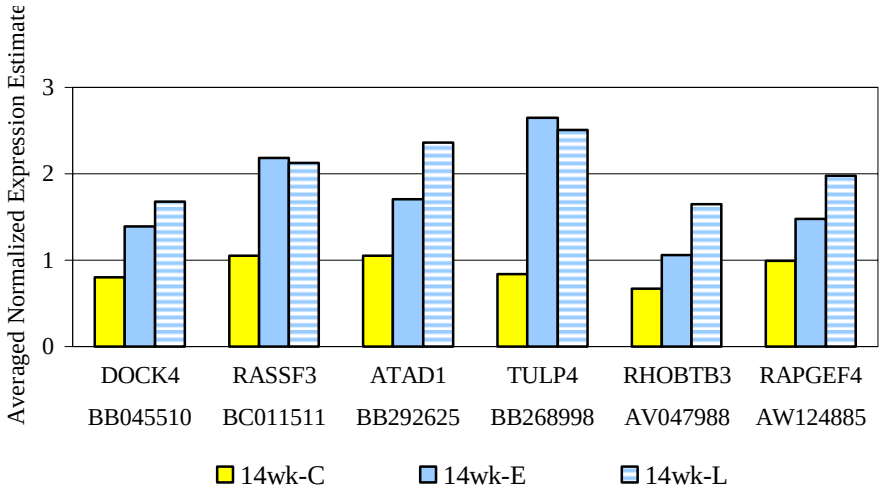

f.

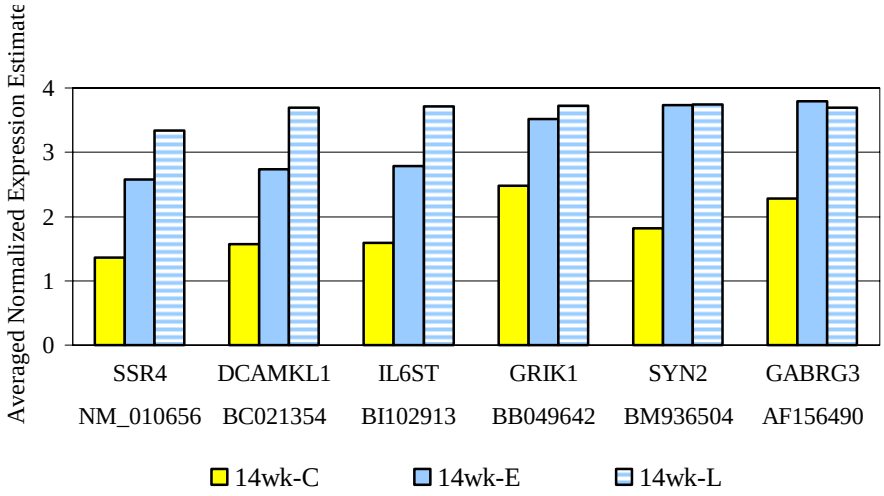

Figure 3.38 Expression Estimates of Genes Involved in Signal Transduction at 14wks.

g.

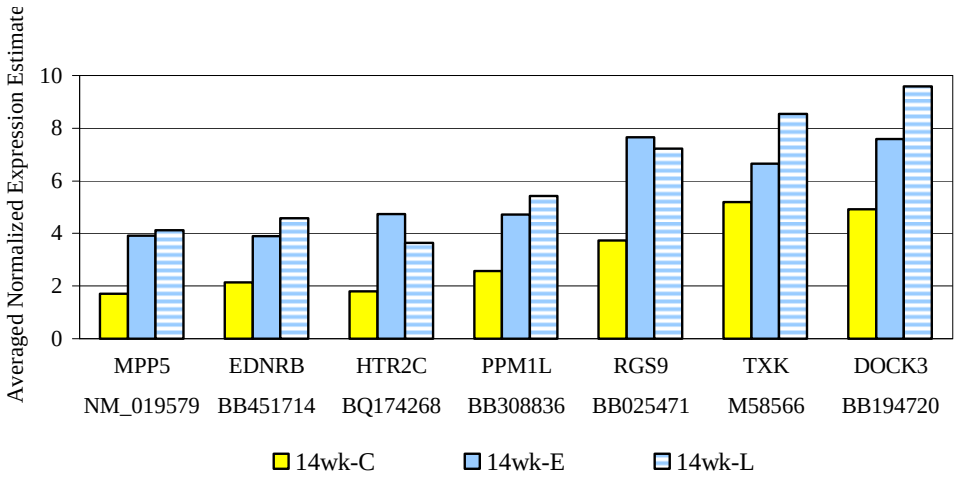

h.

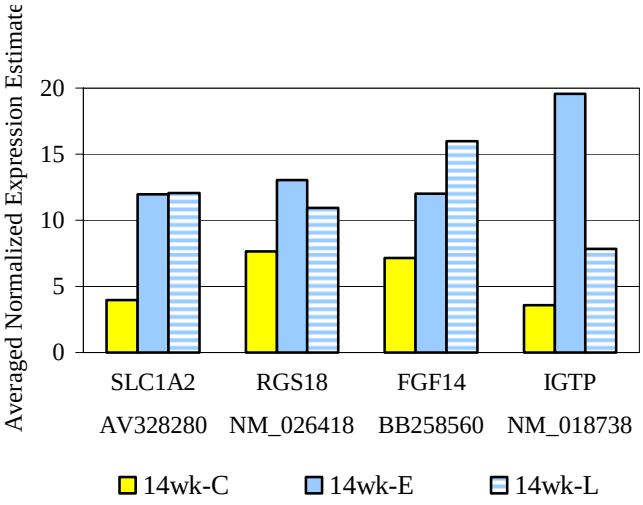

Table 3.21 Differential Expression of Genes Involved in Signal Transduction. Replicate RNA samples from each treatment group were hybridized to separate arrays. The average of replicate normalized expression estimates for each sample group was used to calculate the fold change difference in expression for each gene in Figures 3.37 and 3.38. Positive fold change values indicate an increase, and negative values indicate a decrease in gene expression in the IFNγ-expressing groups. Values in grey indicate the Student's t-test p-value was greater than 0.1.

			Fold Change (IFN-γ-expressing / non-expressing)			
Accession No.	Gene Symbol	Gene Name	11wk-E	11wk-L	14wk-E	14wk-L
NM_133900	ARFRP1	ADP-ribosylation factor related protein 1	**-1.89**	**-1.27**	1.54	1.44
AV028400	ARFRP1	ADP-ribosylation factor related protein 1	-1.17	**-1.49**	**-1.90**	**-1.90**
BG072448	ARHGEF2	rho/rac guanine nucleotide exchange factor (GEF) 2	1.16	1.00	**1.33**	**1.60**
BB292625	ATAD1	ATPase family, AAA domain containing 1	1.33	1.40	**1.61**	**2.24**
BB385044	CD3Z	CD3 antigen, zeta polypeptide	**-1.55**	-1.30	1.38	1.39
BC021354	DCAMKL1	double cortin and calcium/calmodulin-dependent protein kinase-like 1	1.19	1.24	**1.74**	**2.35**
NM_010828	DLL3	delta-like 3 (Drosophila)	-1.06	1.02	**-1.42**	**-1.61**
BB194720	DOCK3	dedicator of cytokinesis 3	-1.10	**1.20**	1.54	**1.95**
BB045510	DOCK4	dedicator of cytokinesis 4	-1.13	-1.14	**1.73**	**2.08**
BB451714	EDNRB	endothelin receptor type B	-1.13	1.03	1.81	**2.14**
BB258560	FGF14	fibroblast growth factor 14	-1.28	1.21	1.68	**2.24**
BF160931	GABARAPL2	GABA(A) receptor-associated protein-like 2	**-1.77**	-1.10	1.59	1.44
AF156490	GABRG3	gamma-aminobutyric acid (GABA-A) receptor, subunit gamma 3	-1.04	-1.05	**1.66**	**1.62**
AU015577	GPCR123	G protein-coupled receptor 123	-1.12	-1.08	**-3.10**	**-2.39**
AV277640	GPR105	G protein-coupled receptor 105	1.00	1.12	**1.42**	**1.52**
BB049642	GRIK1	glutamate receptor, ionotropic, kainate 1	**-1.16**	-1.11	**1.42**	**1.51**

Accession No.	Gene Symbol	Gene Name	Fold Change (IFN-γ-expressing / non-expressing) 11wk-E	11wk-L	14wk-E	14wk-L
BQ174268	HTR2C	5-hydroxytryptamine receptor 2C	1.03	1.57	**2.63**	2.02
NM_018738	IGTP	interferon gamma induced GTPase	1.60	1.10	**5.44**	2.18
BI102913	IL6ST	IL-6 signal transducer	1.03	1.04	**1.75**	**2.34**
BB283493	LPHN3	latrophilin-3, Ca+2-independent alpha-latrotoxin receptor homolog 3; lectomedin 3	-1.04	1.00	**-2.14**	**-1.92**
BF472806	MAGI-1	membrane associated guanylate kinase, WW and PDZ domain containing 1	**-2.02**	**1.25**	1.46	1.30
NM_016693	MAP3K7	mitogen activated protein kinase kinase kinase 7	1.12	1.24	**-1.45**	**-1.55**
NM_019579	MPP5	membrane protein, palmitoylated 3 (MAGUK p55 subfamily member 5)	-1.16	1.06	**2.28**	**2.40**
U10551	MRAS	muscle and microspikes RAS	1.03	-1.20	**1.59**	2.05
BB249447	PCTK1	PCTAIRE-motif protein kinase 1	1.10	-1.28	**-2.09**	**-2.41**
NM_008845	PIP5K2A	phosphatidylinositol-4-phosphate 5-kinase, type II, alpha	-1.10	-1.20	**1.88**	**2.15**
AV209892	PKIG	protein kinase inhibitor, gamma	-1.32	-1.59	**-1.79**	**-2.06**
BB308836	PPM1L	protein phosphatase 1 (formerly 2C)-like	-1.12	1.22	**1.84**	**2.11**
AV023830	PRKACA	protein kinase, cAMP dependent, catalytic, alpha	1.04	-1.13	-1.54	**-1.62**
NM_025980	PRKACA	protein kinase, cAMP dependent, catalytic, alpha	1.18	-1.03	**1.53**	**1.62**
AK005230	RAB2B	RAB2B protein	**-2.23**	-1.32	1.45	1.53
AW124885	RAPGEF4	Rap guanine nucleotide exchange factor (GEF) 4	1.42	1.15	1.49	**1.99**
BC011511	RASSF3	Ras association (RalGDS/AF-6) domain family 3	-1.03	1.00	**2.09**	**2.03**
NM_026418	RGS18	regulator of G-protein signaling 18	-1.07	-1.07	**1.70**	1.43
BB233670	RGS2	regulator of G-protein signaling 2	-1.09	-1.23	-1.49	**-1.81**
BB025471	RGS9	regulator of G-protein signaling 9	-1.12	1.25	**2.04**	**1.93**

Accession No.	Gene Symbol	Gene Name	Fold Change (IFN-γ-expressing / non-expressing) 11wk-E	11wk-L	14wk-E	14wk-L
AV047988	RHOBTB3	Rho-related BTB domain containing 3	1.06	1.58	1.57	**2.45**
NM_053271	RIMS2	regulating synaptic membrane exocytosis 2	1.36	1.05	-1.88	**-2.32**
BB014721	SEH1L	SEH1-like	1.03	-1.23	-1.83	**-2.04**
AV328280	SLC1A2	glutamate transporter	2.20	1.07	**2.99**	**3.01**
AV069725	SOCS-7	suppressor of cytokine signaling 7	1.06	-1.10	**-1.41**	**-1.88**
NM_010656	SSR4	signal sequence receptor, delta	-1.08	1.23	1.89	**2.45**
BM936504	SYN2	synapsin II	-1.12	-1.20	**2.05**	**2.06**
BB388293	SYT1	synaptotagmin 1	1.17	1.26	**-2.03**	-1.65
AV138438	SYT7	synaptotagmin 7	1.16	-1.12	**-2.17**	-2.05
NM_021297	TLR4	toll-like receptor 4	-1.05	-1.16	**1.57**	**1.44**
NM_134131	TNFAIP8	TNF-alpha-induced protein 8	-1.21	-1.04	**2.12**	**1.71**
BB268998	TULP4	tubby like protein 4	1.48	1.08	**3.15**	**2.99**
M58566	TXK	TXK tyrosine kinase	1.13	-1.20	1.28	**1.65**
BB154367	YWHAQ	tyrosine 3-monooxygenase/ tryptophan 5-monooxygenase activation protein, theta	-1.05	1.05	**1.49**	**1.64**

Figure 3.39 Expression Estimates of Genes Involved in Transport at 11wks. a-b) Gene symbols and Accession numbers are plotted on the x-axis; the average of replicate normalized expression values for each treatment group (as described in Materials and Methods) is plotted on the y-axis. In some cases, a gene is represented on the microarray set more than once by different accession numbers. Fold change values are listed in Table 3.22.

a.

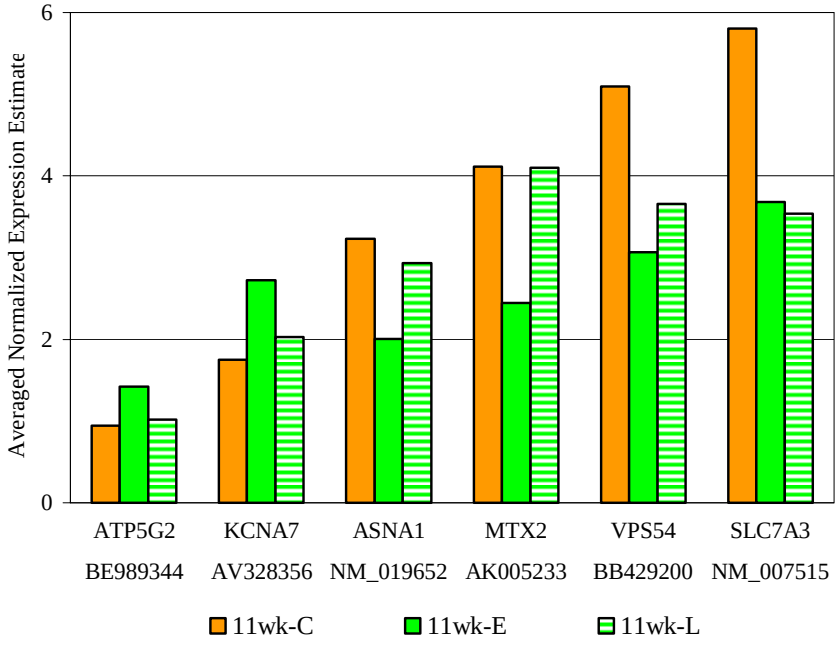

b.

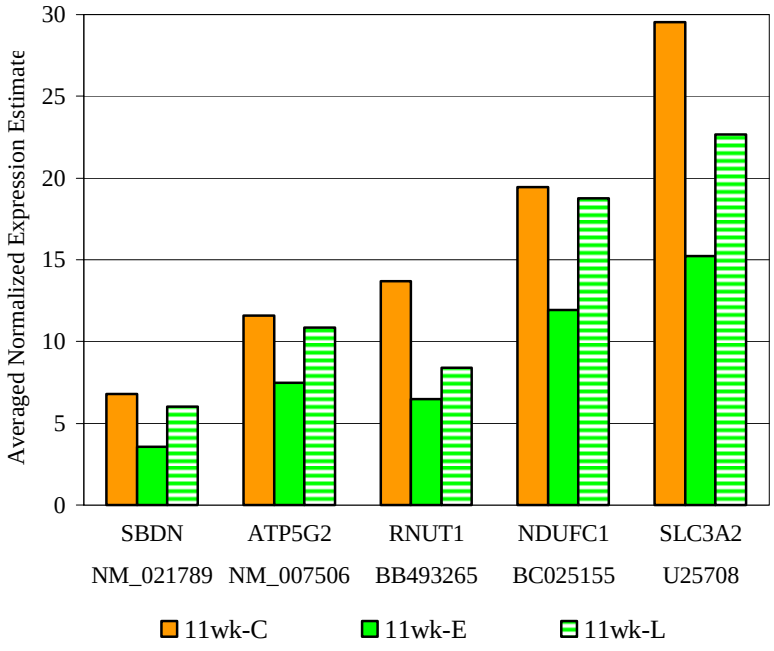

Figure 3.40 Expression Estimates of Genes Involved in Transport at 14wks. a-h) Gene symbols and Accession numbers are plotted on the x-axis; the average of replicate normalized expression values for each treatment group (as described in Materials and Methods) is plotted on the y-axis. In some cases, a gene is represented on the microarray set more than once by different accession numbers. Fold change values are listed in Table 3.22.

a.

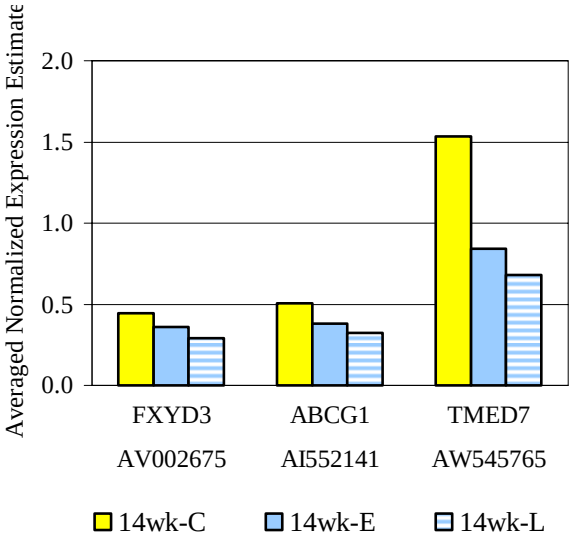

b.

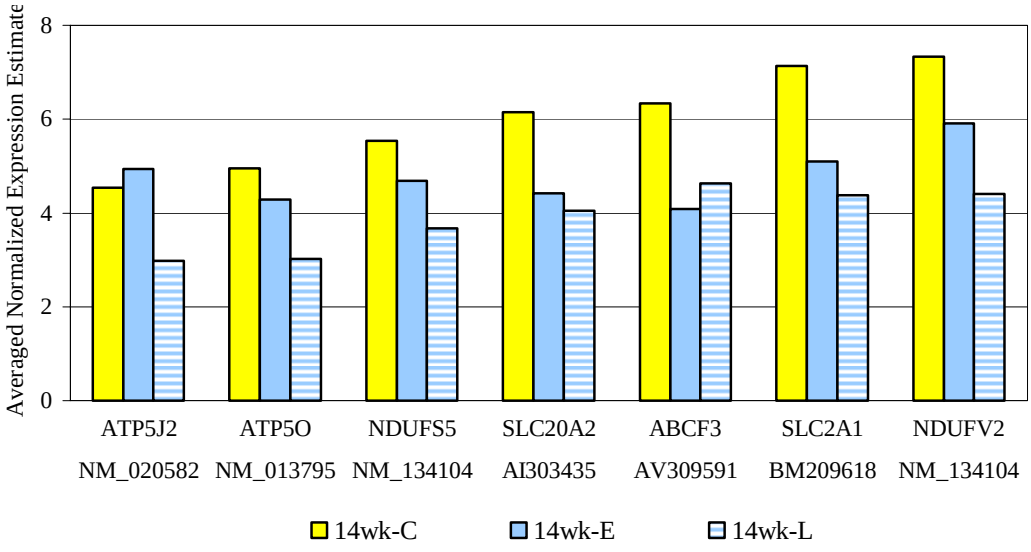

Figure 3.40 Expression Estimates of Genes Involved in Transport at 14wks.

c.

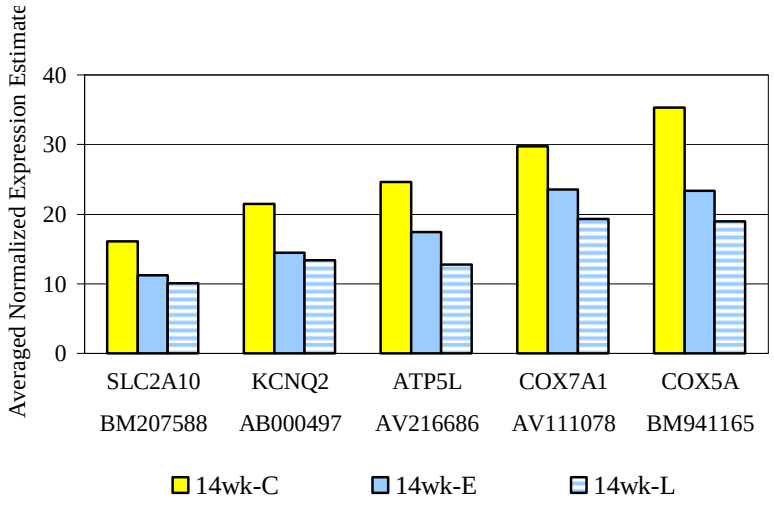

d.

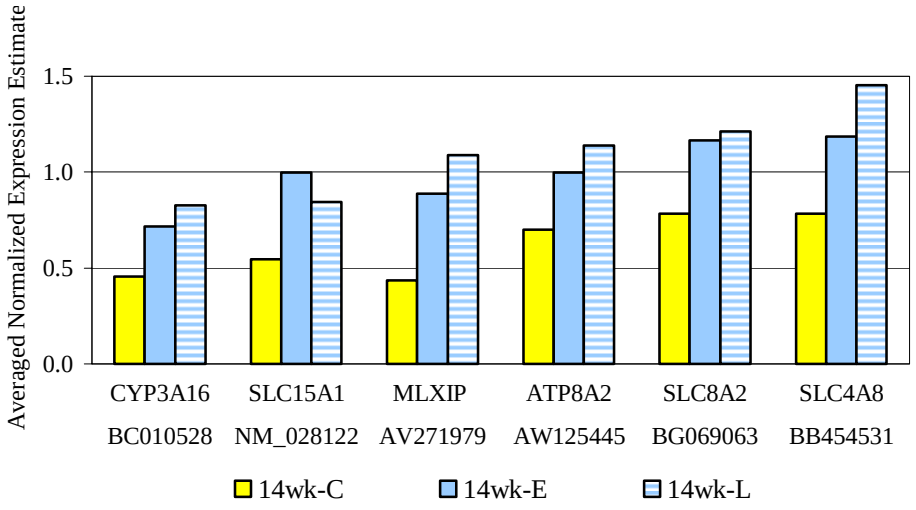

Figure 3.40 Expression Estimates of Genes Involved in Transport at 14wks.

e.

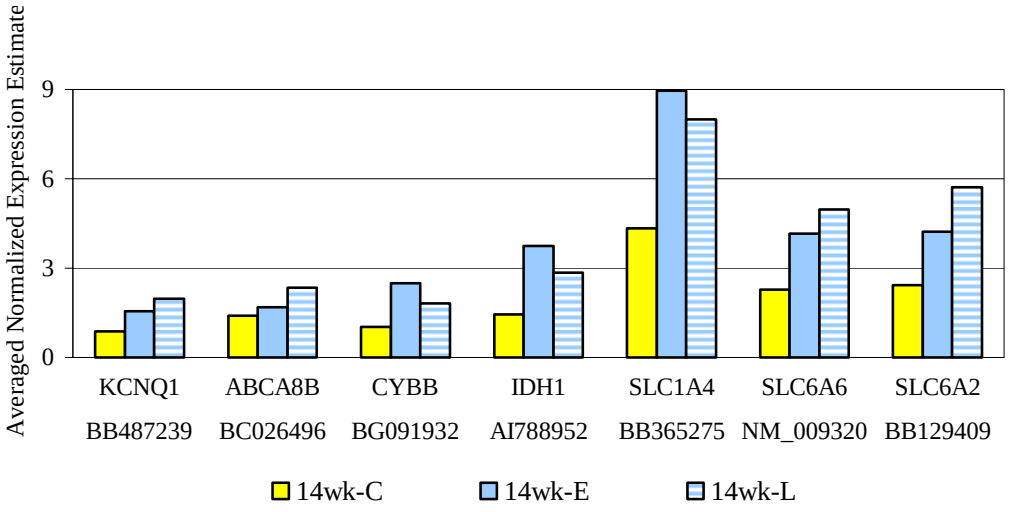

f.

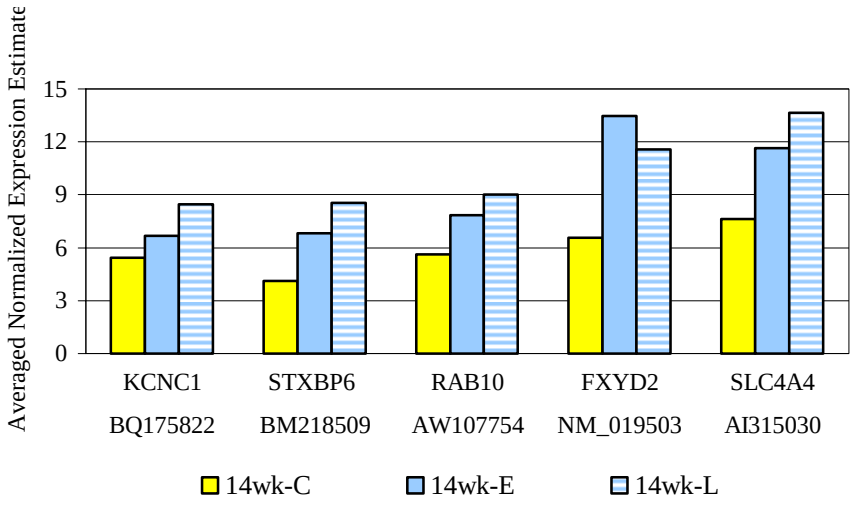

Figure 3.40 Expression Estimates of Genes Involved in Transport at 14wks.

g.

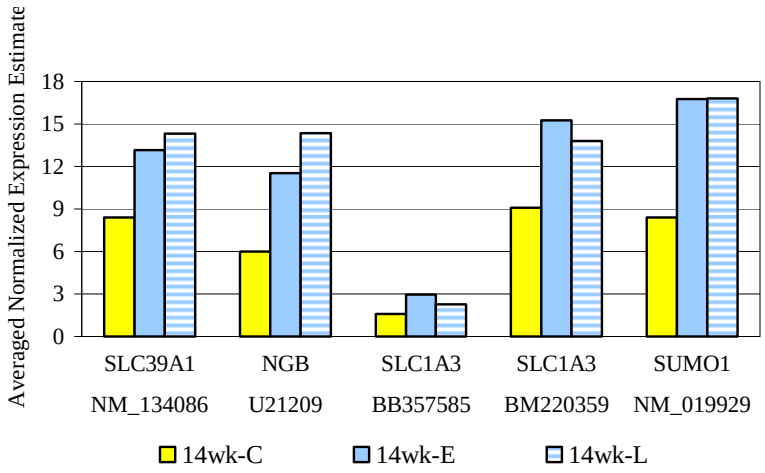

h.

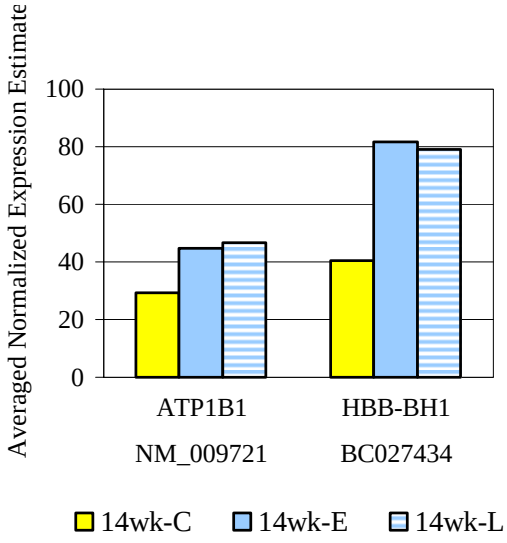

Table 3.22 Differential Expression of Genes Involved in Transport. Replicate RNA samples from each treatment group were hybridized to separate arrays. The average of replicate normalized expression estimates for each sample group was used to calculate the fold change difference in expression for each gene in Figures 3.39 and 3.40. Positive fold change values indicate an increase, and negative values indicate a decrease in gene expression in the IFNγ-expressing groups. Values in grey indicate the Student's t-test p-value was greater than 0.1.

			Fold Change (IFN-γ-expressing / non-expressing)			
Accession No.	Gene Symbol	Gene Name	11wk-E	11wk-L	14wk-E	14wk-L
BC026496	ABCA8B	ATP-binding cassette, sub-family A (ABC1), member 8b	1.24	1.09	1.21	**1.68**
AV309591	ABCF3	ATP-binding cassette, sub-family F (GCN20), member 3	-1.05	-1.03	**-1.55**	**-1.37**
AI552141	ABCG1	ATP-binding cassette, sub-family G (WHITE), member 1	-1.12	-1.28	**-1.33**	**-1.55**
NM_019652	ASNA1	arsA (bacterial) arsenite transporter, ATP-binding, homolog 1	**-1.61**	-1.10	1.31	1.12
NM_009721	ATP1B1	ATPase, Na+/K+ transporting, beta 1 polypeptide	-1.04	1.18	**1.52**	**1.59**
NM_007506	ATP5G2	ATP synthase, H+ transporting, mitochondrial F0 complex, subunit c (subunit 9), isoform 2	**-1.55**	-1.07	1.70	1.52
BE989344	ATP5G2	ATP synthase, H+ transporting, mitochondrial F0 complex, subunit c (subunit 9), isoform 2	**1.51**	1.08	-1.07	-1.05
NM_020582	ATP5J2	ATP synthase, H+ transporting, mitochondrial F0 complex, subunit f, isoform 2	-1.51	-1.18	1.09	**-1.53**
AV216686	ATP5L	ATP synthase, H+ transporting, mitochondrial F0 complex, subunit g	-1.07	-1.22	-1.41	**-1.93**
NM_013795	ATP5O	ATP synthase, H+ transporting, mitochondrial F1 complex, O subunit	**-1.34**	-1.16	-1.16	**-1.64**
AW125445	ATP8A2	ATPase, aminophospholipid transporter-like, class I, type 8A, member 2	1.20	1.11	**1.43**	**1.63**
BM941165	COX5A	cytochrome c oxidase, subunit Va	**-1.20**	**-1.13**	**-1.52**	**-1.87**
AV111078	COX7A1	cytochrome c oxidase, subunit VIIa 1	**-1.19**	-1.15	-1.26	**-1.54**

Accession No.	Gene Symbol	Gene Name	Fold Change (IFN-γ-expressing / non-expressing) 11wk-E	11wk-L	14wk-E	14wk-L
BG091932	CYBB	cytochrome b-245, beta polypeptide	1.36	-1.09	**2.43**	1.77
BC010528	CYP3A16	cytochrome P450, 3a16	1.13	1.21	**1.57**	**1.81**
NM_019503	FXYD2	FXYD domain-containing ion transport regulator 2	-1.44	-1.05	**2.05**	1.76
AV002675	FXYD3	FXYD domain-containing ion transport regulator 3	1.01	1.00	**-1.23**	**-1.53**
BC027434	HBB-BH1	hemoglobin Z, beta-like embryonic chain	-1.14	-1.14	**2.01**	**1.95**
AI788952	IDH1	isocitrate dehydrogenase 1 (NADP+), soluble	-1.13	-1.01	**2.59**	1.97
AV328356	KCNA7	potassium voltage-gated channel, shaker-related subfamily, member 7	**1.55**	1.16	-1.47	-1.63
BQ175822	KCNC1	potassium voltage gated channel, Shaw-related subfamily, member 1	1.11	1.32	1.22	**1.55**
BB487239	KCNQ1	potassium voltage-gated channel, subfamily Q, member 1	1.50	1.03	**1.79**	**2.28**
AB000497	KCNQ2	potassium voltage-gated channel, subfamily Q, member 2	-1.08	-1.17	-1.49	**-1.60**
AV271979	MLXIP	Mlx interactor MIR	-1.37	-1.40	2.04	**2.50**
AK005233	MTX2	metaxin 2	**-1.68**	1.00	1.65	1.51
BC025155	NDUFC1	NADH dehydrogenase (ubiquinone) 1, subcomplex unknown, 1	**-1.63**	-1.04	2.00	1.67
NM_134104	NDUFS5	NADH dehydrogenase (ubiquinone) Fe-S protein 5	-1.32	1.01	-1.18	**-1.50**
NM_134104	NDUFV2	NADH dehydrogenase (ubiquinone) flavoprotein 2	**-1.48**	-1.20	-1.24	**-1.67**
U21209	NGB	neuroglobin	1.02	**1.15**	1.93	**2.40**
AW107754	RAB10	RAB10, member RAS oncogene family	-1.15	1.02	**1.39**	**1.60**
BB493265	RNUT1	RNA, U transporter 1	**-2.11**	**-1.63**	1.03	-1.34
NM_021789	SBDN	synbindin	**-1.90**	-1.13	1.64	1.59
BB357585	SLC1A3	solute carrier family 1, member 3	-1.28	-1.18	**1.87**	1.43

Accession No.	Gene Symbol	Gene Name	Fold Change (IFN-γ-expressing / non-expressing) 11wk-E	11wk-L	14wk-E	14wk-L
BM220359	SLC1A3	solute carrier family 1, member 3	-1.43	-1.10	**1.68**	1.52
NM_028122	SLC15A1	solute carrier family 15 (oligopeptide transporter), 1	-1.41	-1.40	**1.83**	1.54
BB365275	SLC1A4	solute carrier family 1 (glutamate/neutral amino acid transporter), member 4	-1.64	-1.23	**2.07**	1.84
AI303435	SLC20A2	solute carrier family 20, member 2	-1.06	-1.20	-1.39	**-1.52**
BM209618	SLC2A1	solute carrier family 2 (facilitated glucose transporter), member 1	1.22	-1.03	**-1.40**	**-1.63**
BM207588	SLC2A10	solute carrier family 2 (facilitated glucose transporter), member 10	1.23	-1.08	**-1.43**	**-1.59**
NM_134086	SLC39A1	solute carrier family 39 (iron-regulated transporter), member 1	-1.13	1.07	**1.57**	**1.71**
U25708	SLC3A2	solute carrier family 3 (activators of dibasic and neutral amino acid transport), member 2	**-1.94**	-1.30	1.64	1.65
AI315030	SLC4A4	solute carrier family 4 (anion exchanger), member 4	-1.02	1.03	**1.53**	**1.79**
BB454531	SLC4A8	solute carrier family 4 (anion exchanger), member 8	-1.24	-1.21	1.51	**1.85**
BB129409	SLC6A2	solute carrier family 6 (neurotransmitter transporter, noradrenalin), member 2	-1.45	1.11	1.74	**2.35**
NM_009320	SLC6A6	solute carrier family 6 (neurotransmitter transporter, taurine), member 6	-1.29	1.00	1.83	**2.19**
NM_007515	SLC7A3	solute carrier family 7 (cationic amino acid transporter, y+ system), member 3	**-1.58**	**-1.64**	1.22	1.07
BG069063	SLC8A2	solute carrier family 8 (sodium/calcium exchanger), member 2	1.53	1.12	**1.49**	**1.54**
BM218509	STXBP6	syntaxin binding protein 6	-1.18	1.02	1.65	**2.07**
NM_019929	SUMO-1	SMT3 suppressor of mif two 3 homolog 3	-1.55	-1.04	**2.00**	**2.00**
AW545765	TMED7	transmembrane emp24 protein transport domain containing 7	1.11	-1.07	-1.82	**-2.26**
BB429200	VPS54	vacuolar protein sorting 54	**-1.66**	-1.39	-1.84	-1.48

Table 3.23 Differential Expression of Genes of Unknown Function. Replicate RNA samples from each treatment group were hybridized to separate arrays. The average of replicate normalized expression estimates for each sample group was used to calculate the fold change difference in expression. Positive fold change values indicate an increase, and negative values indicate a decrease in gene expression in the IFNγ-expressing groups. Values in grey indicate the Student's t-test p-value was greater than 0.1.

			Fold Change (IFN-γ-expressing / non-expressing)			
Accession No.	Gene Symbol	Gene Name	11wk-E	11wk-L	14wk-E	14wk-L
AA681807	AGPAT3	1-acylglycerol-3-phosphate O-acyltransferase 3	1.28	1.42	**2.55**	**2.54**
AK005060	AGXT2L1	alanine-glyoxylate aminotransferase 2-like 1	1.48	**2.15**	1.38	1.49
U48399	AR	androgen receptor	-1.17	-1.05	**2.28**	**2.54**
BB167922	ARR3	arrestin 3, retinal	1.21	-1.14	**-2.40**	-2.02
AB030194	B3GALT4	UDP-Gal:betaGlcNAc beta 1,3-galactosyltransferase, polypeptide 4	-1.03	-1.18	-1.48	**-2.18**
BB175696	BAALC	brain and acute leukemia, cytoplasmic	1.06	**1.22**	**2.07**	**2.24**
NM_011793	BCS1L	BCS1-like (yeast)	**-2.18**	-1.37	1.32	1.14
BC018174	BTBD3	BTB/POZ domain containing 3	1.19	-1.05	**1.92**	**1.86**
BB199960	BTBD7	BTB/POZ domain containing 7	-1.05	1.04	**1.93**	**2.80**
NM_133781	CAB39	calcium binding protein 39	-1.04	1.54	**2.55**	**2.90**
BG261945	CALR	calreticulin	-1.36	1.62	1.40	**2.17**
AF251705	CD300D	CD300d anigen, immunoglobulin superfamily, member 7	1.00	-1.09	**1.68**	1.20
AV375176	CENTD1	centaurin, delta 1	**-1.52**	-1.09	1.68	1.81
NM_007755	CPEB2	cytoplasmic polyadenylation element binding protein 2	-1.05	1.06	2.03	**2.80**
BM933756	CRHR	corticotropin releasing hormone receptor 1	-1.03	-1.42	-1.51	**-2.05**
NM_133656	CRKO	v-crk sarcoma virus CT10 oncogene homolog (avian)	-1.12	1.11	**2.85**	**2.89**
NM_009977	CST8	cystatin 8 (cystatin-related epididymal spermatogenic)	1.08	-2.02	**2.21**	1.30

Accession No.	Gene Symbol	Gene Name	Fold Change (IFN-γ-expressing / non-expressing) 11wk-E	11wk-L	14wk-E	14wk-L
BC021452	DEAF1	deformed epidermal autoregulatory factor 1 (Drosophila)	1.06	-1.19	**2.72**	**2.38**
NM_013642	DUSP12	dual specificity phosphatase 12	1.01	1.16	1.42	**2.16**
AK009744	DUTP	deoxyuridine triphosphatase	-1.51	1.09	2.04	**2.20**
NM_019808	ENH	enigma homolog	1.04	-1.03	**2.22**	**2.61**
BB817332	FLRT2	fibronectin leucine rich transmembrane protein 2	1.04	1.29	1.45	**2.09**
AV026617	FOSB	FBJ osteosarcoma oncogene B	-1.11	1.07	2.33	**3.46**
NM_018734	GCL	germ cell-less homolog	-1.17	-1.59	**2.62**	1.11
NM_010260	GEM	GTP binding protein (gene overexpressed in skeletal muscle)	1.10	-1.33	**10.94**	3.20
BB315012	GLA	galactosidase, alpha	1.25	1.12	1.90	**2.82**
AK011217	GTL3	gene trap locus 3	**-1.91**	-1.09	1.74	1.64
NM_019440	GUCY1B3	guanylate cyclase 1, soluble, beta 3	1.32	1.08	**6.96**	2.80
AK013709	HNRPAB	heterogeneous nuclear ribonucleoprotein A/B	**-2.06**	-1.15	1.54	1.53
BB390704	LAMP2	lysosomal membrane glycoprotein 2	-1.21	-1.17	**2.05**	**1.83**
BB041834	LASP1	LIM and SH3 protein 1	-1.09	-1.06	1.37	**2.04**
BB440867	LT1	Lurcher transcript 1	1.27	1.21	1.98	**2.43**
AB076722	MURR1	U2af1-rs1 region 1	**-1.29**	**-1.30**	-1.31	**-2.01**
AU067119	NAPB	N-ethylmaleimide sensitive fusion protein attachment protein beta	-1.33	**1.29**	**2.98**	**3.73**
AU067119	NAPB	N-ethylmaleimide sensitive fusion protein attachment protein beta	-1.35	1.21	**2.54**	**3.08**
BQ033138	OAZ3	ornithine decarboxylase antizyme 3	-1.73	-2.41	**3.45**	1.32
AK013804	P2RY2	purinergic receptor P2Y, G-protein coupled 2	-1.45	-1.01	1.62	**2.03**
BC027089	PAP	pancreatitis-associated protein	1.15	1.04	**1.90**	**2.09**
AA389937	PCNT2	pericentrin 2	-1.35	1.12	1.93	**2.13**

Accession No.	Gene Symbol	Gene Name	Fold Change (IFN-γ-expressing / non-expressing) 11wk-E	11wk-L	14wk-E	14wk-L
BB320388	PCNX	pecanex homolog	1.05	-1.12	-1.73	**-2.00**
BB428358	PEX2	peroxisome biogenesis factor 2	-1.04	1.07	**1.67**	**1.75**
BG916808	POP7	Pop7 homolog	1.06	-1.17	**3.32**	1.66
BB823786	PUM1	pumilio 1	-1.25	1.08	1.96	**2.11**
AV364488	RAB40B	Rab40b, member RAS oncogene family	**-2.10**	-1.18	1.68	1.52
BB667227	RBBP4	retinoblastoma binding protein 4	-1.02	-1.02	**-2.27**	-1.74
BC004607	REEP3	receptor expression enhancing protein 3	1.02	1.03	**1.46**	**1.98**
NM_009776	SERPINI1	EST	1.02	-1.01	**2.61**	1.73
BC026135	SH2BP1	SH2 domain binding protein 1	-1.22	-1.14	**2.21**	**2.02**
AK018248	TCBA1	T cell lymphoma breakpoint associated target 1	**-1.72**	-1.12	1.86	1.74
BG065782	TCEB1L	cysteine-rich hydrophobic domain 1	-1.15	1.17	**1.70**	**2.11**
AV026664	TDG	thymine DNA glycosylase	-1.57	1.27	2.00	**2.53**
NM_011579	THAP4	THAP domain containing 4	2.05	1.63	**13.98**	2.93
BB707122	TIPARP	TCDD-inducible poly(ADP-ribose) polymerase	1.04	1.07	1.70	**2.02**
BQ177170	TM4SF6	transmembrane 4 superfamily member 6	-1.93	-1.45	2.61	**2.12**
BB310819	TSGA8	testis-specific protein A; zinc finger protein	1.18	1.16	**-2.75**	-2.05
BF682223	UGP2	UDP-glucose pyrophosphorylase 2	-1.47	1.04	**1.83**	**2.08**
AV370025	UGP2	UDP-glucose pyrophosphorylase 2	-1.36	-1.06	**2.00**	**2.11**
AF424698	UGP2	UDP-glucose pyrophosphorylase 2	-1.52	1.05	2.29	**2.44**
AK009297	WDR33	WD repeat domain 33	-1.30	1.10	**1.75**	**2.11**
BM938007	ZSWIM6	zinc finger Zswim6	1.08	1.02	**2.15**	**1.76**

Table 3.24 Differential Expression of ESTs. Replicate RNA samples from each treatment group were hybridized to separate arrays. The average of replicate normalized expression estimates for each sample group was used to calculate the fold change difference in expression. Positive fold change values indicate an increase, and negative values indicate a decrease in gene expression in the IFNγ-expressing groups. Values in grey indicate the Student's t-test p-value was greater than 0.1.

	Fold Change (IFN-γ-expressing / non-expressing)			
Accession No.	11wk-E	11wk-L	14wk-E	14wk-L
BQ174667	**1.89**	**2.83**	-1.98	1.01
BB703394	**1.68**	1.04	1.12	1.11
NM_008935	**1.55**	1.34	1.19	1.07
BQ175915	**1.51**	1.23	1.18	1.16
BE946605	**-2.22**	-2.17	1.19	1.09
BI655075	**-2.19**	-2.17	2.39	1.68
NM_026526	**-2.04**	-2.17	2.04	1.57
AI596632	**-1.99**	-2.17	1.53	1.65
BG071076	**-1.89**	**-1.43**	1.01	1.15
BF100837	**-1.85**	-2.17	1.37	1.36
BQ175587	**-1.83**	-2.17	1.28	1.15
BB795206	**-1.79**	-2.17	1.35	1.45
BG060788	**-1.69**	**-1.73**	1.29	1.21
AW108203	**-1.67**	-2.17	1.26	1.01
BC024944	**-1.66**	-2.17	1.30	1.10
BB731805	**-1.64**	-2.17	1.72	1.59
BG067009	**-1.58**	-2.17	1.79	1.80
AW121365	**-1.57**	-2.17	-1.98	-1.72
AK012222	**-1.57**	-2.17	1.22	1.13
BG975168	**-1.53**	**-1.32**	1.14	-1.72

	Fold Change (IFN-γ-expressing / non-expressing)			
Accession No.	11wk-E	11wk-L	14wk-E	14wk-L
BF018149	**-1.52**	**-1.20**	1.39	1.13
BM118290	**-1.52**	**-1.30**	1.33	1.36
AF408433	**-1.52**	-2.17	1.33	1.43
AK003715	**-1.52**	**-1.20**	1.31	1.25
BB239907	**-1.51**	-2.17	1.41	1.38
AW550321	**-1.51**	-2.17	1.55	1.49
BQ176278	**-1.51**	**-1.23**	1.40	1.40
BI690696	**-1.50**	1.05	1.24	1.14
AV338249	-1.79	**-1.55**	-1.98	-1.72
BI440542	-1.79	**-1.70**	-1.98	-1.72
BB297094	1.18	**1.78**	-1.98	**2.05**
BB130348	1.16	-2.17	**2.93**	**3.37**
BM211445	1.40	1.33	**2.28**	**3.31**
BM941198	1.02	1.05	**2.45**	**3.24**
BG069278	-1.79	-2.17	**2.92**	**3.04**
BB026312	-1.79	1.07	**2.80**	**2.68**
BB484070	1.15	1.11	**2.83**	**2.60**
BB303443	1.26	1.11	**2.81**	**2.40**
AI746482	1.77	1.08	**1.64**	**2.38**
BQ174216	1.08	1.26	**1.77**	**2.33**
AK020915	1.23	-2.17	**2.11**	**2.25**
AI646720	1.38	1.32	**1.69**	**2.19**
BB325849	-1.79	1.01	**2.18**	**2.18**
BE955100	1.52	1.03	**1.85**	**2.16**
AK003329	-1.79	-2.17	**2.08**	**2.14**

	Fold Change (IFN-γ-expressing / non-expressing)			
Accession No.	11wk-E	11wk-L	14wk-E	14wk-L
BB534387	-1.79	-2.17	**2.22**	**2.14**
BM238331	1.15	1.09	**1.53**	**2.14**
AK012260	1.02	-2.17	**3.11**	**2.13**
BE692107	1.21	1.01	**2.04**	**2.08**
BG093966	1.24	1.23	**2.07**	**2.07**
BF158817	-1.79	1.08	**2.64**	**2.06**
BB256501	-1.79	1.29	**1.59**	**2.05**
BM123174	-1.79	1.01	**1.87**	**2.04**
BB667201	-1.79	**1.22**	**1.93**	**2.04**
AK018550	-1.79	-2.17	**1.65**	**2.03**
AK017198	-1.79	1.06	**1.93**	**1.94**
BB245259	**1.46**	-2.17	**1.63**	**1.93**
AK020045	1.06	1.35	**1.58**	**1.92**
AW146109	-1.79	-2.17	**2.02**	**1.90**
BB736474	-1.79	-2.17	**1.94**	**1.80**
BF660952	1.06	-2.17	**1.82**	**1.79**
BG064688	1.05	1.17	**1.76**	**1.76**
C86506	-1.79	-2.17	**1.99**	**1.76**
BB397845	1.03	-2.17	**1.56**	**1.67**
BB277237	-1.79	-2.17	**1.50**	**1.64**
BI076831	1.18	1.11	**1.54**	**1.63**
BE647363	-1.79	1.03	**1.50**	**1.63**
BF158817	-1.79	**1.16**	**1.92**	**1.61**
AV173139	1.22	1.13	**1.56**	**1.59**
BM241342	-1.79	-2.17	**1.92**	**1.59**

	Fold Change (IFN-γ-expressing / non-expressing)			
Accession No.	11wk-E	11wk-L	14wk-E	14wk-L
AU046270	-1.79	1.11	**1.53**	**1.53**
BB029886	1.00	1.01	**1.62**	**1.52**
AK019515	-1.79	1.08	**1.56**	**1.51**
AV087417	-1.79	-2.17	**1.58**	**1.50**
BM238672	1.29	1.33	1.81	**3.03**
BG066534	-1.79	1.10	2.17	**2.69**
BB455080	1.28	-2.17	1.83	**2.68**
NM_134017	-1.79	**1.34**	2.41	**2.68**
BE825099	-1.79	1.13	2.39	**2.61**
AK018202	-1.79	-2.17	1.89	**2.59**
BM249924	1.01	1.11	1.68	**2.55**
AK009258	-1.79	-2.17	1.62	**2.55**
AV313375	-1.79	-2.17	2.35	**2.50**
AK017401	1.04	1.13	1.52	**2.50**
AK016275	-1.79	1.07	2.49	**2.42**
BG066534	-1.79	1.06	1.88	**2.41**
AU040379	1.67	-2.17	1.82	**2.41**
BG070342	-1.79	1.11	1.99	**2.37**
BB118847	-1.79	1.10	1.85	**2.27**
BM198273	1.17	-2.17	2.55	**2.22**
BM937727	-1.79	-2.17	1.51	**2.22**
AW123199	1.05	1.14	1.62	**2.21**
AK007420	-1.79	-2.17	1.33	**2.20**
AV340255	-1.79	1.12	1.71	**2.19**
BB277790	1.01	1.20	1.87	**2.19**

	Fold Change (IFN-γ-expressing / non-expressing)			
Accession No.	11wk-E	11wk-L	14wk-E	14wk-L
BB215068	-1.79	1.06	1.71	**2.19**
BG797225	-1.79	-2.17	1.69	**2.19**
BM239943	-1.79	1.20	1.49	**2.18**
AK011527	1.22	1.07	1.59	**2.13**
AK012530	-1.79	-2.17	1.68	**2.12**
BB179947	-1.79	1.20	1.39	**2.10**
BG075224	-1.79	1.11	1.60	**2.06**
AU067727	-1.79	1.05	1.53	**2.00**
BB748887	1.13	1.01	1.75	**2.00**
BB153043	1.20	**1.22**	1.36	**1.98**
BB648310	1.35	1.32	1.47	**1.97**
BQ174527	1.55	1.25	1.59	**1.95**
AI597033	1.21	-2.17	1.15	**1.95**
BQ033939	1.16	1.10	1.50	**1.93**
BE979956	1.50	-2.17	2.35	**1.90**
AV029732	-1.79	**1.33**	1.70	**1.88**
BB131938	1.06	1.15	1.54	**1.87**
AV168216	-1.79	1.00	1.60	**1.80**
BF134200	1.18	-2.17	1.28	**1.80**
BF467246	-1.79	1.03	1.55	**1.79**
BE980200	1.42	1.16	1.31	**1.78**
NM_130879	1.14	1.00	1.48	**1.78**
BF465935	-1.79	1.17	1.40	**1.76**
BM211160	-1.79	-2.17	1.66	**1.76**
BB162048	-1.79	**-1.21**	1.53	**1.75**

	Fold Change (IFN-γ-expressing / non-expressing)			
Accession No.	11wk-E	11wk-L	14wk-E	14wk-L
BM942252	1.34	1.23	1.21	**1.74**
BF714941	1.14	-2.17	1.19	**1.73**
BB028677	1.25	1.08	1.21	**1.73**
AV108872	-1.79	1.02	**1.43**	**1.72**
BG918834	1.09	1.12	1.52	**1.71**
BB306048	1.28	1.11	1.32	**1.70**
BG069269	1.27	-2.17	1.48	**1.69**
AV104668	1.04	-2.17	**1.46**	**1.67**
BB632261	-1.79	1.08	1.83	**1.64**
BM117570	1.36	-2.17	1.42	**1.63**
BG067686	1.18	1.31	1.18	**1.61**
AB041803	1.35	1.12	1.13	**1.61**
BG067058	1.33	1.09	1.20	**1.61**
BB038914	1.19	1.19	**1.41**	**1.60**
AU046270	-1.79	1.27	1.54	**1.59**
BM125576	**-1.35**	-2.17	1.46	**1.58**
AV320152	-1.79	1.01	-1.98	**1.57**
BM205987	-1.79	-2.17	1.27	**1.56**
BM217857	1.29	1.16	1.22	**1.56**
BG063085	1.00	1.04	1.23	**1.56**
AW489349	1.07	-2.17	**1.47**	**1.55**
BM240795	1.25	**1.30**	1.18	**1.53**
BE951394	-1.79	1.02	**1.48**	**1.53**
AV338133	-1.79	-2.17	1.19	**1.52**
BB256400	1.20	1.25	1.38	**1.52**

	Fold Change (IFN-γ-expressing / non-expressing)			
Accession No.	11wk-E	11wk-L	14wk-E	14wk-L
BB259670	**-1.26**	-2.17	1.40	**1.52**
BB266350	-1.79	1.12	1.02	**1.52**
BB360713	-1.79	1.03	**1.46**	**1.51**
AA124924	1.03	-2.17	**1.30**	**1.51**
BB206107	1.03	-2.17	**1.24**	**1.51**
BC006682	-1.79	1.06	**1.44**	**1.50**
BG076081	-1.79	-2.17	1.41	**1.50**
BG092512	1.12	-2.17	**6.02**	1.82
BM241271	-1.79	-2.17	**2.49**	1.24
BC010291	-1.79	-2.17	**2.30**	1.05
BC021340	1.02	-2.17	**2.30**	1.37
NM_134083	-1.79	-2.17	**2.24**	1.96
BB668084	1.03	-2.17	**2.13**	1.03
BC021353	-1.79	-2.17	**1.86**	1.47
D45203	-1.79	1.21	**1.76**	1.65
AV334671	-1.79	-2.17	**1.73**	**1.33**
BG075830	-1.79	1.05	**1.66**	1.61
AJ428067	1.12	1.12	**1.65**	1.35
AW552116	1.30	1.10	**1.61**	**1.41**
BB183736	-1.79	1.03	**1.60**	**1.44**
BB284338	-1.79	1.02	**1.59**	1.50
BB317673	-1.79	-2.17	**-2.16**	**-2.35**
BB396413	1.07	-2.17	**-2.06**	**-2.24**
AY037804	-1.79	-2.17	**-1.94**	**-2.09**
AI467657	1.69	1.14	**-1.85**	**-2.07**

	Fold Change (IFN-γ-expressing / non-expressing)			
Accession No.	11wk-E	11wk-L	14wk-E	14wk-L
AW539538	-1.79	-2.17	**-2.92**	**-2.02**
BB699319	-1.79	-2.17	**-1.59**	**-1.99**
AV377712	1.04	**-1.21**	**-1.79**	**-1.86**
AV277957	-1.79	**-1.16**	**-1.68**	**-1.79**
BG073424	-1.79	-2.17	**-1.71**	**-1.75**
AW491150	1.13	-2.17	**-1.63**	**-1.72**
AK019929	-1.79	1.05	**-2.41**	**-1.71**
AK020028	1.01	-2.17	**-1.50**	**-1.64**
BF225441	-1.79	-2.17	**-1.75**	**-1.62**
BB536648	-1.79	-2.17	**-1.70**	**-1.52**
AV069567	-1.79	-2.17	-1.98	**-2.67**
BB458460	-1.79	-2.17	-1.98	**-2.38**
BE992311	-1.79	-2.17	-1.98	**-2.23**
BB209438	1.06	-2.17	-1.98	**-2.20**
BC021536	-1.79	-2.17	**-1.47**	**-2.13**
BB400326	1.00	-2.17	-1.98	**-2.13**
BB035728	1.03	-2.17	-1.98	**-2.11**
BB440272	1.11	-2.17	-1.98	**-2.10**
BC024693	-1.79	**-1.16**	-1.98	**-2.10**
BB108987	1.04	-2.17	-1.98	**-2.05**
BB258427	1.12	-2.17	-1.98	**-2.02**
BB541793	1.16	-2.17	-1.98	**-2.02**
BB794177	1.18	-2.17	-1.98	**-1.96**
BB122985	1.35	-2.17	-1.98	**-1.96**
AI415469	-1.79	**-1.34**	**-1.40**	**-1.88**

	Fold Change (IFN-γ-expressing / non-expressing)			
Accession No.	11wk-E	11wk-L	14wk-E	14wk-L
BM936011	-1.79	-2.17	-1.98	**-1.87**
BB321110	-1.79	-2.17	-1.98	**-1.82**
BB284482	-1.79	-2.17	-1.98	**-1.79**
W65070	-1.79	-2.17	1.15	**-1.78**
BB251205	1.04	-2.17	-1.98	**-1.74**
AV249015	1.05	1.02	**-1.42**	**-1.72**
AV347904	-1.79	-2.17	**-1.32**	**-1.68**
BM899529	-1.79	-2.17	-1.98	**-1.67**
BB397392	-1.79	-2.17	-1.98	**-1.64**
AV056885	**-1.18**	**-1.22**	-1.98	**-1.64**
BB049966	-1.79	-2.17	-1.98	**-1.64**
BG797460	-1.79	-2.17	-1.98	**-1.60**
BI320076	-1.79	-2.17	**-1.39**	**-1.58**
BG067784	1.03	1.06	-1.98	**-1.57**
N28111	-1.79	-2.17	**-1.26**	**-1.57**
BB172440	1.03	1.00	**-1.41**	**-1.57**
BB487787	-1.79	1.05	**-1.32**	**-1.56**
BC013667	1.09	-2.17	-1.98	**-1.56**
BC024955	1.01	-2.17	**-1.25**	**-1.55**
BB258011	1.02	1.00	-1.98	**-1.52**
AV175293	-1.79	-2.17	**-1.46**	**-1.51**
BF459077	1.04	1.00	-1.98	**-1.50**
BG069690	1.05	-2.17	**-1.31**	**-1.50**
BB238478	-1.79	-2.17	**-2.14**	-1.72
BB309880	1.10	1.00	**-2.12**	-1.72

	Fold Change (IFN-γ-expressing / non-expressing)			
Accession No.	11wk-E	11wk-L	14wk-E	14wk-L
BM117872	1.00	-2.17	**-1.95**	-1.72
BE685667	2.35	1.04	**-1.78**	-1.72
AW456636	-1.79	-2.17	**-1.74**	-1.72
AV343258	-1.79	-2.17	**-1.66**	-1.72
BB811311	1.07	**-1.14**	**-1.57**	**-1.47**
BM118846	1.14	1.01	**-1.57**	-1.72
AI503942	-1.79	**-1.21**	**-1.55**	-1.72
C77386	1.00	-2.17	**-1.53**	-1.72
BM243944	-1.79	1.05	**-1.52**	-1.72

CHAPTER FOUR

CONCLUSION

1. Affymetrix GeneChip® Technology

The manufacturing of Affymetrix GeneChips® can be viewed in detail at www.affymetrix.com. Briefly, a GeneChip® is comprised of a small quartz wafer that is reactive to light energy by covalently-linked surface molecules. Photolithographic masks are used to direct the placement of ATCG nucleotides in a series of reactions that results in the synthesis of 25-mer oligonucleotides covalently linked to the array surface. These oligonucleotides, or "probes," are designed to complement specific, usually unique, mRNA sequences. For each gene or EST (hereafter referred to as gene) represented on the array, there are perfect match (PM) probes, which are exact complements of their target sequence; and for each PM probe, there is a mismatch (MM) probe, which is mutated at the 13th base. A "probe pair" then is a single set of PM and MM probes. For each target sequence, there are 11-20 probe pairs (collectively the "probe set"), depending on the specific GeneChip,® at different locations on the array. Altogether on a single mouse genome array (MOE 430), for example, there are ~45,000 target sequences represented by ~100 million probes.

Target RNA is amplified by first reverse transcribing to cDNA; then in vitro transcription incorporating biotin is used to synthesize biotin-labeled cRNA. The labeled cRNA is fragmented, added to control target sequences, and hybridized to the probe sequences on the array. Post hybridization, the array is washed and stained with R-phycoeurythrin-

streptavidin, which has a very high affinity for biotin. The array is then scanned for R-phycoerythrin signal and the individual intensity for each PM and MM probe is recorded. These intensity values must be summarized to generate a single, meaningful, estimate of expression for each gene and EST on the array.

2. Microarray Analysis

On Affymetrix GeneChips® the PM probes measure the specific binding of a particular target sequence, and the MM probes are intended to measure non-specific binding. In order to generate a single value of expression that accurately represents the relative amount of starting target sequence in a sample, the hybridization signals for the probe set must be mathematically summarized. The first algorithm offered by Affymetrix, Microarray Suite (MAS) 4.0, simply subtracts the MM signal from its corresponding PM signal and averages (Tukey biweight) the differences for the probe set (Affymetrix, 1999). This algorithm assumes the variance is equal for all probes, which is not the case, since the variance increases with increasing signal values (Irizarry et al., 2003a). The inaccuracy of MAS 4.0 spawned the evolution of several different algorithms, each attempting to provide precise, statistically and biologically sound measure of expression.

Using spike-in and dilution experiments, Irizarry et al. (2003a) formed a detailed comparison of the most widely used analysis programs. They evaluated the current Affymetrix algorithm, MAS 5.0 (Affymetrix, 2001), which is an improvement over MAS 4.0 in that it substitutes the MM value with a CT value, where CT = MM when MM < PM, and CT is a value less than PM when MM ≥ PM, which is the case for approximately one-third of all probes (Irizarry et al., 2003b; Naef et al., 2002). While MAS 5.0 is more accurate than

MAS 4.0, it is still dependent on the variance between probes, which is problematic since the variance between probes is great. In fact, the standard deviation between probes is approximately 5 times greater than the standard deviation between arrays (Li and Wong, 2001; Irizarry et al., 2003b).

Li and Wong (2001) developed a multiplicative model (dChip) where the expression estimate is the PM-MM value minus the error estimate, divided by an estimate of the probe affinity effect. Estimating probe affinity effects, however, requires numerous arrays, and the error in this model is assumed to have normal distribution (Irizarry et al., 2003a). The Miles group (Zhang et al., 2002; Kennedy et al., 2006) developed the S-score analysis tool, which provides an accurate determination of statistically significant differential expression compared to the RMA algorithm used in our experiments here; however, it does not determine relative gene expression estimates. Therefore, one may know whether a gene is expressed at significantly different levels between samples, but not the relative robustness of expression in each sample.

The RMA model was chosen for this work based on its success in spike-in and dilution experiments compared to the algorithms described above (Irizarry et al., 2003a). RMA is a log scale linear model in which the PM value is corrected for background, normalized across sets of arrays, and log transformed to give T(PM). T(PM) is then equal to the sum of the $\log_2$ scale expression value on the arrays, the log scale affinity effects for the probe sets, and the error estimate (Irizarry et al., 2003a). Importantly, this model ignores the MM value based on evidence that mathematical and biological subtraction of the non-specific binding MM is meant to represent is not always the same (Irizarry et al., 2003a). Spike-in and dilution experiments indicate that RMA is superior to MAS and dChip models in expression estimate

precision, fold change consistency, and specificity and sensitivity of determining differential expression (Irizarry et al., 2003a).

3. Limitations of Microarray Experiments

Microarray technology allows entire genomes to be surveyed for transcription regulation changes simultaneously in response to external stimuli, transgene expression, gene mutations, disease, and many other treatment schemes. In many experiments, certain outcomes or genes of interest may be predicted; however, unexpected, uncharacterized and unknown genes are often found to be differentially regulated and can lead to the identification of novel genes and novel gene functions.

Microarray analysis is an excellent launching pad for plucking out a small number of potentially important genes among thousands; however, as with any technology, there are limitations. Controlling the variance between samples and between arrays is essential in order to maximize the usefulness of array results. The Affymetrix system used here has demonstrated excellent precision across numerous arrays with spike-in control RNA such that the variance between arrays has become nearly negligible (https://www.affymetrix.com/support/downloads/manuals/data_analysis_fundamentals_manual.pdf). RNA isolation, amplification reactions, and hybridization are more real potential sources of variability. In all of experiments described here, the equipment, reagents, and techniques were extremely consistent. Also, the ratios of RNA to protein (260/280 absorbance) were within the acceptable range (1.8 -2.1), and gel electrophoresis indicated that the RNA was not degraded. Probe pairs are designed with a 3' bias for target sequences; whereas, control sequences have both 5' and 3' probes. The ratio of 5' to 3' binding of the controls was very low, also

indicative of in tact RNA. The largest source of variability between samples, therefore, was most likely from biological inconsistencies between experimental animals and primary cell cultures. This notion has also been suggested in Affymetrix technical manuals (www.affymetrix.com/support). Ideally, a large cohort of replicates would be analyzed for control and experimental groups; however, there are obvious limitations to the number of replicates that can feasibly be achieved when working with cell cultures, transgenic animals, and relatively costly technology.

Biological variability is difficult to control and, the author believes, warrants adjustment of the parameters that determine statistical significance between control and experimental samples. For this reason, a p-value cutoff of 0.1 was used instead of the more traditional 0.01 or 0.05, proposing that this results in fewer false negatives than it causes false positives. An argument for this is the observation that the largest fold changes in gene expression are principally measured when a gene is not constitutively expressed (or expressed at very low levels) in one group and highly expressed in another. Analysis of these and other data support the concept that it is at these high levels of transcription the biological variance expands. With few replicate samples, small degrees of variance quickly lead to large p-values, even when a biologically significant difference in expression is evident. On the other side of the coin, increasing the p-value cutoff opens the door for false positives when genes that are constitutively expressed in one group are moderately up- or downregulated in another group. Here, it becomes more difficult to determine whether larger standard deviations among replicates are the result of normal biological variance or due to sample processing error or array artifact. For smaller fold change values between constitutively-expressed genes, it becomes more important to restrict significance to lower p-values as there

is a greater probability of obtaining false positives. These caveats have been taken into consideration when reporting array analysis results for these experiments.

4. Immature OLs Respond Differently to IFN-γ than Mature OLs

Reported effects of IFN-γ on oligodendrocytes cultures have varied among groups. Vartanian et al. (1995) observed cell death in both developing and mature OLs exposed to the cytokine; whereas, other groups found cell metabolism and proliferation to be disrupted (Agresti et al., 1996), but no IFN-γ-induced cell death (Agresti et al., 1996; Turnley et al., 1991). Previous studies in our lab demonstrated apoptotic cell death in immature OLs after 2 days of IFN-γ exposure and necrotic cell death in mature populations after 4-7 days of cytokine exposure (Baerwald et al., 1998).

As is discussed in further detail in section 5, evidence is mounting that suggests not only the developmental stage of OLs, but also the timing and dose of IFN-γ exposure are important factors in its effect on OLs and (re)myelination (Gao et al., 2000; Lin et al., 2005, 2006, unpublished data). For example, Turnley et al. (1991) treated developing OL cultures with 20U/mL of IFN-γ and observed no cell death. In contrast, Baerwald et al. (1998) showed that after 2 days of IFN-γ exposure at 100U/mL, developing OLs extended fewer processes and a higher percentage of cells underwent apoptosis (as measured by TUNEL assay). Baerwald et al. (1998) also examined the effect of IFN-γ on mature cells by allowing progenitors to develop for 7 days in culture before treating them with 100U/mL IFN-γ for several days. After 2 and 4 days of cytokine exposure they observed a decrease in MBP, PLP, CGT, MAG and CNP message, and an increase in MHC class I and GAPDH message. They did not see evidence of apoptosis, but rather necrosis in these cells.

Here we treated progenitor cells with 100U/mL IFN-γ for 24 hours, and with the same dose for 48 hours, we treated OLs that had been allow to mature for 3 days in differentiation-promoting medium. We measured mRNA expression by microarray hybridization and predicted that the immature and mature OL populations would respond differently to IFN-γ exposure. Accordingly, we found some differential gene regulation between the two groups of cells as summarized in Table 4.1.

After 1 day of IFN-γ exposure, immature cells showed an increase in message for myelin proteins MBP, PLP, and CNP compared to non-treated controls (Table 4.1). Cholesterol biosynthesis enzymes, including the rate-liming enzyme HMGCR, along with the cholesterol transporter ApoE were also upregulated in these cells. In contrast, we found either no change or only a slight decrease in these genes in mature OLs exposed to IFN-γ. One possible explanation for the increase in myelin-related gene expression in the immature but not mature OLs is a link between IFN-γ exposure and the stage of development. Another possibility, however, is that a short course (24hrs) of IFN-γ elicits different effects than the longer courses (2-4 days) that have resulted in downregulation of myelin genes (Baerwald et al., 1998; Lin et al., 2005).

The most robust changes in expression were observed in MHC genes and in genes involved in protein processing and degradation. Both MHC class I and class II genes were upregulated in immature and mature OLs exposed to IFN-γ. The upregulation of class I and class I processing genes was more robust in mature cells, while the induction of class II and class II processing genes was more robust in immature cells.

The expression of IFN-γ receptor did not change significantly upon IFN-γ exposure in either cell population; though, immature cells treated with the cytokine expressed

approximately 57% more receptor than did IFN-γ-treated mature cells. Nevertheless, the mature cells were exposed to IFN-γ longer than the immature cells (2 days versus 1 day), which perhaps accounts for the increase in class I expression.

An explanation for the increased class II expression in the immature cells is that progenitor cells have been shown to express more class II than mature OLs (Turnley et al., 1991), although, mature OLs in the presence of physiological levels of glucocorticoid are also able to express some class II (Bergsteindottir et al., 1992). It is likely, then, that the immature cells in culture are intrinsically capable of higher class II expression.

We hypothesized that since OLs are already generating large amounts of membrane lipid and protein, which must go through the ER, the additional robust expression of MHC and protein processing machinery (Table 4.1), which also utilize the ER, could compound the ER stress; and moreover, this ER stress would be the source of apoptotic death in OLs. Cells respond to ER stress by upregulating protein folding chaperones, increasing retrograde transport of molecules out of the ER, increasing protein degradation, and decreasing protein translation (Rutkowski and Kaufman, 2004; Rao et al., 2004; Ma and Hendershot, 2001). We observed an upregulation that was more robust in IFN-γ-treated immature than mature cells in protein folding chaperones including HSPA9A and HSPCA and in the translation initiation factor eIF2A. Concurrently, in response to IFN-γ treatment of mature OLs, Lin et al. (2005) observed an increase in the ER stress markers BIP and CHOP, and an increase in the phosphorylation of eIF2A, which has been shown to attenuate protein translation in response to ER stress (Lin et al., 2005; Jousse et al., 2003).

Additionally, we observed a decrease that was more prominent in immature than mature IFN-γ-treated OLs in additional translation initiation factors including eIF2C1 and eIF4E,

which may represent a decrease in protein translation (Table 4.1). Furthermore, several genes involved in ubiquitin-mediated and 26S proteasome-mediated protein degradation were upregulated, but were not consistently higher in the immature or mature cells after cytokine exposure.

There was also evidence of an oxidative stress response in the immature OLs by the strong upregulation of the oxidase inhibitor CYBA along with antioxidant-inducing transcription factors NFE2L2 and NFkB1. Moreover, we found evidence of increased apoptosis in the immature cells by the upregulation of the DNA fragmentation gene CIDE-B, and its downregulation in mature cells. This is consistent with reports that mature OLs are more resistant to IFN-γ-induced cell death (Baerwald et al., 1998). Additionally, IGF-1, which promotes early differentiation in progenitor cells and has a protective effect on OL survival (Ye et al., 1995; Mason et al., 2000; Gao et al., 2002), was robustly expressed in non-treated immature OLs, ~10 times the average expression on the array and ~6 times higher than in non-treated mature OLs. This agrees with the expectation that there would be more actively differentiating cells after 1 day in differentiation-promoting medium than after 5 days. In both immature and mature populations, IFN-γ treatment resulted in a decrease in IGF1; however, the decrease was considerably less in the mature cells, which may again point to their resistance against the harmful effects of IFN-γ.

Taken together, these data suggest that while there is robust MHC and protein processing genes in both immature and mature OLs in response to IFN-γ exposure, there may be more severe ER stress elicited in the immature cells, which may then lead to apoptosis. Therefore, it would appear that the detrimental effects of IFN-γ on OLs are influenced by the developmental stage of the cells and perhaps the length of time they are exposed to IFN-γ.

Moreover, these data suggest that the deleterious effects are a result of robust induction of antigen presenting and protein processing genes, which tax the ER and elicit stress. Since microarray analysis measures mRNA, determining the protein levels of these genes and the phosphorylation state of eIF2A will provide a clearer understanding of the ER stress response and apoptosis in immature versus mature cells exposed to IFN-γ.

Table 4.1 Results Summary of Immature and Mature OLs Exposed to IFN-γ. Replicate RNA samples from each treatment group were hybridized to separate arrays. The average of replicate normalized expression estimates for each sample group was used to calculate the fold change difference in expression for each gene. Positive fold change values indicate an increase, and negative values indicate a decrease in gene expression in the IFNγ-treated groups. Values in gray indicate the Student's t-test p-value was greater than 0.1; the asterisk indicates there was one sample for each treatment. Underlined values indicate the gene was represented by more than one accession number on the array and the fold change values were averaged.

	Fold Change (IFN-γ-tx OLs / Non-tx OLs)		
Gene Name	Immature	Mature	Gene Function
IFN-γ Signal Transduction			
IFN-γ receptor	**-1.32**	**-1.19***	receptor for IFN-γ
JAK	**1.52**	**1.35***	binds IFN-γ receptor and is phosphorylated
STAT1	**19.7**	**17.3**	binds phosphorylated JAKs, translocates to nucleus, induces GAS sequence-containing genes
SOCS-1	**1.75**	**2.15***	binds phosphorylated JAKs, prevents STAT1 gene induction
Myelin-Related Genes			
CNP	**2.38**	1.03	cell membrane extension
MBP	**3.43**	1.12	myelin compaction
PLP	**2.14**	-1.34	myelin compaction
HMGCR	**1.54**	1.18	rate-limiting step in cholesterol synthesis
APOE	**2.13**	**1.09**	cholesterol transport & recycling
Protein Processing			
MHC Class I	**6.59**	**9.41**	presents antigen recognized by CD8+ T cells
B_2M	**6.96**	**11.5**	transport of class I antigen to cell surface

Gene Name	Fold Change (IFN-γ-tx OLs / Non-tx OLs) Immature	Mature	Gene Function
TAP1	**15.7**	**21.5**	protein transport in and out of ER
PSMB9	**25.5**	**30.5**	20S proteasome-mediated protein degradation
MHC Class II	**6.94**	**3.87**	presents antigen recognized by CD4+ T cells
MHC class II transactivator	**8.11**	**3.49**	transports class II from nucleus to endosome
CD74 invariant chain	**25.2**	**21.6**	transports class II out of the endosome
cathepsin S	**3.51**	2.37	class II endosomal processing
HERC6 ubiquitin ligase	**4.22**	**7.01**	ubiquitin-mediated protein degradation
ubiquitin D	**14.9**	**33.9**	ubiquitin-mediated protein degradation
cathepsin Y	**8.36**	**1.44***	proteolysis & peptidolysis
poly(ADP-ribose) polymerase 9 (PARP9)	**11.3**	**13.4***	proteolysis & peptidolysis
ER Stress Response			
heat shock protein, A (HSPA9A)	**3.17**	1.14	protein folding chaperone
heat shock protein 1a (HSPCA)	**2.62**	**1.74***	protein aggregation prevention, protein folding chaperone, ubiquitin-mediated protein degradation
eIF2A	**4.01**	**3.10**	protein translation initiation (phosphorylated form attenuates protein translation)
eIF2C1	**-1.93**	**-1.13***	protein translation initiation
eIF4E	**-1.89**	**-1.37***	protein translation initiation
Oxidative Stress Response			
cytochrome b558 alpha (CYBA)	**5.26**	1.44	inhibits oxidase
NF-E2-related factor 2 (NFE2L2)	**3.58**	1.32	transcription factor that induces anti-oxidant genes
NF kappa B p105 subunit (NFkB1)	**2.53**	1.35	transcription factor that induces anti-oxidant genes

Gene Name	Fold Change (IFN-γ-tx OLs / Non-tx OLs) Immature	Mature	Gene Function
Apoptosis			
cell death-inducing DNA fragmentation factor, alpha subunit-like effector B (CIDE-B)	**2.85**	**-1.54***	DNA fragmentation - induction of apoptosis
Survival			
insulin-like growth factor I	**-3.57**	**-2.00**	promotes cell survival
Miscellaneous Genes			
complement component 1, q subcomponent, gamma polypeptide (C1QG)	**7.31**	**1.26***	classical complement activation
serine (or cysteine) proteinase inhibitor, clade G (C1 inhibitor), member 1 (SERPING1)	**4.44**	**7.09**	complement activation inhibitor
chemokine (C-X-C motif) ligand 11	**21.6**	**3.03***	induces chemotactic response in activated T cells
Fc IgG receptor III	**6.44**	**2.11**	promotes macrophage activation & cytokine release
integrin alpha L	**2.14**	**1.11***	T cell induction of EAE
leukocyte antigen MRC-OX44 (CD53)	**4.52**	1.34	may promote cell survival and resistance to H2O2
CD9 antigen	**2.16**	**-1.59**	associates with integrins at cell surface, upregulated in response to brain pathogenesis
coronin, actin-binding protein 1B	**2.85**	1.18	regulates cell motility

5. Timing of IFN-γ Induction Influences the Outcome of Remyelination

Increasing evidence suggests that the timing of IFN-γ expression relative to a demyelinating insult influences the outcome of remyelination (Gao et al., 2000; Lin et al., 2005, 2006, unpublished data). Transgenic animals expressing low levels of IFN-γ commensurate with MBP expression are asymptomatic and resistant to cuprizone-induced demyelination (Gao et al., 2000); whereas, under the same transgenic system, animals expressing elevated levels of IFN-γ exhibit tremor, astrogliosis and hypomyelination (Corbin et al., 1996; Horwitz et al., 1997). In the cuprizone model, IGF1 expression increases with increasing demyelination (Komoly et al., 1992; Mason et al., 2000; Jurevics et al., 2002). In low IFN-γ-expressing animals, IGF1 expression is markedly increased prior to the demyelinating insult, and demyelination is less severe (Gao et al., 2000). In addition, there is a slight increase in the number of astrocytes and microglia present in the corpus collosum prior to demyelination in the low-level expressers; however, there is very little sign of microglia activation, astrogliosis, or oligodendrocyte cell loss during cuprizone treatment in these animals (Gao et al., 2000).

The timing of IFN-γ induction does not affect demyelination or EAE severity.

The double transgenic (GFAP/tTA x TRE/IFN-γ) mice used in the experiments reported here express elevated levels of IFN-γ, are hypomyelinated, and tremor (Lin et al., 2004, 2005, 2006). IFN-γ was effectively suppressed in these animals with doxycycline from conception to 6 weeks of age. The early expressers were released from dox at the same time cuprizone treatment began and showed appreciable levels of IFN-γ two weeks later when demyelination was evident, but not yet complete. In the late expressers, IFN-γ was induced

two weeks into cuprizone treatment and was again detected two weeks later when the corpus collosum was fully demyelinated. The difference in the timing of IFN-γ induction did not affect the extent of demyelination by cuprizone (Lin et al., 2006, unpublished data). In a separate experiment, the double transgenic animals were immunized with MOG to induce EAE, and IFN-γ induction was timed such that marked cytokine levels occurred concomitantly with the peak of disease severity; therefore, IFN-γ did not affect the degree of demyelination.

Very few oligodendrocytes remain in the corpus collosum at 11wks when demyelination is maximal (Matsushima and Morell, 2001; Mason et al., 2000; Lin et al., 2006), thus, the changes in gene regulation we measured at 11wk-E and 11wk-L likely originated from the large population of astrocytes that appear upon OL loss, and $NG2^{+}$ progenitors, which infiltrate the corpus collosum beginning around 4wks of cuprizone treatment. A summary of these results in gene regulation is shown in Table 4.2.

The only substantial change in gene regulation in the late IFN-γ expressers at the peak of demyelination was in MHC class I, and this induction was still significantly less than that observed in the early expressers (Table 4.2). In these experiments, MHC induction may have occurred in astrocytes and/or the few remaining OLs left in the corpus collosum at 11wks.

In the early expressers, IFN-γ was present before demyelination reached maximum; therefore, more OLs were presumably exposed to the cytokine. Accordingly, we found measurable induction of MHC class I and II in the early expressers (Table 4.2). There was also evidence of decreased protein synthesis by the downregulation of RNU22 and several ribosomal proteins including RPS4X, as well as a decrease in genes involved in cell metabolism including PHGDH and PHPT1 (Table 4.2). This decrease in global protein

synthesis and metabolism message may represent a shutting down of $NG2^+$ progenitors in response to IFN-γ. This is supported by observations from previous experiments in our lab that detected an initial increase in $NG2^+$ cells at 10wks, but a decrease in progenitors at 12wks in the early expressers (Lin et al., 2006; Lin and Popko, unpublished data).

Table 4.2 Results Summary of Gene Regulation at Peak Demyelination in Response to IFN-γ Expression. Replicate RNA samples from each treatment group were hybridized to separate arrays. The average of replicate normalized expression estimates for each sample group was used to calculate the fold change difference in expression for each gene. Positive fold change values indicate an increase, and negative values indicate a decrease in gene expression in the IFNγ-treated groups. Values in gray indicate the Student's t-test p-value was greater than 0.1. Underlined values indicate the gene was represented by more than one accession number on the array and the fold change values were averaged.

	Fold Change (IFN-γ-expressing / non-expressing)		
Gene Name	11wk-E	11wk-L	Gene Function
IFN-γ Signal Transduction			
IFN-γ receptor	**-1.08**	**-1.18**	receptor for IFN-γ
JAK	**-1.03**	**-1.15**	binds IFN-γ receptor and is phosphorylated
STAT1	**-1.05**	**-1.43**	binds phosphorylated JAKs, translocates to nucleus, induces GAS sequence-containing genes
SOCS-1	-1.21	-1.26	binds phosphorylated JAKs, prevents STAT1 gene induction
Protein Processing			
MHC Class I	**10.9**	**3.62**	presents antigen recognized by CD8+ T cells
proteasome subunit beta type 3	**-1.74**	**-1.09**	20S proteasome-mediated protein degradation
MHC Class II	**6.61**	**1.51**	presents antigen recognized by CD4+ T cells
ubiquitin-specific ligase 11	**-1.96**	-1.10	ubiquitin-mediated protein degradation
amyloid beta (A4) precursor protein-binding, family A, member 1 binding protein	**-2.18**	-1.09	proteolysis & peptidolysis

Gene Name	Fold Change (IFN-γ-expressing / non-expressing) 11wk-E	11wk-L	Gene Function
ER Stress Response			
heat shock binding protein 1	**-1.56**	**-1.14**	protein folding chaperone
heat shock protein E1	**-1.59**	**-1.38**	protein folding chaperone
RNA, U22 small nucleolar	**-2.76**	**-1.69**	protein synthesis
ribosomal protein S4, X-linked	**-2.36**	-1.23	protein synthesis
Miscellaneous Genes			
cyclin-dependent kinase 4	**-2.31**	**-1.33**	cell cycle
activating transcription factor 5	**-2.60**	-1.82	differentiation
metallothionein-like 5	**-2.35**	**-1.48**	differentiation
anaphase promoting complex 5	**-1.89**	-1.11	cell growth
mini chromosome maintenance deficient 7	**-1.95**	-1.33	cell growth
enhancer of rudimentary	**-2.03**	-1.13	metabolism
3-phosphoglycerate dehydrogenase	**-2.25**	-1.26	metabolism
phosphohistidine phosphatase 1	**-2.01**	-1.05	metabolism
coronin, actin-binding protein 1A	**-2.53**	-1.24	regulates cell motility
coronin, actin-binding protein 1C	**-2.20**	-1.27	regulates cell motility
cadherin 13	**-1.81**	-1.21	cell adhesion
H3 histone 3B	**-1.81**	-1.18	nucleic acid binding
RNA binding motif protein 5	**2.08**	-1.07	nucleic acid binding
membrane associated guanylate kinase, WW and PDZ domain containing 1	**-2.02**	**1.25**	signal transduction
Rab2b	**-2.23**	-1.32	signal transduction

Early expression of IFN-γ suppressed remyelination.

After 6 weeks of cuprizone treatment and 2 weeks of recovery without the toxicant, control animals showed an increase in myelin gene expression, an increase in mature OLs with a proportionate decrease in progenitor cells, and a ~48% recovery of remyelinated axons (Lin et al., 2006). In contrast, the early expressers showed a decrease in myelin gene expression, fewer mature OLs, an increase in the number of astrocytes and macrophages, and a ~27% recovery of remyelinated axons (Lin et al., 2006).

Microarray analysis revealed robust upregulation of a large cohort of antigen presenting and processing genes in the early expressers. These results are summarized in Table 4.3. Both MHC class I and class II were upregulated along with genes involved in their processing and assembly, including B_2M, TAP1 and proteasome genes PSMB9 and PSME1, CD74 invariant chain, and cathepsin S. The processing of class I occurs in the ER, and several recent experiments have indicated that the robust upregulation of MHC class I by IFN-γ in OLs, particularly actively myelinating OLs, leads to ER stress and that this ER stress is at least partially responsible for the observed OL cell death during remyelination (Lin et al, 2005, 2006, unpublished data). In addition to the large induction of MHC and protein processing genes, we also observed an increase in genes involved in protein degradation, including ubiquitin-specific ligase 18, cathepsin C and PARP9 (Table 4.3). These data point toward an ER stress condition in the remyelinating corpus collosum; however, we did not find appreciable induction of protein folding chaperones, downregulation of protein translation initiators, or an upregulation of apoptotic genes. Additional experiments in our lab, however, have demonstrated robust induction of MHC and a ~2-fold increase in the ER stress markers BIP and CHOP in the early expressers (Lin et

al., 2005). CHOP protein was also found to be upregulated ~1.8-fold at this time point (Lin et al., 2005). Moreover, our lab has also reported that early IFN-γ expression results in a ~66% reduction in the number of mature $CC1^+$ OLs and only ~27% remyelination compared to ~48% in controls at 14wks (Lin et al., 2005).

Our analysis indicated a ~2.5-fold upregulation JAK and a ~3.3-fold upregulation of STAT1, which are downstream modulators of IFN-γ signaling. Altogether, these data strongly suggest that IFN-γ induction prior to the completion of demyelination results in decreased remyelination and fewer mature OLs, which may, at least in part, be due to ER stress induced by robust induction of MHC and protein processing genes.

Late expression of IFN-γ enhanced remyelination.

Compared to controls, animals in which IFN-γ had been induced two weeks into cuprizone treatment showed an increase in myelin gene expression, an equal number of mature OLs, an increase in the number of astrocytes that was equal to the early expressers, an increase in macrophages that was less than the early expressers, and remarkably, an increase in remyelination (55% vs. 48% in controls, $p<0.05$) (Lin et al., unpublished data).

Concordantly, in our array experiments, we observed a much weaker induction of downstream IFN-γ signaling genes. To that end, while JAK was upregulated slightly more in the late expressers (~2.9-fold) than in the early expressers (~2.5-fold), STAT1 was upregulated only slightly in the late expressers (~1.5-fold) compared to early expressers (~3.3-fold) (Table 4.3).

In accordance with diminished IFN-γ signal transduction, we observed less induction of MHC class I and II and very little upregulation of MHC processing and transport genes than in the early expressers. Furthermore, there was no increase, or only a slight increase, in

expression of IFN-γ-sensitive genes that were upregulated in the early expressers, including interferon-inducible protein 1, interleukin 6 receptor alpha, interleukin 13 receptor alpha 1, macrophage activation 2, and IFN-γ-induced GTPase (Table 4.3).

Consistent with previous experiments in our lab, we found an increase in myelin gene expression, including MBP, MAL, and QK, which supports the observation of increased remyelination in the late IFN-γ expressers compared to non-expressers (Lin et al., unpublished data). Together, these data support other work in our lab suggesting IFN-γ expression after complete demyelination has a beneficial effect on subsequent remyelination.

Table 4.3 Results Summary of Gene Regulation during Robust Remyelination in Response to IFN-γ Expression. Replicate RNA samples from each treatment group were hybridized to separate arrays. The average of replicate normalized expression estimates for each sample group was used to calculate the fold change difference in expression for each gene. Positive fold change values indicate an increase, and negative values indicate a decrease in gene expression in the IFNγ-treated groups. Values in gray indicate the Student's t-test p-value was greater than 0.1. Underlined values indicate the gene was represented by more than one accession number on the array and the fold change values were averaged.

	Fold Change (IFN-γ-expressing / non-expressing)		
Gene Name	14wk-E	14wk-L	Gene Function
IFN-γ Signal Transduction			
IFN-γ receptor	**-1.18**	**-1.09**	receptor for IFN-γ
JAK	**2.54**	**2.94**	binds IFN-γ receptor and is phosphorylated
STAT1	**3.32**	**1.48**	binds phosphorylated JAKs, translocates to nucleus, induces GAS sequence-containing genes
SOCS-1	-1.21	-1.26	binds phosphorylated JAKs, prevents STAT1 gene induction
Myelin-Related Proteins			
myelin and lymphocyte protein	1.58	**1.61**	axo-paranode adhesion
myelin basic protein	1.49	**1.73**	myelin compaction
quaking	**2.14**	**3.13**	stabilizes MBP mRNA, regulates MAG splicing
Protein Processing			
MHC Class I	**51.0**	**21.9**	presents antigen recognized by CD8+ T cells
B_2M	**3.59**	**2.51**	transport of class I antigen to cell surface
TAP1	**1.98**	-1.06	protein transport in and out of ER
proteasome subunit beta type 9 (PSMB9)	**4.62**	1.57	20S proteasome-mediated protein degradation

Gene Name	Fold Change (IFN-γ-expressing / non-expressing) 14wk-E	14wk-L	Gene Function
proteasome 28 subunit, alpha (PSME1)	**2.28**	1.46	immunoproteasome-mediated protein degradation
MHC Class II	**39.4**	**9.43**	presents antigen recognized by CD4+ T cells
CD74 invariant chain	**6.36**	2.07	transports class II out of the endosome
cathepsin S	**1.79**	1.50	class II endosomal processing
ubiquitin-specific ligase 18	**2.34**	1.25	ubiquitin-mediated protein degradation
cathepsin C	**2.15**	1.66	proteolysis & peptidolysis
poly(ADP-ribose) polymerase 9 (PARP9)	**2.06**	1.48	proteolysis & peptidolysis
Protein Synthesis			
ribosomal protein 24	**-1.48**	**-1.96**	protein biosynthesis
ribosomal protein L27	**-1.22**	**-1.74**	protein biosynthesis
ribosomal protein 35	**-1.40**	**-2.06**	protein biosynthesis
ribosomal protein 37a	**-1.13**	**-1.63**	protein biosynthesis
Miscellaneous Genes			
interferon-inducible protein 1	**3.56**	**1.64**	immune response
interleukin 6 receptor, alpha	**2.05**	**1.07**	immune response
interleukin 13 receptor, alpha 1	**2.11**	**1.61**	immune response
macrophage activation 2	**8.41**	1.77	immune response
cadherin 11	**2.06**	**3.29**	cell adhesion
vascular cell adhesion molecule 1	**2.06**	**1.72**	cell adhesion
zinc finger CCDC domain containing 6	**3.04**	**2.14**	nucleic acid binding
Kruppel-like factor 4	1.32	**2.19**	transcription factor

Gene Name	Fold Change (IFN-γ-expressing / non-expressing) 14wk-E	14wk-L	Gene Function
nucleotide binding oligomerization domain 27	**3.05**	**1.70**	transcription factor
period homolog 2	**1.85**	**3.83**	transcription factor
prolactin regulatory element binding	**-2.81**	**-3.17**	transcription factor
RNA-binding region containing protein 2	**2.45**	**3.47**	transcription factor
IFN-γ-induced GTPase	**5.44**	2.18	signal transduction

Possible indirect effects of IFN-γ on remyelination.

The amount of astrogliosis was the same in the early and late expressers during remyelination; however, there were fewer macrophages in the late expressers. Therefore, it is reasonable to surmise that IFN-γ may also exert indirect damaging effects on OLs and remyelination via these cells (Lin et al., 2006, unpublished data). Activated macrophages release TNFα, which has been shown to negatively affect OLs in culture and exacerbate demyelination in vivo; and its cytotoxic effects are made worse by the presence of IFN-γ (Andrews et al., 1998; Merrill et al., 1993; for additional references see Plant et al., 2004). Macrophages have the role of phagocytosing debris, which at lesion sites would include apoptotic OLs and corresponding myelin sheath, thus perhaps the presence of macrophages in lower numbers in the late expressing animals plays a beneficial role in preparing lesion sites for remyelination, while in the early expressers the increase in IFN-γ recruits a detrimental number of macrophages (see also Lin et al., 2006).

Studies in our lab have also demonstrated a larger number of astrocytes after 4 weeks of cuprizone treatment in the corpus collosum of late-expressing animals compared to early expressers (Lin et al., 2006, unpublished data). Perhaps, then, the increase in astrocytes prior to remyelination has some suppressive effect on macrophage and T cell recruitment and/or a positive effect on progenitor cells recruited to the lesion site (see also Lin et al., 2006). This remains to be demonstrated, however.

Altogether, previous experiments in our lab and our results here make a strong argument for a dual role for IFN-γ, one that is time- and dose-dependent, on oligodendrocyte survival and remyelination after immune- and non-immune-mediated demyelination. Immature OLs in culture die after a shorter course of IFN-γ treatment than do mature OLs (Baerwald et al.,

1998). In addition, expression of IFN-γ before the peak of demyelination negatively affects the outcome of remyelination; whereas, expression of the cytokine at full demyelination enhances remyelination as evidenced by a decrease in the number of mature OLs and the number of remyelinated axons in the early expressers compared to an increase in the number of mature OLs and the number of remyelinated axons in the late expressers (Lin et al., 2006, unpublished data). Furthermore, microarray analysis presented here demonstrates that immature OLs exposed to IFN-γ yield a greater increase in genes involved in MHC antigen presentation, protein processing, ER stress response, oxidative stress response, apoptosis, and the immune response. The concomitant upregulation of myelin-associated, proliferation, and survival genes may be attributed to sampling at a time IFN-γ exerted both beneficial and harmful effects. Differential gene expression was observed in the same functional groups of genes in mature OLs exposed to the cytokine, but overall the response was diminished compared to immature OLs. We also observed a more robust induction of immune response, MHC antigen and protein processing, and possibly ER stress response genes during remyelination when IFN-γ had been present prior to the height of demyelination. Moreover, IFN-γ expressed later not only resulted in a suppressed immune response, but also an increase in myelin-associated genes and differentiation-promoting genes. Sorting out the downstream factors, both direct and indirect, in response to IFN-γ stimulus at the different time points has potentially therapeutic benefit in mitigating immune-mediated demyelination and promoting myelin repair.

6. Future Directions

A. Investigation of selected differentially expressed genes. While microarray technology is a useful tool for global gene expression survey, further investigation is necessary to corroborate the level of differential expression and downstream protein translation as well as elucidate gene function. In both experiments presented here, several less well characterized genes and numerous ESTs were significantly differentially regulated, and these are excellent candidates for further investigation by quantitative RT-PCR, ELISA or Western blot as well as gain-of-function (targeted expression) or loss-of-function (knock-out or mutation) analysis. Other example candidate genes of interest would be those with potential T cell recruiting and activation properties. ER stress seems to be a key factor in OL cell death in response to IFN-γ, and certain genes have been identified as important in the ER stress response in OLs, nevertheless, our analysis provides preliminary data that may identify additional key genes involved in that process.

B. Virtually all cells express the IFN-γ receptor, therefore, even though the corpus collosum, which is densely populated by oligodendrocytes, was used in our analysis, and the OL cell cultures used in these experiments were highly selective for OLs, other cell types were also present. Combining a knock-out line of mice for one IFN-γ receptor subtype with a transgenic line with forced expression of the knocked out receptor subtype targeted to oligodendrocytes in a second combination with double transgenic IFN-γ expressing animals would allow evaluation of the response solely of OLs to the presence of IFN-γ at different time points relative to cuprizone-induced demyelination and EAE immunization. Primary mix glial cultures could also be studied in this way from knock-out X transgenic animal lines. Such experiments have been initiated in the lab of Brian Popko.

C. The JAK-STAT pathway is activated in response to IFN-γ-receptor binding and leads to the induction of several IFN-sensitive genes, which likely contribute to its adverse effects on OLs. Both JAK and STAT were found to be robustly upregulated in response to IFN-γ in these experiments. Suppressor of cytokine signaling-1 (SOCS1) interrupts JAK-STAT binding and thwarts IFN-γ signaling. Exploiting SOCS1 expression in OLs has a potential therapeutic benefit, and initial experiments in our lab have demonstrated very promising results (see addendum: Balabanov et al., in press).

Given the dual nature of IFN-γ signaling and its differential effects on demyelination and myelin repair, therapeutic strategies aimed at diminishing demyelination and promoting reparative myelin will likely depend on the timing of IFN-γ suppression. Other challenges include the complex cascade of cross-reactive signal transduction and transcription regulation that may be both detrimental and beneficial, if not necessary, for mitigating the effects of immune-mediated demyelinating disorders.

ADDENDUM

Title: Suppressor of cytokine signaling 1 expression protects oligodendrocytes from the deleterious effects of interferon-gamma

Authors and author addresses: Roumen Balabanov[1,2], Krystle Strand[3,4], April Kemper[5], Ji Yeon Lee[1,2], and Brian Popko [1,2]

[1]Jack Miller Center for Peripheral Neuropathy and [2]Department of Neurology, The University of Chicago, Chicago, IL. [3]Neuroscience Center and [4]Curriculum for Neurobiology, University of North Carolina, Chapel Hill, NC, [5]Department of Pathology, Wake Forest University Baptist Medical Center, Winston Salem, NC 27157, USA.

Corresponding author: Dr. Brian Popko, Jack Miller Center for Peripheral Neuropathy, The University of Chicago, Department of Neurology, 5841 S. Maryland Ave, MC2030, Chicago, IL 60637 (email: bpopko@uchicago.edu).

Keywords: transgenic mice, SOCS1, interferon-gamma, myelin, oligodendrocytes, Stat1

Acknowledgments: This work was supported by grants from the National Institutes of Health (NIH; grants NIH K08 NS5040901 [to R.B.] and NIH R01 NS34939 [to B.P.] and the Myelin Repair Foundation [to B.P.]. We are appreciative of Dr. Wendy Macklin and Dr. Douglas Hilton for their kind gifts of DNA plasmids. The authors also acknowledge the helpful contribution of discussions with colleagues at the Myelin Repair Foundation.

ABSTRACT:

Interferon-gamma (IFN-γ) is a pleiotropic cytokine produced by T cells and natural killer (NK) cells that has been implicated as a deleterious factor in the immune-mediated demyelinating disorder multiple sclerosis. In vitro, purified developing and mature oligodendrocytes have been shown to die in the presence of IFN-γ by apoptosis and necrosis, respectively. Moreover, transgenic expression of IFN-γ in the CNS of mice during development results in tremor, hypomyelination and oligodendrocyte cell loss; and IFN-γ expression in adult animals following demyelinating insults inhibits remyelination. In order to examine the molecular mechanisms of IFN-γ-induced oligodendrocyte injury, we generated a transgenic mouse line (*PLP/SOCS1*) that exhibits diminished oligodendrocyte responsiveness to IFN-γ due to the targeted expression of the suppressor of cytokine signaling 1 (SOCS1) in these cells. We demonstrate that oligodendrocytes in the *PLP/SOCS1* transgenic mice are protected against the injurious effect of IFN-γ. Our data indicate that IFN-γ exerts a direct deleterious effect on developing oligodendrocytes. The capacity of SOCS1 to inhibit the effects of IFN-γ suggests a therapeutic approach toward protection of myelinating oligodendrocytes against the harmful effects of inflammation.

INTRODUCTION:

Interferon-gamma (IFN-γ) is a pleiotropic cytokine produced by T cells and natural killer (NK) cells that is involved in a number of immune processes (Billiau, 1996). IFN-γ is critical to the immunoregulation of autoimmune demyelinating disorders of the central nervous system (CNS) (Panitch et al, 1987; Galbinski et al., 1999; Tran et al., 2000; Skurkovich et al., 2001, Steiman 2001). In addition, IFN-γ provides an intricate link between inflammation and oligodendrocyte injury. Upon stimulation with IFN-γ, oligodendrocytes upregulate the expression of major histocompatibility (MHC) class I molecules, as well as other surface ligands and receptors (e.g., Fas, Hsp70, and TNF-αR) that are believed to facilitate cell-mediated cytotoxicity (Agresti et al., 1998; Pouly et al., 2000; Trougott et al., 2001).

IFN-γ has the capacity to adversely affect oligodendrocytes and the process of myelination. In vitro, developing oligodendrocytes die by apoptosis and mature oligodendrocytes succumb to necrosis in the presence of IFN-γ (Agresti et al., 1996; Baerwald et al., 1998; Andrews et al., 1998; Lin et al., 2005). Transgenic expression of IFN-γ in the CNS of mice during the first few weeks of postnatal development results in hypomyelination and oligodendrocyte cell loss (Corbin et al., 1996; LaFerla et al., 2000; Lin et al., 2005). Moreover, the induction of IFN-γ expression following demyelinating insults significantly inhibits the remyelination process (Lin et al., in press). Oligodendrocyte injury in these models has been related to dysregulation of protein synthesis and trafficking, accumulation of unfolded proteins in the endoplasmic reticulum (ER), and triggering of a proapoptotic stress response (i.e. ER stress response) (Baerwald et al., 2000; Lin et al., 2005).

The molecular mechanism of IFN-γ–mediated injury to developing oligodendrocytes, however, remains unclear. Because of the global effects of IFN-γ on the CNS, either direct or indirect (via microglia) modes of oligodendrocyte injury are possible. Therefore, differentiating between oligodendrocyte-specific and multicellular effects would allow for a better understanding of the molecular mechanisms involved in IFN-γ–mediated oligodendrocyte injury.

Suppressors of cytokine signaling (SOCS) are a family of proteins that inhibit intracellular Jak/Stat signaling and effectively "switch off" the signal transduction pathway (Starr et al., 1997; Song and Shuai 1998; Stark et al., 1998; Sakamoto et al., 2000; Levy and Darnell, 2002). SOCS proteins are key intracellular regulators of cytokine-mediated homeostasis, ensuring a controlled cellular response (Yasukawa et al., 2000; Kubo et al., 2003). SOCS1 is of particular interest because of its function as a regulator of cellular responsiveness to IFN-γ (Starr et al., 1998; Bullen et al., 2001; Alexander et al., 1999; Tunley et al., 2001, 2002; Chong et al., 2001; Federici et al., 2002). Interestingly, the levels of SOCS1 expression in the CNS under both normal and inflammatory conditions are very low and virtually undetectable in oligodendrocytes (Polizzotto et al., 2000; Wang and Campbell, 2002; Maier et al., 2002).

In this report we describe a transgenic line of mice that ectopically expresses SOCS1 in oligodendrocytes under the transcriptional control of the gene encoding the myelin protein proteolipid protein (PLP). *PLP/SOCS1* mice exhibit a normal phenotype with diminished oligodendrocyte responsiveness to IFN-γ. Moreover, we demonstrate that enforced expression of SOCS1 protects oligodendrocytes against the injurious effects of IFN-γ during development.

MATERIALS AND METHODS:

PLP/SOCS1 mouse line

The transgenic mouse line *PLP/SOCS1* was generated using a construct containing a PLP expression cassette and SOCS1 cDNA (Figure 1A). The PLP expression cassette (a kind gift of Dr. Wendy Macklin, Cleveland Clinic, Cleveland, OH) has been described elsewhere and has been used for oligodendrocyte-specific expression of a number of transgenes (Wight et al., 1993; Fuss et al., 2000; Doerflinger et al., 2003; Gonzales et al., 2005). We used a SOCS1 cDNA clone (kindly provided by Douglas Hilton [Walter and Eliza Hall Institute, Melbourne, Australia]) (Starr et al., 1998) that contained a Flag-epitope sequence that served as a marker for SOCS1 expression in polymerase chain reaction (PCR)-based or anti-Flag antibody-based detection methods (Einhauer and Jungbauer, 2001). Briefly, the Flag-SOCS1 cDNA was excised from the original expression vector pEF-FLAG-I/m4A2 with *Xba*I. The fragment was Klenow filled and subcloned into an intermediate vector (modified pNEB/193 vector) at the *Sma*I restriction site. The resulting pNEB193/SOCS1 vector was further digested with *Asc*I (partial digestion) and *Pac*I to release the Flag-SOCS1 fragment, which was subcloned into the polylinker region of the PLP expression cassette at the same restriction sites. The PLP/SOCS1 vector was digested with *ApaI* and *Sac*II (partial digestion) and a linear 15-kb transgene was isolated for microinjection into fertilized (C57BL/6J × DBA/2J) oocytes. Offspring positive for the transgene were identified by amplifying tail DNA by PCR using transgene-specific primers. The identified founders were subsequently bred with C57BL/6J mice (Jackson Laboratories, Bar Harbor, ME) establishing a transgenic line.

IFN-γ–overexpressing Mice

The transgenic mice *MBP/IFN-γ* (line 172) and *GFAP/tTA × TRE/IFN-γ* (lines 184/110 and 184/67) that overexpress IFN-γ in the CNS have been described elsewhere (Corbin et al., 1996; Gao et al., 2000; Lin et al., 2004, 2005). Briefly, *MBP/IFN-γ* (line 172) mice are transgenic animals in which IFN-γ expression is driven by the myelin basic protein (MBP) transcriptional control region (Gao et al., 2000). *GFAP/tTA × TRE/IFN-γ* are double-transgenic mice obtained by mating single-transgenic *GFAP/tTA* (line 184) to single-transgenic *TRE/IFN-γ* (lines 110 and 67) mice. The two *TRE/IFN-γ* mouse lines, line 110 and line 67, used in the experiments produce different amounts of IFN-γ when crossed to *GFAP/tTA* mice (184/110 and 184/67) (Lin e al., 2004, 2005). *GFAP/tTA × TRE/IFN-γ* is a tetracycline-off-inducible system in which the glial fibrilary acidic protein (GFAP) transcriptional control region drives the expression of tTA, which in turn, binds to the TRE (tet responsive element) and initiates the expression of IFN-γ. Administration of doxycycline suppresses tTA DNA binding and IFN-γ expression, and doxycycline removal allows for temporally-controlled induction of IFN-γ expression (Gao et al., 1999).

Mouse breeding and examination

IFN-γ-overexpressing mice were crossed to the *PLP/SOCS1* mice in double-transgenic, (*MBP/IFN-γ × PLP/SOCS1*) and triple-transgenic (*GFAP/tTA × TRE/IFN-γ × PLP/SOCS1*) mating systems. *MBP/IFN-γ × PLP/SOCS1* (172 × *PLP/SOCS1*) mating was performed according to a standard mating protocol. The *GFAP/tTA × TRE/IFN-γ × PLP/SOCS1* matings were performed in a 2-step mating process: *GFAP/tTA* mice (line 184) were initially crossed to *PLP/SOCS1*mice, and double-positive (184 × *PLP/SOCS1*) offspring were then

crossed to the *TRE/IFN-γ* lines 110 and 67, separately. This second mating step was performed according to the previously described "tet-off" protocol. Doxycycline 0.05mg/ml (Sigma-Aldich) was added to the water of impregnated female mice until embryonic day 14, after which the animals were switched back to normal water, thereby allowing initiation of IFN-γ transcription, which peaks during the postnatal period (Lin et al., 2005).

The litters of the mating systems (F1 generation) were examined daily and sacrificed at postnatal day 21. Clinical evaluation included behavioral observation and challenged ladder walking to elicit tremor. Histological examination included quantitation of the number and density of oligodendrocytes and examination of the myelination patterns. Brain tissue was simultaneously obtained from each animal at the time of sacrifice to verify and measure the expression of IFN-γ and Flag-SOCS1 (see below). The clinical and histological findings were subsequently stratified according to genotype. All animal procedures were conducted in compliance with the National Institutes of Health *Guide for Care and Use of Laboratory Animals* and were approved by the Institutional Animal Care and Use Committee at The University of Chicago.

Polymerase-chain reaction and Genotyping

All experimental animals were genotyped using isolated tail DNA (Biotek 2000 automatic system, Beckman-Coutler, Fullerton, CA). PCR (Qiagen,Valencia, CA) for transgene detection was performed using the following transgene-specific screening primers: Flag-SOCS1 sense primer, 5'-CCAGGACGACGATGACAAGA-3' and Flag-SOCS1 anti-sense primer, 5'-TCAGGGGTCCCCA ATAGAAG-3'; MBP/IFN-γ sense primer, 5'-ATGAGGAAGAGCTGCAAAGC-3', and MBP/IFN-γ anti-sense primer, 5-

GGTGACAGACTC CAAGCACA-3'; GFAP/tTA sense primer, 5'-TCGCTTTCCTCTGAACGCTTCTCG-3' and GFAP/tTA anti-sense primer, 5'-TCTGAACGCTGTGACTTGGAGTGTCC-3'; TRE/IFN-γ sense primer 5'-CGAATTCGAGCTCGG TACCC-3' and TRE/IFN-γ anti-sense primer 5'-CCATCCTTTGCCATTCCTCCAG-3' (Integrated DNA Technologies Inc.).

Northern blots and Quantitative PCR (Q-PCR)

Total RNA was isolated from the examined animals with TRIzol reagent (Invitrogen Corp., Carlsbad, CA). Northern blots were performed by separating 20μg of total RNA in a 1.2% denaturing agarose gel. The samples were transferred to a nylon membrane and hybridized overnight with a SOCS1 probe that had been randomly labeled by PCR (GenAmp2400; Perkin-Elmer, Welleslay, MA) with [α-^{32}P] dCTP and [α-^{32}P] dATP (New England Nuclear/Perkin-Elmer, Welleslay, MA). Kodak film was exposed to the hybridized membrane at −80ºC for 48hrs and was developed using the M7B Kodak processor (Kodak, Rochester, NY). To evaluate the relative levels of total RNA present in each lane the membrane was stripped and hybridized with a radiolabeled probe specific for the 28S ribosomal RNA (Baerwald et al., 1998).

Quantitative (Q-PCR, or real-time PCR) was performed by first reverse transcribing 1μg of DNAaseI-treated (Invitrogen) total RNA using oligo(dT)$_{12-18}$ and SuperScript II reverse transcriptase (Invitrogen RT-PCR kit). Q-PCR was performed using 20ng of the cDNA in a reaction containing iQSupermix and the following primers and probes for Flag-SOCS1 and IFN-γ: Flag-SOCS1 sense primer, 5'-GATGACAAGACGCGCCAG ATG -3', Flag-SOCS1 anti-sense primer, 5'-GAGGACGAGGAGGGCTCTGA-3', and Flag-SOCS1 probe, 5'-

56FAM-CGCACCCAGCTGGC AGCCGACATT-3BHQ-1/-3'; IFN-γ sense primer, 5'-GATATCTCGAGGAACTGGCAAAA-3', 5'- IFN-γ anti-sense primer 5'-CTACAAAGAGTCTGAGGTAGAAAGAGATAAT-3', and IFN-γ probe 5'-FAM-TGGTGACATGAAAATCCTGCAGAGCCA-BHQ1-3'; GAPDH sense primer 5'-CTCAACTACATGGTCTACATGTTCCA-3'; GAPDH anti-sense primer 5'-CCATTCTCGGCCTTGACTGT-3', and GAPDH probe, 5'-5TxRd-XN/TGACTCCACTCACGGCAAATTCAACG-3BHQ-2-3' (Integrated DNA Technologies, Inc.). The reactions were performed using a BioRad I-cycler Real-Time PCR unit, under the following conditions: 1 cycle at 95ºC for 3 min, 40 cycles at [95ºC for 30 s and 60ºC for 30 s] (Bio-Rad Laboratories). The mRNA levels of Flag-SOCS1 and IFN-γ were normalized to the expression levels of GAPDH based on threshold cycles (Flag-SOCS1/GAPDH and IFN-γ/GAPDH ratios) (Lin et al., 2005).

Western Blot and Immunoprecipitation

Total lysates from brain and spleen of several *PLP/SOCS1* mice and wild-type mice were obtained by tissue homogenization in RIPA buffer (Santa Cruz Biotechnology, Santa Cruz, CA). After incubation on ice for 15 min, lysates were centrifuged at 14,000 rpm for 30 min and the supernatants collected. Protein samples (50μg) were electrophoresed on 15% SDS-polyacrylamide gels, transferred to PVDF membranes (Trans-blot SD apparatus, Bio-Rad Laboratories), incubated overnight with mouse anti-Flag antibody (M2, diluted to 1:1000) (Sigma-Aldrich, St. Louis, MO), and detected with ECL Western blot detection reagents (Amersham Biosciences, Piscataway, NJ). Flag protein (Sigma-Aldrich), a polymer of the Flag oligopeptide, was used as a positive control for the reaction.

Immunoprecipitation was performed with an immunoprecipitation kit (Roche Molecular Biochemicals, Indianapolis, IN) by incubating the protein extracts from the brain and spleen of *PLP/SOCS1* and wild-type mice with anti-Flag antibody (M2) for 4 hrs at 4˚C, followed by overnight incubation with protein A/C agarose at 4ºC. The immune complexes were collected by centrifugation at 14,000 rpm for 20S and the protein was separated from protein A/C agarose with kit-supplied reagents. Western blot of the immunoprecipitated protein was performed as described above.

Immunohistochemistry

Animals were anesthetized with 0.01 ml/g of 2.5% Avertin (Sigma-Aldrich) administered intraperitoneally and perfused with saline followed by 2% paraformaldehyde for 10 min. Brains were removed, postfixed for 1hr with 2% paraformaldehyde, cryopreserved with 30% sucrose for 48 h, prepared as frozen blocks (OCT compound, Sacura, Torrance, CA), and sectioned at a thickness of 7μm at −20ºC (Leica CM1800 cryostat, Leica Microsystems). Prior to immunostaining, the sections were treated with 0.1% Triton X-100 (Sigma-Aldrich) for 10 min and incubated with 10% bovine serum albumin (Sigma-Aldrich) or goat serum (Invitrogen) for 30 min. Indirect immunostaining was performed by sequential incubation with primary antibodies (for 2 h at room temperature or overnight at 4ºC) and FITC-conjugated or Cy3-congugated secondary antibodies (for 30 min). All of the following primary and secondary antibodies used in the study were commercially available: mouse and rabbit anti-Flag antibody (dilution, 1:100; Sigma-Aldrich), mouse anti-CC1 antibody (dilution, 1:20; Oncogene), mouse MHC class I antibody (dilution, 1:100; Chemicon International, Temecula, CA), mouse anti-PLP, proteolipid protein, antibody (dilution, 1:100;

Chemicon International), mouse and rabbit anti-SOCS1 antibody (dilution, 1:100; Santa Cruz Biotechnology, Santa Cruz, CA), rabbit anti-Stat1 antibody (dilution, 1:100; Santa Cruz Biotecnology), anti-mouse or anti-rabbit FITC-conjugated secondary antibody (dilution, 1:100; Jackson Immunoresearch, Bar Harbor, ME), and anti-mouse or anti-rabbit Cy3-congugated antibody (dilution, 1:500; Jackson Immunoresearch). The immunostained sections were mounted using Vectorshield mounting medium containing DAPI nuclear stain (Vector Laboratories, Burlingame, CA) and examined using a fluorescent microscope (Axoplan; Carl Zeiss Microimaging).

Oligodendrocyte cell density was assessed digitally using Axiovision software, at postnatal day 21, as previously described (Lin et al., 2005). The brains were sectioned sagittally through the corpus callosum dividing the brain in two symmetrical halves. Ten frozen sections from each half were prepared at 7μm thickness, and numbered in the sequence of their preparation. The brains of three animals per study group were prepared in this fashion. Following the CC1 immunostaining the corresponding area of corpus callosum of each section was digitally selected and the corresponding total area obtained. CC1 cell counting was performed manually within the selected areas of each section, and the number of CC1 positive cells per square area (mm^2) calculated. The results were presented as mean±SD of CC1 (+) cells/ mm^2 with n=3 animals per study group.

Electron Microscopy

Mice selected for electron microscopy studies were perfused with 4% paraformaladehyde and 2.5% glutaraldehyde. Brains were harvested, and white matter structures were sectioned using a stereotype microscope (Wild M3C; Wild AG, Heebrugg, Switzerland). The tissue

was further postfixed in osmium tetroxide and embedded in freshly prepared Epoxy resin (Epon-812; Electron Microscope Sciences, Fort Washington, PA) for 48 hrs at 60ºC. The resin blocks were sectioned at 90nm using Leica Ultracut ultramicrotome (Leica Microsystems) and stained with 5% uracyl acetate and 2.5% lead citrate. Utrastructure of the tissue samples was examined using the Tecnai-F30 transmission electron microscope (FEI Company, Hillsboro, OR).

Myelination patterns of the examined animals were assessed at postnatal day 21 by calculating the percent unmyelinated axons and ratio of the axon/fiber diameters (G ratio) with Image J software (National Institutes of Health, Bethesda, MD) as previously described (Lin at al., 2005). The brains were sectioned sagittally through the corpus callosum dividing the brain in two symmetrical halves. Approximately $2mm^3$ samples from the genu and the splenum of both halves of corpus callosum were obtained using a stereotype microscope (Wild M3C, Heebrugg, Switzerland). The orientation of the specimen in the resin blocks yielding axonal crosssections (well seen myelin rings) was chosen, and established by toluedine blue staining of a few sample sections. The resin blocks with the chosen orientation were processed for electron microscope examination. Randomly selected areas were examined and ten representative pictures from both genu and corpus callosum were obtained at 12000X magnification. The number of unmyelinated axons was assessed by manual counting of axons that lacked myelin and were encircled solely by their own plasma membrane. All unmyelinated axons present in the representative images were counted, and their percentage calculated by examining a total of five hundred axons per tissue sample. The G ratio (axonal diameter/fiber diameter ratio) of myelinated axons was assessed by digitally selecting the area encircled by the inner and outer surfaces of the myelin sheath,

obtaining the axonal (inner) and the fiber (outer) diameters, and dividing their corresponding values (axonal diameter/fiber diameter ratio). The brains of three animals per group were examined, and the G ratios of a total of 150 nerve fibers from both genu and splenum were examined. The results were presented as mean±SD of G ratio and percent unmyelinataed axons with n=3 animals per study group.

Mixed Primary Oligodendrocyte Cultures and Stat1 Translocation Assay

Mixed primary oligodendrocyte cultures were prepared as previously described (Baerwald et al., 2000). Briefly, brain tissue was harvested from 2-3-day-old newborn pups of PLP*/SOCS1* and C57Bl/6J matings. Because the litters contained transgenic and wild-type pups, the brain of each animal was processed individually, cultured separately, and later genotype matched. Each brain was digested separately using 0.25% trypsin and 10μg/ml of DNAaseI (Invitrogen) in Dulbecco's modified Eagle's medium (DMEM) for 20 min at 37ºC, and cells were cultured on separate poly-D-lysine-coated 75-mm^2 flasks (Sigma-Aldrich). The cultures were maintained with 10% fetal bovine serum DMEM at 37ºC with 5% CO_2 for 12 days, and then switched to a defined medium containing 5μl/ml of insulin, 50μg/ml of transferrin, 30nM of selenium, 10nM of biotin, 10nM of progesterone, 15nM of T3, 0.1% bovine serum albumin, and 1% ampicillin-streptomycin (Sigma-Aldrich). On the fifth day of differentiation, the cultures were treated with 100U/mL of IFN-γ (Calbiochem, San Diego, CA) for 30 min. Dual immunostaining for anti-PLP and anti-Stat1 antibodies, and DAPI nuclear staining were performed as described above. The Stat1 nuclear translocation assay was performed in six separate culture preparations. One hundred PLP positive cells were

manually counted in both wild-type and *PLP/SOCS1* cultures. The results were presented as mean±SD percent cells positive for Stat1 nuclear translocation.

Statistical analysis

All data were generated from 3 independent experiments. Means, standard deviations, and *p*-values were calculated using Average, Stdev, and Anova in Microsoft Excel (Microsoft, Redmond, WA). A statistically significant difference was defined as a *p*-value of < 0.05.

RESULTS:

Characterization of the PLP/SOCS1 Transgenic Mouse Line

The PLP/SOCS1 transgenic mice, which were generated as described in the Material and Methods section, were designed to express Flag epitope-tagged SOCS1 in myelinating cells (Fig. 1A). These mice exhibit no phenotypic abnormalities, breed and produce transgenic progeny in a Mendelian fashion, and live a normal life span. Histological evaluation, including electron microscopy, performed at different time points up to 1 year of age revealed no significant differences in the myelination patterns or the number, density, or morphology of oligodendrocytes (see below) between transgenic and wild-type littermates.

Expression of the PLP/SOCS1 transgene was characterized at postnatal day 21using several methods. Northern blot analysis with a SOCS1 cDNA hybridization probe revealed a band of increased intensity in RNA samples from the brains of transgenic mice relative to control brain samples but not from other tissues (Fig. 1B). Real-time PCR analysis with transgene-specific primers revealed the highest concentrations of transgene-derived SOCS1 mRNA in brain, spinal cord, and sciatic nerve, with significantly lower levels in other organs

including heart, thymus, spleen, and liver (Fig. 1C). Transgene expression appeared to be stable up to 12 months of age (data not shown).

Western blot analysis, using an antibody to the Flag tag, revealed a 19-kD band corresponding to the expected size of SOCS1 in the *PLP/SOCS1* brain lysates, but not in wild-type brain lysates or *PLP/SOCS1* spleen lysates (Fig. 1D). To further confirm Flag-SOCS1 protein expression, we performed immunoprecipitation with the anti-Flag antibody, which again detected a 19-kD positive band in the *PLP/SOCS1* brain immunoprecipitates, but not in the wild-type brain or *PLP/SOCS1* spleen immunoprecipitates (Fig. 1E).

Indirect immunostaining of wild-type and *PLP/SOCS1* brains with both anti-SOCS1 and anti-Flag antibodies also demonstrated expression of the transgene (Fig. 1F-I). We detected both anti-Flag and anti-SOCS1 immunopositivity only in *PLP/SOCS1* brains.

To localize the expression of Flag-SOCS1 in the CNS, we performed dual immunostaining of wild-type and *PLP/SOCS1* brain tissue with the anti-Flag antibody and either anti-PLP antibody, a marker for myelin, or anti-CC1 antibody, a marker for the oligodendrocyte cell body. We found a strong colocalization between anti-PLP and anti-Flag antibodies, as well as between anti-CC1 and anti-Flag antibodies (data not shown), suggesting that Flag-SOCS1 was localized to the white matter and oligodendrocytes (Fig. 2). Non-colocalizing immunopositivity for anti-Flag, anti-PLP or anti-CC1 antibodies was not detected.

We were also able to detect the expression of Flag-SOCS1 in primary mixed oligodendrocyte cultures established from transgenic animals by dual immunostaining with anti-PLP and anti-Flag antibodies (Fig. 3). Expression of Flag-SOCS1 was detected only in cultures from *PLP/SOCS1* animals and only in cells expressing PLP. Virtually all PLP-positive cells were also positive for Flag-SOCS1. The colocalization between anti-Flag and

anti-PLP immunoreactivity appeared to involve both the cell body and cell processes (Fig. 3F).

Oligodendrocytes from PLP/SOCS1 Mice Exhibited Diminished Responsiveness to IFN-γ

The responsiveness of *PLP/SOCS1* oligodendrocytes to IFN-γ was studied in primary mixed glial cultures. To determine whether expression of transgenic SOCS1 would interfere with the nuclear translocation of the IFN-γ-signaling molecule Stat1, the cell cultures were treated with 100U/mL of IFN-γ for 30 min and immunostained using anti-PLP and anti-Stat1 antibodies along with the DAPI nuclear stain (Fig. 4). Examination of Stat1 subcellular localization in wild-type cultures revealed strong colocalization with DAPI-positive nuclei in all cells, including PLP-positive oligodendrocytes. In contrast, subcellular localization of Stat1 in *PLP/SOCS1* cultures revealed a differential response to IFN-γ. In transgenic PLP-positive oligodendrocytes, Stat1 remained in the cytoplasm and did not colocalize with cell nuclei in the presence of IFN-γ, (Fig. 4E–H). This was in contrast to the response of the surrounding PLP-negative cells, which, similarly to wild-type cells, responded to IFN-γ with Stat1 nuclear translocation. Virtually all PLP positive oligodendrocytes (96±3 cells) in the wild-type cultures responded to IFN-γ stimulation with Stat1 nuclear translocation. In contrast, Stat1 nuclear translocation was detected only in occasional PLP positive oligodendrocytes (6±2 cells) following IFN-γ stimulation ($p<0.05$).

We next characterized the responsiveness of PLP/SOCS1 oligodendrocytes to IFN-γ in vivo using the induction of major histocompatibilty complex class I (MHC class I) molecule expression as an indication of IFN-γ sensitivity. The capacity of SOCS1 to inhibit IFN-γ–mediated induction of MHC class I molecule was examined in a double-transgenic system.

MBP/IFN-γ (line 172) single-transgenic mice, which express a low level of IFN-γ in the CNS (Gao et al., 2000), were mated to *PLP/SOCS1* mice, and the single and double transgenic progeny were examined for differences in MHC class I molecule expression (Figure 5). MHC class I molecule expression was neither detectable in control wild-type mice nor *PLP/SOSC1* mice (Fig. 5A–D). Consistent with previous reports, *MBP/IFN-γ* mice exhibited upregulated expression of the MHC class I molecule, with diffuse protein localization along the myelin sheath (Fig. 5E, F) (Corbin et al., 1996). The double-transgenic mice (*MBP/IFN-γ* × *PLP/SOCS1*), however, displayed a differential pattern of MHC class I molecule expression (Fig. 5G–J). As shown in Figure 5, oligodendrocytes and myelin positive for Flag-tagged SOCS1 did not express detectable levels of MHC class I molecule, whereas, cells negative for transgene expression, and in close proximity to the SOCS1-positive cells, demonstrated strong immunoreactivity. Similar differential upregulation of MHC class I molecule expression was observed following the direct administration of IFN-γ in the brain of *PLP/SOCS1* mice (data not shown). Together, these data indicate that oligodendrocytes from *PLP/SOCS1* mice display diminished responsiveness to IFN-γ.

PLP/SOCS1 Mice Were Protected against Injurious IFN-γ Effects During Development

Transgenic expression of IFN-γ in the CNS of developing mice results in oligodendrocyte loss and hypomyelination (Corbin et al., 1996; Lin et al 2005). To determine whether SOCS1 expression could protect developing oligodendrocytes from the injurious effects of IFN-γ, we crossed *PLP/SOCS1* mice to three transgenic mouse lines overexpressing IFN-γ in the CNS at different levels: *MBP/IFN-γ* (line 172), *GFAP/tTA* × *TRE/IFN-γ* (lines 184/110) and *GFAP/tTA* × *TRE/IFN-γ* (lines 184/67) and the following three mating systems were

established (detailed in the Material and Methods): *MBP/IFN-γ×PLP/SOCS1* (172 × *PLP/SOCS1*, a double transgenic system) and *GFAP/tTA × TRE/IFN-γ × PLP/SOCS1* (184/110×*PLP/SOCS1* and 184/67×*PLP/SOCS1*, two triple-transgenic systems). The litter (F1 generation) of each mating system was divided into four study groups depending on their genotype: wild-type/single transgenic controls, mice expressing IFN-γ only, mice expressing SOCS1 only and mice expressing both IFN-γ and SOCS1. A total of 40 animals per mating system (10 animals per each study group) were collected and examined clinically and histologically at postnatal day 21.

Phenotypic comparisons of littermates were performed from birth to postnatal day 21 and evaluation consisted of behavioral observation and challenged ladder walking to elicit tremor. *MBP/IFN-γ* (line 172) mice express low levels of IFN-γ in the CNS and displayed no behavioral abnormalities, in accordance with findings reported elsewhere (Corbin et al., 1996). Mice from the F1 generation of the *MBP/IFN-γ×PLP/SOCS1* (172 × *PLP/SOCS1)* mating system similarly displayed no behavioral abnormalities regardless of genotype. Double-transgenic *GFAP/tTA × TRE/IFN-γ* (lines 184/110) and *GFAP/tTA × TRE/IFN-γ* (lines184/67) mice display mild to moderate tremor that appears during the second postnatal week and peaks by 21 days of age (Lin et al., 2004; 2005). Mice from the F1 generation of the *GFAP/tTA × TRE/IFN-γ × PLP/SOCS1* mating systems exhibited tremor, the incidence of which was dependent on genotype (Table 1). The phenotypes of wild-type mice and single-transgenic mice (*GFAP/tTA* [184], *TRE/IFN-γ* [67 and 110], and *PLP/SOCS1*) were clinically normal. The tremoring phenotype, which varied in severity, was identified in almost all double-transgenic *GFAP/tTA × TRE/IFN-γ* mice overexpressing IFN-γ: 80% (8/10) of 184/110 mice and 100% (10/10) of 184/67 mice. Triple-transgenic *GFAP/tTA* ×

TRE/IFN-γ × *PLP/SOCS1* mice overexpressing both IFN-γ and SOCS1 appeared to be protected**,** because only 10% (1/10) of 184/110 × *PLP/SOCS1* mice, and 30% (3/10) of 184/67 × *PLP/SOCS1* mice developed tremor.

The clinically examined littermates of all three transgenic mating systems were further evaluated for histological abnormalities at postnatal day 21. Three animals per study group from each mating system were examined histologically for oligodendrocyte and myelin abnormalities. Brain tissue was obtained from each animal at the time of sacrifice (prior to the fixating perfusion) and total RNA isolated. The possibility that SOCS1 expression affected the expression of the IFN-γ transgene was examined in all three transgenic mating systems using quantitative PCR (Q-PCR) (Fig. 6A). IFN-γ expression was detected in *MBP/IFN-γ* single-transgenic and *MBP/IFN-γ* × *PLP/SOCS1* double-transgenic littermates of the 172×*PLP/SOCS1* transgenic system, in *GFAP/tTA* × *TRE/IFN-γ* double-transgenic and *GFAP/tTA* × *TRE/IFN-γ* × *PLP/SOCS1* triple-transgenic littermates of the184/110 × *PLP/SOCS* transgenic system, and in *GFAP/tTA* × *TRE/IFN-γ* double-transgenic and *GFAP/tTA* ×*TRE/IFN-γ* × *PLP/SOCS1* triple-transgenic littermates of the 184/67 × *PLP/SOC1* transgenic system. Two characteristics of IFN-γ expression were observed. First, the three mating systems differed in their expression levels; *MBP/IFN-γ* × *PLP/SOCS1* (172 × PLP/SOCS1) expressed the lowest, and *GFAP/tTA* × *TRE/IFN-γ* × *PLP/SOCS1* (184/67 × *PLP/SOC1*) expressed the highest IFN-γ levels. Secondly, the littermates of the same mating system, expressing IFN-γ only or both IFN-γ and SOCS1, did not differ in their expression levels. We found no detectible levels of IFN-γ in the wild-type, the *GFAP/tTA* and *TRE/IFN-γ* single-transgenic, and the *PLP/SOCS1* littermates (Fig. 6A).

The cerebra of three animals per study group from all transgenic mating systems were processed for immunohistochemical analysis with the CC1 antibody to determine oligodendrocyte density (Fig. 6B and Fig. 7). The *MBP/IFN-γ* mice expressed the lowest levels of IFN-γ in the CNS compared to *GFAP/tTA ×TRE/IFN-γ* mice, and displayed no significant abnormalities in CC1-positive cell density, in accordance with results reported previously (Gao et al., 2000). We found no statistically significant difference in the oligodendrocyte density among mice from the F1 generation of the *MBP/IFN-γ × PLP/SOCS1* (172×*PLP/*SOCS1) mating system. In the triple-transgenic systems (*GFAP/tTA × TRE/ IFN-γ × PLP/SOCS1*), we found that the oligodendrocyte density in mice from the F1 generation differed depending on genotype (Fig. 6B and Fig. 7). Wild-type mice and the single-transgenic mice *(PLP/SOCS1, GFAP/tTA,* and *TRE/IFN-γ)* had comparable oligodendrocyte densities. We found severe dose-dependent oligodendocyte loss in the *GFAP/tTA × TRE/IFN-γ* mice overexpressing IFN-γ, compared with the wild-type and single-transgenic littermates: approximately 20% of oligodendrocytes were lost in 184/110 mice (from 146±6 CC1 (+) cells/mm^2 in the wild-type mice to 115±8 CC1 (+) cells/mm^2 in the IFN-γ mice), and approximately 40% were lost in 184/67 mice (from 144±5 CC1 (+) cells/mm^2 in the wild-type mice to 79±9 CC1 (+) cells/mm^2 in the IFN-γ overexpressing mice). In contrast, *GFAP/tTA × TRE/IFN-γ × PLP/SOCS1* triple-transgenic littermates that overexpressed both IFN-γ and SOCS1 lost statistically significantly fewer oligodendrocytes compared with mice overexpressing IFN-γ only: approximately 8% of oligodendrocytes were lost in 184/110 × *PLP/SOCS1* mice (from 141±6 CC1 (+) cells/mm^2 in the *PLP/SOCS1* mice to 129±6 CC1 (+) cells/mm^2 in the IFN-γ and SOCS1 overexpressing mice), and approximately 15% were lost in 184/67 × *PLP/SOCS1* mice (from 142±5 CC1 (+) cells/mm^2

in the *PLP/SOCS1* mice to 112±7 CC1 (+) cells/mm^2 in the IFN-γ and SOCS1 overexpressing mice) (Fig. 6B and Fig. 7).

Myelination patterns in the harvested cerebra were further evaluated with electron microscopy, and the level of myelination was assessed by calculating the G ratio (axon diameter/fiber diameter ratio) and the percentage of unmyelinating axons (Fig. 6C and D, and Fig. 8). We found no statistically significant difference in G ratios among wild-type, the *MBP/IFN-γ* (172) and *PLP/SOCS1* single-transgenic, and double transgenic littermates from the *MBP/IFN-γ* × *PLP/SOCS1* (172 × *PLP/SOCS1*) mating system. In the triple-transgenic systems (*GFAP/tTA* × *TRE/IFN-γ* × *PLP/SOCS1*), significant differences in G ratios were found among the F1 generation mice, depending on genotype (Fig. 6C and Fig. 7). G ratios among the wild-type and the *GFAP/tTA*, *TRE/IFN-γ*, and *PLP/SOCS1* single-transgenic littermates were similar. IFN-γ-overexpressing *GFAP/tTA* × *TRE/IFN-γ* littermates displayed significantly increased G ratios (±SD) indicating hypomyelination (defined as a G ratio >0.8): 0.89 ± 0.02 for 184/110 mice and 0.95 ± 0.04 for the 184/67 mice (Fig. 6C). In contrast, their triple-transgenic (*GFAP/tTA* × *TRE/IFN-γ* × *PLP/SOCS1*) littermates overexpressing both IFN-γ and SOCS1 had significantly lower G ratios (±SD): 0.75 ± 0.03 (within the normal range) for 184/110 × *PLP/SOCS1* mice, and 0.82 ± 0.08 for 184/67 × *PLP/SOCS1* mice (Fig. 6C and Fig. 8).

The myelin abnormalities were further quantified by determining the percentage of unmyelinated axons in the various transgenic genotypes (Fig. 6D). We found no significant difference in the percentage of unmyelinated axons (less than 9%) among the F1 generation littermates of the *MBP/IFN-γ* × *PLP/SOCS1* (172× *PLP/SOCS1*) double-transgenic system, regardless of genotype (Fig. 6D). In the triple-transgenic *GFAP/tTA* × *TRE/IFN-γ* ×

PLP/SOCS1 systems, however, the distribution of unmyelinated axons differed depending on genotype (Fig. 6D). There was a significantly increased percentage of unmyelinated axons in IFN-γ-overexpressing *GFAP/tTA* × *TRE/IFN-γ* littermates compared to wild-type and single-transgenic control mice: 41% ±6 in 184/110 mice and 57%±7 in 184/67 mice. In contrast, triple-transgenic *GFAP/tTA* × *TRE/IFN-γ* × *PLP/SOCS1* overexpressing both IFN-γ and SOCS1 had a significantly lower percentage of unmyelinated axons compared with mice overexpressing IFN-γ alone: only 13%±3 for 184/110× *PLP/SOCS1* mice and 17%±4.5 for 184/67× *PLP/SOCS1* mice (Fig. 6D). Together, these data demonstrate that oligodendroglial expression of SOCS1 protects mice from the clinical and morphological consequences of IFN-γ expression in the CNS during development.

DISCUSSION:

The presence of the T-cell-derived cytokine IFN-γ within the CNS is believed to play a critical role in the pathogenesis of immune-mediated demyelinating disorders (Panitch et al, 1987; Galbinski et al., 1999; Tran et al., 2000; Vartanian et al., 1996; Horwitz et al. 1997; Steinman, 2001)**.** Nevertheless, the cellular target of the cytokine's effect remains unresolved. In this report we describe the generation of transgenic mice in which the oligodendrocytes display a significantly reduced capacity to respond to IFN-γ. These mice are protected from the injurious effect of ectopic expression of IFN-γ within the CNS, suggesting that a direct deleterious effect of IFN-γ on oligodendrocytes contributes to immune-mediated disease pathogenesis. As discussed below, the work described has significant clinical implications.

Transgenic animals that ectopically express IFN-γ in the CNS during postnatal development are hypomyelinated and contain reduced numbers of oligodendrocytes (Corbin et al., 1996; LeFerla et al., 2000; Lin et al., 2005). Moreover, the induction of IFN-γ expression in the CNS following demyelinating insults results in reduced oligodendroglial repopulation of the demyelinating lesions and impaired remyelination (Lin et al., in press). Previously reported data from our laboratory suggests that the presence of IFN-γ in the CNS activates an ER stress response in oligodendrocytes, which contributes to the observed pathological effects (Lin et al, 2005; in press). It is unclear, however, if the injurious effect of IFN-γ on oligdodendrocytes is a result of a direct action or whether it represents a secondary effect, possibly through microglial activation.

IFN-γ has also been shown to have harmful effects on oligodendrocytes and their progenitors in vitro. There is considerable evidence to suggest that at least part of the injurious effect of this cytokine is mediated through the activation of microglial cells. IFN-γ-treated microglia release cytotoxic agents, including nitric oxide and tumor necrosis factor alpha, that are known to be damaging to oligodendrocytes (Merrill et al., 1991, 1993, Loughlin et al., 1997). Studies using purified oligodendrocytes in vitro, however, suggest that the cytokine may have a direct, harmful effect on oligodendrocytes (Torres et al., 1995; Agresti et al., 1996; Baerwald et al., 1998; Andrews et al., 1998; Lin et al., 2005). IFN-γ has been shown to inhibit cell cycle exit of oligodendroglial progenitor cells, which may predispose these cells to apoptotic death (Chew et al., 2005). Additionally, IFN-γ has been shown to be a very powerful apoptotic-inducing agent for developing oligodendrocytes (Baerwald et al., 1998, 2000; Lin et al., 2005). Oligodendrocytes that have been allowed to differentiate in vitro to the point of expressing mature oligodendroglial markers are less

sensitive to the presence of the cytokine, although they do eventually succumb to necrosis (Baerwald et al., 1998).

In an effort to differentiate direct versus indirect effects of IFN-γ on oligodendrocytes in vivo, we generated transgenic mice that exhibited diminished oligodendrocyte-specific responsiveness to IFN-γ. Transgenic mice expressing either the dominant-negative form of IFN-γ receptor subunit 1 (IFNGR1) or the suppressor of cytokine signaling 1 (SOCS1) have been previously described (Flodstrom et al., 2001; Gonzales at al., 2005, Hindinger et al., 2005). Overexpression of the dominant-negative form of IFNGR1 resulted in accelerated degradation of wild-type IFNGR1 and elimination of the IFN-γ cellular binding sites (Dighe et al., 1994). SOCS1 is an intracellular protein that blocks IFN-γ mediated Stat1 activation (i.e., phosphorylation) by Jak kinases (Starr et al., 1997; Song and Shuai 1998; Sakamoto et al., 2000; Yasukawa et al., 2000; Kubo et al., 2003; Stark et al., 1998; Levy and Darnell, 2002). Mouse mutants with a targeted null mutation in the SOCS1 gene exhibit abnormal hypersensitivity to IFN-γ and die of multi-organ failure in the presence of normal levels of the cytokine (Starr et al., 1998; Alexander et al., 1999; Bullen et al., 2001). Moreover, forced expression of SOCS1 has been shown to result in a state of IFN-γ unresponsiveness in a variety of cell types (Tunley et al., 2001, 2002; Chong et al., 2001, Federici et al., 2002; Flodstom et al., 2001).

The *PLP/SOCS1* mice exhibited no phenotypic or histological abnormalities, indicating that Stat1 activation is not required for normal oligodendrocyte development, even though its involvement in growth factor signaling has been suggested in vitro (Dell'Albani et al., 1998). Our finding is supported by the phenotypic characteristics of Stat1 (−/−) knockout mice, which displayed no oligodendrocyte or myelin abnormalities but do have significantly

impaired IFN-γ cellular responses (Meraz et al., 1996). Thus, it appears that Stat1 activation plays a differential role in oligodendorocyte injury and development.

Functional examination of the *PLP/SOCS1* mice further demonstrated a diminished oligodendrocyte-specific responsiveness to IFN-γ, including inhibition of Stat1 activation (i.e. phosphorylation) and nuclear translocation, and MHC class I molecule upregulation. When crossed with transgenic mice overexpressing IFN-γ in the CNS, *PLP/SOCS1* mice were protected from the deleterious clinical and histological effects of IFN-γ. IFN-γ-overexpressing transgenic mice that also carried the PLP/SOCS1 transgene displayed significant oligodendrocyte and myelin preservation and lower prevalence of tremor compared to IFN-γ expressing mice without the PLP/SOCS1 transgene. Results of our study thereby indicate that IFN-γ exerts a direct injurious effect on developing oligodendrocytes.

Overexpression of SOCS1 provided cellular protection to oligodendrocytes, suggesting that inhibition of IFN-γ signaling results in reduced cellular effects. Wild-type oligodendrocytes, as reported by others and also observed by us, express nearly undetectable amounts of SOCS1 under normal, and even inflammatory conditions, and have much lower SOCS1 expression compared to the surrounding glial and inflammatory cells (Polizzotto et al., 2000; Wang and Campbell 2002; Maier et al., 2002). Such low constitutive expression may limit the oligodendrocyte capacity for effective downregulation of IFN-γ/Jak/Stat1 signaling, resulting in enhanced IFN-γ cellular effects. The rescuing effect of SOCS1 overexpression in oligodendrocytes that was observed in our experimental system supports this possibility.

Circumstantial and experimental evidence suggests that IFN-γ plays a deleterious role in the immune-mediated demyelinating disorder multiple sclerosis (Popko et al., 1997,

Steinman 2001). IFN-γ is found in demyelinated lesions and its levels in cerebrospinal fluid correlate with disease severity (Vartanian et al., 1996; Calabresi et al., 1998; Becher et al., 1999; Moldovan et al., 2003). Administration of IFN-γ to MS patients exacerbated the disease, and neutralizing antibodies to IFN-γ have been shown to delay disease progression (Panitch et al, 1987; Skurkovich et al., 2001). Diminishing the local effect of IFN-γ, perhaps through the targeted expression of SOCS1 by oligodendrocytes, could prove to be therapeutically beneficial. Remyelinating oligodendrocytes after a demyelinating insult are more sensitive to the presence of IFN-γ (Lin et al., in press); therefore, such protection might be particularly useful for the promotion of remyelination.

Stem cell therapy is rapidly gaining interest as a potential therapeutic approach to demyelinating disorders such as multiple sclerosis and adrenoleukodystrophy (review in Keirstead 2005). The success of such an approach would appear to be limited, however, in immune-mediated demyelinating disorders, since the harsh environment created by the inflammatory response would remain. Perhaps stem cells engineered to be resistant to the harmful cytokines present in the extracellular milieu of the breached CNS would stand a better chance of surviving and accomplishing remyelination. It is, therefore, of therapeutic interest to identify signaling pathways that play differential roles in oligodendrocyte injury and development. Our results describing inhibition of IFN-γ–mediated oligodendrocyte injury without induction of any observable oligodendrocyte or myelin abnormalities provide support for such an approach.

In summary, we have demonstrated that the forced expression of SOCS1 in oligodendrocytes of transgenic mice protects against the deleterious effects of IFN-γ on oligodendrocytes and the process of myelination. Our results strongly indicate that the

deleterious effect of IFN-γ on myelinating oligodendrocytes is due, at least in part, to a direct adverse effect on these cells. Moreover, our work suggests that forced expression of SOCS1 in oligodendrocytes might provide protection against the harsh environment in immune-mediated demyelinating disorders.

Figure 1. Expression of Flag-SOCS1. A. PLP/SOCS1 construct contains 2.4Kb of the PLP 5' flanking DNA, exon 1(no ATG), intron 1(diagonally striped boxes), Flag-SOCS1 and SV40 polyA signal sequence. Expression of the PLP/SOCS1 transgene was characterized at postnatal day 21using several methods. B. Northern blot analysis demonstrated Flag-SOCS1 expression in *PLP/SOCS1* brain, lane 2 (T, transgenic brain), compared to wild-type brain, lane 1 (WT, wild-type brain). C. Q-PCR analysis with transgene-specific primers revealed the highest concentrations of transgene-derived SOCS1 mRNA were in the brain, spinal cord, and sciatic nerve, with significantly lower levels in other organs. D. Western blot. E. Immunoprecipitation. Both demonstrated a single 19 KD Flag positive band, the expected molecular weight of SOCS1, only in the lanes loaded with brain samples from *PLP/SOCS1* mice (brain fSOCS1+). Flag protein was used as a positive control for the antibody reaction; 15% SDS-PAGE, anti-Flag (M2) antibody. Immunostaining with anti-SOCS1/FITC (F, H), and anti-Flag/FITC antibodies (G, I) demonstrated positive signal only in *PLP/SOCS1* (H, I, green), and not in the wild-type mouse samples (F, G). Cell nuclei were contrastained with ethidium bromide (F-I, red). Coronal section sections of thalamic fiber; Bar=20µm.

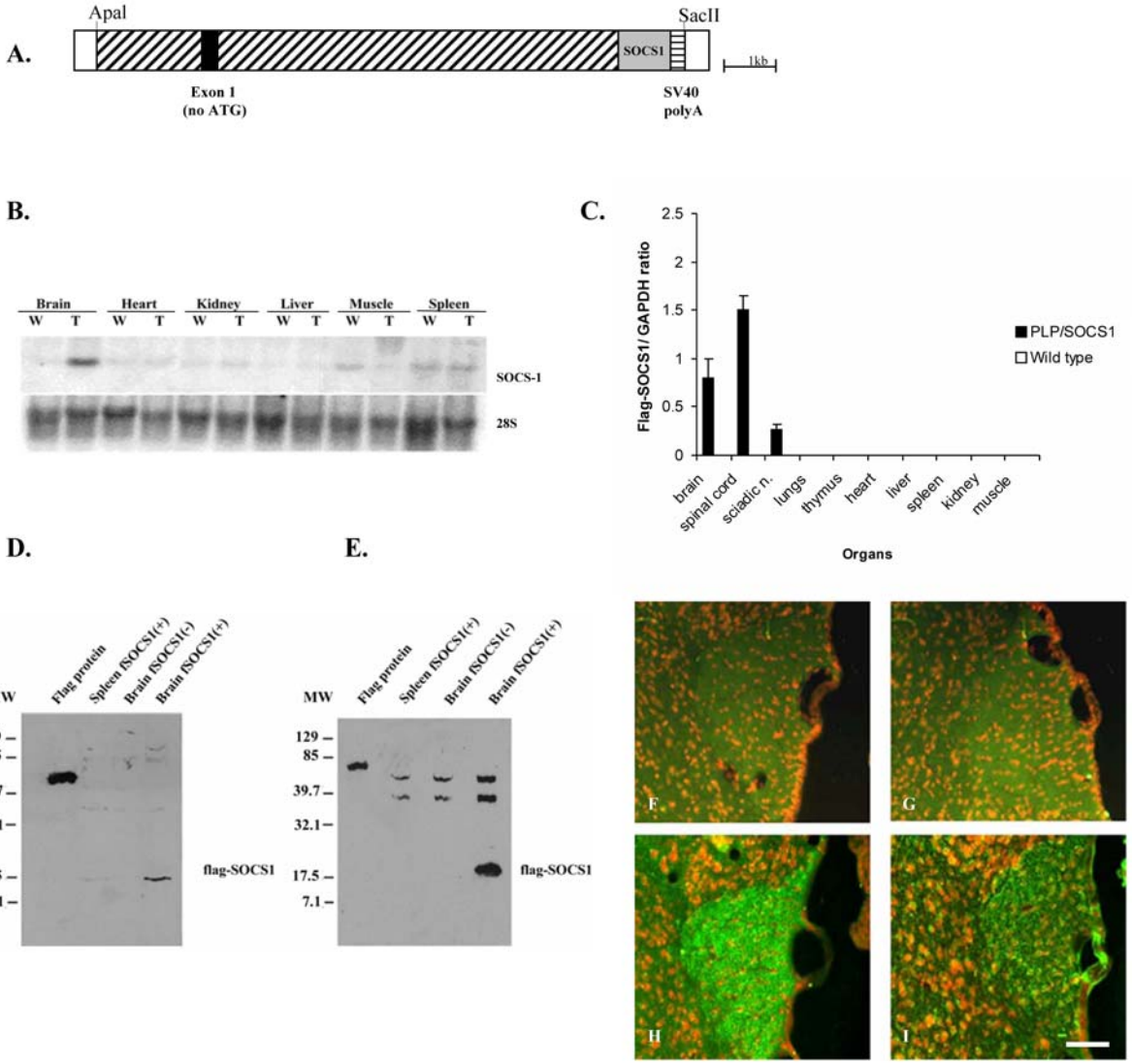

Figure 2. Colocalization of Flag-SOCS1 and PLP in vivo. Dual immunostaining of wild-type (A-C, top row) and *PLP/SOCS1* (D-F, bottom row) cerebellar tissue, harvested at postnatal day 21, was performed using anti-PLP/Cy3 (A, D, red) and anti-Flag/FITC (B, E, green) antibodies, and DAPI nuclear stain (C, F, blue). PLP positive structures of the wild-type samples (A, red) demonstrated no immunopositivity for anti-Flag (B) and no signal colocalization was established (C). In contrast, PLP positive structures of *PLP/SOCS1* samples (D) expressed Flag-SOCS1 (E), and strong co-localization between the anti-PLP and anti-Flag immunopositivity was detected (F, yellow color signifies co-localization). Sagittal sections of cerebellum; Bar=20μm.

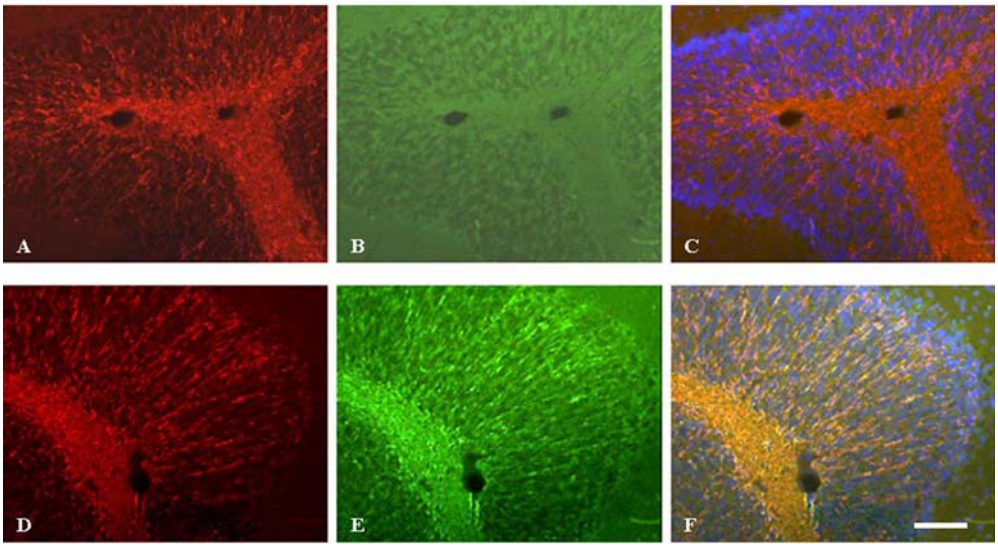

Figure 3. **Colocalization of flag-SOCS1 and PLP in vitro.** Dual immunostaining of wild-type (A-C, top row) and *PLP/SOCS1* (D-F, bottom row) mixed primary oligodendrocyte cultures was performed using anti-PLP/FITC (A, D, green) and anti-Flag/Cy3 (B, E, red) antibodies. PLP positive oligodendrocytes in the wild-type culture (A) demonstrated no immunopositivity for anti-Flag (B), and no signal colocalization was established (C). In contrast, PLP positive oligodendrocytes (D) in the *PLP/SOCS1* cultures expressed Flag-SOCS1 (E), and strong colocalization between anti-PLP and anti-Flag signals was detected (F). Flag-SOCS1 appeared to be localized in the cell body (large arrows) and cell processes (small arrows) of oligodendrocytes. Bar=20μm.

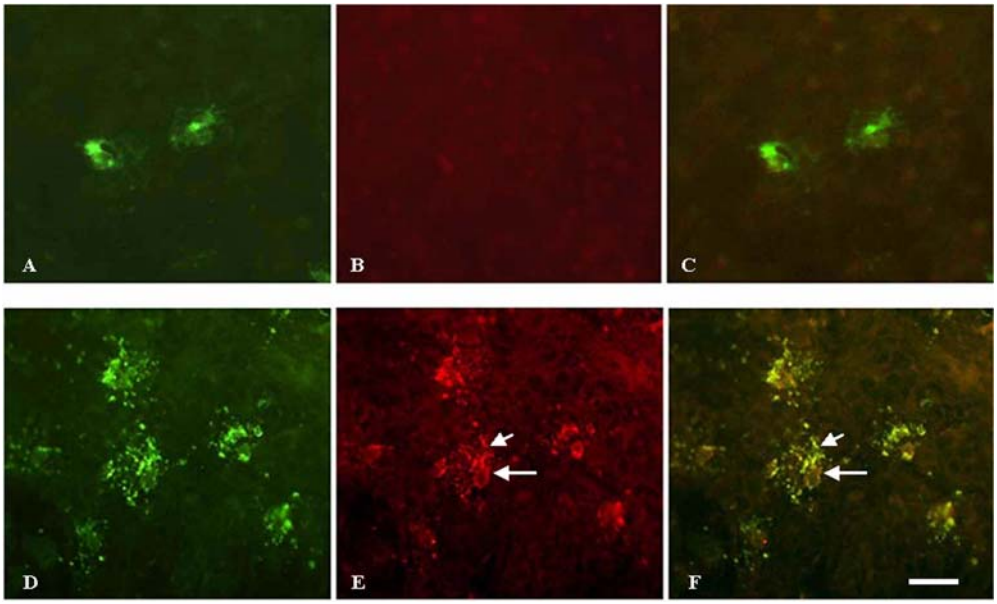

Figure 4. Differential inhibition of Stat1 nuclear translocation. Mixed primary oligodendrocyte cultures from wild-type (A-D; top row) and *PLP/SOCS1* (E-H; bottom row) mice were stimulated with 100U IFN-γ for 30 min, and dual immunostainings using anti-PLP/Cy3 (A, E; red), anti-Stat1 (B, F; green), and DAPI nuclear stain (D, H; blue) were performed and the fluorescent signals digitally overlayed (C and G, overlay between PLP/Cy3 and Stat1/FITC signals; D and H, overlay between PLP/Cy3, Stat1/FITC and DAPI signals). In the wild-type cultures, Stat1 was colocalized with DAPI stained nuclei of all cells, including the PLP positive oligodendrocytes (small arrows) (B, D, colocalization between Stat1 and DAPI). In the *PLP/SOCS1* cultures, Stat1 was colocalized with DAPI positive nuclei of the PLP negative cells (small arrows), but not of the PLP positive oligodendrocytes (large arrows). Stat1 in the PLP positive oligodendrocytes did not colocalize with DAPI stained nuclei, but remained in the cytoplasm (large arrows) (F, H). Bar=10μm.

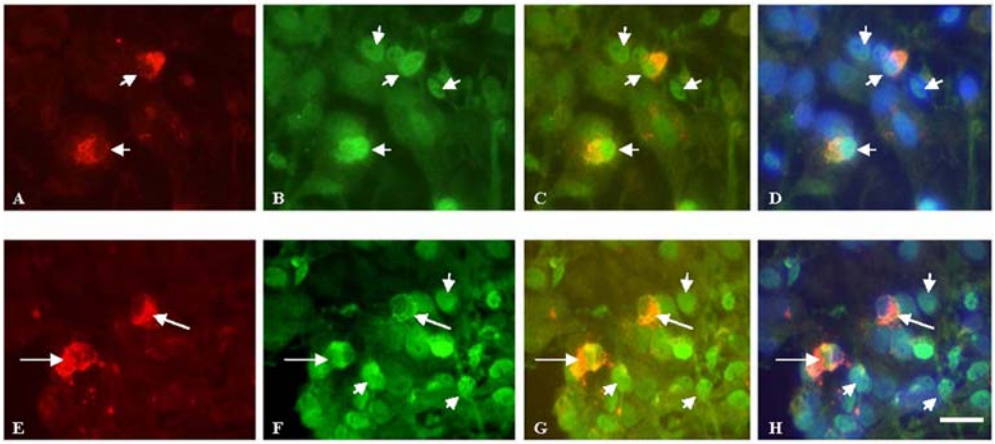

Figure 5. Differential expression of MHC class I molecule in *MBP/IFN-γ* x *PLP/SOCS1* mice. Wild-type (A, B), *PLP/SOCS1* (C, D), *MBP/IFN-γ* (E, F) and *MBP/IFN-γ* × *PLP/SOCS1* (G, H, I, J) mouse brains, harvested at postnatal day 21, were dual immunostained with anti-MHC class I/FITC (A, C, E, G, I; green) and anti-flag/Cy3 (B, D, F, H, J; red) antibodies, and DAPI nuclear stain (J, blue). Wild-type samples (A, B) were double negative. *PLP/SOCS1* samples were negative for MHC class I molecule (C) and positive for Flag (D). *MBP/IFN-γ* samples were single positive for MHC class I molecule (E) and negative for Flag (F). Double transgenic *MBP/IFN-γ* × *PLP/SOCS1* samples were double positive for MHC class I molecule (G) and Flag (H). Higher magnification of *MBP/IFN-γ* × *PLP/SOCS1* samples (outlined square in G, H) revealed differential distribution of the immunopositivity (I, J); MHC class I positive cells (large arrows) were negative for Flag, whereas Flag positive cells (small arrows) were negative for MHC class I molecules. Sagittal sections of corpus callosum; Bar=20μm (A-H); Bar=10μm (I, J).

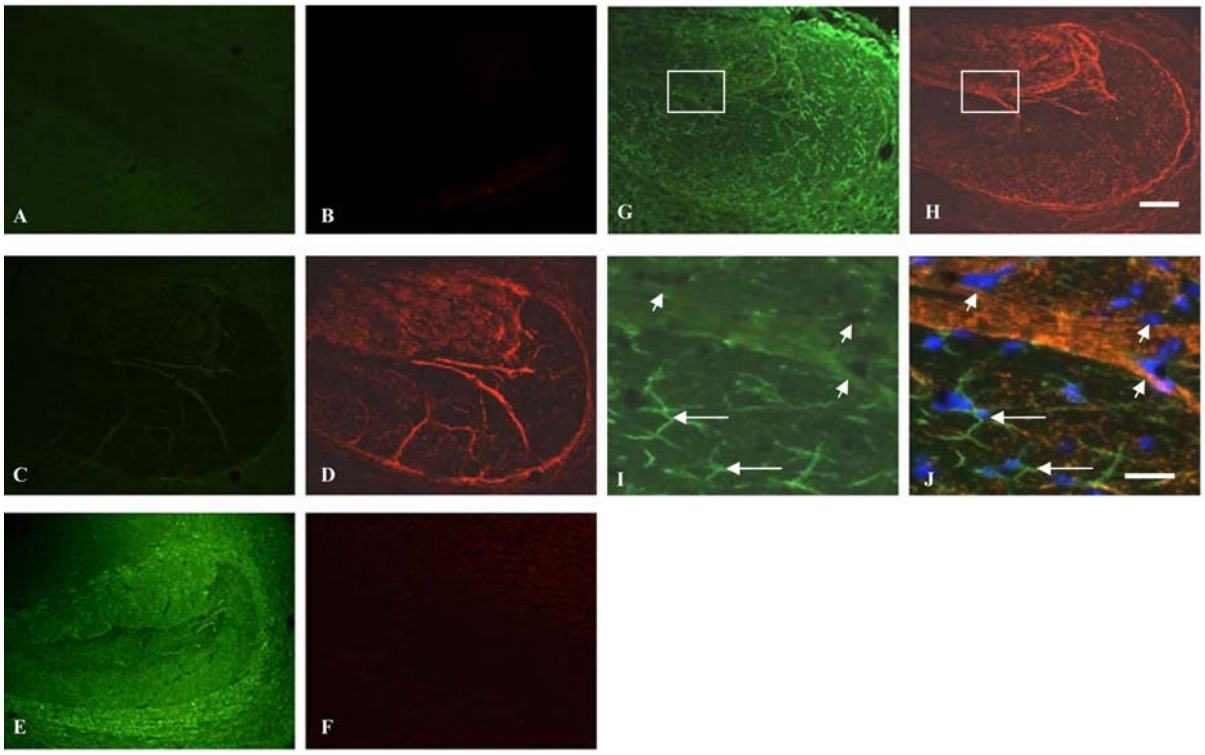

Figure 6. SOCS1-mediated protection of oligodendrocytes and myelin. The IFN-γ expression (A), oligodendrocyte density (CC1 cells/mm^2) (B), G ratio (C), and percent unmyelinated axons (D) were examined among littermates of three transgenic systems: 172×*PLP/SOCS1,* 184/110×*PLP/SOCS1* and 184/67×*PLP/SOCS1* at postnatal day 21 (see Results for complete description). The relative amount of IFN-γ expression differed among the systems but no statistical difference was found in the levels of expression between littermates from the same transgenic system overexpressing either IFN-γ only (IFN-γ) or both IFN-γ and SOCS1 (IFN-γ×SOCS1) (A). The IFN-γ overexpressing littermates (IFN-γ) displayed significant dose-dependent oligodendrocyte cell loss (B) and hypomyelination (C, D) as compared to the wild type, single transgenic control (wt/cntrl) and *PLP/SOCS1* littermates (* $p<0.05$, n=3 per study animals). The triple transgenic littermates expressing both IFN-γ and SOCS1 (IFN-γ×SOCS1) displayed significant oligodendrocyte (B) and myelin preservation (C, D) as compared to those overexpressing IFN-γ only (IFN-γ) (** $p<0.05$, n=3 animals per study group).

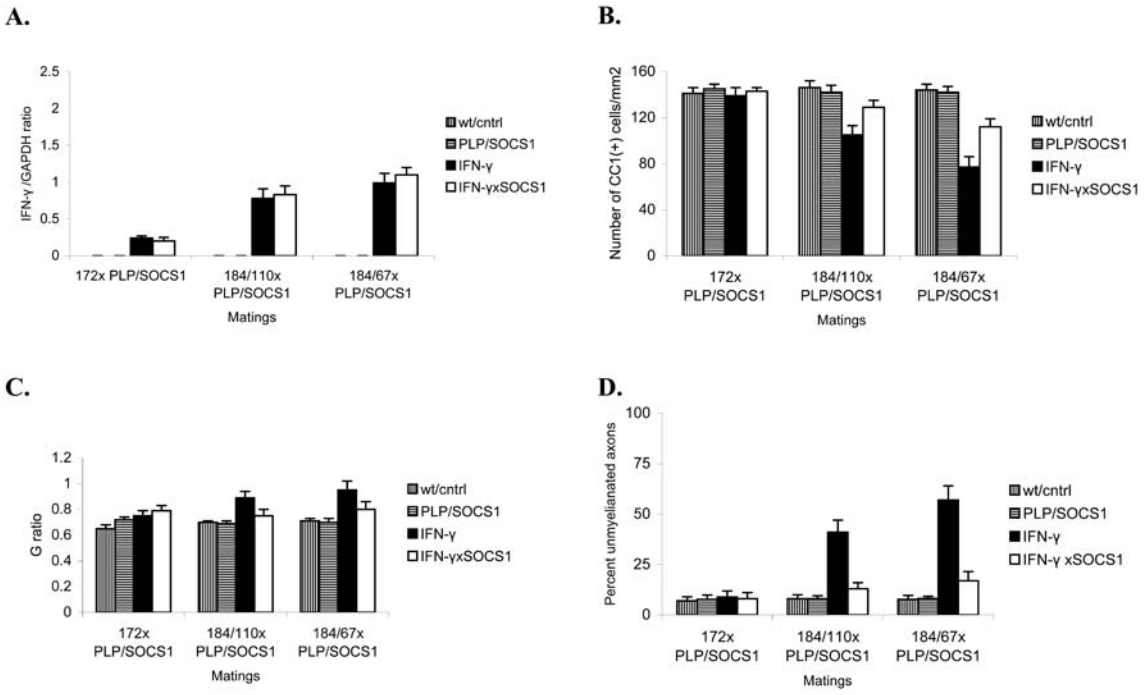

Figure 7. SOCS1-mediated oligodendrocyte protection. Representative images of the quanitated areas from *GFAP/tTA* × *TRE/IFN-γ* × *PLP/SOCS1* (184/67× *PLP/SOCS1*) mice at postnatal day 21: A. Wild-type; B. *PLP/SOCS1*; C. 184/67 and D; 184/67 ×*PLP/SOCS1*. Immmunostaining with CC1/Cy3 (red) and DAPI nuclear stain (blue). Sagittal sections of corpus callosum; Bar=20μm. Note the loss of CC1 positivity in the sample from an IFN-γ-overexpressing mouse (C) compared to the samples from wild-type (A) and *PLP/SOCS1* mice (B), and the significant oligodendrocyte preservation in the sample from a mouse overexpressing both IFN-γ and SOCS1 (D).

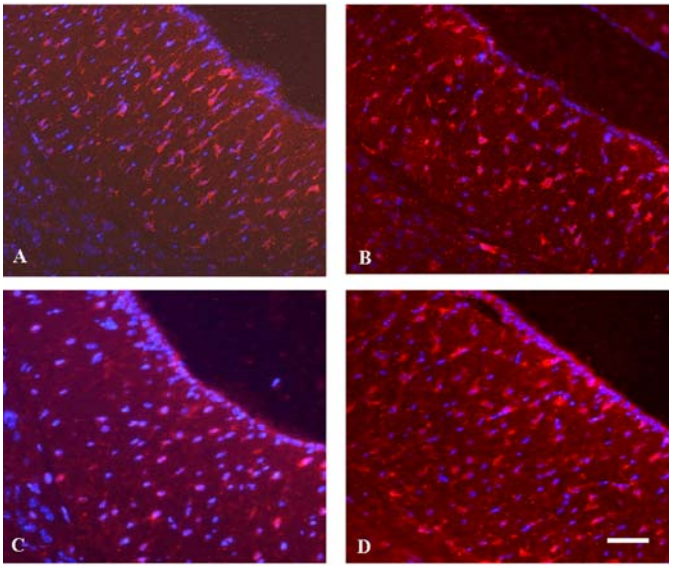

Figure 8. SOCS1-mediated myelin protection. Representative images of the quanitated areas from *GFAP/tTA × TRE/IFN-γ × PLP/SOCS1* (184/67×*PLP/SOCS1*) mice at postnatal day 21: A. Wild-type; B. *PLP/SOCS1*; C. 184/67 and D; 184/67×*PLP/SOCS1*. Electron micrographs of corpus callosum; Bar=500nm. Note the hypomyelination in the sample from an IFN-γ-overexpressing mouse (C) compared to the samples from wild type (A) and PLP/SOCS1 mice (B), and the significant myelin preservation in the sample from a mouse overexpressing both IFN-γ and SOCS1 (D).

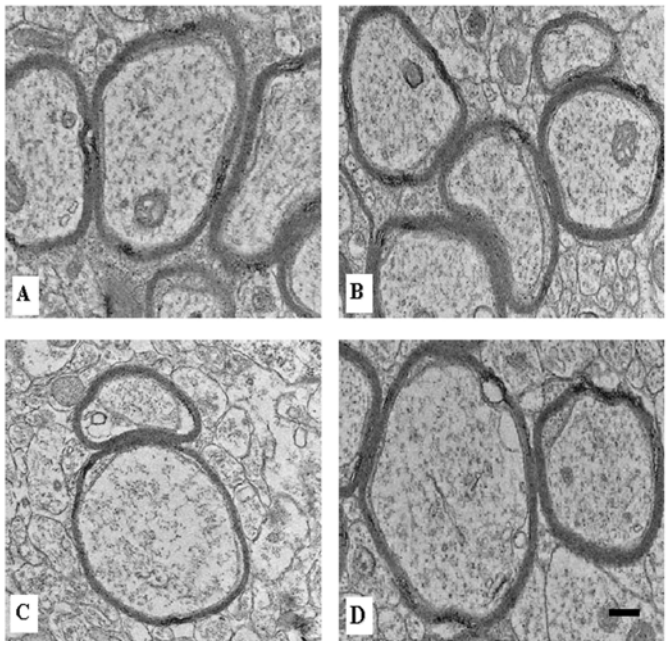

Table1. Incidence of tremor among the transgenic littermates

	Wild-type/controls	SOCS1	IFN-γ	IFN-γ×SOCS1
172×PLP/SOCS1	0%	0%	0%	0%
184/110×PLP/SOCS1	0%	0%	80% (8/10)	10% (1/10)
184/67×PLP/SOCS1	0%	0%	100% (10/10)	30% (3/10)

Littermates from three transgenic mating systems, 172 × *PLP/SOCS1*, 184/110×*PLP/SOCS1* and 184/67×*PLP/SOCS1* were stratified according to their genotype into four groups: Wild-type/control mice, mice expressing SOCS1 only, mice expressing IFN-γ only and mice expressing both IFN-γ and SOCS1. Ten mice per group were clinically followed during the first three postnatal weeks and the incidence of tremor recorded.

REFERENCES:

Agresti C, Bernardo A, Del Russo N, Marziali G, Battistini A, Aloisi F, Levi G, Coccia E (1998) Synergistic stimulation of MHC class I and IRF-1 gene expression by IFN-gamma and TNF-alpha in oligodendrocytes. Eur J Neurosci 10:2975-2983.

Agresti C, D'Urso D, Levi G (1996) Reversible inhibitory effects of interferon-gamma and tumor necrosis factor-alpha on oligodendroglial lineage cell proliferation and differentiation in vitro. Eur J Neurosci 8:1106-11016.

Alexander W. Starr R, Fenner J, Scott C, Handman E, Spring N, Corbin J, Cornish, A Darwishe R, Owczarek C, Kay T, Nicola N, Hertzog P, Metcalf D, Hilton D (1999) Socs1 is a critical inhibitor of interferon-gamma signaling and prevents the potentially fatal action of this cytokine. Cell 98:598-608.

Andrews T, Zhang P, Bhat N (1998) TNFalpha potentiates IFN gamma-induced cell death in oligodendrocyte progenitors. J Neurosci Res 54:574-583.

Becher B, Giacomini PS, Pelletier D, McCrea E, Prat A, Antel J (1999) Interferon-gamma secretion by peripheral blood T-cell subsets in multiple sclerosis: correlation with disease phase and interferon-beta therapy. Ann Neurol 45:247-250.

Baerwald K, Popko B (1998) Developing and mature oligodendrocytes respond differently to the immune cytokine interferon-gamma. J Neurosci Res 52:230-239.

Baerwald K, Corbin J, Popko B (2000) Major histocompatibility complex heavy chain accumulation in the endoplasmic reticulum of oligodendrocytes results in myelin abnormalities. J Neurosci Res 15:160-169.

Billiau A (1996) Interferon-γ: biology and role in pathogenesis. Adv Immunol 62:61-130.

Bullen D, Darwich R, Metcalf D, Handman E, Alexander W (2001) Neutralization of interferon-gamma in neonatal SOCS1-/- mice prevents fatty degeneration of the liver but not subsequent inflammatory disease. Immunol 2001, 104:92-98.

Calabresi P, Tranquill L, McFarland H, Cowan E (1998) Cytokine gene expression in cells derived from CSF of multiple sclerosis patients. J Neuroimmunol 14:198-205.

Chew L., King W., Kenedy A, Gallo V (2005) Interferon-gamma inhibits cell cycle exit in differentiating oligodendrocyte progenitor cells. Glia 52:127-143.

Chong M, Thomas H, Kay T (2001) gamma-Interferon signaling in pancreatic beta-cells is persistent but can be terminated by overexpression of suppressor of cytokine signaling-1. Diabetes 50:2744-2751.

Corbin J, Kelly D, Rath E, Baerwald K, Suzuki K, Popko B (1996) Targeted CNS expression of interferon-gamma in transgenic mice leads to hypomyelination, reactive gliosis, and abnormal cerebellar development. Mol Cell Neurosci 7:354-370.

Dell'Albani, Kahn M, Cole R, Condorelli D, Giuffrida-Stela A, Vellis J (1998) Oligodendrocyte survival factors, PFGF-AA and CNTF, activate Jak/STAT signaling pathways. J Neurosci Res 54:191-205.

Dighe A, Richards E, Old L, Schreiber R (1994) Enhanced in vivo growth and resistance to rejection of tumor cells expressing dominant negative IFN gamma receptors. Immunity 1:447-456.

Doerflinger N, Macklin W, Popko B (2003) Inducible site-specific recombination in myelinating cells. Genesis 35:63-72.

Einhauer A, Jungbauer A (2001) The flag peptide, a versatile fusion tag for the purification of recombinant proteins. J Biochem Biophys 49:455-465.

Federici M, Giustiziri M, Scarponi C, Girolomini G, Albanesi C (2002) Impaired IFN-gamma-dependent inflammatory response in human keratinocytes overexpressing the suppressor of cytokine signaling 1. J Immunol 169:434-443.

Flodstrom M, Maday A, Balakrisha D, Cleary M, Yoshimura A, Starvetnick N (2001) Target cell defense prevents development of diabetes after viral infection. Nat Immunol 3: 373-382.

Fuss B, Mallon B, Phan T, Ohlemeyer C, Kirchoff F, Nishiyama A, Macklin W (2000) Purification and analysis of in vivo-differentiated oligodendrocytes expressing the green fluorescent protein. Dev Biol 218:259-274.

Gao X, Gilling T, Ye P, D'Ercole J, Matsushima G, Popko B (2000) Interferon-γ protects against cuprizone-induced demyelination. Mol Cell Neurosci 16:338-349.

Gao X, Kemper A, Popko B (1999) Advanced transgenic and gene-targeting approachs. Neurochem Res 24:1183-1190.

Glabinski A, Kranowski M, Han Y, Owens T, Ransohoff R (1999) Chemokine expression in GRO mice (lacking interferon-gamma) with experimental autoimmune encephalomyelitis. J Neurovirol 51:95-101.

Gonzales J, Bergmann C, Fuss B, Hinton D, Kangas C, Macklin W, Stohlman S (2005) Expression of dominant negative IFN-γ receptor on mouse oligodendrocytes. Glia 51:22-34.

Hindinger C, Gonzalez J, Bergmann C, Fuss B, Hinton D, Atkinson R, Macklin W, Stohlman S (2005) Astrocyte expression of a dominant-negative interferon-gamma receptor. J Neurosci Res 82:20-31.

Horwitz M, Evans C, McGavern D, Rodriguez M, Oldstone M (1997) Primary demyelination in transgenic mice expressing interferon-gamma. Nature Med 3:1037-1041.

Keirstead H (2005) Stem cells for the treatment of myelin loss. Trends Neurosci 28:677-683.

Kubo M, Hanada T, Yoshimura A (2003) Suppressors of cytokine signaling and immunity. Nature Immunol 4:1169-1176.

LaFerla F, Sugarman M, Lane T, Leissring M (2000) Regional dysplasia in transgenic mice with astrocyte-derived expression of interferon-gamma. J Mol Neurosci 15:45-59.

Levy D, Darnell J (2002) Stats: transcriptional control and biological impact. Nature Rev Mol Cell Biol 651-662.

Lin W, Kemper A, McCarthy K, Pytel P Wang J, Campbell I, Utset M, Popko B (2004) Interferon-gamma induces medullobalstoma in the developing cerebellum. J Neurosci 24:10074-10083.

Lin W, Harding H, Ron D, Popko B (2005) Endoplasmic reticulum stress modulates the response of myelinating oligodendrocytes to the immune cytokine interferon-gamma. J Cell Biol 169:603-612.

Lin W, Kemper A, Dupree J, Harding H, Ron D, Popko B. Interferon-gamma inhibits central nervous system remyelination through a process modulated by endoplasmic reticulum stress. Brain (in press).

Loughlin A, Copelman C, Hall A, Armer T, Young B, Landon D, Cuzner M (1997) Myelination and remyelination of aggregate rat brain cell cultures enriched with macrophages. J Neurosci Res 47:384-392.

Maier J, Kincaid C, Pagenstecher A, Campbell I (2002) Regulation of signal transducer and activator of transcription and suppressor of cytokine-signaling gene expression in the brain of mice with astrocyte-targeted production of interleukin-12 or experimental autoimmune encephalomyelitis. Am J Pathol 160:271-288.

Merrill J, Zimmerman R (1991) Natural and induced cytotoxicity of oligodendrocytes by microglia is inhibitable by TGF beta. Glia 4:327-31.

Merrill J, Ignarro L, Sherman M, Melinek J, Lane T (1993) Microglial cytotoxicity of oligodendrocytes is mediated through nitric oxide. J Immunol 151:2132-2141.

Meraz M, White J, Sheehan K, Bach E, Roding S, Dighe A, Kaplan D, Riley J, Greenlund A, Campbell D, Caver-Moore K, Dubois R, Clark R, Aguet M, Schreiber R (1996) Targeted disruption of Stat1 gene in mice reveals unexpected physiological specificity in the Jak/STAT signaling pathway. Cell 84:431-442.

Moldovan IR, Rudick RA, Cotleur AC, Born SE, Lee JC, Karafa MT, Pelfrey CM (2003) Interferon gamma responses to myelin peptides in multiple sclerosis correlate with a new clinical measure of disease progression. J Neuroimmunol 141:132-140.

Panitch N, Hirsch R, Haley A, Johnson K (1987) Exacerbations of multiple sclerosis in patients treated with gamma interferon. Lancet 1:893-895.

Polizzotto M, Bartlett P, Turnley A (2000) Expression of "suppressor of cytokine signaling" (SOCS) genes in the developing and adult mouse nervous system. J Compar Neurol 423:348-358.

Popko B, Corbin J, Baerwald K, Dupree J, Garcia A (1997) The effects of interferon-gamma on the central nervous system. Mol Neurobiol 14:19-35.

Pouly S, Becher B, Blain M, Antel J (2000) Interferon-gamma modulates human oligodendrocyte susceptibility to Fas-mediated injury. J Neuropathol Exp Neurol 59:280-286.

Sakamoto H, Kinjyo I, Yoshimura A (2000) The janus kinase inhibitor, Jab/SOCS1, is an interferon-gamma inducible gene and determines sensitivity to interferons. Leuk Lymphoma 38:49-58.

Skurkovich S, Boiko A, Beliaeva I, Buglak I, Alekseeva T, Smirnova T, Kulakova O, Tchechonin V, Gurova O, Deomina T, Favarova O, Skurkovith B, Gusev E (2001) Randomized study of antibodies to IFN-gamma and TNF-alpha in secondary progressive multiple sclerosis. Mult Scler 7:277-284.

Song M, Shuai K (1998) The suppressor of cytokine signaling (SOCS1) and SOCS3 but not SOCS2 proteins inhibit interferon-mediated antiviral and antiproliferative activities. J Biol Chem 25:35056-35062.

Steiman L (2001) Blockade of gamma interferon might be beneficial in MS. Mult Scler 7:275-276.

Stark G, Kerr I, Williams B, Silverman R, Schreiber R (1998) How cells respond to interferons. Ann Rev Biochem 67:257-264.

Starr R, Wilson T, Viney E, Murray L, Rayner J, Jenkins J, Brendan J, Gonda T, Alexander W, Metcalf D, Nicola N, Hilton J (1997) A family of cytokine inducible inhibitors of signaling. Nature 387:917-921.

Starr R. Donald M, Elefanty A, Brysha, M, Wilson T, Nicola A, Hilton D, Alexander W (1998) Liver degeneration and lymphoid deficiency in mice lacking suppressor of cytokine signaling-1. PNAS USA 95:14395:14999.

Torres C, Aranguez I, Rubio N (1995) Expression of interferon-gamma receptors on murine oligodendrocytes and its regulation by cytokines and mitogens. Immunology 86:250-255.

Tran E, Prince E, Owens T (2000) IFN-gamma shapes invasion of the central nervous system via regulation of chemokines. J Immunol 164:2759-2768.

Traugott U (2001) Evidence for immunopathogenesis. In: Handbook of Multiple sclerosis (Cook S, ed) 3d edition, pp163-192, New York: Marcel Deker.

Tunley A, Starr R, Bartlett P (2002) Failure of sensory neurons to express class I MHC is due to differential SOCS1 expression. J Neuroimmunol 123:35-40.

Tunley A, Starr R, Bartlett P (2001) SOCS1 regulates interferon-gamma mediated sensory neuron survival. Neuroreport 16:3443-3445.

Vartanian T, Li Y, Zhao M, Stefansson K (1995) Interferon-γ induced oligodendrocyte cell death: implications for the pathogenesis of multiple sclerosis. Mol Med, 1:732-743.

Wang J, Campbell I (2002) Cytokine signaling in the brain: putting a SOCS in it? J Neurosci Res 67:423-427.

Wight P, Duchala C, Readhead C, Macklin W (1993) A myelin proteolipid protein-lacZ fusion protein is developmentally regulated and targeted to the myelin membrane in transgenic mice. J Cell Biol 123:443-454.

Yasukawa H, Sasaki A, Yoshimura A (2000) Negative regulation of signaling pathways. Annu Rev Immunol 18:143-164.

REFERENCES

Affymetrix. 1999 [cited 2002]. Microarray Suite User Guide, Version 4. [Internet]. Available from: www.affymetrix.com/support/technical/manuals.affx

Affymetrix. 2001 [cited 2002]. Microarray Suite User Guide, Version 5. [Internet]. Available from: www.affymetrix.com/support/technical/manuals.affx

Agresti C, D'Urso, D, Levi G. 1996. Reversible inhibitory effects of interferon-gamma and tumour necrosis factor-α on oligodendroglial lineage cell proliferation and differentiation *in vitro*. Eur J Neuroscience 8:1106-1116.

Andrews T, Zhang P, Bhat NR. 1998. TNFalpha potentiates IFNgamma-induced cell death in oligodendrocyte progenitors. J Neurosci Res 54:574-583.

Arnett HA, Fancy SP, Alberta JA, Zhao C, Plant SR, Kaing S, et al. 2004. bHLH transcription factor Olig1 is required to repair demyelinated lesions in the CNS. Science 306: 2111-2115.

Awatramani R, Scherer S, Grinspan J, Collarini E, Skoff R, O'Hagan D, Garbern J, Kamholz J. 1997. Evidence that the homeodomain protein Gtx is involved in the regulation of oligodendrocyte myelination. J Neurosci 17(17):6657-6668.

Badea T, Niculescu F, Soane L, Shin M, Rus, H. 1998. Molecular cloning and characterization of RGC-32, a novel gene induced by complement activation in oligodendrocytes. J Biol Chem 273(41):26977-26981.

Baerwald KD, Popko B. 1998. Developing and mature oligodendrocytes respond differently to the immune cytokine interferon-gamma. J Neurosci Res 52:230-239.

Baerwald KD, Corbin JG, Popko B. 2000. Major histocompatibility complex heavy chain accumulation in the endoplasmic reticulum of oligodendrocytes results in myelin abnormalities. J Neurosci Res 59:160-169.

Balabanov R, Popko B. 2005. Myelin repair: developmental myelination redux? [Review]. Nat Neurosci 8:262-264.

Banninger G, Reich NC. 2004. STAT2 nuclear trafficking. J Biol Chem 279(38):39199-39206.

Barres BA. 1999. Neuron-Glial Interactions. In: Cowen WM, Jessel TM, Zipursky SL. Molecular and Cellular Approaches to Neural Development. Oxford, Oxford University Press.

Barres BA, Hart IK, Coles HS, Burne JF, Voyvodic JT, Richardson WD, Raff MC. 1992. Cell death and control of cell survival in the oligodendrocyte lineage. Cell 70:31-46.

Barres BA, Lazar MA, Raff MC. 1994. A novel role for thyroid hormone, glucocorticoids and retinoic acid in timing oligodendrocyte development. Development 120:1097-1108.

Barres BA, Schmid R, Sendnter M, Raff MC. 1993. Multiple extracellular signals are required for long-term oligodendrocyte survival. Development 118:283-275.

Ben-Hur T, Rogister B, Murray K, Rougon G, Dubois-Dalcq M. 1998. Growth and fate of PSA-NCAM^{+} precursors of the postnatal brain. J Neurosci 18:5777-5788.

Benveniste E, Benos D. 1995. TNF-α and IFN-gamma-mediated signal transduction pathways: effects on glial cell expression and functions. FASEB J 9:1577-1584.

Bergsteindottir K, Brennan A, Jessen KR, Mirsky R. 1992. In the presence of dexamethasone, gamma interferon induces rat oligodendrocytes to express major histocompatibility complex class II molecules. PNAS 89(19):9054-9058.

Billiau A, Heremans H, Vandekerckhove F, Dijkmans R, Sobis H, Meulepas E, Carton H. 1988. Enhancement of experimental allergic encephalomyelitis in mice by antibodies against IFN-gamma. J Immunol 140:1506-1510.

Boehm UTK, Groot M, Howard JC. 1997. Cellular responses to interferon-gamma. Annu Rev. Immunol. 15:749-795.

Bostrom K, Zebboudj A, Yao Y, Lin T, Torres A. 2004. Matrix GLA protein stimulates VEGF expression through increased transforming growth factor-beta1 activity in endothelial cells. J Biol Chem 279(51):52904-52913.

Brás A, Martinez-A C, Baixeras E. 1997. B cell receptor cross-linking prevents Fas-mediated cell death by inactivating the IL-1-β-converting enzyme protease and regulating Bcl-2/Bcl-x expression. J Immun 159:3168-3177.

Bronstein JM, Chen K, Tiwari-Woodruff S, Kornblum HI. 2000. Developmental expression of OSP/claudin-11. J Neurosci Res 60(3):284-290.

Calder VL, Wolswijk G, Noble M. 1988. The differentiation of O-2A progenitor cells into oligodendrocytes is associated with a loss of inducibility of Ia antigens. Eur J Immunol 18:1195-1201.

Ciechanover A. 1994. The ubiquitin-proteasome proteolytic pathway. Cell 79:13-21.

Collarini EJ, Kuhn R, Marshall CJ, Monuki ES, Lemke G, Richardson WD. 1992. Down-regulation of the POU transcription factor SCIP is an early event in oligodendrocyte differentiation in vitro. Development 116(1):193-200.

Compston A, Coles A. 2002. Multiple sclerosis. [Review]. Lancet 359:1221-1231.

Connor JR, Menzies SL. 1990. Altered cellular distribution of iron in the central nervous system of myelin deficient rats. Neuroscience 34:265-271.

Connor JR, Pavlick G, Karli D, Menzies SL, Palmer C. 1995. A histochemical study of iron-positive cells in the developing rat brain. J Comp Neurol 355:111-123.

Cooney RN. 2002. Suppressors of cytokine signaling (SOCS): inhibitors of the JAK/STAT pathway. [Review]. Shock. 17(2):83-90.

Corcoran C, Luo X, He Q, Jiang C, Huang Y, Sheikh M. 2005. Genotoxic and endoplasmic reticulum stresses differentially regulate TRB3 expression. Cancer Biol Ther 4(10):1063-1067.

Coux O, Tanaka K, Goldberg A. 1996. Structure and functions of the 20S and 26S proteasomes. Annu Rev Biochem 65:801-847.

Crone C. 1986. The Blood-Brain Barrier; A Modified Tight Epithelium. In: Suckling AJ, Rumsby MG, and Bradbury MWB, editors. Blood-Brain Barrier in Health Disease. UK: Ellis Horwood. p17-40.

Davey GM, Heath WR, Starr R. 2006. SOCS1: a potent and multifaceted regulator of cytokines and cell-mediated inflammation. Tissue Antigens. 67(1):1-9.

De Angelis DA, Braun PE. 1996. Binding of 2',3'-cyclic nucleotide 3'-phosphodiesterase to myelin: an in vitro study. J Neurochem 66(6):2523-2531.

Baron W, Metz B, Bansal R, Hoekstra D, de Vries H. 2000. PDGF and FGF-2 signaling in oligodendrocyte progenitor cells: regulation of proliferation and differentiation by multiple intracellular signaling pathways. Mol Cell Neurosci 15(3):314-29.

Dubois-Dalcq M. 1987. Characterization of a slowly proliferative cell along the oligodendrocyte differentiation pathway. EMBO J 6:2587-2595.

Duong TT, St. Louis J, Gilbert JJ, Finkelman FD, Strejan GH. 1992. Effect of anti-interferon-gamma and anti-interleukin-2 monoclonal antibody treatment on the development of actively and passively induced experimental allergic encephalomyelitis in the SJL/J mouse. J Neuroimmunol 36:105-115.

Eisenbarth GS, Walsh FS, Nirenberg M. 1979. Monoclonal antibody to a plasma membrane antigen of neurons. PNAS 76:4913-4917.

Emoto Y, Manome Y, Meinhardt G, Kisaki H, Kharbanda S, Robertson M, Ghayur T, Wong WW, Kamen R, Weichselbaum R. 1995. Proteolytic activation of protein kinase C delta by an ICE-like protease in apoptotic cells. EMBO J 14(24):6148-6156.

Erne B, Sansano S, Frank M, Schaeren-Wiemers N. 2002. Rafts in adult peripheral nerve myelin contain major structural myelin proteins and myelin and lymphocyte protein (MAL) and CD59 as specific markers. J Neurochem 82(2):550-582.

Espejo C, Penkowa M, Demestre M, Montalban X, Martinez-Caceres EM. 2005. Time-course expression of CNS inflammatory, neurodegenerative tissue repair markers and metallothioneins during experimental autoimmune encephalomyelitis. Neuroscience 132(4):1135-1149.

Farkas I, Baranyi L, Ishikawa Y, Okada N, Bohata C, Budai D, Fukuda A, Imai M, Okada H. 2002. CD59 blocks not only the insertion of C9 into MAC but inhibits ion channel formation by homologous C5b-8 as well as C5b-9. J Physiol 539(2):537-545.

Ferber IA, Brocke S, Taylor-Edwards C, Ridgway W, Dinisco C, Steinman L, et al. 1996. Mice with a disrupted IFN-gamma gene are susceptible to the induction of experimental autoimmune encephalomyelitis (EAE). J Immunol 156:5-7.

Francois C, Nguyen-Legros J, Percheron G. 1981. Topographical and cytological localization of iron in rat and monkey brains. Brain Res 215:317-322.

Franklin RJ. 2002. Why does remyelination fail in multiple sclerosis? [Review]. Nat Rev Neurosci 3:705-714.

ffrench-Constant C, Colognato H, Franklin R. 2004. The mysteries of myelin unwrapped. Science 304:688-689.

Fruttiger M, Karlsson L, Hall AC, Abramsson A, Calver AR, Bostrom H, Willets K, Berthold C-H, Heath JK, Betsholtz C, Richardson WD. 1999 Defective oligodendrocyte development and severe hypomyelination in PDGF-A knockout mice. Development 126:457-467.

Fulda S, Debatin KM. 2002. IFNgamma sensitizes for apoptosis by upregulating caspase-8 expression through the Stat1 pathway. Oncogene 21(15):2295-2308.

Gao X, Kemper A, Popko B. 1999. Advanced transgenic and gene-targeting approaches. Neurochem Res 24:1181-1188.

Gao X, Gillig TA, Ye P, D'Ercole AJ, Matsushima GK, Popko B. 2000. Interferon-gamma protects against cuprizone-induced demyelination. Mol Cell Neurosci 16(4):338-349.

Gilgun-Sherki Y, Melamed E, Offen D. 2004. The role of oxidative stress in pathogenesis of multiple sclerosis: the need for effective antioxidant therapy. J Neurol 251(3):261-268.

Gow A, Friedrich Jr. VL, Lazzarini RA. 1994. Many naturally occurring mutations of myelin proteolipid protein impair its intracellular transport. J Neurosci Res 37:574-583.

Gow A, Lazzarini RA. 1996. A cellular mechanism governing the severity of Pelizaeus-Marzbacher Disease. Nature Gen 13:422-428.

Gow A, Southwood CM, Lazzarini RA. 1998. Disrupted proteolipid protein trafficking results in oligodendrocyte apoptosis in an animal model of Pelizaeus-Merzbacher Disease. J Cell Biol 140:925-934.

Gow A, Southwood CM, Li JS, Pariali M, Riordan GP, Brodie SE, Danias J, Bronstein JM, Kachar B, Lazzarini RA. 1999. CNS myelin and sertoli cell tight junction strands are absent in Osp/claudin-11 null mice. Cell 99(6):649-59.

Graesser D, Mahooti S, Madri J. 2000. Distinct roles for matrix metalloproteinase-2 and alpha4 integrin in autoimmune T cell extravasion and residency in brain parenchyma during experimental autoimmune encephalomyelitis. J Neuroimmunol 109(2):121-131.

Grinspan JB, Stern JL, Pustilnik SM, Pleasure D. 1990. Cerebral white matter contains PDGF-responsive precursors to O2A cells. J Neurosci 10:1866-1873.

Gutowski NJ, Newcombe J, Cuzner ML. 1999. Tenascin-R and C in multiple sclerosis lesions: relevance to extracellular matrix remodeling. Neuropathol Appl Neurobiol 25:207-214.

Harding HP, Zeng H, Zhang Y, Jungries R, Chung P, Plesken H, Sabatini DD, Ron D. 2001. Diabetes mellitus and exocrine pancreatic dysfunction in *PERK*-/- mice reveals a role for translational control in secretory cell survival. Mol Cell 7:1153-1163.

Harding HP, Zhang Y, Ron D. 1999. Protein translation and folding are coupled by an endoplasmic-reticulum-resident kinase. Nature 397:271-274.

Harding HP, Zhang Y, Bertolotti A, Zeng H, Ron D. 2000. *Perk* is essential for translational regulation and cell survival during the unfolded protein response. Mol Cell 5:897-904.

Harroch S, Furtado GC, Brueck W, Rosenbluth J, Lafaille J, Chao M, Buxbaum JD, Schlessinger J. 2002. A critical role for the protein tyrosine phosphatase receptor type Z in functional recovery from demyelinating lesions. Nat Genet 32(3):411-414.

Hershko A, Ciechanover A. 1992. The ubiquitin system for protein degradation. Annu Rev Biochem 61:761-807.

Holz A, Schwab ME. 1997. Developmental expression of the myelin gene MOBP in the rat nervous system. J Neurocytol 26(7):467-477.

Horwitz MS, Evans CF, Klier FG, Oldstone MB. 1999. Detailed in vivo analysis of interferon-gamma induced major histocompatibility complex expression in the central nervous system: astrocytes fail to express major histocompatibility complex class I and II molecules. Lab Invest 79:235-242.

Iijima W, Ohtani H, Nakayama T, Sugawara Y, Sato E, Nagura H, Yoshie O, Sasano T. 2003. Infiltrating CD8+ T cells in oral lichen planus predominantly express CCR5 and CXCR3 and carry respective chemokine ligands RANTES/CCL5 and IP-10/CXCL10 in their cytolytic granules: a potential self-recruiting mechanism. Am J Pathol 163(1):261-268.

Irizarry RA, Bolstad BM, Collin F, Cope LM, Hobbs B, Speed TP. 2003a. Summaries of Affymetrix GeneChip probe level data. Nucleic Acids Res. 31(4)e15:1-8.

Irizarry RA, Hobbs B, Collin F, Beazer-Barclay Y, Antonellis K, Scherf U, Speed T. 2003b. Exploration, normalization, and summaries of high density oligonucleotide array probe level data. Biostatistics 4(2):249-264.

Issazadeh S, Mustafa M, Ljungdahl A, Hojeberg B, Dagerlind A, Elde R, Olsson T. 1995. Interferon-gamma, interleukin 4 and transforming growth factor β in experimental autoimmune encephalomyelitis in Lewis rats: dynamics of cellular mRNA expression in the central nervous system and lymphoid cells. J Neurosci Res 40:579-590.

Jia S, Li Y, Parodo J, Kapus A, Fan L, Rotstein O, Marshall J. 2004. Pre-B cell colony-enhancing factor inhibits neutrophil apoptosis in experimental inflammation and clinical sepsis. J Clin Invest 113(9):1318-1327.

Jin S and Conti M. 2002. Induction of the cyclic nucleotide phosphodiesterase PDE4B is essential for LPS-activated TNF-alpha responses. PNAS USA 99(11):7628-7633.

Johnsson N, Marriott G, Weber K. 1988. p36, the major cytoplasmic substrate of src tyrosine protein kinase, binds to its p11 regulatory subunit via a short amino-terminal amphiphatic helix. EMBO J 7:2435-2442.

Jousse C, Oyadomari S, Novoa I, Lu P, Zhang Y, Harding H, Ron D. 2003. Inhibition of a constitutive translation initiation factor 2α phosphatase, CReP, promotes survival of stressed cells. J Cell Biol 163(4):767-775.

Jurevics H, Largent C, Hostettler J, Sammond DW, Matsushima GK, Kleindienst A, et al. 2002. Alterations in metabolism and gene expression in brain regions during cuprizone-induced demyelination and remyelination. J Neurochem 82:126-136.

Kagawa T, Ikenaka K, Inoue Y, Kuriyama S, Tsujii T, Nakao J, Nakajima K, Aruga J, Okano H, Mikoshiba K. 1994 Glial cell degeneration and hypomyelination caused by overexpression of myelin proteolipid protein gene. Neuron 13:427-442.
Kennedy RE, Archer KJ, Miles MF. 2006. Empirical Validation of the S-Score Algorithm in the Analysis of Gene Expression Data. BMC Bioinformatics 7(1):154 [Epub ahead of print].

Kim HJ, Kim SG. 2002. Alterations in cellular Ca(2+) and free iron pool by sulfur amino acid deprivation: the role of ferritin light chain down-regulation in prooxidant production. Biochem Pharmacol 63(4):647-657.

Kitani T, Okuno S, Fujisawa H. 2003. Growth phase-dependent changes in the subcellular localization of pre-B-cell colony-enhancing factor. FEBS Lett 544(1-3):74-78.

Komoly S, Hudson LD, Webster HD, Bondy CA. 1992. Insulin-like growth factor I gene expression is induced in astrocytes during experimental demyelination. PNAS 89:1894-1898.

Komuro I, Schalling M, Jahn L, Bodmer R, Jenkins NA, Copeland NG, Izumo S. 1993. Gtx: a novel murine homeobox-containing gene, expressed specifically in glial cells of the brain and germ cells of testis, has a transcriptional repressor activity in vitro for a serum-inducible promoter. EMBO J 12(4):1387-1401.

Krebs DL, Hilton DJ. 2000. SOCS: physiological suppressors of cytokine signaling. J Cell Sci. 113(Pt 16):2813-9.

Kumar L, Feske S, Rao A, Geha RS. 2005. A 10-aa-long sequence in SLP-76 upstream of the Gads binding site is essential for T cell development and function. PNAS 102(52):19063-19068.

Kwon M, MacLeod TJ, Zhang Y, Waisman DM. 2005. S100A10, annexin A2, and annexin a2 heterotetramer as candidate plasminogen receptors. Front Biosci 10:300-325.

Lander ES, Weinberg RA. 2000. Genomics: journey to the center of biology. Science 287(5459):1777-1782.

Lee J, Gravel M, Zhang R, Thibault P, Braun P. 2005. Process outgrowth in oligodendrocytes is mediated by CNP, a novel microtubule assembly myelin protein. J Cell Biol 170(4):661-673.

Leegwater PA, Vermeulen G, Konst AA, Naidu S, Mulders J, Visser A, et al. 2001. Subunits of the translation initiation factor eIF2B are mutant in leukoencephalopathy with vanishing white matter. Nat Genet 29:383-388.

Lepej SZ, Rode OD, Jeren T, Vince A, Remenar A, Barsic B. 2005. Increased expression of CXCR3 and CCR5 on memory CD4+ T-cells migrating into the cerebrospinal fluid of patients with neuroborreliosis: the role of CXCL10 and CXCL11. J Neuroimmunol 163(1-2):128-134.

LeVine SM, Macklin WB. 1990. Iron-enriched oligodendrocytes: a reexamination of their spatial distribution. J Neurosci Res 26:508-512.

Li C, Wong W. 2001. Model-based analysis of oligonucleotide arrays: expression index computation and outlier detection. PNAS 98:31-36.

Li Y, Atashi J, Hayes C, Reap E, Hunt S, Popko B. 1995. Morphological and molecular response of the MOCH-1 oligodendrocyte cell line to serum and interferon-gamma: possible implications for demyelinating disorders. J Neurosci Res 40:189-198.

Lin W, Kemper A, Dupree JL, Harding HP, Ron D, Popko B. 2006. Interferon-{gamma} inhibits central nervous system remyelination through a process modulated by endoplasmic reticulum stress. Brain. Feb 27; [Epub ahead of print] .

Lin W, Harding HP, Ron D, Popko B. 2005. ER stress modulates the response of myelinating oligodendrocytes to the immune cytokine interferon-gamma. J Cell Biol 169:603-612.

Lin W, Kemper A, McCarthy KD, Pytel P, Wang JP, Campbell IL, Utset MF, Popko B. 2004. Interferon-γ induced medulloblastoma in the developing cerebellum. J Neurosci 24(45):10074-10083.

Liu Y, Liu W, Song XD, Zuo J. 2005. Effect of GRP75/mthsp70/PBP74/mortalin overexpression on intracellular ATP level, mitochondrial membrane potential and ROS accumulation following glucose deprivation in PC12 cells. Mol Cell Biochem 268(1-2):45-51.

Lu Z, Ku L, Chen Y, Feng Y. 2005. Developmental abnormalities of myelin basic protein expression in fyn knock-out brain reveal a role of fyn in posttranscriptional regulation. J Biol Chem 280(1):389-395.

Ma Y, Hendershot L. 2001. The unfolding tale of the unfolded protein response. [Review]. Cell 107:827-830.

Mahley RW. 1988. Apolipoprotein E: cholesterol transport protein with expanding role in cell biology. Science 240(4852):622-630.

Magnus T, Schreiner B, Korn T, Jack C, Guo H, Antel J, Ifergan I, Chen L, Bischof F, Bar-Or A, Wiendl H. 2005. Microglial expression of the B7 family member B7 homolog 1 confers strong immune inhibition: implications for immune responses and autoimmunity in the CNS. J Neurosci 25(10):2537-2546.

Marg A, Shan Y, Meyer T, Meissner T, Brandenburg M, Vinkemeier U. 2004. Nucleocytoplasmic shuttling by nucleoporins Nup153 and Nup214 and CRM1-dependent nuclear export control the subcellular distribution of latent Stat1. J Cell Biol 165(6):823-833.

Martin R, McFarland HF. 1995. Immunological Aspects of Experimental Allergic Encephalomyelitis and Multiple Sclerosis. Critical Rev. Clinical Lab. Sciences 32(2):121-182.

Martin R, McFarland HF, McFarlin D. 1992. Immunological aspects of demyelinating diseases. Ann Rev Immunol 10:153-187.

Mason JL, Jones JJ, Taniike M, Morell P, Suzuki K, Matsushima GK. 2000. Mature oligodendrocyte apoptosis precedes IGF-1 production and oligodendrocyte progenitor accumulation and differentiation during demyelination/remyelination. J Neurosci Res 61:251-262.

Massa PT, Ozato K, McFarlin DE. 1993. Cell type-specific regulation of major histocompatibility complex (MHC) class I gene expression in astrocytes, oligodendrocytes, and neurons. Glia 8:201-207.

Matsushima GK, Morell P. 2001. The neurotoxicant, cuprizone, as a model to study demyelination and remyelination of the central nervous system. [Review]. Brain Pathol 11:107-116.

Mauch D, Nagler K, Schumacher S, Goritz C, Muller E, Otto A, Pfrieger F. 2001. CNS synaptogenesis promoted by glia-derived cholesterol. Science 294(5545):1354-1357.

McCarron RM, Wang L, Racke MK, McFarlin DE, Spatz M. 1993 Cytokine-regulated adhesion between encephalitogenic T lymphocytes and cerebrovascular endothelial cells. J Neuroimmunol 43:23-30.

McKinnon RD, Dubois-Dalcq M.1996. Cytokines and Growth Factors in the Development and Regeneration of Oligodendrocytes. In: Benveniste RM, Ransohoff EN. Cytokines and the CNS. New York. CRC Press**:** 85-113.

McKinnon RD, Matsui T, Dubois-Dalcq M, Aaronson SA. 1990. FGF modulates the PDGF-driven pathway of oligodendrocyte development. Neuron 5:603-614.

McKinnon RD, Smith C, Behar T, Smith T, Dubois-Dalcq M. 1993. Distinct effects of bFGF and PDGF on oligodendrocyte progenitor cells. Glia 7:245-254.

McMorris FA, Smith TM, Desalvo S, Furlanetto RW. 1986. Insulin-like growth factor 1/somatomedin C: a potent inducer of oligodendrocyte development. PNAS 83:822-826.

Meller R, Stevens S, Minami M, Cameron J, King S, Rosenzweig H, Doyle K, Lessov N, Simon R, Stenzel-Poore M. 2005. Neuroprotection by osteopontin in stroke. J Cereb Blood Flow Metab 25(2):217-225.

Merrill JE, Ignarro LJ, Sherman MP, Melinek J, Lane TE. 1993. Microglial cell cytotoxicity of oligodendrocytes is mediated through nitric oxide. J Immunol 151:2132-2141.

Miller S, McRae B, Vanderlugt C, Nikcevich K, Pope J, Pope L, Karpus W. 1995. Evolution of the T-cell repertoire during the course of experimental immune-mediated demyelinating diseases. Immunol Rev 144:225-244.

Moos T, Morgan EH. 2000. Transferrin and transferrin receptor function in brain barrier systems. Cell Mol Neurobiol 20:77-95.

Morell P, Barrett CV, Mason JL, Toews AD, Hostettler JD, Knapp GW, Matsushima GK. 1998. Gene expression in brain during cuprizone-induced demyelination and remyelination. Mol Cell Neurosci 12(4-5):220-227.

Morell P, Jurevics H. 1996. Origin of cholesterol in myelin. Neurochem Res 21(4):463-470.

Morell P, Quarles RH, 1999. Myelin Formation, Structure, and Biochemistry. In: Siegal GJ, Agranoff BW, Albers RW; Fisher SK, Uhler MD, editors. Basic Neurochemistry, Molecular, Cellular, and Medical Aspects. 6th ed. Philadelphia: Lippincott, Williams & Wilkins. p.117-143.

Morita K, Sasaki H, Fujimoto K, Furuse M, Tsukita S. 1999. Claudin-11/OSP-based tight junctions of myelin sheaths in brain and Sertoli cells in testis. J Cell Biol 145(3): 579-588.

Muse E, Jurevics H, Toews A, Matsushima G, Morell P. 2001. Parameters related to lipid metabolism as markers of myelination in mouse brain. J Neurochem 76(1):77-86.

Mustafa MI, Diener P, Hojeberg B, Van der Meide P, Olsson T. 1991. T cell immunity and interferon-gamma secretion during experimental allergic encephalomyelitis in Lewis rats. J Neuroimmunol 31:165-177.

Naef F, Lim DA, Patil N, Magnasco M. 2002. DNA hybridization to mismatched templates: a chip study. Phys Rev E Stat Nonlin Soft Matter Phys 65(4 Pt 1):040902.

Noble M, Murray K, Stroobant P, Waterfield MD, Riddle P. 1988. Platelet-derived growth factor promotes division and motility and inhibits premature differentiation of the oligodendrocyte/ type-2 astrocyte progenitor cell. Nature 333:560-562.

Noseworthy JH. 1999. Progress in determining the causes and treatment of multiple sclerosis. Nature 399(Supplement):A40-A47.

Okada T, Yoshida H, Akazawa R, Negishi M, Mori K. 2002. Distinct roles of activating transcription factor 6 (ATF6) and double-stranded RNA-activated protein kinase-like endoplasmic reticulum kinase (PERK) in transcription during the mammalian unfolded protein response. Biochem J 366:585-594.

Page K, Hollister R, Hyman B. 1998. Dissociation of apolipoprotein and apolipoprotein receptor response to lesion in the rat brain: an in situ hybridization study. Neuroscience 85(4):1161-1171.

Panitch HS. 1992. Interferons in multiple sclerosis. A review of the evidence. [Review] Drugs 44:946-962.

Panitch HS, Hirsch RL, Schindler J, Johnson KP. 1987. Treatment of multiple sclerosis with gamma interferon: exacerbations associated with activation of the immune system. Neurology 37:1097-1102.

Park S-Y, Seol J-W, Lee Y-J, Cho J-H, Kang H-S, Kim I-S, Park S-H, Kim T-H, Yim JH, Kim M, Billiar TR, Seol D-W. 2004. IFN-γ enhances TRAIL-induced apoptosis through IRF-1. Eur J Biochem 271:4222-4228.

Pesheva P, Probstmeier R. 2000. Association of tenascin-R with murine brain myelin membranes: involvement of divalent cations. Neurosci Letters 283:165-168.

Pesheva P, Gloor S, Schachner M, Probstmeier R. 1997. Tenascin-R is an intrinsic autocrine factor for oligodendrocyte differentiation and promotes cell adhesion by a sulfatide-mediated mechanism. J Neuroscience 17:4642-4651.

Plant S, Arnett H, Ting J. 2004. Astroglial-derived lymphotoxin-α exacerbates inflammation and demyelination, but not remyelination. Glia 49:1-14.

Poirier J, Baccichet A, Dea D, Gauthier S. 1993. Cholesterol synthesis and lipoprotein reuptake during synaptic remodelling in hippocampus in adult rats. Neuroscience 55(1):81-90.

Popko B, Baerwald KD. 1999. Oligodendroglial response to the immune cytokine interferon gamma. [Review]. Neurochem Res 24:331-338.

Popko B, Corbin JG, Baerwald KD, Dupree J, Garcia AM. 1997. The effects of interferon-γ on the central nervous system. [Review] Mol Neurobiol 14:19-35.

Power C, Kong P-A, Trapp BD. 1996. Major histocompatibility complex class I expression in oligodendrocytes induces hypomyelination in transgenic mice. J Neurosci Res 44:165-173.

Quarles R. Glycoproteins of myelin sheaths. 1997. J Mol Neurosci 8:1-12.

Raff MC, Lillien LE, Richardson WD, Burne JF, Noble MD. 1988. Platelet-derived growth factor from astrocytes drives the clock that times oligodendrocyte development in culture. Nature 333:562-565.

Raff MC, Mirsky R, Fields KL, Lisak RP, Dorfman SH, Silberberg DH, Gregson NA, Leibowitz S, Kennedy MC. 1978. Galactocerebroside is a specific cell-surface antigenic marker for oligodendrocytes in culture. Nature 274:813-816.

Raine, CS. 1994. The Dale E. McFarlin Memorial Lecture: The immunology of the multiple sclerosis lesion. Ann Neurol 36:S61-S72.

Raine, CS. 1997. Oligodendrocytes and central nervous system myelin. In Davis RL and Robertson DM, editors. Textbook of Neuropathology. 3rd ed. Baltimore, Williams & Wilkins: p 137 –164.

Ransohoff RM, Bö L. 1996. Cytokines in CNS Inflammation: Status of Experimental Autoimmune Encephalomyelitis and Multiple Sclerosis as Cytokine-Regulated Delayed-Type Hypersensitivity Reactions. In: Ransohoff RM, Beneveniste EN, editors. Cytokines and the CNS. 2nd ed. New York, CRC Press: p 221-237.

Rao RV, Ellerby HM, Bredesen DE. 2004. Coupling endoplasmic reticulum stress to the cell death program. [Review]. Cell Death Differ 11:372-80.

Raza SM, Fuller GN, Rhee CH, Huang S, Hess K, Zhang W, Sawaya R. 2004. Identification of necrosis-associated genes in glioblastoma by cDNA microarray analysis. Clin Cancer Res 10(1 Pt 1):212-221.

Readhead C, Schneider A, Griffiths I, Nave K-A. 1994. Premature arrest of myelin formation in transgenic mice with increased proteolipid protein gene dosage. Neuron 12:583-595.

Renno T, Lin J, Piccirillo C, Antel J, Owens T. 1994. Cytokine production by cells in cerebrospinal fluid during experimental autoimmune encephalomyelitis in SJL/J mice. J Neuroimmunol 49:1-7.

Rodriguez M, Miller D. 1994. Immune promotion of central nervous system remyelination. Prog Brain Res 103:343-355.

Rodriguez M, Scheithauer B. 1994. Ultrastructure of multiple sclerosis. Ultra Pathol 18:3-13.

Rodriguez M, Scheithauer B, Forbes G, Kelly P. 1993. Oligodendrocyte injury is an early event in lesions of multiple sclerosis. Mayo Clinic Proc 68:627-636.

Roland M, McFarland H. 1995. Immunological aspects of experimental allergic encephalomyelitis and multiple sclerosis. [Review] Crit Rev Clin Lab Sci 32:121-182.

Ron D. 2002. Translational control in the endoplasmic reticulum stress response. [Review]. J Clin Invest 110:1383-1388.

Rutkowski D, Kaufman R. 2004. A trip to the ER: coping with stress. [Review]. Trends Cell Biol 14:20-28.

Sato Y, Nakamura R, Satoh M, Fujishita K, Mori S, Ishida S, Yamaguchi T, Inoue K, Nagao T, Ohno Y. 2005. Thyroid hormone targets matrix Gla protein gene expression associated with vascular smooth muscle calcification. Circ Res 97(6):550-557.

Satoh J, Kim SU, Kastrukoff LF, Takei F. 1991. Expression and induction of intercellular adhesion molecules (ICAMs) and major histocompatibility complex (MHC) antigens on cultured murine oligodendrocytes and astrocytes. J Neurosci Res 29:1-12.

Schneider-Schaulies J, Kirchhoff F, Archelos J, Schachner M. 1991. Down-regulation of myelin-associated glycoprotein on Schwann cells by interferon-gamma and Tumor necrosis factor-α affects neurite outgrowth. Neuron 7:995-1005.

Schachner M, Kim SK, Zehnle R. 1981. Developmental expression in central and peripheral nervous system of oligodendrocyte cell surface antigens (O antigens) recognized by monoclonal antibodies. Dev Biol 83(2):328-338.

Schaeren-Wiemers N, Bonnet A, Erb M, Erne B, Bartsch U, Kern F, Mantei N, Sherman D, Suter U. 2004. The raft-associated protein MAL is required for maintenance of proper axon--glia interactions in the central nervous system. J Cell Biol 166(5):731-742.

Selvaraju R, Bernasconi L, Losberger C, Graber P, Kadi L, Avellana-Adalid V, Picard-Riera N, Van Evercooren AB, Cirillo R, Kosco-Vilbois M, Feger G, Papoian R, Boschert U. 2004. Osteopontin is upregulated during in vivo demyelination and remyelination and enhances myelin formation in vitro. Mol Cell Neurosci 25(4):707-721.

Sethna MP, Lampson LA. 1991. Immune modulation within the brain: recruitment of inflammatory cells and increased major histocompatibility antigen expression following intracerebral infection of interferon-gamma. J Neuroimmunol 34:121-132.

Shuai K, Ziemiecki A, Wilks AF, Harpur AG, Sadowski HB, Gilman MZ, Darnell JE. 1993. Polypeptide signalling to the nucleus through tyrosine phosphorylation of Jak and Stat proteins. Nature 366(6455):580-3.

Simmons RD, Willenborg DO. 1990. Direct injection of cytokines into the spinal cord causes autoimmune encephalomyelitis-like inflammation. J Neurol Sci 100:37-42.

Skoff RP. 1995. Programmed cell death in the dysmyelinating mutants. Brain Path 5:283-288.

Skurkovich S, Boiko A, Beliaeva I, Buglak A, Alekseeva T, Smirnova N, Kulakova O, Tchechonin V, Gurova O, Deomina T, Favorova OO, Skurkovic B, Gusev E. 2001. Randomized study of antibodies to IFN-gamma and TNF-alpha in secondary progressive multiple sclerosis. Mult Scler 7(5):277-284.

Smith CUM. 1996. Elements of Molecular Neurobiology. 2nd ed. New York (NY): John Wiley & Sons Ltd. 522 p.

Solodukhin AS, Caldwell HL, Sando JJ, Kretsinger RH. 2002. Two-dimentional crystal structures of protein kinase C-delta, its regulatory domain, and the enzyme complexed with myelin basic protein. Biophys J 82(5): 2700-2708.

Sommer I, Schachner M. 1981. Monoclonal antibodies (01 to 04) to oligodendrocyte cell surfaces: an immunocytological study in the central nervous. Dev Biol 83(2):311-327.

Southwood CM, Garbern J, Jiang W, Gow A. 2002. The unfolded protein response modulates disease severity in Pelizaeus-Merzbacher disease. Neuron 36:585-596.

St. Pierre B, Merrill J, Dopp J. 1996. Effects of cytokines on CNS cells: Glia. In: Ransohoff RM, Beneveniste EN, editors. Cytokines and the CNS. 2nd ed. New York, CRC Press: p 151-168.

Steffen BJ, Butcher EC, Engelhardt B. 1994. Evidence for involvement of ICAM-1 and VCAM-1 in lymphocyte interaction with endothelium in experimental autoimmune encephalomyelitis in the central nervous system in the SJL/J Mouse. Am J Path 145:189-201.

Steiniger B, van der Meide PH. 1988. Rat epedyma and microglia cells express class II MHC antigens after intravenous infusion of recombinant gamma interferon. J Neuroimmunol 19:111-118.

Steinman L. 2001. Blockade of gamma interferon might be beneficial in MS [Review]. Mult Scler 7:275-276.

Stidworthy MF, Genoud S, Li WW, Leone DP, Mantei N, Suter U, et al. 2004. Notch1 and Jagged1 are expressed after CNS demyelination, but are not a major rate-determining factor during remyelination. Brain 127:1928-1941.

Sullivan P, Mezdour H, Aratani Y, Knouff C, Najib J, Reddick R, Quarfordt S, Maeda N. 1997. Targeted replacement of the mouse apolipoprotein E gene with the common human APOE3 allele enhances diet-induced hypercholesterolemia and atherosclerosis. Am Soc Biochem Mol Biol 272(29):17972-17980.

Suzuki T, Urano T, Tsukui T, Horie-Inoue K, Moriya T, Ishida T, Muramatsu M, Ouchi Y, Sasano H, Inoue S. 2005. Estrogen-responsive finger protein as a new potential biomarker for breast cancer. Clin Cancer Res 11(17):6148-6154.

Suzuki K, Kikkawa T. 1969. Status spongiosus of CNS and hepatic changes induced by cuprizone (biscyclohexanone oxalydihydrazone). Am J Path 54:307-325.

Suzumura A, Silberberg DA, Lisak RP. 1986. The expression of MHC antigens on oligodendrocytes: induction of polymorphic H-2 expression by lymphokines. J Neuroimmunol 11:179-190.

Tau G, Rothman P. 1999. Biologic functions of the IFN-gamma receptors. Allergy 54(12):1233-1251.

Tiwari-Woodruff SK, Buznikov AG, Vu TQ, Micevych PE, Chen K, Kornblum HI, Bronstein JM. 2001. OSP/claudin-11 forms a complex with a novel member of the tetraspanin super family and beta1 integrin and regulates proliferation and migration of oligodendrocytes. J Cell Biol 153(2): 295-305.

Tosic M, Gow A, Dolivo M, Domanska-Janik K, Lazzarini RA, Matthieu J-M. 1996. Proteolipid/DM-20 Proteins Bearing the Paralytic Tremor Mutation in Peripheral Nerves and Transfected Cos-7 Cells. Neurochem Res 21(No 4):423-430.

Trapp B, Bö L, Mork S, Chang A. 1999. Pathogenesis of tissue injury in MS lesions. [Review]. J Neuroimmunol 98:49-56.

Turnley AM, Miller JFAP, Bartlett PF. 1991. Regulation of MHC Molecules on MBP positive oligodendrocytes in mice by IFN-g and TNF-a. Neurosci Lett 123:45-48.

Utz U, McFarland HF. 1994. The role of T cells in multiple sclerosis: Implications for therapies targeting the T cell receptor. J Neuropath Exp Neurol 53:351-358.

Vartanian T, Li Y, Zhao M, Stefansson K. 1995 Interferon-γ–induced oligodendrocyte cell death: implications for the pathogenesis of multiple sclerosis. Mol Med 1:732-743.

Venezie R, Toews A, Morell P. 1995. Macrophage recruitment in different models of nerve injury: lysozyme as a marker for active phagocytosis. J Neurosci Res 40(1):99-107.

Watanabe M, Toyama Y, Nishiyama A. 2002 Differentiation of proliferated NG2-positive glial progenitor cells in a remyelinating lesion. J Neurosci Res 69:826-836.

Voorthius JAC, Uitdehaag BMJ, De Groot CJA, Goede PH, Van der Meide PH, Dijkstra CD. 1990. Suppression of experimental allergic encephalomyelitis by intraventricular administration of interferon-gamma in Lewis rats. Clin Exp Immunol 81:183-188.

Wegner M. 2001. Expression of transcription factors during oligodendroglial development. Microsc Res Tech 52:746-752.

Willenborg DO, Fordham S, Bernard CC, Cowden WB, Ramshaw IA. 1996. IFN-gamma plays a critical down-regulatory role in the induction and effector phase of myelin oligodendrocyte glycoprotein-induced autoimmune encephalomyelitis. J Immunol 157:3223-3227.

Wissing D, Mouritzen H, Egeblad M, Poirier GG, Jäättelä M. 1997. Involvement of caspase-dependent activation of cytosolic phospholipase A_2 in tumor necrosis factor-induced apoptosis. PNAS 94(10):5073-5077.

Wolf LA, Laster SM. 1999. Characterization of arachidonic acid-induced apoptosis. Cell Biochem Biophys 30:353-368.

Wong D, Dorovini-Zis K.1992. Upregulation of Intercellular Adhesion Molecule-1 (ICAM-1) Expression in Primary Cultures of Human Brain Microvessel Endothelial Cells by Cytokines and Lipopolysaccharide. J. Neuroimmunol. 39:11-21.

Wong GH, Bartlett PF, Clark-Lewis I, Battye F, Schrader JW. 1984. Inducible Expression of H-2 and Ia Antigens on Brain Cells. Nature 310: 688-691.

Wu JI, Reed RB, Grabowski PJ, Artzt K. 2002. Function of quaking in myelination: regulation of alternative splicing. PNAS 99(7):4233-4238.

Wu T, Angus CW, Yao XL, Logun C, Shelhamer JH. 1997. P11, a unique member of the S100 family of calcium-binding proteins, interacts with and inhibits the activity of the 85-kDa cytosolic phospholipase A2. J Biol Chem 272(27):17145-17153.

Yamano T, Murata S, Shimbara N, Tanaka N, Chiba T, Tanaka K, Yui K, Udono H. 2002. Two distinct pathways mediated by PA28 and hsp90 in major histocompatibility complex class I antigen processing. J Exp Med 196(2):185-196.

Ye P, Carson J, De'Ercole A. 1995. Insulin-like growth factor-I influences the initiation of myelination: studies of the anterior commissure of transgenic mice. Neurosci Lett 201:235-238.

Yool D, Montague P, McLaughlin M, McCulloch MC, Edgar JM, Nave KA, Davies RW, Griffiths JR, McCallion, AS. 2002. Phenotypic analysis of mice deficient in the major myelin protein MOBP, and evidence for a novel Mobp isoform. Glia 39(3):256-267.

Yoshikawa H. 2001. Myelin-associated oligodendrocyte basic protein modulates the arrangement of radial growth of the axon and the radial component of myelin. Med Electron Microsc 34(3):160-164.

Zhang L, Wang L, Ravindranathan A, Miles MF. 2002. A new algorithm for analysis of oligonucleotide arrays: application to expression profiling in mouse brain regions. J Mol Biol 317(2):225-235.

Zhi H, Zhang J, Hu G, Lu J, Wang X, Zhou C, Wu M, Liu Z. 2003. The deregulation of arachidonic acid metabolism-related genes in human esophageal squamous cell carcinoma. Int J Cancer 106:327-333.

Zimmermann A, Trilling M, Wagner M, Wilborn M, Bubic I, Jonjic S, Koszinowski U, Hengel H. 2005. A cytomegaloviral protein reveals a dual role for STAT2 in IFN-{gamma} signaling and antiviral responses. J Exp Med 201(10):1543-1553.

Zobiack N, Rescher U, Ludwig C, Zeuschner D, Gerke V. 2003. The annexin 2/S100A10 complex controls the distribution of transferrin receptor-containing recycling endosomes. Mol Biol Cell 14(12): 4896-4908.

Zhou Q, Choi G, Anderson DJ. 2001. The bHLH Transcription Factor Olig2 Promotes Oligodendrocyte Differentiation in Collaboration with Nkx2.2. Neuron 31(5):791-807.